Towards multifidelity uncertainty quantification for multiobjective structural design

Jérémy Lebon

Par **Jérémy LEBON**

Towards multifidelity uncertainty quantification for multiobjective structural design

Thèse présentée
pour l'obtention du grade
de Docteur de l'UTC

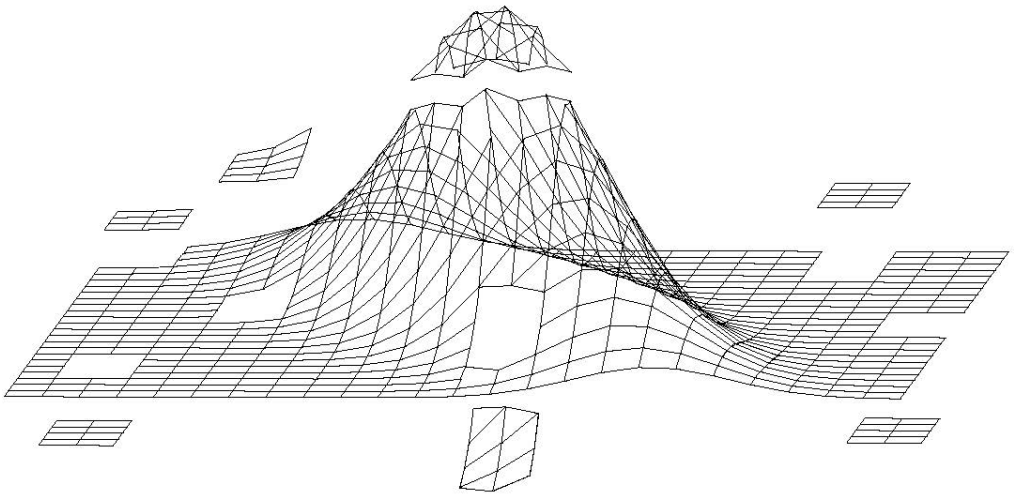

Soutenue le 12 décembre 2013
Spécialité : Mécanique avancée

D2123

Université libre de Bruxelles
École polytechnique de Bruxelles

Université de Technologie de Compiègne
École doctorale de l'UTC

Towards multifidelity uncertainty quantification for multiobjective structural design

Thèse de doctorat

Défense publique du **12 Décembre 2013**

en vue de l'obtention du

Titre de Docteur en Sciences de l'Ingénieur
de l'Université libre de Bruxelles
et du
Grade de docteur en Sciences Appliquées
de l' Université de Technologie de Compiègne
Specialité : Mécanique avancée

par

LEBON Jérémy

Jury de thèse

Membres:	Pr. DERAEMAEKER Arnaud	Université libre de Bruxelles
	Pr. LEMAIRE Maurice	Institut Français de Mécanique Avancée
	Pr. TISON Thierry	Université de Valenciennes
	Pr. VILLON Pierre	Université de Technologie de Compiègne
	Dr. Ing. ZENTNER Irmela	Research Engineer, Électricité De France
Promoteurs :	Ass. Pr. FILOMENO COELHO Rajan	Université libre de Bruxelles
	Dr. Ing. BREITKOPF Piotr	CNRS, Université de Technologie de Compiègne
Co-Promoteur :	Pr. BOUILLARD Philippe	Université libre de Bruxelles

Service BATir (Construction, Architecture & Urbanisme)
Bruxelles, ULB, Belgique

Laboratoire Roberval
Compiègne, UTC, France

To my parents,
To my sister,
To my grandmother,
In memory of Sully, Léon, Lucet, Emilia, Mickaelle

Acknowledgements

Now comes the time to write the last page of this thesis work, bringing by the way my student journey to an end. Here are a few words full of gratitude to those who contributed to make this journey a success, so rich in lessons, in both scientific and personal sides.

First and foremost, I would like to express my sincere gratitude to my supervisors Ass. Pr. Rajan Filomeno Coelho and Pr. Piotr Breitkopf for their invaluable scientific and human support and guidance throughout this research work.

I wish to thank the members of the jury, namely Pr. DERAEMAEKER Arnaud, Pr. LEMAIRE Maurice, Pr. TISON Thierry, Pr. VILLON Pierre, Dr. Ing. ZENTNER Irmela for their relevant questions and comments during both private and public defenses. I hope we may keep such fruitful exchanges in the future.

I would like also to thank my colleagues from BATir in Brussels and from Roberval in Compiègne with which I spent a huge amount of time during office hours and beyond. Thanks to all of you for the moments we shared.

Last but not least, without the unconditional support of my family despite the long distance, my brother in arms, Frédéric, and my beloved partner Sabine, nothing would have been possible.

Finally, I would like to gratefully acknowledge the support provided for this work under the BB2B project from the Innoviris institution (Bruxelles Capitale).

Abstract

This thesis aims at Multi-Objective Optimization under Uncertainty in structural design. We investigate Polynomial Chaos Expansion (PCE) surrogates which require extensive training sets. We then face two issues: high computational costs of an individual Finite Element simulation and its limited precision. From numerical point of view and in order to limit the computational expense of the PCE construction we particularly focus on sparse PCE schemes. We also develop a custom Latin Hypercube Sampling scheme taking into account the finite precision of the simulation. From the modeling point of view, we propose a multifidelity approach involving a hierarchy of models ranging from full scale simulations through reduced order physics up to response surfaces. Finally, we investigate multiobjective optimization of structures under uncertainty. We extend the PCE model of design objectives by taking into account the design variables. We illustrate our work with examples in sheet metal forming and optimal design of truss structures.

Outline

Chapter 1

Introduction

1.1 Introduction

Numerical models are extensively used in science disciplines such as physics, chemistry, computational engineering, biological and social sciences, etc. These are aimed at providing a better understanding of real world phenomena. In mechanical engineering, they are devoted to play a central role in the analysis and design of structures and processes. They provide an invaluable tool to the engineer to the search for the best performing structures and processes. In most of real-life applications, the performances are assessed simultaneously by multiple criteria (cost, environmental impact, safety, robustness). It has been now commonly admitted that uncertainties are inherent of this process and may have a non-negligible influence on the design performances.

In this thesis work we explore two issues the engineer has to face: the quantification of the impact of uncertainties on the design (Uncertainty quantification), and its incorporation into an optimization process with multiple criteria (Multiobjective Optimization under Uncertainty).

Uncertainty Quantification (UQ) Along the elaboration process of the numerical models, approximations are made. They result from the implementation into a computer code of an imperfect abstraction (the mathematical model) of the reality (the real experiment). Figure 1.1 proposes to identify three sources of approximations involved in the construction of a numerical model.

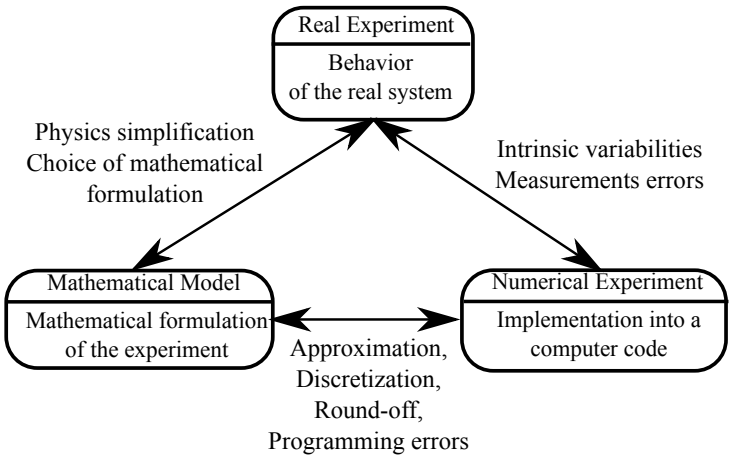

Figure 1.1: A possible illustration for uncertainty sources

One of them is issued from the elaboration of the mathematical model of real experiment. It describes the underlying physics of the observed phenomenon. The induced errors are due to simplifications or lack of knowledge that the mathematical abstraction of the physical system may suffer from (simplified physics error) but also to the choice of the underlying mathematical formulation (Galerkin formulation instead of strong FEM formulation, etc). The implementation of the mathematical model into a computer code also generates its own type of errors. It encompasses the necessary approximation/discretization errors as well as the numerical and round-off errors, and programming errors. Finally, a third source of errors may be emphasized by repeatedly performing the real experiment under the same configuration:

different results may though be observed as a result of errors in measurements, of the evolution in time and space of material properties, the environmental conditions, etc.

All these errors laid end to end, may lead simulation results to represent the underlying physics with a low level of fidelity. The question of the accuracy of the simulation results must be inevitably confronted. This topic is addressed in the literature by the *Verification*[1] and *Validation* domain[2] (V&V) [OTH04] as well as Uncertainties Quantification (UQ). This thesis work is concerned with the latter domain where the errors are preferentially referred to "uncertainties". Different theories to represent uncertainties are provided in the literature (fuzzy logic, confidence theory, probabilistic,...). This thesis focuses on the probabilistic viewpoint: uncertainty sources are described by random variables characterized by a probability density function[3].

UQ provides the engineer with valuable tools to assess the impact of the designed process design and sensitivity analysis, reliability based design and variability analysis:

- *Robust design and Sensitivity analysis* are aimed at quantifying the contribution of each random input variable to the variability of the response [SAA+10]. One may distinguish between two types of approaches addressing the sensitivity analysis from two different points of view. The local sensitivity analysis focuses on small variations of the input parameters around a nominal value and studies how the model response is affected; the global sensitivity analysis focuses on quantifying the output uncertainty due to changes of input parameters (taken either separately or in combination) in their entire range of variation.

- *The reliability* of a system is defined as the assessment of its failure probability, that is the non-satisfaction of its expected performance [LCM09]. As a system is usually composed of subsystems, the failure of the system may be caused by different scenarii caused by the failure of one or more components to be identified.

- Finally, the *variability study* aims at completely characterizing the output probability density function.

Achieving these tasks firstly requires the definition of the probabilistic model. It consists in identifying the uncertain input data and to model them according to their respective (joint) probability density function (*Identification*). Then, to assess their impact onto the model output, one has to transform the modeled uncertainties on the input variables to output statistical (e.g. statistical moments) or probabilistic quantities of interest (e.g. probability density function). This process forms the *propagation of uncertainties*. Two approaches may then be distinguished: *intrusive* methods consist in adapting the governing equations of the deterministic model to uncertainty propagation; and *non-intrusive* methods, which make use of a series of calls to the deterministic model to propagate the uncertainties. In this thesis, we consider the non-intrusive uncertainty propagation scheme enabling the use of complex in-house or commercial simulation codes. In this context, the UQ process is illustrated in Fig1.2.

[1] *Verification* aims at assessing the accuracy of the solution in the context of the study by comparing in some useful sense the consistency of the numerically obtained results with some trustworthy experimental results at hand (Do we solve right the equations?)

[2] *Validation* consists in providing a quantitative description of the distance between the real experiment, the numerical model or the real-life system it is aimed to represent (Do we solve the right equation?).

[3] The notions of random variables and probability density function are described in more details in Chapter 2

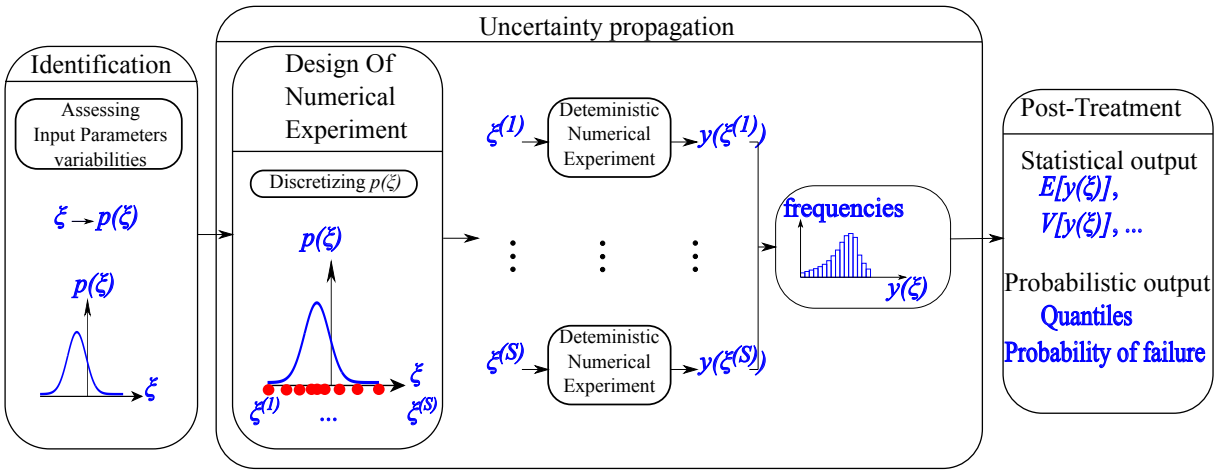

Figure 1.2: Steps for non-intrusive uncertainty quantification

Once the stochastic model has been identified, a Design Of Experiment (DoE) is built on the stochastic variables with respect to their probability density function. For each point in the DoE, deterministic calls to the numerical model are performed. A post-treatment phase allows to retrieve the statistical (histogram, mean, variance, etc.) and/or the probabilistic (quantiles, probability of failure, etc.) data of interest. The uncertainty propagation phase is computationally expensive as a single call to the numerical model may already be costly and numerous calls may be necessary to assess the stochastic and/or probabilistic quantities of interest.

Optimization Under Uncertainty (OUU) The second issue addressed in this thesis concerns the multiplicity of pontentially competing criteria required to assess the performances of a structure.

The incorporation of uncertainties [EGWJT02] transposes the concepts of robustness, and reliability into the optimization context.

- *Robust design optimization* is aimed at identifying the most performing responses with a particular insight on their sensitivity to random perturbation of design variables or parameters.
- *Reliability-based design optimization* incorporates the failure probability as a constraint of the optimization problem.

Figure 1.3 plots a straightforward manner to perform optimization under uncertainty in a non intrusive context.

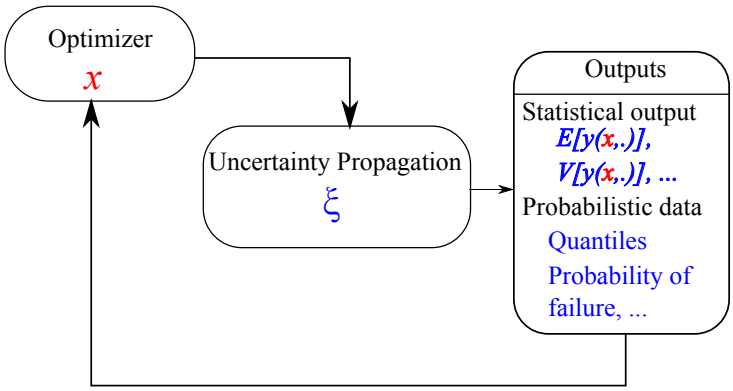

Figure 1.3: Double-Loop optimization process under uncertainty

The assessment of robustness and reliability measure usually require the computation of statistical data (mean/variance) and or probabilistic data such quantiles and probability of failure. The robustness and the reliability enters the optimization problems either as objective of constraints and may then be assessed each time a new solution is provided by the optimizer. The optimization and uncertainty quantification loops may then be nested which leads to high computational costs. Strategies to overcome this limitation have ben developed. One way to circumvent it consists in multifidelity approaches whose numerical challenges are addressed in more details in the next section.

1.2 Numerical challenges

As in practice both OUU and UQ are performed by repeated calls to the (deterministic) numerical model, the computational expense may rapidly become unaffordable. Multifidelity approaches address this issue by combining in a hierarchical manner two levels of numerical models: a "high-fidelity" model which is characterized by a high accuracy but also a high computational cost is combined with "low-fidelity" model less accurate but also less computationally costly.

1.2.1 On the development of metamodel in multifidelity approaches

Categorization of surrogate models Non-intrusive schemes based on surrogate-based approaches have been proposed in optimization and uncertainty propagation domains:

- on the UQ side, the **Chapter 2** provides an overview of computational methods and shows that the Polynomial Chaos Expansion (PCE) has been widely extended and adapted to deal with computationally costly and high-dimensional black-box functions;
- on the optimization side, optimization strategies for computationally costly and high-dimensional black-box simulations [SW10] as well as metamodeling techniques for optimization [WS07] are proposed.

In the following the original computational model will be referred as the "high-fidelity" model, and the surrogate model as the "low-fidelity" model as it is less accurate than the original numerical model.

One may classify these approaches as "multi-fidelity" or "variable-fidelity" when physics-based and non-physics surrogates are considered:

- physics-based surrogates built from partial convergence of the "high -fidelity" model [BBM$^+$00], those based on simplified physics [dSR08], those based on a coarse discretization [ALG$^+$99, VHS02, SLZ$^+$11];
- interpolating or regression-based response surface from a Design of Experiment (DoE) evaluated with "high-fidelity" simulations. When the derivatives are available, one may build a first order consistent approximation [WG95]. When only the function evaluation is available, general approaches, such as general least square, polynomial response surface[MAC09], kriging [Ste99, Cre90], moving least squares [LS81, NTV92], radial basis function [B$^+$00] may be used to build a global approximation from the available set of points.

The non-physics based approaches do not perform well in high dimensions ("curse of dimensionality"). Their accuracy depends on the underlying "high-fidelity" model and may be sensitive to the type and to the size of the DoE used. Moreover, the computational expense related to the training phase depends on the cost of the underlying "high-fidelity model". Finally tuning such metamodel is not straightforward (e.g. excessive smoothing, overfiting). Physics-based approaches do not suffer from these issues but have to be specifically built for one application, thus may not be always available.

In the UQ domain, during the last two decades, the Polynomial Chaos Expansion (PCE) has been widely used to propagate uncertainties (**Chapter 2**). Broadly speaking, the PCE [Gha91] is a metamodel that is intended to give an approximation of the stochastic behavior of a function y (*scalar random process*). When a single random variable ξ is considered, the P^{th}-order PCE of y is defined as:

$$y = \sum_{i=0}^{P-1} \gamma_i \Psi_i(\xi) \tag{1.1}$$

where $\boldsymbol{\xi}_{\mathcal{S}}$ are standardized random variables, and $\boldsymbol{\gamma} = \{\gamma\}_{i=0}^{P-1}$ the set of PCE coefficients which have to be computed during the training phase.

On the validation of surrogate based approaches Twofold challenge has to be tackled:

- ensuring the convergence of the multifidelity surrogates,
- ensuring the accuracy/stability of the underlying "high-fidelity" model.

Convergence of hierarchical approaches In the optimization field, the key point is to guarantee that the surrogate-based optimization process converges to an optimum of the original model. In the UQ field, the key point is to guarantee that the surrogate-based UQ approach converges in terms of statistical measures of the system responses (e.g. the output variances, sensitivities, robustness measures, probability measures)

In the optimization field, rigorous approaches combining in a hierarchical way a "low-" and "high-'' fidelity model are referred to surrogate-based optimization and/or model management framework [ALG$^+$01]. The premise of this methodology is to claim that a surrogate based on a physics-based low-fidelity model

and an interpolant of the discrepancy may provide a more cost-effective approximation of the high fidelity model. A proof of convergence is ensured provided that one employs a sufficiently rigorous verification (e.g. trust region methodology) and that the surrogate model satisfies first-order [AL01] and sometimes even second order [EGC$^+$04] consistency conditions with the underlying high-fidelity model. In the trust region methodology, the "low-fidelity" model values are corrected to fit the "high-fidelity" model values (up to the second order if necessary) using either additive, multiplicative, or combined multiplicative-additive correction functions on a set of collocation points. In addition, to guarantee that the progress made with the "lower-fidelity" model also leads to an improvement with the "higher-fidelity" model, the "lower-fidelity" model is regularly updated using systematical calls to the "high-fidelity" model.

In the UQ field, the use of *non-physics* based metamodel is usually not discussed or is highlighted a posteriori by assessing error measures on the statistical or probability data of interest. Moreover, in some cases, adaptive sampling is used in order to update the metamodels and control its accuracy in a particular space region [DSB11b, WCS$^+$13]. It is only recently that [NE12] investigates the extension of the classic multi-fidelity optimization concepts to the uncertainty quantification fields. The "low-fidelity" model values are corrected using combined additive-multiplicative correction function to match the high-fidelity values on some collocation points, and the non-intrusive PCE is trained on the low-fidelity model to propagate the uncertainty.

On the accuracy/stability of the "high-fidelity model". In the optimization field, ensuring the accuracy and/or the stability of the "high-fidelity" model and of the gradients in the whole domain of interest belongs to the "good practice rules" (e.g. the minimum step size of the finite difference scheme is assessed a priori). In UQ, these instabilities may be treated as epistemic uncertainties through diverse approaches such as interval analysis, possibility theory, evidence theory or probability theory [HJOS10, HD03].

When considering the high-fidelity model as a black-box, no direct mapping is provided from the input variables $\boldsymbol{\xi} = [\xi_1, \xi_2, \ldots, \xi_M]$ to the derivatives of a selected output function y, except in seldom cases where the black-box itself provides it. Thus a numerical scheme has to be used in order to compute the sensitivities (i.e the derivatives) of the model. In this thesis, we are interested in the model output stability with respect to the variation of the variable ξ_i, $i \in \{1, \ldots, M\}$ assessed by the following non dimensional finite difference scheme :

$$\mu_i = \frac{\Delta y(\xi_i)}{\Delta \xi_i} \times \frac{\xi_i \text{nom}}{y(\xi_i^{\text{nom}})} \tag{1.2}$$

where ξ_i^{nom}, $i \in \{1, \ldots, M\}$ is a nominal value.

$$\Delta y(\xi_i) = y\left(\xi_i^{\text{nom}} + \frac{\Delta \xi_i}{2}\right) - y\left(\xi_i^{\text{nom}} - \frac{\Delta \xi_i}{2}\right). \tag{1.3}$$

When decreasing the order of magnitude of the perturbation ($-\log(\Delta\xi)$ increasing), the non-dimensional sensitivity μ_i computed for the "high-fidelity" model exhibits subsequent behaviors illustrated in a qualitative manner[4] on Fig.1.4:

[4]For a quantitative illustration see Fig.7 in Chapter 3 or Fig.13 in Chapter 4

1. firstly, for "large" variation of $\Delta\xi_i$, the variation μ_i reveals the non-linear behavior of the model. No brutal variation of μ_i is observed and the model is considered as trustworthy.
2. secondly, μ_i stabilizes around a constant value $\bar{\mu_i}$ where the model may be considered as linear.
3. thirdly, on reaching the threshold Ⓑ, μ_i becomes unstable.
4. finally, the threshold Ⓐ shows the model sensitivity limit: for this range of variation, the model is not sensitive anymore.

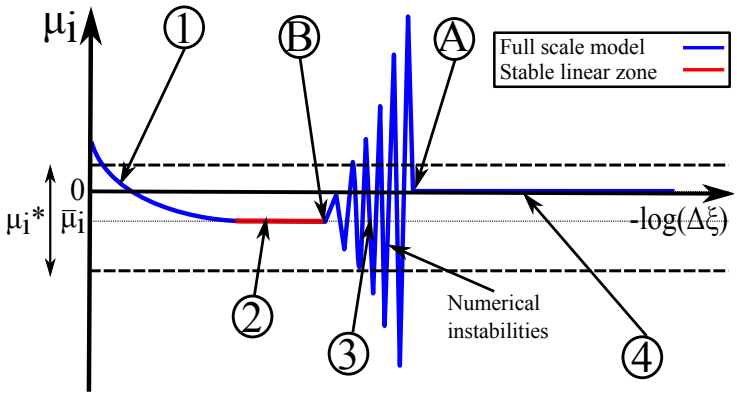

Figure 1.4: Typical sensitivity results issued from actual computation

In both optimization and UQ domains, comparing the model error with the variation magnitude of the output function is of paramount importance to ensure the validity of the approach. To do so, one may arbitrarily define a resolution threshold δ_i^* on ξ_i determined from an acceptable value of μ_i arbitrarily defined. δ_i^* is then defined as.

$$\delta_i^* = \underset{\Delta\xi_i}{\operatorname{argmin}}\ \mu_i(\Delta\xi_i) > \mu_i^*, i \in \{1, \ldots, M\}. \tag{1.4}$$

When evaluating two sample points $\xi_i^{(1)}$ and $\xi_i^{(2)}$ one considers model response trustworthy when $\Delta\xi = |\xi_i^{(1)} - \xi_i^{(2)}| \geq \delta_i^*$ and erroneous otherwise.

In this work, we focus on the observation that the resolution threshold and the variation range of the training data may be close. The number of achievable simulations by the "high-fidelity" model is not only limited by the cost of an individual simulation but also by its intrinsic resolution. Thus one has to face two issues: firstly, an insufficient number of "high-fidelity" simulations may harm the accuracy of the response surface, secondly, a too high number of simulations may introduce numerical noise which also directly leads to an inaccurate surrogate model.

1.2.2 MultiObjective Optimization under Uncertainty (MOOU)

In real-life applications the solution of the optimization problem involving possibly competing criteria is not unique: a set of best compromise solutions (called Pareto set) is sought rather than a single solution.

The Pareto set P^* is then defined as the set of all non-dominated solutions in the design variable space Ω: $P^* = \{\boldsymbol{x}^* \in \Omega \mid \nexists \boldsymbol{x} \in \Omega; \boldsymbol{y}(\boldsymbol{x}) \succeq \boldsymbol{y}(\boldsymbol{x^*})\}$ and the Pareto front defines its representation in the objective function space. The symbol "$\succeq$" defines the dominance concept between the vectors $\boldsymbol{y}(\boldsymbol{x})$ and $\boldsymbol{y}(\boldsymbol{x^*})$ such as $\forall i \in \{1, ..., m\}, y_i(\boldsymbol{x}) \leq y_i(\boldsymbol{x^*})$ and $\exists i \in \{1, ..., m\} \mid y_i(\boldsymbol{x}) < y_i(\boldsymbol{x^*})$. The Fig.1.5 illustrates Pareto fronts for two different values of α. The best performing solutions are obtained for a minimization of the functions y_1 and y_2.

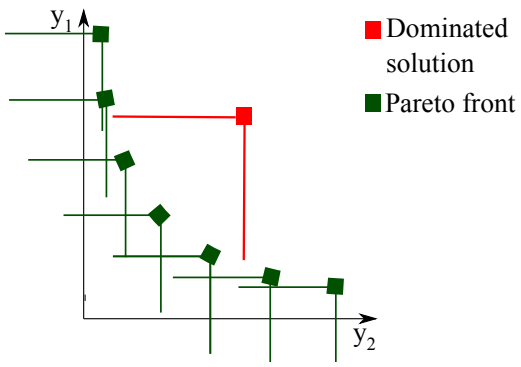

Figure 1.5: Illustration of dominated and non dominated solutions. The red vector of objectives is dominated by 3 green vectors. The green vectors are not dominated and form the Pareto front.

Extending the classical concepts for single objective robust design optimization and reliability based optimization to multiobjective optimization is not straightforward. Notably, [DG05, HGB07] extends the concept of reliability and robustness in the multi-objective space by defining y robustness frontiers of the Pareto front and [RFC10] defines stochastic Pareto front ruled by a probability of dominance.

Moreover, in most of the studies (e.g. [YCL+11]), the influence of uncertainties is rarely considered using a metamodel approach. The formulation of the optimization problem has to be adapted and the notion of robustness and reliability has to be defined in conjunction with the dominance notion. Thus, the development of a non-intrusive stochastic metamodel strategy, specially when a complete probabilistic description might be useful to compute the probability of failure (e.g. in Reliability Based Optimization) is a challenged we address in this thesis work.

1.3 Contributions of the thesis

The contribution of this thesis is twofold.

- The issue of Uncertainty Quantification with high fidelity model characterized by inadequate resolution for uncertainty propagation is illustrated in **Chapter 3** and in **Chapter 4**. It highlights that a careful attention has to be given to the validation of the high-fidelity model to perform uncertainty quantification. In fact the variation range of the stochastic variables may be smaller than the resolution to the model.

- The incorporation of uncertainty into a multi-objective optimization in a non intrusive framework is addressed in **Chapter 5**, based on the hierarchical combination of two metamodels: one for

the deterministic variation of design variables and the other to assess the variability of the model response for each set of design variables.

In the following sections we discuss both issues.

1.3.1 A multifidelity approach for springback variability assessment

In this section we illustrate the first contribution of this thesis using an example of deep drawing of metal parts. The deep drawing process is a manufacturing process which aims at permanently changing the shape of a metal sheet through the action of a moving punch forming the metal against a motionless die (Fig.1.6(a)). When the loading is removed, additional deformations appear and the so called springback phenomenon occurs (Fig.1.6(b)).

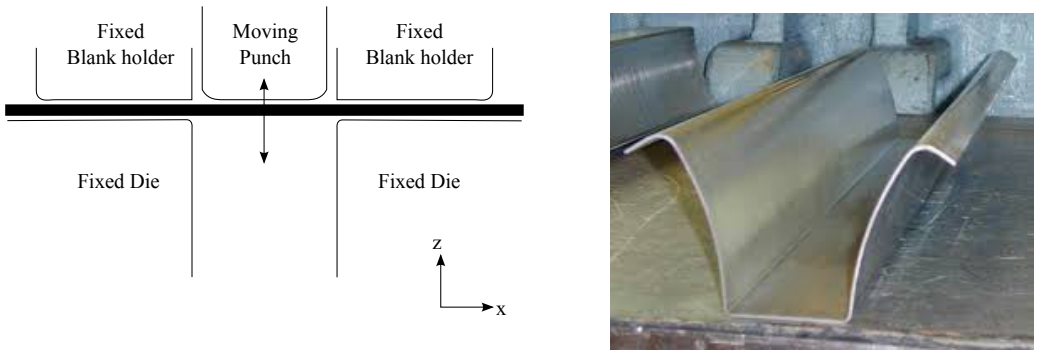

(a) Geometrical configuration of the modeled Numisheet'93 benchmark

(b) Illustration of springback shape [Car09]

Figure 1.6: Springback phenomenon for a 2D deep drawn U-shaped metal sheet

To perform a variability study of the post springback shape, we propose a two-pronged approach .

A first ingredient consists in defining a physics-based "low-fidelity" model with a finer resolution to replace the "high-fidelity" model for small variation of parameters. A custom sparse stochastic surrogate (Sparse PCE, where only the most relevant term of the PCE are retained) is then used to perform the variability study onto the newly "low-fidelity" "high-resolution" model.

The simulation of the springback process provides a noisy numerical behavior against small thickness variations. The FEM model may be considered as trustworthy for a resolution which represents a tolerance on the thickness around $\frac{1}{20}$ of its nominal value. The resolution of the numerical model is thus clearly insufficient to perform a variability study on the tolerance range. Three aspects of the FE implementation of the deep drawing process may be responsible for these numerical instabilities: the coarsity of the mesh, the incorrect stress integration through the thickness and the contact algorithm. Improving the FE model needs (among other) to refine the discretization of the model in every direction preserving the same aspect ratio which leads to excessive computational cost. We choose to combine both models: the FE "high-fidelity" model by a "lower-fidelity" physics-based metamodel with both features: a lower computational cost and a higher resolution.

Such a metamodel has been recently proposed by [LQBRJ12]. It describes the deep drawing process

of a 2D metal sheet as a 2D plain strain Bending-Under-Tension process (B-U-T) in a semi-analytical framework combining an analytical approach with a FE model (assuming negligible shear stress).

The contact occurring during the deep drawing process is modeled here using an analytical approach inducing consequently no numerical instabilities. Up to 200 integrations points are considered. In this configuration, the impact the numerical noise on the springback shape parameters is drastically reduced.

We have trained the PCE model on the B-U-T physics-based surrogate in order to perform a variability study of the springback shape parameters. The coefficients of the PCE are computed using a regression based approach from a Design of Experiment (DoE) defined by a standard Latin-Hypercube Sampling. We propose a stochastic model representing up to 8 independent random variables for the springback shape parameter study.

A well known limitation of the PCE lies in the computational cost to compute the full set of coefficients when the number of variables or the degree increases. We here choose to apply the Least Angle Regression Stagewise (LARS) method [BS08c] on an 7^{th} order PCE and the empirical error estimate as the stopping criterion.

The savings in computational cost is significant since in each case only a fourth of the coefficients are needed to reach the convergence on each of the function representative of the springback shape with a preserved accuracy.

This approach demonstrates that the use of simplified physics-based model allows for accurate UQ and acceptable computational costs.This approach is not limited to 2D and opens the way to the use of other types of physics-based metamodels such as one-step or PGD/POD.

1.3.2 Adapting the sampling to the model resolution: Fat-Latin Hypercube sampling

To train the stochastic metamodel, a compromise has to be found in the distribution and the size of the set of training points. In fact, a too small number of simulations leads to an excessive smoothing of the response surface while a too high number of simulations may introduce numerical noise leading by the way to the same lack of accuracy of the stochastic metamodel.

In **Chapter 3**, the compromise is addressed. A modified LHS scheme is proposed in order to take into account the resolution of the model. It provides an upper bound on the sampling density. A coherent metamodel scheme based on the PCE is built taking into account this upper bound on sampling density, and the lower bound given by the regression approach to compute the PCE coefficients.

The main idea is to build around each sampling point a restricted area free from other samples while preserving the LHS property. The characteristic size of each area is parameterized by the *a priori* identified model resolution δ_i^*, $\{i = 1, \ldots, M\}$ in each of the M dimensions.

Depending on the chosen norm, different shapes of the restricted area are considered. Here, an illustration is given for the $\mathcal{L}_\infty$ and the $\mathcal{L}_2$ norms.

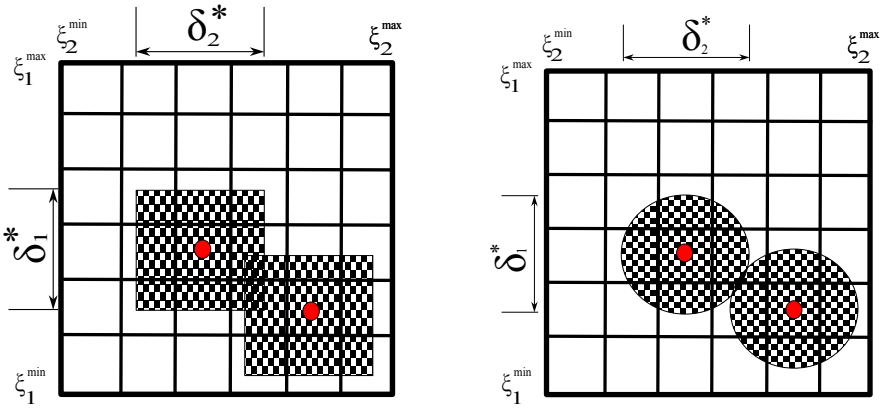

(a) Fat-LHS$^{\mathcal{L}_\infty}$ (b) Fat-LHS$^{\mathcal{L}_2}$

Figure 1.7: Sensitivity restricted area shape around two sampling points for $\mathcal{L}_\infty$ and $\mathcal{L}_2$ in 2D

The "Fat-LHS" scheme provides a dense sampling along with a maximum number S_{ub} of samples respecting the model resolution. With this limited number of samplings, we train a sparse version of PCE where only the most significant terms are kept.

The efficiency of the Fat-LHS is illustrated on the variability assessment of springback of a 2D deep drawn metal sheet. It exhibits a higher convergence rate to the two first statistical moments than a similar size LHS (without taking into account the model resolution). On a higher dimension test case (8D), the convergence results for the different truncation strategies are compared. The sampling is then coupled with an adapted metamodel strategy in order to efficiently propagate the uncertainties at low computational costs.

1.3.3 Towards Multi-objective Optimization Under Uncertainty

In this section, we address the incorporation of uncertainty treatment into a multi-objective optimization process using surrogate-models in a non-intrusive framework. After a brief recall on the basics of the multi-objective optimization under uncertainty, we present the following original contributions:

- the development of a non-intrusive hierarchical stochastic metamodels based on Moving-Least Squares (MLS) and PCE;
- its application to multi-objective reliability based optimization of space truss structures.

Evolutionary population-based algorithms are designed to efficiently address multi-objective optimization problems these optimization problems due to their ability to possibly provide many of the Pareto-optimal solutions in a single algorithm iteration [Fog97, And02]. We use Non Sorted Genetic Algorithm II [Deb02] for 3 reasons: low computational complexity, elitist approach and ability to preserve diversity in the population.

$\boldsymbol{\xi} = [\xi_1, \ldots, \xi_M]$ are the M independent *stochastic* variables described by their probability density function. $\boldsymbol{x}$ represent the set *deterministic* design variables. $\boldsymbol{y}(\boldsymbol{x}, \boldsymbol{\xi}) = [y_1(\boldsymbol{x}, \boldsymbol{\xi}), \ldots, y_m(\boldsymbol{x}, \boldsymbol{\xi})]$ is the vector of the m *stochastic* objective functions

Instead of comparing each objective function separately, one may take into account of the intrinsic multi-objective nature of the problem by checking the probabilistic non-dominance ([Tei01]) $P_{\text{non-dominance}} \equiv P[\boldsymbol{y}(\boldsymbol{x},\boldsymbol{\xi}) \succ \boldsymbol{\zeta}] \geq \alpha$ assessing that the vector of the objective functions $\boldsymbol{y}(\boldsymbol{x},\boldsymbol{\xi}) = [y_1(\boldsymbol{x},\boldsymbol{\xi}), y_2(\boldsymbol{x},\boldsymbol{\xi})]$ should dominate the set of quantiles $\boldsymbol{\zeta}$ with a minimum probability level (user defined) α while satisfying constraints (such as reliability for example). The Fig.1.8 illustrates Pareto fronts for two different values of α. The best performing solutions are obtained for a minimization of the functions y_1 and y_2. When the values of α increases, the stochastic Pareto front represented by the non dominated quantiles ζ moves farther from the deterministic one being more and more *conservative*.

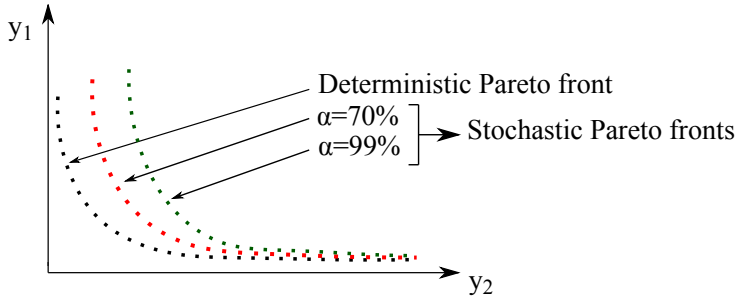

Figure 1.8: Stochastic Pareto fronts

The proposed formulation is implemented into the Non Sorted Genetic Algorithm II [Deb02] without any modification.

The challenge consists in the computation of the non-dominance probability for each set of solution produced by the algorithm. A straightforward approach would consist in building a polynomial chaos expansion of each provided solution. The statistical quantities and non-dominance probability needed are then computed exclusively using this approximation.

We propose a hierarchical metamodeling approach. It consists in a surrogate model providing an original mapping from the mixed deterministic-stochastic variable space to the response function space. The first step consists in building a metamodel of the PCE coefficients:

$$x \mapsto \tilde{\gamma}_i(x), \qquad i = 0, \ldots, P-1 \tag{1.5}$$

and then to reconstruct the PCE for each design variable provided by the algorithm:

$$(x,\xi) \mapsto y(x,\xi) = \sum_{i=0}^{P-1} \tilde{\gamma}_i(x)\Psi_i(\xi) \tag{1.6}$$

resulting in an increased computational efficiency.

We validate the proposed approach by comparing the obtained stochastic Pareto set with a Monte Carlo sampling under different probability levels. An explicit two-variable test case allows to analytically compute the response surface and to compare it with those obtained by an MLS approximation of the PCE coefficients. A perfect agreement is observed. A second test case deals with the multi-objective sizing optimization of three 3D linear elastic truss structures. In most of the situations the combination of second order MLS interpolation of the PCE coefficients provides the best results. The influence of the

PCE order is investigated. In most of the cases the second order approximation is better, highlighting a possible overfiting phenomenon when the approximation order increases or a sampling size is too small. Finally, the sizing optimization of trusses is verified using Monte Carlo Simulations.

1.4 Thesis outline

The original contributions of this thesis are organized in the following manner:

- **Chapter 2** presents a literature review with a special insight firstly on general UQ methodologies and then a focus on the spectral methods for uncertainty propagation. For the latter approach the numerous challenges are put into evidence as well as the concepts proposed in the literature.

- **Chapters 3, 4 and 5** refer either to our published articles (**Chapter 4**, **Chapter 5**) or to papers under review (**Chapter 3**). **Chapter 3** and **Chapter 4** rise the question of the trust to give to the nominal model in the context of uncertainty propagation for variability study. Answers are proposed in the field of metal forming where highly non linear phenomena such as material non linearities, contact friction, springback, ... occur, and which makes in practice the stability of the numerical model difficult to control. In fact, when considering the springback prediciton of the 2D U-shaped deep drawn metal sheet, a large variety of results is observed [MNOW93] when modifying the experiment parameters or when changing the software used to predict the springback values. However the stochastic analysis of metal forming processes requires both a high precision and low cost numerical models in order to take into account very small perturbations on inputs (physical as well as process parameters) and to allow for numerous repeated analysis in a reasonable time. **Chapter 3** addresses this issue by presenting an original two-pronged approach based on the combination of a semi-analytical model dedicated to plain strain deep drawing based on a Bending-Under-Tension numerical model (B-U-T model) to accurately predict the influence of small random perturbations around a nominal solution estimated with a full scale Finite Element Model (FEM). A custom sparse variant of the Polynomial Chaos Expansion (PCE) is used to model the propagation of uncertainties through this model at low computational cost. In **Chapter 4**, a particular attention is given to the definition of an adapted Design of Experiment (DoE) taking the model sensitivity into account which limits the number of sampling points. The construction of an adaptive sparse PCE based on the limited set of data is investigated.

  Chapter 5 proposes a metamodel based Multi-Objective Optimization under uncertainty based on a hierarchical metamodel approach with respect to the deterministic and random input parameters.

- Finally, **Chapter 6** gives the general conclusions and discussions/perspectives of the presented work.

Bibliography

[AL01] N M Alexandrov and R M Lewis. An overview of first-order model management for engineering optimization. *Optimization and Engineering*, 2(4):413–430, 2001.

[ALG+99] N M Alexandrov, R M Lewis, C R Gumbert, L L Green, and P A Newman. Optimization with variable-fidelity models applied to wing design. Technical report, DTIC Document, 1999.

[ALG+01] N M Alexandrov, R M Lewis, C R Gumbert, L L Green, and P A Newman. Approximation and model management in aerodynamic optimization with variable-fidelity models. *Journal of Aircraft*, 38(6):1093–1101, 2001.

[And02] O Andrzej. *Evolutionnary algorithms for Single and Multicriteria Design Optimisation*. Physica Verlag, 2002.

[B+00] M.D Buhmann et al. Radial basis functions. *Acta numerica*, 9(1):1–38, 2000.

[BBM+00] M.H Bakr, J W Bandler, K Madsen, J E Rayas-Sanchez, and J Sondergaard. Space-mapping optimization of microwave circuits exploiting surrogate models. *Microwave Theory and Techniques, IEEE Transactions on*, 48(12):2297–2306, 2000.

[BS08] G Blatman and B Sudret. Sparse polynomial chaos expansions and adaptive stochastic finite elements using a regression approach. *Comptes Rendus Mécanique*, 336(6):518–523, 2008.

[Car09] J Carbonniere. *Contribution à l'analyse du retour élastique en emboutissage*. PhD thesis, Institut National des Sciences Appliquées de Lyon, 2009.

[Cre90] N Cressie. The origins of kriging. *Mathematical Geology*, 22(3):239–252, 1990.

[Deb02] K Deb. A fast and elitist multiobjective genetic algorithm: Nsga ii. *IEEE Transactions on Evolutionary Computation*, 6(2), 2002.

[DG05] K Deb and H Gupta. Searching for robust pareto-optimal solutions in multi-objective optimization. In Carlos A. Coello Coello, Arturo Hernández Aguirre, and Eckart Zitzler, editors, *Evolutionary Multi-Criterion Optimization*, volume 3410 of *Lecture Notes in Computer Science*, pages 150–164. Springer Berlin / Heidelberg, 2005.

[DSB11] V Dubourg, B Sudret, and J-M Bourinet. Reliability-based design optimization using kriging surrogates and subset simulation. *Structural and Multidisciplinary Optimization*, 44(5):673–690, 2011.

[dSR08] T de Souza and B Rolfe. Multivariate modelling of variability in sheet metal forming. *Journal of Material Processing Technology*, 203:1–12, 2008.

[EGC+04] MS Eldred, AA Giunta, SS Collis, NA Alexandrov, and RM Lewis. Second-order corrections for surrogate-based optimization with model hierarchies. In *Proceedings of the 10th AIAA/ISSMO Multidisciplinary Analysis and Optimization Conference, Albany, NY,, Aug*, 2004.

[EGWJT02] M S Eldred, A A Giunta, S F Wojtkiewicz Jr, and T G Trucano. Formulations for surrogate-based optimization under uncertainty. In *Proc. 9th AIAA/ISSMO Symposium on Multidisciplinary Analysis and Optimization, number AIAA-2002-5585, Atlanta, GA*, volume 189, page 346, 2002.

[Fog97] D B Fogel. The advantages of evolutionary computation. *Bio Computing and emerging computation*, 1997.

[Gha91] R Ghanem. *Stochastic finite Elements: A spectral approach*. Springer, 1991.

[HD03] J C Helton and F J Davis. Latin hypercube sampling and the propagation of uncertainty in analyses of complex systems. *Reliability Engineering & System Safety*, 81(1):23–69, 2003.

[HGB07] B Sendhoff H-G Beyer. Robust optimization – a comprehensive survey. *Computer Methods in Applied Mechanics and Engineering*, 196:3190–3218, 2007.

[HJOS10] Jon C Helton, Jay D Johnson, William L Oberkampf, and Cédric J Sallaberry. Representation of analysis results involving aleatory and epistemic uncertainty. *International Journal of General Systems*, 39(6):605–646, 2010.

[LCM09] M Lemaire, A Chateauneuf, and J-C Mitteau. *Structural Reliability*. Wiley/ISTE,, 2009.

[LQBRJ12] G Le Quilliec, P Breitkopf, J-M Roelandt, and P Juillard. Semi-analytical approach for plane strain sheet metal forming using a bending-under-tension numerical model. *International Journal of Material Forming*, (DOI 10.1007/s12289-012-1122-7), 2012.

[LS81] P Lancaster and K Salkaukas. Surfaces generated by moving least squares methods. *Mathematics of Computation*, 37(155):141–158, 1981.

[MAC09] R H Myers and C M Anderson-Cook. *Response surface methodology: process and product optimization using designed experiments*, volume 705. Wiley. com, 2009.

[MNOW93] A Makinouchi, E Nakamachi, E Onate, and R H Wagoner, editors. *Numisheet'93 2nd International Conference, Numerical Simulatoin of 3-D Sheet Metal Forming Process - Verification of Simulation with Experiment*. Riken Tokyo, 1993.

[NE12] LWT Ng and MS Eldred. Multifidelity uncertainty quantification using nonintrusive polynomial chaos and stochastic collocation. In *Proceedings of the 14th AIAA Non-Deterministic Approaches Conference, number AIAA-2012-1852, Honolulu, HI*, volume 43, 2012.

[NTV92] B Nayroles, G Touzot, and P Villon. Generalizing the finite element method: Diffuse approximation and diffuse elements. *Computational Mechanics*, 10:307–318, 1992.

[OTH04] W L Oberkampf, T G Trucano, and C Hirsch. Verification, validation, and predictive capability in computational engineering and physics. *Applied Mechanics Reviews*, 57(5):345–384, 2004.

[RFC10] Ph. Bouillard R. Filomeno Coelho. Multiobjective reliability-based optimization with stochastic metamodels. *Evolutionary Computation*, 2010.

[SAA+10] A Saltelli, P Annoni, I Azzini, F Campolongo, M Ratto, and S Tarantola. Variance based sensitivity analysis of model output. design and estimator for the total sensitivity index. *Computer Physics Communications*, 181(2):259–270, 2010.

[SLZ+11] G Sun, G Li, S Zhou, W Xu, X Yang, and Q Li. Multi-fidelity optimization for sheet metal forming process. *Structural and Multidisciplinary Optimization*, 44(1):111–124, 2011.

[Ste99] M L Stein. *Interpolation of spatial data: some theory for kriging*. Springer, 1999.

[SW10] S Shan and G G Wang. Survey of modeling and optimization strategies to solve high-dimensional design problems with computationally-expensive black-box functions. *Structural and Multidisciplinary Optimization*, 41(2):219–241, 2010.

[Tei01] J Teich. Pareto-front exploration with uncertain objectives. In Springer-Verlag, editor, *Evolutionary Multi-Criterion Optimization, First International Conference (EMO 2001)*, volume 1993, pages 314–328, 2001.

[VHS02] R Vitali, R T Haftka, and B V Sankar. Multi-fidelity design of stiffened composite panel with a crack. *Structural and Multidisciplinary Optimization*, 23(5):347–356, 2002.

[WCS+13] J Winokur, P Conrad, I Sraj, O Knio, A Srinivasan, W C Thacker, Y Marzouk, and M Iskandarani. A priori testing of sparse adaptive polynomial chaos expansions using an ocean general circulation model database. *Computational Geosciences*, pages 1–13, 2013.

[WG95] L Wang and R V. Grandhi. Improved two-point function approximations for design optimization. *AIAA Journal*, 33(9):1720–1727, 2013/05/07 1995.

[WS07] G Gary Wang and S Shan. Review of metamodeling techniques in support of engineering design optimization. *Journal of Mechanical Design*, 129:370, 2007.

[YCL+11] W Yao, Chen, W Luo, M van Tooren, and J Guo. Review of uncertainty-based multidisciplinary design optimization methods for aerospace vehicles. *Progress in Aerospace Sciences*, 47(6):450–479, 2011.

Chapter 2

Non-intrusive Polynomial Chaos Expansion for uncertainty quantification

2.1 Introduction and general concepts

In the past decades a copious amount of work has been devoted to the characterization of the impact of uncertainties on the behavior of a mechanical system described by numerical models. A first step in their quantification may consists in the categorization of the uncertainties. This topic is subjected to many discussions by statisticians and engineers, but two concepts are clearly distinguished and commonly admitted : *epistemic* uncertainties are reducible uncertainties by means of gathering more data or by refining the model; on the opposite, *random* or *aleatory* uncertainties are irreducible uncertainties, intrinsic to the components or to the environment of the real experiment. However, the classification of uncertainties into one of these two categories may depend on the context of the study but is of paramount importance. [KD09] highlights that a correct a priori identification of the types of uncertainties allows to identify (hence to elaborate) reasonable strategies in order to a priori reduce the uncertainties at the end of the line: a wrong categorization may influence the results from several orders of magnitude.

To quantitatively assess their influence, one may classify the methodologies into two groups: *intrusive* and *non-intrusive* methodologies. The formers require mathematical developments of the governing equations to produce, most of the time, semi-analytical solutions for the stochastic analysis. This class of methods present a major drawback: their implementation tends to become complex and analytically cumbersome in case of highly non linear physical systems. One may then prefer the use non-intrusive techniques which consider the numerical simulation process as a *black-box*. This section only deals with the latter class of methodologies described on a probabilistic framework.

First and foremost, a brief recall on the probabilistic description of uncertainties is provided together with a classification and a short review of the non-intrusive approaches for UQ. It essentially aims at pointing out the notations and to provide the reader with an overview of non intrusive UQ.

The second section forms the heart of this chapter. It is dedicated to the class of spectral methodologies taking their roots in functional evaluation of the stochastic data of interest. A special focus is provided on the use of the Polynomial Chaos Expansion (PCE) in a non-intrusive context. Since the groundbreaking work of [Gha91], this methodology has encountered a growing interest and has been used in many different fields. This section highlights the evolution of the Polynomial Chaos Expansion from its initial formulation as Hermite-Homogeneous Polynomial Chaos to the most recent advances. The goal of this section is not to systematically provide a deep insight into each theoretical advances but more to guide the interesting reader by providing him in an organized manner some fundamental references to the field.

2.1.1 Mathematical framework

2.1.1.1 Probabilistic space

The observation of a random phenomenon provides uncertain outcomes which nevertheless may follow a regular distribution for a large number of trials. The set of all possible outcomes, denoted Ω is called the "elementary sample space". The result of one trial, is a subset $\omega \in \Omega$ called "elementary event". The set of all admissible events associated to aprobability measure $p_{\mathcal{F}}$ forms a σ-algebra associated with Ω denoted by $\mathcal{F}$. Finally, the triplet $(\Omega, \mathcal{F}, p_{\mathcal{F}})$ forms the "probability space".

2.1.1.2 Random variable, Stochastic process, Random field

Random Variable A random variable ξ is a measurable function defined on the σ-algebra $\mathcal{F}$ with values in a Borel set $\mathcal{B}(\mathbb{R})$

$$\begin{aligned} \xi : \mathcal{F} &\to \mathcal{B}(\mathbb{R}) \\ \omega &\mapsto \xi(\omega). \end{aligned} \tag{2.1}$$

In this thesis we assume that the uncertainties can be modeled using a finite number random variables gathered into a M-sized random vector $\boldsymbol{\xi} = \{\xi_1, \dots, \xi_M\}$. We thus define the random vector $\boldsymbol{\xi}$ as a measurable function defined on the σ-algebra $\mathcal{F}$ with values in a Borel set of $\mathbb{R}^M$ denoted $\mathcal{B}(\mathbb{R}^M)$.

$$\begin{aligned} \xi : \mathcal{F} &\to \mathcal{B}(\mathbb{R}^M) \\ \omega &\mapsto \boldsymbol{\xi}(\omega). \end{aligned} \tag{2.2}$$

The dimensions of the random vector $\boldsymbol{\xi}$ are denoted using subscript, while their realizations are denoted by superscripts: $\xi_i^{(j)}$ denotes the j^{th} realization of the i^{th} component of the random vector $\boldsymbol{\xi} = \{\xi_1, \dots, \xi_M\}$.

Let ξ be any of the components of $\boldsymbol{\xi}$ and τ one realization of ξ. In this thesis work, we consider that $\boldsymbol{\xi}$ is completely characterized by a *continuous* probability density function (pdf) $p_\xi(\xi)$ whose integral over the sample space $\mathbb{R}$ is called the cumulative probability density function (cdf). The mean value of the random variable ξ is given by:

$$\mu = E[\xi] = \int_{\mathbb{R}} \tau \mathrm{d}p_\xi(\tau) \tag{2.3}$$

where $\{\xi = \tau\} = \{\omega \in \Omega | \xi(\omega) = \{\tau\}\}$ and $\mathrm{d}p(\xi = \tau) = p_\xi(\tau) = p_{\mathcal{F}}(\{\xi = \tau\})$.

The variance V of the random variable is given by:

$$V = \int_{\mathbb{R}} (\tau - \mu)^2 \mathrm{d}p_\xi(\tau) \tag{2.4}$$

The n-th order moment is given by

$$E[\xi^n] = \int_{\mathbb{R}} \tau^n \mathrm{d}p_\xi(\tau) \tag{2.5}$$

In this thesis work, we only consider real random variables with finite second order moment ($E[\xi^2] < \infty$). We denote the corresponding vectorial space by $\mathcal{L}^2(\mathcal{B}(\mathbb{R}), \mathcal{T}, P_\xi)$.

Considering now two random variables $\boldsymbol{\xi} = \{\xi_1, \xi_2\}$, the joint probability density function is naturally denoted p_{ξ_1,ξ_2} or more concisely $p_{\boldsymbol{\xi}}$. The covariance between these two random variables is denoted

$$C(\boldsymbol{\xi}) = E\left[(\xi_1 - \mu_{\xi_1}) \times (\xi_2 - \mu_{\xi_2})\right]. \tag{2.6}$$

The correlation factor ρ_{ξ_1,ξ_2} is given by:

$$\rho_{\xi_1,\xi_2} = \frac{C(\boldsymbol{\xi})}{\sigma_{\xi_1}\sigma_{\xi_2}}. \tag{2.7}$$

A random field A random field $y(\boldsymbol{x},\omega)$ [Adl81] may be defined as a collection of random variables indexed by a continuous parameter $\boldsymbol{x}$ defined on a bounded set $\mathcal{D} \in \mathbb{R}^d$ with value in $\mathbb{R}$ (Eq. 2.8). A one-dimensional random field ($\mathcal{D} \in \mathbb{R}$) is usually called a stochastic process.

$$\begin{aligned} y :&\mathbb{R}^d \times \Omega \to \mathbb{R} \\ &(\boldsymbol{x},\omega) \mapsto y(\boldsymbol{x},\omega). \end{aligned} \tag{2.8}$$

For a chosen $\boldsymbol{x}_0 \in \mathcal{D}$, $y(\boldsymbol{x}_0,.)$ is a random variable. One denotes by $\boldsymbol{y}(\boldsymbol{x}_0) = \{y(\boldsymbol{x}_0,\omega_1),\dots,y(\boldsymbol{x}_0,\omega_S)\}$ the set of S realizations of the random field. Its mean is then defined as:

$$\mu(\boldsymbol{x}_0) = \int_\Omega y(\boldsymbol{x}_0,\omega)\mathrm{d}p_y(\boldsymbol{x}_0,\omega) \tag{2.9}$$

The continuity of a random field is often characterized by its *mean-square* continuity:

$$\begin{aligned} &E[\|\boldsymbol{y}(\boldsymbol{x},.)\|^2] < \infty, \forall \boldsymbol{x} \in \mathcal{D} \\ &\lim_{x\to x_0} E[\|\boldsymbol{y}(\boldsymbol{x},.) - \boldsymbol{y}(\boldsymbol{x_0},.)\|^2] = 0 \end{aligned} \tag{2.10}$$

The matrix-valued covariance function of the random field taken as the covariance function between two distinct $\boldsymbol{x}_1, \boldsymbol{x}_2$:

$$C(\boldsymbol{x}_1,\boldsymbol{x}_2) = E\left[(y(\boldsymbol{x}_1,.) - \mu(\boldsymbol{x}_1)) \times (y(\boldsymbol{x}_2,.) - \mu(\boldsymbol{x}_2))\right] \tag{2.11}$$

The correlation factor ρ_{ξ_1,ξ_2} is given by:

$$\rho_{y(\boldsymbol{x}_1,.),y(\boldsymbol{x}_2,.)} = \frac{C(\boldsymbol{x}_1,\boldsymbol{x}_2)}{\sigma_{y(\boldsymbol{x}_1,.)}\sigma_{y(\boldsymbol{x}_1,.)}} \tag{2.12}$$

2.1.2 Common concepts for probabilistic approaches

Building a stochastic model usually consists in two steps. The first one is concerned with the proper identification of the random inputs by a finite number M of random variables (such as parameters of the system, material properties, etc.) or processes (random time dependent loading,etc.) [Fra65]. For Gaussian random variables and processes, the identification is straightforward as they are completely determined by the two first statistical moments (mean and covariance). This is however not the case in general for non Gaussian processes and their identification still remains an open research area [YS88, WC94, SG02a, PPS02, LCS07]

The second one consists in identifying the (joint) probability distribution of the random variables, fields of interest. Two approaches may be distinguished:

- *A direct approach* consists in directly constructing the probability function p_ξ based on information theory (i.e using only the information at hand on ξ).
- *An indirect approach* consists in introducing a measurable mapping h between the random vector $y(\xi)$ of unknown probability density function (p.d.f) p_y to the random vector ξ whose p.d.f p_ξ is known: $y(\xi) = h(\xi)$. Then, $p_y(y)$ is the transformation of $p_\xi(\xi)$ by h. This method is advantageous

when experiments are available. It also allows to develop non-intrusive approaches by defining the mapping function h independently from the physical model.

2.1.2.1 An overview of direct approaches

Maximum Entropy Principle The Maximum Entropy Principle [Jay82, Gif08] is based on the definition of a unique measure which quantifies the amount of uncertainties represented by a discrete probability density function, namely the *entropy measure*. It follows the natural intuition that a "broad" probability distribution represents more uncertainty than a "sharp" one. Let ξ be any component of the random vector $\boldsymbol{\xi} = \{\xi_1, \ldots, \xi_M\}$. Let us assume now that ξ has been evaluated in S samples denoted $\xi^{(1)}, \ldots, \xi^{(S)}$ each sample associated with the probability $p_\xi(\xi^{(i)})$, $i = 1, \ldots, S$ such as $\sum_{i=1}^{S} p_\xi(\xi^{(i)}) = 1$. The entropy measure is given by:

$$T(p_\xi(\xi^{(1)}, \ldots, \xi^{(S)})) = -K \sum_{i}^{S} p_\xi(\xi^{(i)}) \ln(p_\xi(\xi^{(i)})) \tag{2.13}$$

where K is a positive constant. To solve the inference problem stated in the direct approach, the only possible unbiased assignment consists in searching the probability distribution which maximizes the entropy with regards to the information at hand. The classical optimization problem to solve may then be stated as:

$$\begin{array}{rl} \max\limits_{p_\xi} & T(p_\xi(\xi^{(1)}, \ldots, \xi^{(S)})) \\ s.t & E[y(\xi)] = \sum_{i=1}^{S} y(\xi^{(i)}) \\ & \sum_{i=1}^{S} p_\xi(\xi^{(i)}) = 1. \end{array} \tag{2.14}$$

The use of Lagrange multipliers λ_0 and λ_1 leads to the following optimal solution:

$$p_\xi(\xi) = e^{-\lambda_0 - \lambda_1 \xi} \tag{2.15}$$

In the multi-variate case where $\boldsymbol{\xi} = \{\xi_1, \ldots, \xi_M\}$ the maximum entropy probability distribution generalizes to [Jay57]:

$$p_{\boldsymbol{\xi}}(\boldsymbol{\xi}) = \sum_{i=1}^{n} \exp(-[\lambda_0 + \lambda_1 \xi_1^{(i)} + \ldots + \lambda_M \xi_M^{(i)}) \tag{2.16}$$

The set of Lagrangian coefficients, may be retrieved by solving the set of equation obtained by replacing the expression of $p_\xi(\xi)$ in the expressed constraints.

Maximum likelihood Let us consider the following problem (also referred as "forward problem") [Mil11]

$$\boldsymbol{y} \approx \boldsymbol{f}(\boldsymbol{\xi}) + \boldsymbol{\epsilon} \tag{2.17}$$

where $\boldsymbol{\xi} = \{\xi_1, \ldots, \xi_M\}$ represents here a vector of model parameters, $\boldsymbol{y} = \{y_1, \ldots, y_r\}$ is a vector of output of interests seen as realizations of random variables, f is a (non-linear) function $\mathbb{R}^M \to \mathbb{R}^r$ and $\boldsymbol{\epsilon} \in \mathbb{R}^r$ a random vector encompassing all possible kind of uncertainties.

Let us assume that a set of observed output is available. The goal of Maximum Likelihood estimation is to retrieve the input parameters which has most likely generated the observed sample. To do so, one has to maximize the following probability $p_{\boldsymbol{\xi}}(\boldsymbol{y}|\boldsymbol{\xi})$, which is called the *Likelihood*.

A trivial (and common) assumption consists in assuming that the random vector $\boldsymbol{\epsilon} \in \mathbb{R}^r$ representing the components of the error produced are independent and identically distributed characterized by a normal probability density function ($E[\epsilon_i] = 0, i = 1, \ldots, r$, the covariance matrix of the error is $\boldsymbol{C} = \sigma^2 \boldsymbol{I}_{r\times r}$ where $\boldsymbol{I}_{r\times r}$ is the $r \times r$ identity matrix). In this case $p_{\boldsymbol{\xi}}(\boldsymbol{y}|\boldsymbol{\xi}) \in \mathcal{N}(\boldsymbol{f}(\boldsymbol{\xi}))$ and the likelihood function becomes

$$\begin{aligned}
\mathcal{L}(\boldsymbol{\xi}) &= \prod_{i=1}^{r} p_{\epsilon_i}(\epsilon_i)) \\
\mathcal{L}(\boldsymbol{\xi}) &= \prod_{i=1}^{r} p_{\epsilon_i}(y_i - f_i(\boldsymbol{\xi})) \\
&= \prod_{i=1}^{r} \exp\left(-\frac{(y_i - f_i(\boldsymbol{\xi}))^2}{2\sigma^2}\right) \\
&= \exp\left(-\sum_{i=1}^{r} \frac{(y_i - f_i(\boldsymbol{\xi}))^2}{2\sigma^2}\right)
\end{aligned} \tag{2.18}$$

Searching for the maximum of this function is equivalent to finding the minimum of $\sum_{i=1}^{r}(y_i - f_i(\boldsymbol{\xi}))^2$ which may be done by any appropriate optimization algorithm or by considering a classical minimum distance leasts square problem. In the general case $\boldsymbol{\epsilon}$ is not supposed to be Gaussian, the Likelihood function may be computed using Monte Carlo Simulations which may be too expensive. Another more efficient consists in using a kernel approximation method.

Bayesian Inference This approach allows to determine the *prior* probability distribution of input parameters $\boldsymbol{\xi} = \{\xi_1, \ldots, \xi_M\}$ when the only information at hand concerns the output of the model $\boldsymbol{y} = \{y_1(\boldsymbol{\xi}), \ldots, y_J(\boldsymbol{\xi})\}$. This process is called inference. In the context of the Bayes' framework, the knowledge about the true values of the parameters before and after having observed the data are described using probability. In the general case one may use inference only in order to refine the probability distribution of the input knowing the outputs, but we present here this approach in the general case where the whole probability density function of the input parameters are searched.

The Bayes' theorem states that:

$$p(\boldsymbol{\xi}|\boldsymbol{y}) = \frac{p(\boldsymbol{y}|\boldsymbol{\xi})p_{\boldsymbol{\xi}}(\boldsymbol{\xi})}{\int p(\boldsymbol{y}|\boldsymbol{\xi})p_{\boldsymbol{\xi}}(\boldsymbol{\xi})d\boldsymbol{\xi}} \tag{2.19}$$

where $p(\boldsymbol{\xi}|\boldsymbol{y})$ is the *posterior* distribution of the parameters values (obtained after having observed the data), $p(\boldsymbol{y}|\boldsymbol{\xi}) = \mathcal{L}(\boldsymbol{\xi})$ is the likelihood function and $p_{\boldsymbol{\xi}}(\boldsymbol{\xi})$ is the *prior* probability density function (obtained before having observed the data) of the parameters values and $\int p(\boldsymbol{y}|\boldsymbol{\xi})p_{\boldsymbol{\xi}}(\boldsymbol{\xi})d\boldsymbol{\xi}$ is a constant (as $p(\boldsymbol{\xi}|\boldsymbol{y})$ is a distribution on $\boldsymbol{\xi}$, $\boldsymbol{y}$ is a constant)

Thus a more concise form of the Bayes theorem may be obtained by:

$$p(\boldsymbol{\xi}|\boldsymbol{y}) \propto (\boldsymbol{y}|\boldsymbol{\xi})p_{\boldsymbol{\xi}}(\boldsymbol{\xi}) \tag{2.20}$$

In the general case, the described inference process consists in refining an *a priori* given set of probabilities (*prior* models) in the light of the observed outputs.

In the case where the input probabilities are unknown, the Bayes' inference approach methodology may often be used in conjunction with the Maximum Entropy Principle. In general, the Bayes theorem offers a robust mean for inference, however vague prior information on the parameter value the posterior remains improper, which may cause serious problems for the verification of complex models [Gey92]. However, if a sufficient amount of information on the prior is available, the Bayes' inference has been successfully use in the literature to assess the confidence in model prediction by comparing the model output with experimental data.

A first direct approach in order to compute the posterior distribution consists in using Monte Carlo Sampling on the prior distribution. The sample produced is thus non optimal with regards to the posterior distribution (many sample points may located in the tail of the posterior probability) and thus the chosen set of parameters with higher posterior probability may not be relevant. The use of Markov Chain Monte Carlo (MCMC) [Ahm08] based on the Metropolis-Hasting's algorithm [CG95] may allow to increase the computational efficiency. MCMC are used to directly sampling the posterior distribution, to build an optimal sample with regards to the posterior distribution. Moreover, it eliminates the need of computing the constant $\int p(\boldsymbol{y}|\boldsymbol{\xi})p_{\boldsymbol{\xi}}(\boldsymbol{\xi})d\boldsymbol{\xi}$.

2.1.2.2 A classification of indirect approaches

Simulation based methodology Monte Carlo Samplings (MCS) is the most direct approach for uncertainty quantification. In the literature, the Monte Carlo simulation is widely used in order to assess the two first statistical moment of a *multi-dimensional* random variable. These quantities are extracted from S independent realizations of random inputs. These are generated from their *a priori* prescribed probability density function. For each realization, the data are fixed and the problem becomes deterministic: the is obtained from a set of deterministic calls to the considered model. From this set of deterministic evaluations, statistical information are extracted (mean, variance, histograms). MCS is then straightforward to apply but a large number of realizations are needed e.g. the mean value typically converges in $1/\sqrt{S}$. Slow convergence rates may incur excessive computational costs, specially when one deterministic simulation is already computationally costly. To accelerate this computational cost, different techniques have been developed in the literature. Among them, Quasi Monte Carlo Simulation, Stratified Sampling and the Latin Hypercube Sampling.

Moment equations In this approach, the objective functional is replaced by its Taylor series expansion around the mean value (of the input random variable). The mean and the variance of the output function of interest are computed using the moments of the input variables. This leads to a more efficient integration of the first and second order moment. The proof is done below only for the 2 first statistical moments using a first order (y_{FO}) and a second order (y_{SO}) Taylor series expansion of the output function. Let y the output function of interest where $\boldsymbol{\xi} = \{\xi_1, \ldots, \xi_M\}$ with mean $\bar{\boldsymbol{\xi}} = \{\bar{\xi}_1, \ldots, \bar{\xi}_M\}$ and let us define its first and second order Taylor series approximation by y_{FO} and by y_{SO} [PNTIG01, MD10]. It is respectively assumed that $y \in \mathcal{C}^1$ and $y \in \mathcal{C}^2$.

$$y_{\mathrm{FO}}(\boldsymbol{\xi}) = y(\bar{\boldsymbol{\xi}}) + \sum_{i=1}^{M} \frac{\partial y}{\partial \xi_i}(\xi_i - \bar{\xi}_i) \tag{2.21}$$

$$y_{\mathrm{SO}}(\boldsymbol{\xi}) = y(\bar{\boldsymbol{\xi}}) + \sum_{i=1}^{M} \frac{\partial y}{\partial \xi_i}(\xi_i - \bar{\xi}_i) + \frac{1}{2!}\sum_{j=1}^{M}\sum_{i=1}^{M} \frac{\partial^2 y}{\partial \xi_i \partial \xi_j}(\xi_i - \bar{\xi}_i)(\xi_j - \bar{\xi}_j). \tag{2.22}$$

After some algebra, the expected value from the mean (unbiased) and from the variance of the output y are approximated by:

$$\bar{y}_{\mathrm{FO}} = y_{\mathrm{FO}}(\bar{\boldsymbol{\xi}}) \tag{2.23}$$

$$\sigma^2(y_{\mathrm{FO}}) = \sum_{i=1}^{M} \left(\frac{\partial y_{\mathrm{FO}}}{\partial \xi_i}\sigma(\xi_i) \right)^2 \tag{2.24}$$

and by

$$\bar{y}_{\mathrm{SO}} = y_{\mathrm{SO}}(\bar{\boldsymbol{\xi}}) + \frac{1}{2!}\sum_{j=1}^{M}\sum_{i=1}^{M} \frac{\partial^2 y}{\partial \xi_i \partial \xi_j}\sigma(\xi_i)\sigma(\xi_j) \tag{2.25}$$

$$\sigma^2(y_{\mathrm{SO}}) = \sum_{i=1}^{M} \left(\frac{\partial y_{\mathrm{SO}}}{\partial \xi_i}\sigma(\xi_i) \right)^2 + \frac{1}{2!}\sum_{j=1}^{M}\sum_{i=1}^{M} \left(\frac{\partial^2 y}{\partial \xi_i \partial \xi_j}\sigma(\xi_i)\sigma(\xi_j) \right)^2 \tag{2.26}$$

In some special cases, where the first and second order derivatives are available, the integration of the first and second order moment may be realized analytically as shown in equations Eq.2.23,2.25 and Eq.2.24, 2.26. However, in most of the case, finite difference schemes are required which leads to unaffordable computational costs when M increases. Moreover, the issue of the truncation the Taylor series expansion is still an open issue as in general no fundamental result proves the *monotonic convergence* of the Taylor series expansion.

Methods dedicated to reliability studies Performing reliability analysis of a mechanical system or process results in determining the probability of a particular event $\boldsymbol{\xi}_{\mathrm{failure}}$ leading to the failure of the structure (the "failure event"). This failure event may usually be expressed as the negative value (by convention) of a criterion $G(\boldsymbol{\xi}_{\mathrm{failure}})$. The probability of failure P_{failure} of the system is then the probability that $G(\boldsymbol{\xi}_{\mathrm{failure}}) < 0$. The set $D_f = \{\boldsymbol{\xi}_{\mathrm{failure}} | G(\boldsymbol{\xi}_{\mathrm{failure}}) < 0\}$ defines the failure domain. The function $\Xi \rightarrow \partial D_f = \{\boldsymbol{\xi}_{\mathrm{failure}} | G(\boldsymbol{\xi}_{\mathrm{failure}}) = 0\}$ defines the border of the failure domain also called limit state function.

First and Second Order Reliability Method These methods consist in approximating the failure domain G by a simpler domain whose probability may be computed analytically. A preliminary step to the construction of the simpler domain consists in transforming the observed random variable $\boldsymbol{\xi}$ into a vector of independent centered normalized Gaussian random variables. In this particular space, the most probable failure point $\boldsymbol{\xi}^*$ also called "conception point" has to be identified. In the transformed space the conception point is the nearest point to the origin (this is due to the "bell symmetric" shape of the Gaussian probability density function.) Computing this point may be done by solving the following optimization problem

$$\begin{aligned} &\min(\|\boldsymbol{\xi}\|^2) \\ &s.t \quad G(\boldsymbol{\xi}_{failure}) \leq 0 \end{aligned} . \tag{2.27}$$

Many algorithms have been proposed in the literature to solve this problem and find the $\boldsymbol{\xi}^*$ which may be referred in the literature as the conception point, the beta point of most probable point (MPP).

Once the MPP has been identified, the FORM consists in building a linear approximation of the limit state function points by defining a hyperplane passing through the design point and orthogonal to the vector $\boldsymbol{\xi}^*$. The probability of failure is then simply approximated by:

$$P_{\text{failure}} \approx \Phi(-\beta), \tag{2.28}$$

where Φ is the standard Gaussian cumulative distribution function and β is the signed distance between the origin and the conception point. The SORM improves the FORM methodology by proposing a second order approximation of the limit state function defined by a paraboloid tangent to the limit state at the conception point. The curvatures of the paraboloid at the design point are computed as the eigenvalues of the Hessian matrix of the limit state function. In this context, the failure probability may then be approximated by :

$$P_{\text{failure}} \approx \Phi(-\beta) \prod_{i=1}^{M} (1 - \alpha_i \beta)^{-1/2} \tag{2.29}$$

where the α_i are the principal curvatures of the paraboloid.

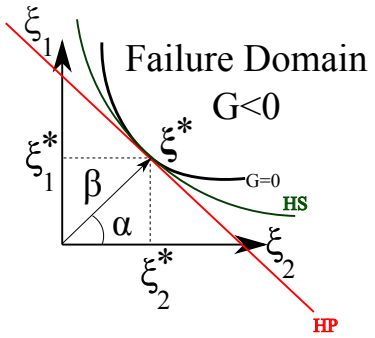

Figure 2.1: Illustration of FORM/SORM methodologies

For relatively small stochastic dimensions and smooth continuous limit state these methodologies provide relatively accurate results with reasonable computational time. However, they are not adapted to discontinuous or multi-modal limit state functions and may lead in these cases to an erroneous estimation of the probability of failure. Moreover, they do not intrinsically provide an error estimator on the probability of failure. Finally, these methodologies require the need of derivatives which are not always available when the function of interest is given in an implicit way (as it is the case in non intrusive approaches). Moreover, in high dimension the computation of the Hessian matrix for the SORM may be prohibitively costly [ZO99]. [KS91] proposes a more efficient iterative algorithm to compute the curvatures at the design point without the need of the Hessian matrix.

Sampling based approach To keep the control on the error committed on the estimated probability of failure, direct integration techniques to assess the reliability of the system may also be used.

The probability of failure is then written in its integral form as:

$$P_{\text{failure}} = \int_G \boldsymbol{\xi} dP_{\boldsymbol{\xi}}(\boldsymbol{\xi}) = E[1_G(\boldsymbol{\xi})], \tag{2.30}$$

where 1_G is the indicator function on G.

The computation of the above integral using brute Monte Carlo simulation becomes rapidly prohibitive in the transformed variable space as most of the sampling will concentrate around the origin of the domain. It may be shown that for low P_{failure}, the coefficient of variation C_V of the MCS estimator converges in $\frac{1}{\sqrt{S}}$. For example, for $P_{\text{failure}} = 10^{-4}$, and a targeted $C_V = 10^{-1}$, 10^6 samples may be needed.

The Importance Sampling methodologies[AB99][ER93] allow to improve the efficiency of the crude MCS by centering the samples around the conception point following a translated probability density function $p_{\text{translated}} = p_\xi(\xi - \xi^*)$. Directional sampling [Bje88], [Mel94, NE00], line sampling [KPS04], subset simulation [AB01]. These advanced methodologies are extended by [SPK04] to be efficient in high dimensions.

Metamodel based approaches A metamodel is a response surface coupled with a sampling strategy which is aimed at describing the behavior of a complex computational model while being less expensive to evaluate. In the context of structural reliability a number of them has been developed in the last decade in order to circumvent the costs and accuracy issues of the proposed FORM and SORM methodologies. In the early 90's, [BB90, Far89, Won85] proposes an adaptive second order polynomial response surface to interpolate the limit state function. To increase the efficiency and the accuracy of the metamodel, statistical information on the basic variables are used in order to update the obtained metamodel. Monte Carlo simulations are then used in conjunction of the metamodel in order to assess the desired reliability estimates. An obvious limitation of this methodology lies in the fact the limit state function has to be smooth enough and continuous. In some practical problems this is clearly not the case: the performance function may highlight multiple design points, and multiple regions that make significant contributions to the failure probability. This question is addressed by [GM04] who proposes an algorithm to identify the multiple points and regions and to interpolate these points using a second-order polynomial response surface whose coefficients are determined using a least square analysis. A measure of the sensitivity of the reliability index is also provided. However, for non-smooth limit state function, the use of second order polynomial response surface may show insufficient accuracy in approximating the limit state function, and large errors may be observed in the computation of the sensitivity of the reliability index, particularly. [YC04a], [KKC10] used Moving Least Squares giving higher weight to the experimental points closer to the design point and allowing the response surface function (RSF) to be closer to the limit state function. The authors in [DSB11b] take advantage of the kriging intrinsic features in order to propagate the approximation error on the limit-state surfaces to the failure probabilities estimates providing thus an empirical error measure. In [LX10] the authors argue that the straightforward sampling on surrogates models may lead to biased results and thus proposes a hybrid approach based on a large sampling of the metamodel in the probability space and refining this sampling using the numerical model in some region of interest. In [Sud12, DSD13] the author proposed an efficient scheme to solve the problem of the potential biasedness in the estimation of a probability of failure due to a direct substitution. It combines the use of an importance sampling strategy guided by a kriging metamodel replacing the indicator function

of the failure domain by a probabilistic function.

2.2 Spectral representation of stochastic field through Polynomial Chaos Expansion

2.2.1 Introduction

This section reviews in more details the construction of the Polynomial Chaos Expansion (PCE). This methodology has been widely used as an alternative to the Monte Carlo Simulation in order to propagate the uncertainty through a deterministic numerical model. From its initial form, many obstacles have to be circumvented for an efficient use. In this section we briefly review these obstacles and the circumventing solutions.

2.2.2 Functional evaluation of a random variable by orthogonal polynomials

2.2.2.1 Functional evaluation of random variable

In practice, random variables of interest are seen as the output of a *deterministic numerical model* $y(\boldsymbol{\xi})$. They often belong to the set of square integrable functions denoted by $\mathcal{L}^2(\mathbb{R}^M, dP_{\boldsymbol{\xi}})$ and defined by:

$$\begin{aligned}\mathcal{L}^2(\mathbb{R}^M, dP_{\boldsymbol{\xi}}) = \{y : \boldsymbol{\xi} \mapsto y(\boldsymbol{\xi}) \in \mathbb{R};\\ E[y^2] := \int_{\mathbb{R}^M} y(\boldsymbol{\xi})^2 dP_{\boldsymbol{\xi}}(\boldsymbol{\xi}) < \infty\}\end{aligned} \tag{2.31}$$

where $\boldsymbol{\Xi} \in \mathbb{R}^M$ since in practice one often deals with a finite number of second order (with finite second order moment) random variables $\boldsymbol{\xi} = \{\xi_1, \ldots, \xi_M\}$.

When this space is equipped with the following inner product, it becomes an Hilbert space:

$$< u, v >_{\mathcal{L}^2(\mathbb{R}^M, dP_{\boldsymbol{\xi}})} = E[uv] = \int_{\mathbb{R}^M} u(\boldsymbol{\xi}) v(\boldsymbol{\xi}) dP_{\boldsymbol{\xi}}(\boldsymbol{\xi}) \tag{2.32}$$

An Hilbertian basis $\{B_i\}_{i\in\mathcal{I}}$ of $\mathcal{L}^2(\mathbb{R}^M, dP_{\boldsymbol{\xi}})$ is a complete set of orthonormal functions verifying the following properties:

$$< B_i, B_j >_{\mathcal{L}^2(\mathbb{R}^M, dP_{\boldsymbol{\xi}})} = \delta_{ij} \tag{2.33}$$

where δ_i, j is the Kronecker symbol and

$$\forall u \in \mathcal{L}^2(\mathbb{R}^M, dP_{\boldsymbol{\xi}}), < B_i, u >= 0, \forall i \in \mathcal{I} \Rightarrow u = 0 \tag{2.34}$$

Finally, each function $y \in \mathcal{L}^2(\mathbb{R}^M, dP_{\boldsymbol{\xi}})$ admits an unique decomposition on this Hilbertian basis:

$$y(\boldsymbol{\xi}) = \sum_{i\in\mathcal{I}} \gamma_i B_i(\boldsymbol{\xi}) \tag{2.35}$$

where γ_i, $i \in \mathcal{I}$ are the coordinate of y projected on the orthonormal basis $\{B_i\}_{i\in\mathcal{I}}$:

$$\begin{aligned}\gamma_i &=< \gamma, B_i >_{\mathcal{L}^2(\mathbb{R}^M, dP_{\boldsymbol{\xi}})} = E[y, B_i] \\ &= \int_{\mathbb{R}^M} y(\boldsymbol{\xi}) B_i(\boldsymbol{\xi}) dP_{\boldsymbol{\xi}}(\boldsymbol{\xi})\end{aligned} \tag{2.36}$$

Several choices have been proposed in the literature in order to construct the Hilbertian basis. Among the most popular, one may find the Karhunen Loève (KL) expansion and the polynomial expansion methods.

2.2.2.2 Link between random variable and orthogonal polynomials

In probability theory, since the preliminary work of Wiener on Brownian motion, the relationship between orthogonal polynomials and random variables has been widely studied [Sch00].

Let $\mathbb{P} = \{H_N(\xi), N \in \mathbb{N}\}$ be a set of monovariate polynomials whose maximal degree is N. Let Φ be a real positive measure. $\mathbb{P}$ forms a set of orthogonal polynomials with respect to the measure Φ if:

$$\int_\Omega H_n(\xi) H_m(\xi) d\Phi(\xi) = K\delta_{nm}, \qquad n, m \in \mathbb{N} \tag{2.37}$$

where δ_{nm} is the Kronecker product and K is a non zero constant (if K=1, $\mathbb{P}$ is orthonormal). A well known property of real orthogonal polynomial lies in the fact that they all may be built using a three terms recurrence relationship on the form:

$$-\xi H_n(\xi) = b_n H_{n+1} + \gamma_n H_n(\xi) + c_n H_{n-1}(\xi), \qquad n \in \mathbb{N} \tag{2.38}$$

where b_n, $c_n \neq 0$ and $c_n/b_{n-1} > 0$

In the space $\mathcal{L}^2(\mathbb{R}, dP_{\boldsymbol{\xi}})$ of continuous second order random variable, the following classical polynomials form an orthogonal basis: they are referred in the literature to the classical orthogonal polynomials of the Askey-scheme:

Pdf type	Density Function	Orthogonal polynomial	Support
Uniform	$\mathbf{1}_{]-1,1[}(\xi)/2$	Legendre: $P_k(\xi)$	$[-1;1]$
Gaussian	$\frac{1}{\sqrt{(2\pi)}} e^{-\xi^2/2}$	Hermite: $H_k(\xi)$	$[-\infty;\infty]$
Gamma	$\xi^a e^{-\xi} \mathbf{1}_{\mathbb{R}^+}(\xi)$	Laguerre: $L_a^k(\xi)$	$[0;+\infty]$
Exponential	e^{-x}	Gen. Laguerre $L_n^{(\alpha)}(x)$	$[0;+\infty]$
Beta	$\mathbf{1}_{]-1;1[}(\xi) \frac{(1-\xi)^a (1+\xi)^b}{B(a)B(b)}$	Jacobi: $J_k(\xi)$	$[-1;1]$

Table 2.1: Classical orthogonal polynomial of the Askey scheme with respect to their probability density function

The resulting expansion of the random variable of interest is readily:

$$y(\omega) = \sum_{i \in \mathbb{J}} \gamma_i H_i(\xi) \tag{2.39}$$

where $\mathbb{J} \subset \mathbb{N}$, $\{H_i\}_{i \in \mathbb{J}}$ is an infinite series of one of the Askey-scheme polynomial, $\xi_{\mathcal{S}}$ the associated

standard variable, $\{\gamma_i\}_{i\in\mathbb{J}}$ the coordinate of the function on the orthogonal polynomial basis.

2.2.3 Construction of Wiener Polynomial Chaos Expansions (PCEs)

N. Wiener [Wie38] proposes for standard Gaussian variable the use of Hermitian polynomial as an Hilbertian basis to construct an approximation of the random variable $y(\boldsymbol{\xi}) \in \mathcal{L}^2(\boldsymbol{\Xi}, dP_{\boldsymbol{\xi}})$. In the following we describe the construction of the original PCE. It is usually named Hermite homogeneous PCE in the literature.

2.2.3.1 Univariate case

Let ξ be any component of $\boldsymbol{\xi}$ supposed to be a Gaussian standardized random variable (which may be obtained using an iso-probabilist transformation [LCM09]) the expansion is readily given by Eq.2.39 where $\{H_i\}_{i\in\mathbb{N}}$ are the mono-variate Hermite polynomials. The first 5 Hermite's polynomials are given below:

$$\begin{aligned} H_0(\xi) &= 1 \\ H_1(\xi) &= \xi^2 - 1 \\ H_2(\xi) &= \xi^3 - 3\xi \\ H_3(\xi) &= \xi^4 - 6\xi^2 + 3 \\ H_4(\xi) &= \xi^5 - 10\xi^3 + 15\xi \end{aligned}$$

A fundamental result for the Hermite homogeneous PCE is established by the Cameron Martin theorem [CM47]. It states that any second-order functional of the Brownian motion (Gaussian random field) can be expanded as a mean-square convergent series in terms of infinite-dimensional Hermite polynomial in Gaussian variables. Thus, the exact (in a mean square sense) PCE of the random variable $y(\xi)$ is readily:

$$y(\xi) = \sum_{i\in\mathbb{N}} \gamma_i H_i(\xi) \tag{2.40}$$

where H_i is the i^{th} degree Hermite polynomial. Exploiting the polynomial orthogonality, the coefficients of the expansion are defined as:

$$\forall i \in \mathbb{N}, \gamma_i = \frac{< y(\xi), H_i(\xi) >}{\|H_i\|^2} \tag{2.41}$$

2.2.3.2 Multi-variate case

In the multi-variate case $\boldsymbol{\xi} = \{\xi_1, \xi_2, \ldots, \xi_M\}$ with M coordinates, according to the independence assumption, the joint probability density function $f_{\boldsymbol{\xi}}(\boldsymbol{\xi})$ may be decomposed on a product of the marginal probability density functions $f_{\xi^{(i)}}$ (Eq.2.42):

$$f(\boldsymbol{\xi}) = \prod_{i=1}^{M} f_{\xi_i}(\xi_i) \tag{2.42}$$

Given the natural inner product for arbitrary function ϕ with respect to each of the marginal proba-

bility function $f_\xi(\xi)$ defined on $\mathcal{D}$

$$< \phi_1, \phi_2 >= \int_{\mathcal{D}} \phi_1(\xi)\phi_2(\xi)f_\xi(\xi)d\xi \tag{2.43}$$

Using the tensor product on these mono-variate polynomials one may obtain an infinite set of multi-variate polynomials (with a preserved orthogonality property) $\boldsymbol{H} = \{H_{\boldsymbol{\alpha}}, \boldsymbol{\alpha} \in \mathbb{N}^M\}$ where $\boldsymbol{\alpha} = \{\alpha_1, \ldots, \alpha_M\} \in \mathbb{N}^M$ is a multi-index set.

$$\mathrm{H}_{\boldsymbol{\alpha}}(\boldsymbol{\xi}) = \otimes_{i=1}^{M} H_{\alpha_i}(\xi_i) \tag{2.44}$$

According to the theorem of Cameron Martin [CM44], the exact polynomial expansion of the functional y is readily

$$y(\boldsymbol{\xi}) = \sum_{\boldsymbol{\alpha}\in\mathbb{N}^M} \gamma_{\boldsymbol{\alpha}} H_{\boldsymbol{\alpha}}(\boldsymbol{\xi}), \tag{2.45}$$

where $\{\gamma_{\boldsymbol{\alpha}}\}$, $\boldsymbol{\alpha} \in \mathbb{N}^M$ are the coefficients of the PCE to be identified

For practical use, one may truncate the full set of tensor product polynomials in order to only retain a *finite set* of polynomial terms.

Classical truncation scheme Among all $\{H_{\boldsymbol{\alpha}}, \boldsymbol{\alpha} \in \mathbb{N}^M\}$ the classical truncation scheme [Gha91, BSL06a, SDK00a] retains only the multi-variate polynomial terms whose degree does not exceed an arbitrarily fixed N leading to the following multi-index set:

$$\mathcal{A}_q^M = \{\boldsymbol{\alpha} \in \mathbb{N}^M, ||\boldsymbol{\alpha}||_q \leq p\}, \tag{2.46}$$

where $||\boldsymbol{\alpha}||_q = \left(\sum_{i=1}^{M} \alpha_i^q\right)^{1/q}$ and $q = 1$. Then, the truncated model may be written as:

$$y^{\mathcal{A}_q^M}(\boldsymbol{\xi}) \approx \sum_{\boldsymbol{\alpha}\in\mathcal{A}_q^M} \gamma_{\boldsymbol{\alpha}} H_{\boldsymbol{\alpha}}(\boldsymbol{\xi}). \tag{2.47}$$

Fig.2.2 gives an illustration of this scheme for a 2-variate 7^{th} order PCE.

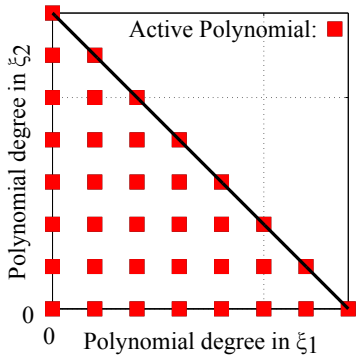

Figure 2.2: Illustration of the classical truncation scheme for a 7^{th} order PCE

The number P of coefficients in the PCE is given by

$$P = \sum_{k=0}^{N} C_{M+k+1}^{k} = \frac{(N+M)!}{N!M!} \tag{2.48}$$

and increases exponentially both with N and M.

A list of the multi-variate Hermitian monomials for $M = 2$ and $N = 3$ is provided below:

i	$\boldsymbol{\alpha} = \{\alpha_1, \alpha_2\}$	H_i
0	$\{0,0\}$	$H_0(\xi_1)H_0(\xi_2) = 1$
1	$\{1,0\}$	$H_1(\xi_1)H_0(\xi_2) = \xi_1$
2	$\{0,1\}$	$H_0(\xi_1)H_1(\xi_2) = \xi_2$
3	$\{2,0\}$	$H_2(\xi_1)H_0(\xi_2) = \xi_1^2 - 1$
4	$\{1,1\}$	$H_1(\xi_1)H_1(\xi_2) = \xi_1\xi_2$
5	$\{0,2\}$	$H_0(\xi_1)H_2(\xi_2) = \xi_2^2 - 1$
6	$\{3,0\}$	$H_3(\xi_1)H_0(\xi_2) = \xi_1^3 - 1\xi_1$
7	$\{2,1\}$	$H_2(\xi_1)H_1(\xi_2) = (\xi_1^2 - 1)\xi_2$
8	$\{1,2\}$	$H_1(\xi_1)H_2(\xi_2) = \xi_1(\xi_2^2 - 1)$
9	$\{0,3\}$	$H_0(\xi_1)H_3(\xi_2) = \xi_2^3 - 3\xi_2$

Table 2.2: Bi-variate Hermitian Polynomials Basis elements up to the order $p = 3$

Note: *One may imagine different ways to classify the obtained multi-variate monomials. When a M dimensional expansion of order N is searched, one may classify the multi-variate monomial by making the value of the M-digits of α evolving according to the "rain drop" algorithm. The previous tabular provides an example with $M = 2$ and $N = 3$.*

2.2.3.3 PCE for stochastic field representation

PCE for random field The extension to the approximation of random process as may introduce an additional non probabilistic variables such as design variable for example gives the following expression:

$$y(\boldsymbol{x},\boldsymbol{\xi}) \approx \sum_{\boldsymbol{\alpha}\in\mathbb{N}^M} \gamma_{\boldsymbol{\alpha}}(\boldsymbol{x})\Psi_{\boldsymbol{\alpha}}(\boldsymbol{\xi}) \tag{2.49}$$

or alternatively

$$y(\boldsymbol{x},\boldsymbol{\xi}) \approx \sum_{\boldsymbol{\alpha}\in\mathbb{N}^M} \gamma_{\boldsymbol{\alpha}}\Psi_{\boldsymbol{\alpha}}(\boldsymbol{x},\boldsymbol{\xi}) \tag{2.50}$$

where Ψ may be built over the tensor product of optimal orthogonal polynomials with regards to the probability measure for each ξ_i, $i = 1,\dots,M_\xi$ and by Legendre polynomial (orthogonal with respect to the uniform distribution) for the x_i, $i = 1,\dots,M_x$ variables [Eld09]. The cost of the latter expansion may become rapidly prohibitive as it increases exponentially with the number $M_\xi + M_x$ of variables (see Eq.2.48).

Let $y(\boldsymbol{x},\omega) : \mathcal{D}\times\Omega \to \mathbb{R}$ be a mean-square continuous random field (i.e. with continuous covariance function) where $\mathcal{D}$ denotes an open, bounded domain with values in $\mathbb{R}^d$, and Ω is the set of *elementary events*.

Let us give a set of points $\boldsymbol{x_1},\dots,\boldsymbol{x_N} \in \mathbb{R}^d$ and $\omega_1,\dots,\omega_S$ a set of S elementary events. Let $\boldsymbol{y}^{(i)} = \boldsymbol{y}(\omega_i) = \{y(\boldsymbol{x}_1,\omega_i),\dots,y(\boldsymbol{x}_N,\omega_i))\}^\top$, $i = 1,\dots,S$ be a real column vector in $\mathbb{R}^N$. Let $\{\bar{y}_1,\dots,\bar{y}_N\}^\top$ the vector of expectations:

$$\forall i \in \{1,\dots,N\}, \bar{y}_i = \frac{1}{S}\sum_{j=1}^{S} y(\boldsymbol{x}_i, w_j). \tag{2.51}$$

Karhunen-Loève decomposition The full Karhunen-Loève expansion [Loe63] is aimed at efficiently reducing the statistical complexity of the random field by achieving its decomposition as a denumerable sum of product functions of the form:

$$\boldsymbol{y}(\omega) = \bar{\boldsymbol{y}} + \sum_{i=1}^{N} \sqrt{\lambda_i}\kappa_i(\omega)\boldsymbol{\varphi}_i \tag{2.52}$$

decoupling the stochastic Ω and deterministic $\mathcal{D}$ spaces.

The suited decomposition may be obtained by orthogonal projection of the stochastic field of interest onto separable Hilbert spaces. The convenience of the Karhunen Loève (KL) expansion stays precisely in the fact that KL expansion is toptimal with regards to the total mean square error. To construct, the Hilbertian basis one performs an eigenvalue decomposition of the covariance operator which may be defined as

$$C(\boldsymbol{x}_i,\boldsymbol{x}_j) = \int_D y(\boldsymbol{x}_i,\omega)y(\boldsymbol{x}_j,\omega)\mathrm{d}p_\omega(\omega),\ (i,j)\in\{1,\dots,N\}^2. \tag{2.53}$$

Replacing y by its collocation vector $\boldsymbol{y}$, an unbiased estimator of the covariance operator may be obtained by:

$$C(\boldsymbol{x}_i,\boldsymbol{x}_j) = \frac{1}{S-1}\sum_{i=1}^{S}(\boldsymbol{y}^{(i)} - \bar{\boldsymbol{y}}_i)^\top(\boldsymbol{y}^{(j)} - \bar{\boldsymbol{y}}_j),\ (i,j)\in\{1,\dots,N\}^2. \tag{2.54}$$

By definition, the covariance kernel function (since $\mathcal{D}$ is bounded), symmetric and positive definite.

It admits a decomposition of the form:

$$\begin{aligned} C &= \sum_{i=1}^{N} \lambda_i \boldsymbol{\varphi_i} \boldsymbol{\varphi_i}^\top \\ &= \sum_{i=1}^{N} \boldsymbol{\phi_i} \boldsymbol{\phi_i}^\top \end{aligned} \tag{2.55}$$

where $\{\lambda_i\}_{i=1}^N$ are the eigenvalues, and $\{\boldsymbol{\varphi}_i\}_{i=1}^N$ the eigenfunctions. They constitute the elements of the Hilbertian basis $\{\boldsymbol{\phi}_i\}_{i=1}^N = \{\sqrt{\lambda_i}\boldsymbol{\varphi}_i\}_{i=1}^N$.

From 2.55, one obtained the following decomposition $\boldsymbol{y}_{\mathrm{KL}}$ of $\boldsymbol{y}(\omega)$:

$$\begin{aligned} \boldsymbol{y}_{\mathrm{KL}}(\omega) &= \bar{\boldsymbol{y}} + \boldsymbol{\phi}\boldsymbol{\phi}^\top \left(\boldsymbol{y}(\omega) - \bar{\boldsymbol{y}}\right) \\ &= \bar{\boldsymbol{y}} + \sum_{i=1}^{N} \boldsymbol{\phi}_i \kappa_i(\omega) \end{aligned} \tag{2.56}$$

where we have introduced $\{\kappa_i\}_{i=1}^N = \{\boldsymbol{\phi}_i^\top (\boldsymbol{y}(\omega) - \bar{\boldsymbol{y}})\}_{i=1}^N$. Out of this definition one may deduce the following properties:

- κ_i are second order random variables
- $\mathrm{E}[\kappa_i] = 0$
- $\mathrm{E}[\kappa_i \kappa_j] = 0 \; i \neq j \in \mathbb{N}$

Consequently, the covariance matrix of $\boldsymbol{\kappa}$ is the identity matrix insuring the independence between the vector components. Moreover, since the underlying random field $\boldsymbol{y}(\omega)$ is generally not gaussian, the $\boldsymbol{\kappa}$ variables are in general non Gaussian variables. Due to the symmetry and to the positiveness of the covariance kernel, the eigenfunctions φ_i form a complete set and exhibit an orthogonality property

$$\boldsymbol{\phi}\boldsymbol{\phi}^\top = I_{N \times N}, \tag{2.57}$$

where $I_{N \times N}$ is the $N \times N$ identity matrix.

Regarding the eigenvalues $\{\lambda_i\}_{i=1}^N$ they form a decreasing sequence of positive values conventionally ordered as follows: $\lambda_1 > \lambda_2 > \lambda_3 > \ldots \to 0$. Moreover, with the additional assumption of mean-square continuity of the random field, this sequence is convergent. From these assertion one may prove that the Karhunen Loève expansion is unique.

In the following we show that the Karhunen Loève expansion is optimal in the mean square sense, i.e increasing the truncation the order of the expansion reduces the total mean square error.

Let us first introduce the following additional notations:

- Let $n < N$ and let us consider $\{\boldsymbol{\phi}\}_{i=1}^n$ the n first eigenvectors, we denote them $\boldsymbol{\phi}_t$,
- Let $\boldsymbol{Y} = \{\boldsymbol{y}(\omega_1), \ldots, \boldsymbol{y}(\omega_S)\}$ and
- $\boldsymbol{C} = \sum_{i=1}^{S} (\boldsymbol{y}^{(i)} - \bar{\boldsymbol{y}})(\boldsymbol{y}^{(i)} - \bar{\boldsymbol{y}})^\top = \boldsymbol{Y}\boldsymbol{Y}^\top$.

A truncated expansion $\boldsymbol{y}^{\mathrm{KLt}}(\omega)$ of $\boldsymbol{y}(\omega)$ is readily

$$\boldsymbol{y}^{\mathrm{KLt}}(\omega) = \bar{\boldsymbol{y}} + \boldsymbol{\phi}_t \boldsymbol{\phi}_t^\top \left(\boldsymbol{y}(\omega) - \bar{\boldsymbol{y}}\right). \tag{2.58}$$

The truncation error ϵ is given by:

$$\begin{aligned}
\epsilon &= \sum_{i=1}^{S} \|\boldsymbol{y}(\omega_i) - \boldsymbol{y}^{\mathrm{KLt}}(\omega_i)\|^2 \\
&= \left(\boldsymbol{y}^{(i)} - \bar{\boldsymbol{y}} - \boldsymbol{\phi}_t \boldsymbol{\phi}_t^\top (\boldsymbol{y}^{(i)} - \bar{\boldsymbol{y}})\right)^\top \left(\boldsymbol{y}^{(i)} - \bar{\boldsymbol{y}} - \boldsymbol{\phi}_t \boldsymbol{\phi}_t^\top (\boldsymbol{y}^{(i)} - \bar{\boldsymbol{y}})\right) \\
&= \sum_{i=1}^{S} (\boldsymbol{y}^{(i)} - \bar{\boldsymbol{y}})(\boldsymbol{I} - \boldsymbol{\phi}_t \boldsymbol{\phi}_t^\top)^\top (\boldsymbol{I} - \boldsymbol{\phi}_t \boldsymbol{\phi}_t^\top)(\boldsymbol{y}^{(i)} - \bar{\boldsymbol{y}}) \\
&= \sum_{i=1}^{S} (\boldsymbol{y}^{(i)} - \bar{\boldsymbol{y}})(\boldsymbol{I} - \boldsymbol{\phi}_t \boldsymbol{\phi}_t^\top)(\boldsymbol{y}^{(i)} - \bar{\boldsymbol{y}}) \\
&= \mathrm{tr}\left(\boldsymbol{Y}^\top \left(\boldsymbol{I} - \boldsymbol{\phi}_t \boldsymbol{\phi}_t^\top\right) \boldsymbol{Y}\right) \\
&= \mathrm{tr}\left(\boldsymbol{C}\left(\boldsymbol{I} - \boldsymbol{\phi}_t \boldsymbol{\phi}_t^\top\right)\right) \\
&= \mathrm{tr}\left(\boldsymbol{C}\right) - \mathrm{tr}\left(\boldsymbol{\phi}_t^\top \boldsymbol{C} \boldsymbol{\phi}_t\right) \\
&= \sum_{i=1}^{N} \lambda_i - \sum_{i=1}^{n} \lambda_i \\
&= \sum_{i=n+1}^{N} \lambda_i
\end{aligned}$$

Thus when increasing the order of the expansion one automatically reduces the total mean square error. In practice one truncates the expansion to a finite number of summands leading to :

$$\boldsymbol{y}(\omega) = \bar{\boldsymbol{y}}(\omega) + \sum_{i=1}^{n} \boldsymbol{\phi_i} \kappa_i(\omega) \tag{2.59}$$

The truncated order may be chosen such that for some $n \leq N$, $\dfrac{\sum_{i=1}^{n} \lambda_i}{\sum_{i=1}^{N} \lambda_i}$ is closed enough to one.

Reduced PCE expansion Let the random n variables κ_j be collected in to a random vector $\boldsymbol{\kappa}$ with value in $\mathbb{R}^n$ and let us approximate them using a PCE of order P and dimension n:

$$\kappa_j(\boldsymbol{\gamma}) = \sum_{\boldsymbol{\alpha}, |\boldsymbol{\alpha}|=1}^{P} \gamma_{\boldsymbol{\alpha}} \mathrm{H}_{\boldsymbol{\alpha}}(\boldsymbol{\xi}) \tag{2.60}$$

where $|\boldsymbol{\alpha}| = \sum_{j=1}^{M} \alpha_j$.

Injecting this reduced expansion into the KL decomposition of the field $\boldsymbol{y}$, one obtains:

$$\boldsymbol{y}(\omega) = \bar{\boldsymbol{y}} + \sum_{i=1}^{n} \left(\sum_{\boldsymbol{\alpha}_i, |\boldsymbol{\alpha}_i|=1}^{P} \gamma_{\boldsymbol{\alpha}_i} \mathrm{H}_{\boldsymbol{\alpha}_i}(\boldsymbol{\xi}) \right) \boldsymbol{\phi}_i. \tag{2.61}$$

We note that $\boldsymbol{\xi}$ is valued in $\mathbb{R}^n$ where n is chosen sufficiently large in order to limit the accuracy loss due to the dimension reduction process.

2.2.4 On the limitation of Wiener Hermite PCE for non Gaussian probability measure

2.2.4.1 Convergence for non Gaussian random variable

According to the Cameron Martin theorem, the PCE converges in a mean square sense for $\mathcal{L}^2$ random variables and stationary stochastic processes. However, as only a few terms of the PCE are retained in many applications this statement is sometimes irrelevant. [KL00] particularly shows on analytical random non Gaussian variables that when increasing the number of terms of the PCE, some metrics are systematically improved: among them, the mean square accuracy, the relative error accuracy, the probability of the PCE approximation of taking non physical values, the probability that the PCE is equal in probability to the true function, the difference between the tails of the true function and the PCE to the upper 1% fractile, the relative errors in variance and kurtosis. When increasing the number of terms all the considered metrics are improved in a monotonic way with different convergence rate, some of them being highlighting particularly slow convergence rates.

Considering the difference between the tails of the true function and the PCE to the upper 1% fractile, in some cases non monotonic convergence are observed: for some non-gaussian random variables increasing the number of terms may not improve the distribution tails making the use of the PCE approaches risky for reliability analysis. Moreover, the authors in [FG07] provide mathematical proofs showing that higher-order statistical moments (i.e., greater than two) computed using homogeneous hermitian PCE may not always converge with the number of terms in the Hermite-PCE series. For example, it is shown that the third absolute moment of the PC approximation for a lognormal random variable does converge, while moments of order four and higher for uniform random variables do not converge. It has been previously demonstrated through numerical study in [FJG04]) who proved that a lack of convergence in the higher-order moments can have a profound effect on the rate of convergence of the tails of the distribution of the PC approximation.

2.2.4.2 On the balance between computational costs and accuracy

The highest challenge consists then in the computation of the PCE coefficients. One may then have to face many different problems:

- in high dimension, the number of terms to compute increases exponentially with the number of variables and with the order of the PCE which may in some cases improve some metrics. This problematic is called the “curse of dimensionality”. To tackle this issue, a special care has to be simulatneously given to the reduction of the number of calls of the exact model in order to compute

a fixed number of coefficient, and to adapt the polynomial basis in order to only capture the basis elements the most significant with regards to the stochastic function to be expanded.

- limited set of data or erroneous set of data introduces [RHB04] its own type of uncertainties. It is then of paramount importance to build a PCE with regards to the data at hand and to be able to evaluate the influence of missing and/or erroneous data on the PCE prediction capability.

2.2.5 PCE for independent non Gaussian probability measure

2.2.5.1 Variable transformation approach

It is possible to put into conformity a physical variable with a normal variable by an adequate transformation called Gaussian anamorphosis (or normal score transformation) [Wac96] or approximate parametric transformation [DM96] but this usually decreases the convergence rate of the expansion [XK03a, XK02a].

2.2.5.2 Generalized PCE

The convergence rate (with the Wiener associated measure) is optimal (exponential) for gaussian process only and degenerates when the probability density function describing the process goes away from the Gaussian distribution. To address this limitation, the authors in [XK02b] and [XLSK02] propose a generalization of the classical PCE. The generalized Polynomial Chaos Expansion (gPCE) has become one of the mostly used metamodel in order to perform UQ. It extends the Wiener-Hermite PCE to a finite set of non gaussian field replacing the Hermite polynomials by more appropriate orthogonal polynomials (with respect of the corresponding measures, see table 2.2.2.2 for correspondence between orthogonal polynomial and associated measures). In a set of papers the authors [XLSK03, XK03a, XK03b, Xiu04, XH05, Xiu07a, Xiu09a, Xiu09b], showed (without providing mathematical proofs) that in many cases a higher convergence rate may be obtained using the orthogonal polynomials of the Askey-scheme in lieu of the Hermite polynomial.

However, for these generalized polynomial basis, despite the demonstration of their efficiency in many cases no proof of convergence has been established until very recently. The authors in [EMSU12] notably show that an arbitrary random variable with finite variance may be expanded in generalized polynomial chaos expansions if the underlying probability measure is uniquely determined by its moment and continuous giving by the way the missing theoretical insight to the gPC.

2.2.5.3 arbitrary PCE (aPCE)

Finally, arbitrary Polynomial Chaos expansion (aPC) [ON12, Rie23] proposed the construction of a PCE basis using only the statistical moments of the random variable computed from the data at hand. It shows that the construction of a polynomial basis of degree d needs the knowledge of a finite number $(2d)$ of the statistical moments of the continuous random variable to be expanded without requiring any knowledge of a probability density function. The degree of the expansion is also required to be not greater than the number of available sampling points. The stochastic analysis is handled using only the data at hand, hence avoiding the subjective association of a parametric probability function to the limited set of data. The complexity of the stochastic analysis is thus aligned with the reliability and

the detail level of the statistical information at hand. However, when limited or erroneous data sets are available epistemic uncertainties are introduced in the model. The proposed methodology does not offer any intrinsic property in order to assess the impact of these kind of uncertainties. External methods to assess their impact are then proposed by the authors such as jacknife and bootstrap. Finally, the authors highlight an improved convergence rate of this approach with regards to the gPC approach on the same limited set of data, but no convergence proof of such an approach has been provided yet. At the current state of the art, no work has been proposed yet in order to extend the aPC technique for correlated random variable.

2.2.5.4 Multi-Element Generalized PCE

The previously proposed generalizations, the Hilbertian basis used for the projection of the random field over the whole stochastic space is made of continuous polynomial functions: they do not allow to treat non continuous probability density function. To address this limitation, the authors in [WK05, WK06a, WK06c, WK06b] introduced Multi-Element generalized Polynomial Chaos Expansion (MEgPC) as an extension of the gPC dedicated to the assessment of non continuous probability density function. It is based on a decomposition of the random space into local elements, and subsequently implements gPC locally within the individual elements. An error control has been developed for the ME-gPC in [WK09].

This methodology shows its limitation in high dimension when no other solution may exists in order to build a partition of the stochastic space.

2.2.6 Computing the PCE coefficients in adequacy with computational ressources

Another well addressed limitation of the PCEs (Hermite, generalized, or arbitrary) appears when the stochastic dimension increases. As shown by Eq. 2.48, when the dimension increases the number of terms in the PCE increases exponentially and may rapidly lead to a situation where the construction of the PCE metamodel itself may become too computationally expensive. This situation is often referred to as an aspect of the "curse of dimensionality". To circumvent this curse, a handfull of methodologies are proposed in the literature proposing to retain only the number of polynomial in the expansion which are significant to describe the response variability.

2.2.6.1 Low rank index set truncation

The most intuitive and direct approach relies on the "sparsity of effects principle". It states that a system is usually dominated by main effects and low-order interactions. Q-norm generalizes the classical truncation scheme by varying $0 \leq q \leq 1$ [BS08a]. Fig.2.3 illustrates a typical truncated index set different for $q = 0.6$ and a 7^{th} order 2-variate PCE.

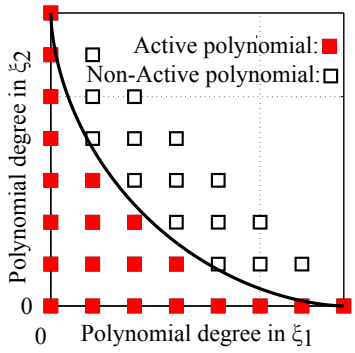

(a) $q = 0.6$

Figure 2.3: Illustration of $Q-$norm truncation with different values of the truncation parameter q for a 7^{th} order PCE

The set of active polynomials in the PCE decomposition is decreased when q decreases. Fig.2.4(a) illustrates the evolution of the number of 2-variate polynomial terms in linear scale against q values, and Fig.2.4(b) shows it for an 8-variate polynomial in log scale.

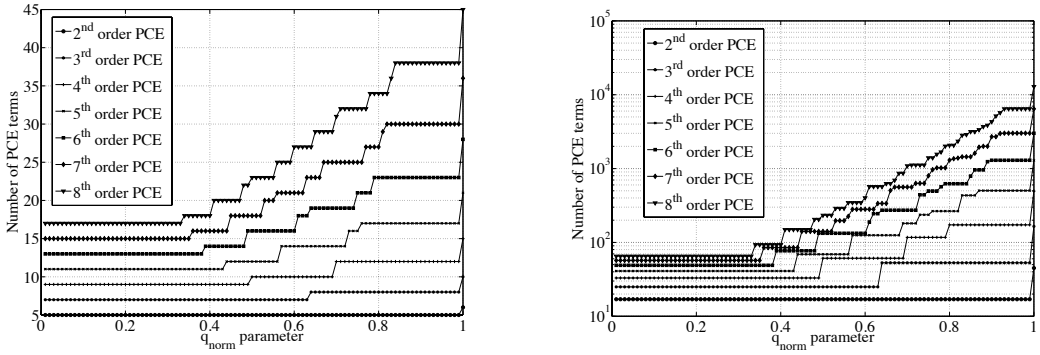

(a) 2-variate

(b) 8-variate

Figure 2.4: Number of polynomials terms in *q-truncated* PCE with regards to the q truncation parameter for 2 and 8 variables

Having performed this *a priori* truncation scheme, the PCE coefficients may then be computed using either a projection scheme exploiting the orthogonality of the PCE basis, or using a collocation scheme. The cost reduction is done using so called "sparse approaches" were the sparsity either characterizes the Design of Experiment (DoE) used to compute the projection coordinates of the random data on the orthogonal polynomial basis (PCE coefficients), or the polynomial basis itself.

2.2.6.2 Adressing the curse of dimensionality using sparse approaches

Non-intrusive spectral projection The projection method uses the orthogonality property of the polynomial basis elements on the Hilbert space of finite variance random variables, $\{H_{\boldsymbol{\alpha}}(\boldsymbol{\xi})\}_{|\boldsymbol{\alpha}|\leq \boldsymbol{P}}$ to compute the coefficients of the expansion $\{\gamma_{\boldsymbol{\alpha}}\}_{|\boldsymbol{\alpha}|\leq \boldsymbol{P}}$:

$$\gamma_{\boldsymbol{\alpha}} = \frac{< y, \mathrm{H}_{\boldsymbol{\alpha}}(\cdot) >}{< \mathrm{H}_{\boldsymbol{\alpha}}(\cdot), \mathrm{H}_{\boldsymbol{\alpha}}(\cdot) >} = \frac{\int_{\mathbb{R}^M} y(\boldsymbol{\xi}) \mathrm{H}_{\boldsymbol{\alpha}}(\xi) \Phi(\boldsymbol{\xi}) d\boldsymbol{\xi}}{\int_{\mathbb{R}^M} \mathrm{H}_{\boldsymbol{\alpha}}(\boldsymbol{\xi})^2 \mathrm{H}_{\boldsymbol{\alpha}}(\boldsymbol{\xi}) d\boldsymbol{\xi}} = \frac{E[y(.)\mathrm{H}_{\boldsymbol{\alpha}}(\cdot)]}{E[\mathrm{H}^2_{\boldsymbol{\alpha}}]} \tag{2.62}$$

Each tensor product involves the computation of a multi-dimensional integral over the support range of the multivariate probability measure. Let us assume that the random variables $\boldsymbol{\xi} = \{\xi_1, \ldots, \xi_M\}$ are all independent standard Gaussian random variables, hence with $\prod_{i=1}^{M} \phi(\xi_i) = \Phi(\boldsymbol{\xi})$ is a M-multivariate standardized Gaussian probability density function obtained from the product of the M one-dimensional standardized Gaussian probability density function.

The integral equation on the denominator is known and easy to compute in the Hermitian case:

$$\begin{aligned}
E[\mathrm{H}^2_{\boldsymbol{\alpha}}] &= < \mathrm{H}_{\boldsymbol{\alpha}}, \mathrm{H}_{\boldsymbol{\alpha}} > \\
&= \int_{\mathbb{R}} \mathrm{H}^2_{\boldsymbol{\alpha}}(\boldsymbol{\xi}) \mathrm{H}_{\boldsymbol{\alpha}}(\boldsymbol{\xi}) d\boldsymbol{\xi} \\
&= \int_{\Xi_1} \ldots \int_{\Xi_M} \Psi^2_j(\xi_1, \ldots, \xi_M) \phi(\xi_1) \ldots \phi(\xi_M) d\xi_1 \ldots d\xi_M \\
&= \int_{\Xi_1} \ldots \int_{\Xi_M} \prod_{j=1}^{M} H^2_{\alpha_j}(\xi_j)) \phi(\xi_1) \ldots \phi(\xi_M) d\xi_1 \ldots d\xi_M \\
&= \prod_{j=1}^{M} \int_{\Xi_j} H^2_{\alpha_j}(\xi_j) \phi(\xi_j) d\xi_j \\
&= \prod_{j=1}^{M} \alpha_j!
\end{aligned} \tag{2.63}$$

Only the integral equation on the numerator is still to be computed

$$\int_{\mathbb{R}^M} y(\omega) \mathrm{H}_{\boldsymbol{\alpha}}(\boldsymbol{\xi}) d\boldsymbol{\xi} \tag{2.64}$$

The key point is to choose the collocation points. In one dimension the choice is straight forward. A one dimensional quadrature rule is aimed at approximating an integrand of the form $\int_{\mathbb{R}} y(\xi)\phi(\xi)d\xi$ by a finite summand number of S terms composed by the product of "weights" $\{w_1, \ldots, w_S\}$ and of evaluations of the output function $y(\xi)$ at some quadrature abscissas $\{\xi^{(1)}, \ldots, \xi^{(S)}\} \in \mathbb{R}$.

$$\mathcal{U}(y) = \sum_{i=1}^{S} y(\xi^{(i)}) w_i \tag{2.65}$$

For example the Gaussian Quadrature rule abscissas are composed of the zeros of the polynomials which are orthogonal to the probability density weighting function and referred in the Wiener-Askey scheme. Numerous studies show that the Gaussian quadrature rule is usually the best choice.

The tensor product of one dimensional quadrature rule generalizes this approach in higher dimension. Let $\boldsymbol{\xi} = \{\xi_1, \ldots, \xi_M\}$, be a M dimensional vector and $i \in \{1, \ldots, M\}$ an index referring to the variables dimensions. For each dimension i, let $\{\xi_i^{(1)}, \ldots, \xi_i^{(m_i)}\}$ be a sequence of abscissas for quadrature on $\mathbb{R}$. For $f \in \mathcal{C}^0(\mathbb{R})$ and $n = 1$ let us introduce a sequence of one dimensional quadrature operators.

$$\mathcal{U}^i(y) = \sum_{j=1}^{m_i} y(\xi_j^i) w_j^i \tag{2.66}$$

with $m_i \in \mathbb{N}$. The Gauss quadrature method allows to compute multivariate integrals by transforming it into a weighted sum. In the M-dimension case such a weighted sum is written:

$$\int_{\mathbb{R}^M} y(\boldsymbol{\xi})\Psi_j(\boldsymbol{\xi})\Phi(\boldsymbol{\xi})d\boldsymbol{\xi} = \sum_{k_1}^{K} \dots \sum_{k_M}^{K} w_{k_1} \dots w_{k_M} y(\xi_{k_1}, \dots, \xi_{k_M}) \tag{2.67}$$

where $\{w_{k_1} \dots w_{k_M}\}$ and $\{\xi_{k_1}, \dots, \xi_{k_M}\}$ are respectively the integration weights and integration points. The integration order K in each direction is assessed by considering the following assertion: if the response $y(\boldsymbol{\xi})$ was polynomial of order p the terms to be integrated $(y_i\boldsymbol{\xi})\Psi_j(\xi))$ would be of maximal order $2p$ and a $K = p + 1$ order integration scheme would give the exact solution. The integration weights and points are computed according to the probabilistic measure considered. In this context for each direction, the integration weights are computed in the following way:

$$w_k = \frac{< H_k, H_k >}{H'_k(\xi_k)H_{k-1}(\xi_k)} \tag{2.68}$$

with H_k the k^{th} order mono-variate Hermitian polynomial.

Considering now the integration points, it is shown that they have to be taken as the roots of the maximal possible order $(2p)$ monomial Hermitian polynomial appearing in the terms to be integrated.

This approach has been used in a number of recent papers notably [GS93, MH03, MK05, XK03a] and some investigations towards an error estimation has been analyzed in [BNT07].

The main limitation of this approach is the exponential growth of the computational cost with the number of variables. If s collocation points are chosen in each of M-dimension, the number of total calls to the exact model is $S = s^M$. Realizing this number of simulations becomes rapidly unfeasible particularly when high computational efforts are demanded for one evaluation of $y(\boldsymbol{\xi})$ and thus limit the use of the tensor product of integration rules to lower dimensions.

Sparse approaches based on Smolyak's algorithm In projection based approaches, the challenge consists in computing at low computational costs the integral Eq.2.64 when the number of random variables become moderately large. Smolyak [**?**] proposes to consider *sparse* tensor product of quadrature rules.

The Smolyak sparse grid quadrature rule is aimed at drastically reducing the number of collocation points while preserving a high level of accuracy. It consists in tensor product of quadrature rules retaining only those where a small number of points are used by the following rules:

For $\mathcal{U}^0 = 0$ and for $i \geq 1$, and $|\boldsymbol{i}| = i_1 + \dots, i_n$, the Smolyak quadrature formula is defined by:

$$\mathcal{A}(w, n) = \sum_{|\boldsymbol{i}| \leq w+n} (\Delta^{i_1} \otimes \dots \otimes \Delta^{i_n}) \tag{2.69}$$

where

$$\Delta^i = \mathcal{U}^i - \mathcal{U}^{i-1} \tag{2.70}$$

which may be equivalently written as:

$$\mathcal{A}(w,n) = \sum_{w+1\leq|\boldsymbol{i}|\leq w+n} (-1)^{w+n-|\boldsymbol{i}|} \binom{n-1}{w+n-|\boldsymbol{i}|} (\mathcal{U}^{i_1} \otimes \ldots \otimes \mathcal{U}^{i_n}) \tag{2.71}$$

For each level index $\boldsymbol{i}$, the number of points considered in the one dimensional quadrature is ruled by a growth function which may be linear or non linear:

$$\text{Clenshaw-Curtis rules } m = \begin{cases} 1i = 1 \\ 2^{i-1} + 1i > 1 \end{cases} \tag{2.72}$$

$$\text{Gauss-Patterson rules } m = 2^i - 1, \tag{2.73}$$

$$\text{Gausisan rules } m = 2i - 1. \tag{2.74}$$

As an extension of this idea, [CEP12] re-examine the Smolyak's algorithm in order to reconstruct the coefficients that naturally corresponds to the sparse grid integration rule. The number of terms in the obtained expansion is consistent with the number of points in the sparse grid integration rule. The key point of the proposed approach is to separately compute the coefficients of the tensor product polynomial expansion for each tensor grid in the sparse grid. Then, the linear combination of the tensor weight is used to linearly combine the coefficients of each tensor expansion. This method produces a pointwise equivalent polynomial surrogate to the one constructed from a linear combination of tensor product Lagrange polynomial.

Cubature rules Cubature rules are specifically adapted to the computation of integrand in high dimension. As in Eq.2.66 they aim at transforming a multi-dimensional integral in a weighted sum, without though using the tensor structure of the multivariate stochastic space. An extensive review of cubature rules may be found in [Coo03, Hab70]. Cubature rules are characterized by a degree "d" for which the equation 2.66 is exact if the integrand is any multi-variate polynomials of degree at most d but not $d+1$. As an example, a set of $d = 2$ cubature rule discussed in [Xiu07b] are generalized for arbitrary integration domain with arbitrary probability measures. Due to the excellent consistency between the number of polynomials in the expansion and the number of required terms, these methods may be highly efficient for smooth (the integration degree remains quite low) high dimensional problems. However these cubature rules may only be built using homogeneous random variables. Moreover, the interpolation accuracy can not systematically be reduced. These limiting assumptions make them superseded in the literature and sparse grid integration rules are preferred.

Regression approach to compute PCE parameters

Classical Collocation Approach Another scheme referred as collocation (or regression scheme) consists in performing least squares regression on the polynomial chaos coefficients. For each design point $\boldsymbol{x}$, a set of S scattered data in the standardized random variable space $\boldsymbol{\Xi} = \{\boldsymbol{\xi}^{(1)}, \ldots, \boldsymbol{\xi}^{(S)}\}$ are sampled.

Then on each of these points the mechanical model (*high fidelity simulations*) PCE coefficients $\boldsymbol{\gamma}$ are obtained by minimizing the least square residual ϵ_{LS}

$$\epsilon_{LS} = \left\| \begin{Bmatrix} y(\omega_1) \\ \vdots \\ y(\omega_S) \end{Bmatrix} - \begin{bmatrix} \mathrm{H}_1(\boldsymbol{\xi}^{(1)}) & \cdots & \mathrm{H}_j(\boldsymbol{\xi}^{(1)}) \\ \vdots & & \vdots \\ \mathrm{H}_1(\boldsymbol{\xi}^{(S)}) & \cdots & \mathrm{H}_j(\boldsymbol{\xi}^{(S)}) \end{bmatrix} \begin{Bmatrix} \gamma_1 \\ \vdots \\ \gamma_j \end{Bmatrix} \right\|^2 . \tag{2.75}$$

It has to be noticed that the results issued from the collocation method is quite sensible to the samples configuration of DOE points: for different sampling, different accuracies on the output can be obtained. Moreover, the number of sampling points taken to solve the system, also influences the accuracy on the outputs. An empirical rule shows that the number of numerical experiments Q giving the best accuracy has to be chosen such as $Q \approx (M-1) \times P$ ([BSL06b]).

Improved Collocation method Collocation methods can be improved by performing a smarter sampling of the collocation points [BSL06a]. Another alternative for the choice of the collocation points consists in constructing them from the roots of the $P+1^{th}$ order mono-variate Hermitian polynomial, where P is the maximal order of the polynomial chaos. Having constructed the M-uplets formed by all the possible combinations of the $P+1$ roots for each stochastic variables $\boldsymbol{\xi}$, only P of them are chosen to solve the system. As $\boldsymbol{\xi}$ follows a multi-normal standardized gaussian distribution, the P M-uplets retained are those with the smallest norm . The number of optimal roots to consider in each direction is an open research issue, but the results by Berveiller and al. suggest that this collocation approach provide a number of collocation point which is more consistent with the number of terms in the PCE than the classical one.

Sparse approaches based on model selection techniques Another method proposed by the authors in [BS08b, BS, BS11] uses model selection techniques (Least Angle Regressions schemes [EHJT04a, EHJT04b, HTF09, HCMF08]) to efficiently select the most relevant polynomial basis elements of the full polynomial chaos expansion. The combination of these methods are particularly interesting since they may be use to build iteratively a sparse polynomial chaos metamodel using a small number approximation. By “small”, the authors the authors mean not greater than the number of terms in the expansion, or even possibly significantly smaller. The selection of the most "relevant" polynomials coefficients are performed using statistical correlation measures between the current models and the exact models evaluated on a reference population of small size. The authors also build an adaptive algorithm to stop adding terms in the polynomial expansion when overfitting is detected. This algorithm is applied to a rigid frame with 21 stochastic variables. The LARS adaptive algorithm is used to build a sparse polynomial representation of the displacement of the structure. [HCMF08]

2.2.6.3 Adressing the limited number and erroneous training data

An alternative approach to compute the PCE coefficients, is to characterize them as a random variables. Some approaches have been developed in very recent years in the literature tackling this problem most of the time in an intrusive manner. A very interesting feature of this proposed approach is that they set the computation of the PCE coefficients as a stochastic inverse problem. The coefficients of the PCE are

seen as random variables. Following the same idea as for aPC, classical direct methods for (maximum likelihood, maximum entropy, Bayes' theorem) are applied in order to assess the most probable values of these coefficients with regards to the data at hand. This approach has been investigated in the framework of stochastic inverse problem where the characteristics of random fields have to be identified using some of their realizations. Most of the time the complexity of the random data of interest is reduced using the KL decomposition:

$$\boldsymbol{y}(\omega) = \sum_{i=1}^{n} \kappa^{(i)}(\omega)\boldsymbol{\phi}_i. \tag{2.76}$$

The random variables $\boldsymbol{\kappa} = \{\kappa_1, \ldots, \kappa_n\}$ are then expanded onto a PCE leading to the following approximation:

$$\boldsymbol{y}(\omega) = \bar{\boldsymbol{y}} + \sum_{i=1}^{n} \left(\sum_{\boldsymbol{\alpha}_i, |\boldsymbol{\alpha}_i|=1}^{P} \gamma_{\boldsymbol{\alpha}_i} \Psi_{\boldsymbol{\alpha}_i}(\boldsymbol{\xi}) \right) \boldsymbol{\phi_i}. \tag{2.77}$$

The coefficients to be identified and seen as random variables are the $\boldsymbol{\Gamma} = \{\boldsymbol{\gamma}\}_{i=1}^{n}$. In a set of papers, [DGS$^+$05b, DGS06, DSG$^+$06, DSG07] investigate the use of the maximum likelihood in order to identify the coefficients $\boldsymbol{\Gamma}$ of the reduced PCE expansion . The likelihood function is then written as a function of the coefficients:

$$\mathcal{L}(\boldsymbol{\Gamma}) = \prod_{i=1}^{N} p_{\boldsymbol{\kappa}}(\boldsymbol{\kappa}^{(i)}|\boldsymbol{\Gamma}) \tag{2.78}$$

where $\boldsymbol{\Gamma} = \{\boldsymbol{\gamma}_{\boldsymbol{\alpha}}, |\boldsymbol{\alpha}| \leq q\}$. Then identifying the $\boldsymbol{\gamma}$ set of coefficients lead to the maximization of $\mathcal{L}(\boldsymbol{\gamma})$:

$$\boldsymbol{\Gamma}^* = \underset{\boldsymbol{\Gamma}}{\operatorname{argmax}}\ \mathcal{L}(\boldsymbol{\Gamma}). \tag{2.79}$$

The authors in [DGS$^+$05b] propose the use of the characteristic function to describe each probability density function. Such a methodology may be costly in high dimension and is not always applicable. In a general way, the computation of the probabilities involve Monte Carlo simulations, thus high computational costs. Moreover, another issue consists in performing efficiently the optimization problem on the likelihood function. The authors in [PSBP07, PFS10, BSS07] specially address these issues.

To circumvent this issue, an alternative method has been proposed quite recently and encounter a growing success. It consists in considering the Bayesian approach in order to estimate the posterior probability of the coefficients knowing some evaluation of the $\boldsymbol{\kappa}$ variables. The Bayes' rule is used:

$$p(\boldsymbol{\gamma}|\boldsymbol{y}) = \frac{p(\boldsymbol{y}|\boldsymbol{\gamma})p_{\boldsymbol{\gamma}}(\boldsymbol{\gamma})}{\int p(\boldsymbol{y}|\boldsymbol{\gamma})p_{\boldsymbol{\gamma}}(\boldsymbol{\gamma})d\boldsymbol{\gamma}} \tag{2.80}$$

$$p(\boldsymbol{\gamma}|\boldsymbol{y}) \propto p(\boldsymbol{y}|\boldsymbol{\gamma})p_{\boldsymbol{\gamma}}(\boldsymbol{\gamma}) \tag{2.81}$$

where $p(\boldsymbol{\gamma}|\boldsymbol{y})$ is the *posterior* distribution of the parameters values (obtained after having observed the data), $p(\boldsymbol{y}|\boldsymbol{\gamma}) = \mathcal{L}(\boldsymbol{\gamma})$ is the likelihood function and $p_{\boldsymbol{\gamma}}(\boldsymbol{\gamma})$ is the *prior* probability density function (obtained before having observed the data) of the parameters values.

The full characterization of the posterior probability density function allows to investigate the impact of data limitations associated with the calibration of parameters on the overall predictive accuracy of the

PCE. Moreover, the Gaussian variables of the PC basis may be seen as the part of the approximation modeling the aleatory uncertainty, as the random PC coefficients represent the epistemic uncertainty.

If no information is available on the set of $\boldsymbol{\gamma}$ coefficients, the prior distribution $p_{\boldsymbol{\gamma}}(\boldsymbol{\gamma})$ a non-informative probability distribution [AGS10] may be arbitrary defined. As usual, the likelihood

$$\mathcal{L}(\boldsymbol{\gamma}) = \prod_{j=1}^{n} p_{\boldsymbol{\kappa}}(\boldsymbol{\kappa}^{(j)}|\boldsymbol{\gamma}) \tag{2.82}$$

may be performed using Monte Carlo simulation or more efficiently using the kernel density method [Sco09]. This framework has firstly been proposed in [GD06] and further developed in [AGS10, MDMV12, BSS10].

2.2.6.4 Adressing simultaneously the two problematics

Finally, [Soi10b, SD10] proposes a general framework based on the stochastic identification of the PCE coefficients of a reduced random field expansion aiming at extending the originally proposed approach to high-dimension (several millions of coefficients) polynomial chaos expansions with random coefficients for non-Gaussian tensor-valued random fields using partial and limited experimental data. The proposed methodology consists in the following steps:

- introducing a family of prior probability models,
- identifying an optimal prior model in the constructed family using the experimental data,
- constructing a statistical reduced order optimal prior model,
- constructing the polynomial chaos expansion with deterministic vector-valued coefficients of the reduced order optimal prior model and finally,
- constructing the probability distribution of random coefficients of the polynomial chaos expansion and identifying the parameters using experimental data.

2.2.7 Why is PCE efficient to perform UQ analysis?

2.2.7.1 PCE for robust design

Having computed the set of PC coefficients, a number of convenient analytical features allows to make the use of these techniques particularly attractive for global and local sensitivity analysis, and design under uncertainty in a general way. In fact, the analytical moments of the responses may be obtained in closed form:

$$\begin{array}{rclcl} E[y(\omega)] & = & \displaystyle\sum_{\boldsymbol{\alpha},|\boldsymbol{\alpha}|\leq P} E[\gamma_{\boldsymbol{\alpha}} \mathrm{H}_{\boldsymbol{\alpha}}(\boldsymbol{\xi})] & = & \gamma_0 \\ \sigma^2[y(\omega)] & = & \displaystyle\sum_{\boldsymbol{\alpha},|\boldsymbol{\alpha}|\leq P} E[\gamma_{\boldsymbol{\alpha}} \mathrm{H}_{\boldsymbol{\alpha}}(\boldsymbol{\xi})]^2 - E[y(\omega)]^2 & = & \displaystyle\sum_{\boldsymbol{\alpha},|\boldsymbol{\alpha}|\leq P} \gamma_{\boldsymbol{\alpha}}^2 E[\mathrm{H}^2] \end{array} \tag{2.83}$$

Local sensitivity analysis Introducing non probabilistic variables such as design variable for example gives the following expression:

$$y(\boldsymbol{\xi}) \approx \sum_{\boldsymbol{\alpha},|\boldsymbol{\alpha}|\leq P} \gamma_{\boldsymbol{\alpha}}(\boldsymbol{x})\mathrm{H}_{\boldsymbol{\alpha}}(\boldsymbol{\xi}) \tag{2.84}$$

The sensitivity of the mean and variance responses may be obtained:

$$\frac{d\mu}{dx} = \frac{d}{dx}\gamma_0(x) \tag{2.85}$$

$$\frac{d\sigma^2}{dx} = \sum_{\boldsymbol{\alpha},|\boldsymbol{\alpha}|\leq P} \frac{d}{dx}\gamma_{\boldsymbol{\alpha}}(x)^2 \tag{2.86}$$

where $\frac{d}{dx}\gamma_{\boldsymbol{\alpha}}$ is defined as (the theorem of uniform convergence being verified):

$$\frac{d}{dx}\gamma_{\boldsymbol{\alpha}} = \frac{<\frac{dy}{dx}, \mathrm{H}_{\boldsymbol{\alpha}}>}{<\mathrm{H}^2_{\boldsymbol{\alpha}}>} \tag{2.87}$$

Due to the independence property, the coefficients computed in the last equation may be interpreted either as the nonprobabilistic sensitivities of the chaos coefficients for the response expansion, or as the chaos coefficients of an expansion for the nonprobabilistic sensitivities of the response. The resulting expansion are valid only for a particular set of nonprobabilistic variables and must be in a first approach computed again each time the nonprobabilistic variable are modified.

Another alternative to compute local sensitivities consists in building the stochastic expansion over both stochastic $\boldsymbol{\xi}$ and deterministic $\boldsymbol{x}$ variables. Considering a bounded domain $x_{\text{upper bound}} \leq x \leq x_{\text{lower bound}}$ with no probabilistic content the PCE expansion then becomes:

$$y(\boldsymbol{x},\omega) \approx \sum_{\boldsymbol{\alpha},|\boldsymbol{\alpha}|\leq P} \gamma_{\boldsymbol{\alpha}}\mathrm{H}_{\boldsymbol{\alpha}}(\boldsymbol{x},\boldsymbol{\xi}) \tag{2.88}$$

where Ψ may be built over the tensor product of optimal orthogonal polynomials with regards to the probability measure for each component of $\boldsymbol{\xi}$ and by Legendre polynomial (orthogonal with respect to the uniform distribution) for each component of $\boldsymbol{x}$. In this case, the statistical moment of interest are computed using the scalar product only on the probabilistic variables:

$$\begin{aligned} E[y]_{\boldsymbol{\xi}}(\boldsymbol{x}) &= \sum_{\boldsymbol{\alpha},|\boldsymbol{\alpha}|\leq P} \gamma_{\boldsymbol{\alpha}} E_{\boldsymbol{\xi}}[\mathrm{H}_{\boldsymbol{\alpha}}(\boldsymbol{\xi},\boldsymbol{x})] \\ \sigma^2[y]_{\boldsymbol{\xi}}(\boldsymbol{x}) &= \sum_{\boldsymbol{\alpha},|\boldsymbol{\alpha}|\leq P} E_{\boldsymbol{\xi}}[\Psi_i(\boldsymbol{\xi},\boldsymbol{x})\gamma_i]^2 - E_{\boldsymbol{\xi}}[y(\boldsymbol{\xi},\boldsymbol{x})]^2 \end{aligned} \tag{2.89}$$

Considering this approach one advantage is that the obtained expansion is valid for the full nonprobabilistic variable range and the sensitivity of the statistical moment does not need the sensitivity of the response to be computed. However, by adding another type of variable, the dimension of the PCE is increased which makes its construction more computationally expensive.

2.2.7.2 PCE for sensitivity study

Global sensitivity analysis Recent work from [Sud08] and [CLMM09] introduces the use of PCE to perform global sensitivity analysis. Two types of methodologies are exposed in the literature.

- The regression based methods based on a linear regression of the output random vector on the output vector. Among these methodologies, one may count the Pearson correlation coefficient and the Partial Correlation Coefficient. These are useful to quantify the effect of random input onto the random output if the stochastic model is nearly linear, but fails when in most of the case when the model is non linear.
- The variance based methodologies are more general. Broadly speaking they are based on a decomposition of the variance of the output of interest into summands

First of all let us give an overview of the Sobol decomposition. We consider $\boldsymbol{\xi} = \{\xi_1, \ldots, \xi_M\} \in \mathbb{R}^M$, M independent identically distributed random variables and $y(\boldsymbol{\xi})$ an output function. The Sobol decomposition of the y function is given by:

$$y^{\text{SOBOL}}(\boldsymbol{\xi}) = \sum_{\boldsymbol{u} \subseteq \{1,2,\ldots,M\}} y_{\boldsymbol{u}}(\boldsymbol{\xi}_{\boldsymbol{u}}), \tag{2.90}$$

where $\boldsymbol{u}$ is a set of integers, $\boldsymbol{\xi}_{\boldsymbol{u}} = (\boldsymbol{\xi}_{u_1}, \ldots, \boldsymbol{\xi}_{u_s})$ with s=card($\boldsymbol{u}$). This summand counts 2^M elements. Each of the terms of this summand (except the mean value $y_0 = \bar{y}$) verifies for any $\boldsymbol{\xi}_{u_i}$ the following property: $\int_\Omega y_{\boldsymbol{u}}(\boldsymbol{\xi}_{\boldsymbol{u}}) p(\xi_i) d\xi_i = 0 \ \forall \boldsymbol{u} \ni i$ which implies the orthogonality of the functions y_u: $\int_{\Omega^M} y_u(\xi_u) y_v(\xi_v) p(\xi) d\xi = 0, \forall u \neq v$ and thus the uniqueness of the Sobol decomposition. Each Sobol function y_u may be computed according to:

$$y_u(\xi_u) = \int_{\mathbb{R}^{M-|u|}} y(\xi) p(\xi_{\sim \boldsymbol{u}}) d\xi_{\sim \boldsymbol{u}} - \sum_{\substack{v \subset \boldsymbol{u} \\ v \neq \boldsymbol{u}}} y_v(\xi_v) \tag{2.91}$$

where $\xi_{\sim \boldsymbol{u}}$ denotes the $\boldsymbol{\xi}$ vector without the $\boldsymbol{u}$ components.

We denote y_0 the mean of the output y, V the total variance of the output y,

$$V = \int_{\mathbb{R}^M} y^2(\xi) p(\xi) d\xi - \bar{y}^2 \tag{2.92}$$

and $V_{\boldsymbol{u}}$ the conditional variances of the Sobol functions $y_{\boldsymbol{u}}$.

$$V_{\boldsymbol{u}} = \int_{\mathbb{R}^s} y_u^2(\xi_u) p(\xi_u) d\xi_u \tag{2.93}$$

Thanks to the orthogonality of the decomposition, we have:

$$V = \sum_{\substack{u \subseteq \{1,2,\ldots,M\} \\ u \neq \emptyset}} V_u \tag{2.94}$$

The Sobol sensitivity indices are then defined as:

$$S_{\boldsymbol{u}} = \frac{V_{\boldsymbol{u}}}{V} \tag{2.95}$$

with the following property:

$$\sum_{\substack{u\subseteq\{1,2,\ldots,M\}\\ u\neq\emptyset}} V_u = V. \tag{2.96}$$

$S_{\boldsymbol{u}}$ denotes the s-order sensitivity index where $s{=}card(\boldsymbol{u})$ and measures the sensitivity of the variance of y due only to the interactions of the variables $\xi_{\boldsymbol{u}}$. One may count 2^M-1 sensitivity indices. As this number may increase rapidly with the number of variable, one defined the total sensitivity indices S_{T_i} by:

$$S_{T_i} = \sum_{\boldsymbol{u}\ni i} S_{\boldsymbol{u}}. \tag{2.97}$$

These express the total sensitivity of the variance of y due to the variable ξ_i alone, and all its interaction with the other variables.

To compute the Sobol indices sampling methods may be used but rapidly become unaffordable. Moreover one may exhibit a straightforward relationship between the polynomial chaos coefficients and the Sobol indices [Sud08]. In fact, due to the orthogonality property of the $\{\Psi\}_{i=0}^{P-1}$ the total variance D may be approximated by:

$$V = \int_{\mathbb{R}^M} y^2(\boldsymbol{\xi})p(\boldsymbol{\xi})d\boldsymbol{\xi} - \bar{y}^2 = \sum_{\boldsymbol{\alpha},|\boldsymbol{\alpha}|\leq P} \gamma_{\boldsymbol{\alpha}}^2 E[\mathrm{H}_{\boldsymbol{\alpha}}^2] \tag{2.98}$$

The Sobol decomposition of y is approximated by the Sobol decomposition of y^{PCE}. The elements y_u^{PCE} of the Sobol decomposition of y^{PCE} may be simply obtained by:

$$y_u^{\mathrm{PCE}}(\xi_u) = \sum_{\beta\in\beta_{\boldsymbol{u}}} \gamma_\beta \mathrm{H}_\beta(\xi_u) \tag{2.99}$$

where the selected indices are

$$\beta_u = \{\beta\in\{1,\ldots,P\}, \mathrm{H}_\beta(\xi) = \prod_{i=1}^{s} H_{\alpha_i^\beta}(\xi_{u_i}), \alpha_i^\beta > 0\} \tag{2.100}$$

The approximated conditional variances may then be expressed as:

$$\tilde{V}_u = \sum_{\beta\in\beta_u} \gamma_\beta^2 E[\mathrm{H}_\beta^2] \tag{2.101}$$

and thus the sensitivity indices as:

$$S_u \approx \tilde{S}_u = \frac{\sum_{\beta\in\beta_u}\gamma_\beta^2 E[\mathrm{H}_\beta^2]}{\sum_{\beta=1}^{P}\gamma_\beta^2 E[\mathrm{H}_\beta^2]} \tag{2.102}$$

2.2.7.3 PCE for reliability study

As mentioned earlier, the PCE is not of suitable used to approximate distribution tails and thus may be adapted in order to compute low probability of failure. Different strategies have been adopted in order to adapt the PCE to the computation of small probabilites. A first attempt has been proposed by the authors in [Gha91, Gha99b] to sample the orthogonal residuals in order to improve the prediction

accuracy of the distribution tails. As a first step [PW07] proposes the use of an adapted PCE to the computation of the failure probability. It defines two methodologies: a "shifted" PCE and a "windowed" PCE inspired from the space discretization in ME-gPC.

2.2.8 An open issue: Extension to correlated non Gaussian random variables

The polynomial chaos expansion extends the random process of interest on a set of polynomials depending on standards random variables. However the observed random variables (denoted $\boldsymbol{\xi}_{obs}$) are usually not standards and may be correlated. One may then transform the random variable into standard non correlated random variables and apply the stochastic expansion into the transformed probability space. Two alternatives are briefly formulated.

One alternative consists in numerically generating optimal orthogonal polynomials and to compute their Gauss points and weights using one of the approaches described in the literature. These approaches produce optimal orthogonal polynomials for an arbitrary probability density function, but a gap in theoretical advances stays wide open concerning the assessment of joint probability distributions of correlated random variables with arbitrary probability density functions.

Another alternative consists in using an non-linear transformation in order to transform non-normal correlated distributions on normal independent distributions. These transformations are usually non linear. Among them one may count, the Nataf transformation, the Rosenblatt transformation, and the Box-Cox transformation.

The input of the Nataf transformation are the marginal density functions and the correlation matrix, it does not need the knowledge of the joint probability density function. The traditional Nataf distribution may be applied if and only if the *copula* relative to the random variables $\xi_1, \ldots, \xi_M$ is normal. However, a generalized Nataf transform has been defined and relax the condition on the copula to the elliptical cases.

The Rosenblatt transformation does not require any condition on the copula type of the random variables but requires the knowledge of the cumulative distribution of conditional random variables, which is usually not provided. The (generalized-)Nataf transformation is more suitable for the common case.

Finally a last alternative has been proposed by [SG04] to generalize the polynomial chaos expansion. It proposes a theoretical insight to construct multivariate orthogonal basis when the $\boldsymbol{\xi}$ variables are dependent. In this case, $\mathcal{L}^2(\mathbb{R}^{\boldsymbol{M}}, dp_{\mathbb{R}^{\boldsymbol{M}}})$ has no more a tensor product structure.

2.3 Conclusion

This chapter offered an overview of the different categories of approaches developed in the literature in order to quantify the impact of uncertainties. A special focus has been provided on the efficient use of the Polynomial Chaos Expansion in Uncertainty Quantification in a probabilistic and non-intrusive framework. Since the preliminary work of Wiener on the homogenous Hermite PCE many developments have been made in order to alleviate some of its initial limitations. (Multi-Element) generalized Polynomial Chaos and arbitrary Polynomial Chaos Expansion mainly addresses the issue of the approximation of non smooth stochastic behaviors exploiting the flexibility in the choice of the polynomial basis. Sparse

approaches based on adaptive strategies investigates the computational cost of the construction of the PCE in high dimensional space aiming at circumventing the curse of dimensionality. Based on the sparsity of effect principle, these strategies aimed at identifying in the expansion terms that are the most significant with regards to the response variability. Finally, an emerging set of methodologies consists in considering the coefficients of the PCE themselves as random variable and to identify them by solving an inverse stochastic problem. These approaches notably allows to quantify the impact of missing data on the accuracy of the produced expansion. Significant contributions within this approach also allows to tackle high dimensional problems. This chapter also points out the limitations of these methodologies opening the way to future work. An open issue has still to be addressed concerning the spectral representation of *correlated* random variables. A way to deal with this limitation would be to consider the tensor decomposition of high-dimensional stochastic fields [GNLC13].

Bibliography

[AB99] SK Au and JL Beck. A new adaptive importance sampling scheme for reliability calculations. *Structural Safety*, 21(2):135–158, 1999.

[AB01] SK Au and J L Beck. Estimation of small failure probabilities in high dimensions by subset simulation. *Probabilistic Engineering Mechanics*, 16(4):263–277, 2001.

[Adl81] R J Adler. *The geometry of random fields*. Siam, 1981.

[AGS10] M Arnst, R Ghanem, and C Soize. Identification of Bayesian posteriors for coefficients of chaos expansions. *Journal of Computational Physics*, 229(9):Pages: 3134–3154, 2010.

[Ahm08] SE Ahmed. Markov chain monte carlo: Stochastic simulation for bayesian inference. *Technometrics*, 50(1):97–97, 2008.

[BB90] CG Bucher and U Bourgund. A fast and efficient response surface approach for structural reliability problems. *Structural safety*, 7(1):57–66, 1990.

[Bje88] P Bjerager. Probability integration by directional simulation. *Journal of Engineering Mechanics*, 114(8):1285–1302, 1988.

[BNT07] I Babuška, F Nobile, and R Tempone. A stochastic collocation method for elliptic partial differential equations with random input data. *SIAM Journal on Numerical Analysis*, 45(3):1005–1034, 2007.

[BS] G Blatman and B Sudret. Éléments finis stochastiques non intrusifs par chaos polynomiaux creux et adaptatifs.

[BS08a] G Blatman and B Sudret. Sparse polynomial chaos expansions and adaptive stochastic finite elements using a regression approach. *Comptes-Rendus Mécanique*, 336:518–523, 2008.

[BS08b] G Blatman and B Sudret. Sparse polynomial chaos expansions and adaptive stochastic finite elements using a regression approach. *Comptes Rendus Mécanique*, 336:518–523, 2008.

[BS11] G Blatman and B Sudret. Adaptive sparse polynomial chaso expansion based on least angle regression. *Journal of Computational Physics*, 230:2345–2367, 2011.

[BSL06a] M Berveiller, B Sudret, and M Lemaire. Stochastic finite element : a non intrusive approach by regression. *Revue Européenne de Mécanique Numérique*, 15:81–92, 2006.

[BSL06b] M Berveiller, B Sudret, and M Lemaire. Stochastic finite element: a non intrusive approach by regression. *European Journal of Computational Mechanics/Revue Européenne de Mécanique Numérique*, 15(1-3):81–92, 2006.

[BSS07] E Blanchard, C Sandu, and A Sandu. A polynomial-chaos-based bayesian approach for estimating uncertain parameters of mechanical systems. In *Proceedings of the ASME 2007 International Design Engineering Technical Conferences & Computers and Information in Engineering Conference IDETC/CIE 2007, 9th International Conference on Advanced Vehicle and Tire Technologies (AVTT)*, pages 4–7. Springer, 2007.

[BSS10] E D Blanchard, A Sandu, and C Sandu. Polynomial chaos-based parameter estimation methods applied to a vehicle system. *Proceedings of the Institution of Mechanical Engineers, Part K: Journal of Multi-body Dynamics*, 224(1):59–81, 2010.

[CEP12] P G Constantine, M S Eldred, and E T Phipps. Sparse pseudospectral approximation method. *Computer Methods in Applied Mechanics and Engineering*, 229:1–12, 2012.

[CG95] S Chib and E Greenberg. Understanding the metropolis-hastings algorithm. *The American Statistician*, 49(4):327–335, 1995.

[CLMM09] T Crestaux, O Le Maıtre, and J-M Martinez. Polynomial chaos expansion for sensitivity analysis. *Reliability Engineering & System Safety*, 94(7):1161–1172, 2009.

[CM44] R H Cameron and W T Martin. Transformations of wiener integrals under translations. *The annals of Mathematics*, 45(2):386–396, 1944.

[CM47] R H Cameron and W T Martin. The orthogonal development of non-linear functionals in series of fourier-hermite functionals. *The Annals of Mathematics*, 48(2):385–392, 1947.

[Coo03] R Cools. An encyclopaedia of cubature formulas. *Journal of Complexity*, 19(3):445–453, 2003.

[DGS+05] C Desceliers, R Ghanem, C Soize, et al. Problème stochastique inverse et représentation sur les chaos pour l'identification expérimentale des champs stochastiques modélisants le comportement des milieux élastiques tridimensionnelles. *Actes du 17ème Congrès Français de Mécanique 2005*, 2005.

[DGS06] C Desceliers, R Ghanem, and C Soize. Maximum likelihood estimation of stochastic chaos representations from experimental data. *International Journal for Numerical Methods in Engineering*, 66(6):978–1001, 2006.

[DM96] O Ditlevsen and H O Madsen. *Structural reliability methods*, volume 178. Citeseer, 1996.

[DSB11] V Dubourg, B Sudret, and J-M Bourinet. Reliability-based design optimization using kriging surrogates and subset simulation. *Structural and Multidisciplinary Optimization*, 44(5):673–690, 2011.

[DSD13] V Dubourg, B Sudret, and F Deheeger. Metamodel-based importance sampling for structural reliability analysis. *Probabilistic Engineering Mechanics*, 33:47–57, 2013.

[DSG+06] C Desceliers, C Soize, R Ghanem, et al. Inverse problem for the identification of chaos representations of random fields using experimental vibrational tests. In *Proceedings of ISMA2006: International Conference on Noise and Vibration Engineering*, volume 1, pages 4117–4123, 2006.

[DSG07] C Desceliers, C Soize, and R Ghanem. Identification of chaos representations of elastic properties of random media using experimental vibration tests. *Computational Mechanics*, 39(6):831–838, 2007.

[EHJT04a] B Efron, T Hastie, I Johnstone, and R Tibshirani. Least angle regression. *Annals of Statistics*, 32:407–451, 2004.

[EHJT04b] B Efron, T Hastie, I Johnstone, and T Tibsirani. Least angle regression. *The annals of statistics*, 32(2):407–451, 2004.

[Eld09] MS Eldred. Recent advances in non-intrusive polynomial chaos and stochastic collocation methods for uncertainty analysis and design. *AIAA Paper*, 2274:2009, 2009.

[EMSU12] O G Ernst, A Mugler, H-J Starkloff, and E Ullmann. On the convergence of generalized polynomial chaos expansions. *ESAIM: Mathematical Modelling and Numerical Analysis*, 46(02):317–339, 2012.

[ER93] S Engelund and R Rackwitz. A benchmark study on importance sampling techniques in structural reliability. *Structural Safety*, 12(4):255–276, 1993.

[Far89] L Faravelli. Response-surface approach for reliability analysis. *Journal of Engineering Mechanics*, 115(12):2763–2781, 1989.

[FG07] RV Field and M Grigoriu. Convergence properties of polynomial chaos approximations for l2 random variables. Technical report, Technical report SAND2007-1262. Sandia National Laboratories, Albuquerque, 2007.

[FJG04] RV Field Jr and M Grigoriu. On the accuracy of the polynomial chaos approximation. *Probabilistic Engineering Mechanics*, 19(1):65–80, 2004.

[Fra65] J N Franklin. Numerical simulation of stationary and non-stationary gaussian random processes. *SIAM review*, 7(1):68–80, 1965.

[GD06] R G Ghanem and A Doostan. On the construction and analysis of stochastic models: characterization and propagation of the errors associated with limited data. *Journal of Computational Physics*, 217(1):63–81, 2006.

[Gey92] C J Geyer. Practical markov chain monte carlo. *Statistical Science*, 7(4):473–483, 1992.

[Gha91] R Ghanem. *Stochastic finite Elements: A spectral approach*. Springer, 1991.

[Gha99] R Ghanem. Ingredients for a general purpose stochastic finite elements implementation. *Computer Methods in Applied Mechanics and Engineering*, 168(1):19–34, 1999.

[Gif08] A Giffin. *Maximum entropy: the universal method for inference*. ProQuest, 2008.

[GM04] S Gupta and CS Manohar. An improved response surface method for the determination of failure probability and importance measures. *Structural Safety*, 26(2):123–139, 2004.

[GNLC13] L Giraldi, A Nouy, G Legrain, and P Cartraud. Tensor-based methods for numerical homogenization from high-resolution images. *Computer Methods in Applied Mechanics and Engineering*, 254(0):154 – 169, 2013.

[GS93] R Ghanem and PD Spanos. A stochastic galerkin expansion for nonlinear random vibration analysis. *Probabilistic Engineering Mechanics*, 8(3):255–264, 1993.

[Hab70] S Haber. Numerical evaluation of multiple integrals. *SIAM review*, 12(4):481–526, 1970.

[HCMF08] T Hesterberg, N H Choi, L Meier, and C Fraley. Least angle and l_1 penalized regression: A review. *Statistics Surveys*, 2:61–93, 2008.

[HTF09] T Hastie, R Tibshirani, and J Friedman. *The Elements of Statistical Learning, Data Mining, Inference and Prediction*. Springer, 2009.

[Jay57] E T Jaynes. Information theory and statistical mechanics. *Physical review*, 106(4):620, 1957.

[Jay82] E T Jaynes. On the rationale of maximum-entropy methods. *Proceedings of the IEEE*, 70(9):939–952, 1982.

[KD09] A D Kiureghian and O Ditlevsen. Aleatory or epistemic? does it matter? *Structural Safety*, 31(2):105–112, 2009.

[KKC10] Soo-Chang K, Hyun-Moo K, and Jinkyo F C. An efficient response surface method using moving least squares approximation for structural reliability analysis. *Probabilistic Engineering Mechanics*, 25(4):365 – 371, 2010.

[KL00] CA Kennedy and WC Lennox. Solution to the practical problem of moments using non-classical orthogonal polynomials, with applications for probabilistic analysis. *Probabilistic engineering mechanics*, 15(4):371–379, 2000.

[KPS04] PS Koutsourelakis, HJ Pradlwarter, and GI Schuëller. Reliability of structures in high dimensions, part i: algorithms and applications. *Probabilistic Engineering Mechanics*, 19(4):409–417, 2004.

[KS91] A D Kiureghian and M D Stefano. Efficient algorithm for second-order reliability analysis. *Journal of engineering mechanics*, 117(12):2904–2923, 1991.

[LCM09] M Lemaire, A Chateauneuf, and J-C Mitteau. *Structural Reliability*. Wiley/ISTE,, 2009.

[LCS07] J Liang, S R Chaudhuri, and M Shinozuka. Simulation of nonstationary stochastic processes by spectral representation. *Journal of engineering mechanics*, 133(6):616–627, 2007.

[Loe63] M Loeve. Probability theory. *Graduate Texts in Mathematics*, 45:12, 1963.

[LX10] J Li and D Xiu. Evaluation of failure probability via surrogate models. *Journal of Computational Physics*, 229(23):8966–8980, 2010.

[MD10] M Martinelli and R Duvigneau. On the use of second-order derivatives and metamodel-based monte-carlo for uncertainty estimation in aerodynamics. *Computers & Fluids*, 39(6):953–964, 2010.

[MDMV12] L Mehrez, A Doostan, D Moens, and D Vandepitte. Stochastic identification of composite material properties from limited experimental databases, part ii: Uncertainty modelling. *Mechanical systems and signal processing*, 27:484–498, 2012.

[Mel94] RE Melchers. Structural system reliability assessment using directional simulation. *Structural safety*, 16(1):23–37, 1994.

[MH03] L Mathelin and M Y Hussaini. *A stochastic collocation algorithm for uncertainty analysis.* Citeseer, 2003.

[Mil11] R B Millar. *Maximum likelihood estimation and inference: with examples in R, SAS and ADMB*, volume 111. John Wiley & Sons, 2011.

[MK05] H G Matthies and A Keese. Galerkin methods for linear and nonlinear elliptic stochastic partial differential equations. *Computer Methods in Applied Mechanics and Engineering*, 194(12):1295–1331, 2005.

[NE00] J Nie and B R Ellingwood. Directional methods for structural reliability analysis. *Structural Safety*, 22(3):233–249, 2000.

[ON12] S Oladyshkin and W Nowak. Data-driven uncertainty quantification using the arbitrary polynomial chaos expansion. *Reliability Engineering & System Safety*, 106:179–190, 2012.

[PFS10] B L Pence, H K Fathy, and J L Stein. A maximum likelihood approach to recursive polynomial chaos parameter estimation. In *American Control Conference (ACC), 2010*, pages 2144–2151. IEEE, 2010.

[PNTIG01] M M Putko, P A Newman, A C Taylor III, and L L Green. Approach for uncertainty propagation and robust design in cfd using sensitivity derivatives. *AIAA paper*, 2528:2001, 2001.

[PPS02] B Puig, F Poirion, and C Soize. Non-gaussian simulation using hermite polynomial expansion: convergences and algorithms. *Probabilistic Engineering Mechanics*, 17(3):253–264, 2002.

[PSBP07] F Perrin, B Sudret, G Blatman, and M Pendola. Use of polynomial chaos expansions and maximum likelihood estimation for probabilistic inverse problems. *18ème Congrès Français de Mécanique (Grenoble 2007)*, 2007.

[PW07] M Paffrath and U Wever. Adapted polynomial chaos expansion for failure detection. *Journal of Computational Physics*, 226(1):263–281, 2007.

[RHB04] JR Red-Horse and Allan S Benjamin. A probabilistic approach to uncertainty quantification with limited information. *Reliability Engineering & System Safety*, 85(1):183–190, 2004.

[Rie23] M Riesz. Sur le problème des moments et le théorème de parseval correspondant. *Acta Litt.*, 1:209–225, 1923.

[Sch00] W Schoutens. *Stochastic Processes and Orthogonal Polynomials*. Springer, 2000.

[Sco09] D W Scott. *Multivariate density estimation: theory, practice, and visualization*, volume 383. Wiley. com, 2009.

[SD10] C Soize and C Desceliers. Computational aspects for constructing realizations of polynomial chaos in high dimension. *SIAM Journal on Scientific Computing*, 32(5):2820–2831, 2010.

[SDK00] B Sudret and A Der Kiureghian. Stochastic finite elements methods and reliability- a state of the art. Technical report, Department of civil and environmental engineering, 2000.

[SG02] S Sakamoto and R Ghanem. Simulation of multi-dimensional non-gaussian non-stationary random fields. *Probabilistic Engineering Mechanics*, 17(2):167–176, 2002.

[SG04] C Soize and R Ghanem. Physical systems with random uncertainties: chaos representations with arbitrary probability measure. *SIAM Journal on Scientific Computing*, 26(2):395–410, 2004.

[Soi10] C Soize. Identification of high-dimension polynomial chaos expansions with random coefficients for non-gaussian tensor-valued random fields using partial and limited experimental data. *Computer methods in applied mechanics and engineering*, 199(33):2150–2164, 2010.

[SPK04] GI Schuëller, HJ Pradlwarter, and PS Koutsourelakis. A critical appraisal of reliability estimation procedures for high dimensions. *Probabilistic Engineering Mechanics*, 19(4):463–474, 2004.

[Sud08] B Sudret. Global sensitivity analysis using polynomial chaos expansions. *Reliability Engineering & System Safety*, 93(7):964–979, 2008.

[Sud12] B Sudret. Meta-models for structural reliability and uncertainty quantification. *arXiv preprint arXiv:1203.2062*, 2012.

[Wac96] H Wackernagel. Multivariate geostatistics: an introduction with applications. In *International Journal of Rock Mechanics and Mining Sciences and Geomechanics Abstracts*, volume 33, pages 363A–363A. Elsevier, 1996.

[WC94] A T Wood and G Chan. Simulation of stationary gaussian processes in [0, 1] d. *Journal of computational and graphical statistics*, 3(4):409–432, 1994.

[Wie38] N Wiener. The homogeneous chaos. *American Journal of Mathematics*, 60(4):897–936, 1938.

[WK05] X Wan and G E Karniadakis. An adaptive multi-element generalized polynomial chaos method for stochastic differential equations. *Journal of Computational Physics*, 209(2):617–642, 2005.

[WK06a] X Wan and G E Karniadakis. Beyond wiener–askey expansions: handling arbitrary pdfs. *Journal of Scientific Computing*, 27(1-3):455–464, 2006.

[WK06b] X Wan and G E Karniadakis. Long-term behavior of polynomial chaos in stochastic flow simulations. *Computer methods in applied mechanics and engineering*, 195(41):5582–5596, 2006.

[WK06c] X Wan and G E Karniadakis. Multi-element generalized polynomial chaos for arbitrary probability measures. *SIAM Journal on Scientific Computing*, 28(3):901–928, 2006.

[WK09] X Wan and G E Karniadakis. Error control in multi-element generalized polynomial chaos method for elliptic problems with random coefficients. *Communications in Computational Physics*, 5(2-4):793–820, 2009.

[Won85] F S Wong. Slope reliability and response surface method. *Journal of Geotechnical Engineering*, 111(1):32–53, 1985.

[XH05] D Xiu and J S Hesthaven. High-order collocation methods for differential equations with random inputs. *SIAM Journal on Scientific Computing*, 27(3):1118–1139, 2005.

[Xiu04] D Xiu. *Generalized (Wiener-Askey) Polynomial Chaos*. PhD thesis, Brown University, 2004.

[Xiu07a] D Xiu. Efficient collocational approach for parametric uncertainty analysis. *Communications in computational physics*, 2(2):293–309, 2007.

[Xiu07b] D Xiu. Numerical integration formulas of degree two. *Applied numerical mathematics*, 2007.

[Xiu09a] D. Xiu. Fast numerical methods for stochastic computations: a review. *Comm. Compu. Phys*, 5:242–272, 2009.

[Xiu09b] D Xiu. Fast numerical methods for stochastic computations: a review. *Communications in computational physics*, 5(2-4):242–272, 2009.

[XK02a] D Xiu and G Karniadakis. The wiener-askey polynomial chaos for stochastic differential equations. *J. Sci. Comput.*, 24(2002):619–644, 2002.

[XK02b] D Xiu and G E Karniadakis. The wiener–askey polynomial chaos for stochastic differential equations. *SIAM Journal on Scientific Computing*, 24(2):619–644, 2002.

[XK03a] D Xiu and G E Karniadakis. Modeling uncertainty in flow simulations via generalized polynomial chaos. *Journal of Computational Physics*, 187(1):137–167, 2003.

[XK03b] D Xiu and G E Karniadakis. A new stochastic approach to transient heat conduction modeling with uncertainty. *International Journal of Heat and Mass Transfer*, 46(24):4681–4693, 2003.

[XLSK02] D Xiu, D Lucor, CH Su, and G E Karniadakis. Stochastic modeling of flow-structure interactions using generalized polynomial chaos. *Transactions American Society of Mechanical Engineers - Journal of Fluids Engineering*, 124(1):51–59, 2002.

[XLSK03] D Xiu, D Lucor, C-H Su, and G E Karniadakis. Performance evaluation of generalized polynomial chaos. In *Computational Science—ICCS 2003*, pages 346–354. Springer, 2003.

[YC04] B D Youn and K K Choi. A new response surface methodology for reliability-based design optimization. *Computers & structures*, 82(2):241–256, 2004.

[YS88] F Yamazaki and M Shinozuka. Digital generation of non-gaussian stochastic fields. *Journal of Engineering Mechanics*, 114(7):1183–1197, 1988.

[ZO99] Y-G Zhao and T Ono. A general procedure for first/second-order reliabilitymethod (form/-sorm). *Structural Safety*, 21(2):95–112, 1999.

Chapter 3

A physics-based metamodel approach for springback variability assessment

In this chapter, we address the stochastic analysis of the U-shaped deep drawing process of a metal sheet using a regression based Polynomial Chaos approach. In this context, very small perturbations of the input variables provide the regression points used to build the PCE. We show that a careful attention has to be paid to the resolution [5] of the "high-fidelity" model used to produce those points. In the following, the resolution of the model is of the same order of magnitude than the range of variation of the stochastic variable. We show in this case, that one possible solution to perform the stochastic analysis, consists in defining an intermediate surrogate model. We here consider a physics based metamodel which highlights two advantages. The first one, is to improve the model resolution, and the second one, is to be less computationally costly. This model may then be used in order to build a Polynomial Chaos of the response.

[5] The resolution of a model has been defined on p.8.

A two-pronged approach for springback variability assessment using sparse polynomial chaos expansion and multi-level simulations

Jérémy Lebon, Guénhaël Le Quilliec, Piotr Breitkopf, Rajan Filomeno Coelho & Pierre Villon

International Journal of Material Forming

ISSN 1960-6206

Int J Mater Form
DOI 10.1007/s12289-013-1126-y

Springer

Int J Mater Form
DOI 10.1007/s12289-013-1126-y

ORIGINAL RESEARCH

A two-pronged approach for springback variability assessment using sparse polynomial chaos expansion and multi-level simulations

Jérémy Lebon · Guénhaël Le Quilliec · Piotr Breitkopf · Rajan Filomeno Coelho · Pierre Villon

Received: 20 December 2012 / Accepted: 7 February 2013

Abstract In this study, we show that stochastic analysis of metal forming process requires both a high precision and low cost numerical models in order to take into account very small perturbations on inputs (physical as well as process parameters) and to allow for numerous repeated analysis in a reasonable time. To this end, an original semi-analytical model dedicated to plain strain deep drawing based on a Bending-Under-Tension numerical model (B-U-T model) is used to accurately predict the influence of small random perturbations around a nominal solution estimated with a full scale Finite Element Model (FEM). We introduce a custom sparse variant of the Polynomial Chaos Expansion (PCE) to model the propagation of uncertainties through this model at low computational cost. Next, we apply this methodology to the deep drawing process of U-shaped metal sheet considering up to 8 random variables.

Keywords Springback variability assessment · Sparse polynomial chaos expansion · Semi-analytical bending-under-tension model

Introduction

In order to accurately assess the springback variability of a formed metal sheet one has to take into account uncertainties linked with the deep drawing process (blank-holder forces, tool radius tolerances, punch speed, etc.) as well as those linked with the physical model parameters (material properties, thickness of the metal sheet, etc.). The assessment of the final springback shape variability relies on the combination of two numerical tools: a numerical model of the deep drawing process and a stochastic process to propagate the uncertainties into this model.

In the context of variability study, the numerical model has to be computed for very small variations of the input parameters. Comparing the model error with the variation magnitude of the output function is of paramount importance to ensure the validity of the variability study. The Finite Element Method (FEM) is a standard tool to construct the numerical model which is used consequently to perform sensitivity analysis on springback of sheet metal forming [1] or to perform reliability analysis (coupled to classical reliability methodology) of the deep drawing process [2]. However, the FEM shows important limitations regarding the variability issues. First of all, to model the highly non-linear phenomena involved (large strains, plasticity, frictional contact, etc.) with a high sufficient accuracy for small variations of the input parameters, the model has to be refined in every direction (decreasing the mesh size while preserving a good enough aspect ratio and increasing the number of integration points). This rapidly leads to unaffordable computational costs, specially when a high number of calls is needed. To circumvent this cost issue, alternative approaches have been proposed: in a sensibility analysis context using an analytical model of the springback [3]; in an optimization context using a "one step" inverse approach for the analysis and optimum process design of deep drawn industrial metal part [4], this model is also used in [5] to train a Moving Least Square surrogate to efficiently perform the optimization. A second limitation is that FEM generates intrinsic errors such as a discretization

J. Lebon (✉) · G. Le Quilliec · P. Breitkopf · P. Villon
Laboratoire Roberval, UMR 7337, Université de Technologie de Compiègne, BP 20529, 60205 Compiègne cedex, France
e-mail: jeremlebon974@gmail.com

J. Lebon · R. Filomeno Coelho
BATir Department CP 194/2, Université Libre de Bruxelles (ULB), 50, avenue Franklin Roosevelt, 1050 Brussels Belgium

Published online: 02 March 2013

error (due to mesh size) and computational errors (round-off, quadrature, ...) [6] (page 93). Contact description and through-thickness integration may play a leading role [7].

Common computational methods propagate the uncertainties defined on the random parameters to the shape of the formed metal sheet based on a sampling of the random input parameters (Monte Carlo simulation, Importance Sampling, etc.) and thus require a relatively high number of calls to the underlying computational model. The authors in [3] use Monte Carlo simulations to perform a sensitivity analysis of the springback with regards to process parameters, [2] and [8] use FORM methodology coupled with an enhanced adaptive Monte Carlo methodology to assess the reliability of the deep drawing process. The use of stochastic metamodels combined with advanced sampling methods offers an alternative to the crude sampling methods. The authors in [9] proposes the use of linear and quadratic response surfaces combined with Monte Carlo Simulation to perform the reliability assessment of sheet metal forming process. In [10], a second order Polynomial Chaos Expansion (PCE) is used as a stochastic response surface to assess the reliability of the formed metal sheet with regards to tolerance criteria. However, in these studies, the number of random variables taken into account by the stochastic response surface is limited.

In this paper, we propose an original two-pronged approach to accurately propagate the uncertainties into a "high resolution" model at low computational cost. Our approach is based on a combination of a stochastic surrogate (PCE) and a physics-based Reduced Order Model (ROM). We demonstrate, that in the case of variability study, as the order of magnitude of the variation range decreases the full scale model prediction becomes unstable. We investigate then regularization features of a "high resolution" physics based ROM, allowing us to reach numerical stability for smaller variations of the input variables. Then, a stochastic surrogate model is trained on the full parameter variation range and it is then used to perform the variability study at low computational cost.

In the second section, we introduce the Polynomial Chaos Expansion (PCE) as a stochastic response surface for the uncertainty propagation. We highlight the need of a numerical model characterized by a high precision for small perturbations of the input variables as well as low computational cost. The third section quantifies the limitations of the FEM modeling with regards to the variability problematic by considering "very" small variations of the input parameters around a nominal value. The two following sections introduce the ingredients of the proposed approach: the semi-analytical deep drawing model based on a plain strain Bending-Under-Tension model (denoted semi-analytical B-U-T in the sequel) and the sparse custom version of the PCE (inspired from [11]) for an enhanced accuracy of the variability study at low computational cost. The fourth section introduces the semi-analytical B-U-T and shows how it allows to alleviate the FEM limitations by side stepping the main numerical noise sources (contact description and through-thickness integration). The fifth section discusses a custom sparse version of the PCE, putting into evidence the need to create a sparse polynomial chaos expansion when the number of random variables increases. Finally, the sixth section of the paper illustrates the methodology on the deep drawing process of U-shaped metal sheet with 8 random variables to assess the variability of the springback shape parameters considering a relatively large number of random variables chosen among the most influential ones [1, 10].

Assessing the springback variability using polynomial chaos expansion

The purpose of this paragraph is to provide the necessary evidence for the following rather than giving a comprehensive introduction to the PCE which may be found in [12, 13].

The PCE is a stochastic metamodel, that is intended to give an intrinsic representation of the stochastic behavior of a function y (*scalar random variable*) that is defined as a function of an input random vector $\boldsymbol{\xi} = \{\xi_1, \xi_2, \ldots, \xi_M\}$ with M coordinates and with prescribed probability density function $f_{\boldsymbol{\xi}}(\boldsymbol{\xi})$ [14]. Its accuracy to predict the variability of the *scalar* output function y highly depends on the underlying "high fidelity model".

Building the multi-variate Hermitian PCE

Assuming that $\boldsymbol{\xi}$ has independent Gaussian components and that y is a second order random variable ($\mathbb{E}[y^2] < \infty$), then according to the Cameron Martin theorem, generalized in M dimensions [15] an exact PCE of y is given by

$$y(\boldsymbol{\xi}) = \sum_{j=0}^{\infty} \gamma_j \Psi_j(\boldsymbol{\xi}), \tag{1}$$

where $\{\Psi_j(\boldsymbol{\xi}),\ j = 0, 1, \ldots, \infty\}$ are the multivariate polynomials orthogonal with respect to the natural inner product

$$< \Psi_k, \Psi_l >= \int \Psi_k(\boldsymbol{\xi})\Psi_l(\boldsymbol{\xi}) \prod_{i=1}^{M} f_{\xi_i}(\xi_i) d\xi_i \tag{2}$$

with $f_{\xi_i}(\xi_i)$ the marginal distribution of the i^{th} component of the random vector $\boldsymbol{\xi}$.

For M independent Gaussian random variables, multivariate Hermitian polynomials exhibit the orthogonality property. Given a degree N, the multi-variate set of M^{N+1}

Hermitian polynomials are built using the tensor product of mono-variate Hermitian polynomials. Practically, only a finite $P < M^{N+1}$ number of terms is retained yielding to the reduced expansion

$$y(\boldsymbol{\xi}) \approx \sum_{j=0}^{P-1} \gamma_j \Psi_j(\boldsymbol{\xi}), \tag{3}$$

where

$$P = \frac{(N+M)!}{N!M!}. \tag{4}$$

In order to properly interpret the sparse PCE algorithm, an appropriate scheme for numbering the multi-variate polynomials of degree $d \leq N$ needs to be introduced. The scheme used is illustrated in Table 1 on an example of a 3rd order Hermitian multi-variate PCE with 2 random variables ξ_1 and ξ_2.

Computing the coefficients of the multi-variate PCE

The PCE accuracy highly depends on the precise computation of its P coefficients. An intrusive Galerkin type approach has been first proposed by [14]. Projections based non-intrusive methods take benefit from the orthogonal properties of the multivariate polynomials of the expansion. Equivalent stochastic collocation is based on a Lagrangian interpolation in the stochastic space [16]. These methods are the most accurate but also become rapidly unaffordable in relatievly high dimensions.

The regression based approach (emphasized in this paper) consists in finding the best set of PCE coefficients $\boldsymbol{\gamma} = [\gamma_0, \ldots, \gamma_{P-1}]$ by minimizing the residual error in the least square sense:

$$\boldsymbol{\gamma} = argmin(\|\mathbf{y}(\boldsymbol{\xi}) - \boldsymbol{\Psi}(\boldsymbol{\xi})\boldsymbol{\gamma}^\top\|^2) \tag{5}$$

yielding to

$$\boldsymbol{\gamma} = (\boldsymbol{\Psi}(\boldsymbol{\xi})\boldsymbol{\Psi}(\boldsymbol{\xi})^\top)^{-1}\boldsymbol{\Psi}(\boldsymbol{\xi})\mathbf{y}(\boldsymbol{\xi}) \tag{6}$$

Table 1 Illustration of the numbering scheme used for a 3rd order PCE with 2 random variables

Bi-variate monomials $\Psi(\xi_1, \xi_2)$			
1	ξ_2	$\xi_2^2 - 1$	$\xi_2^3 - 3\xi_2$
ξ_1	$\xi_1\xi_2$	$\xi_1\left(\xi_2^2 - 1\right)$	
$\xi_1^2 - 1$	$\left(\xi_1^2 - 1\right)\xi_2$		
$\xi_1^3 - 3\xi_1$			
Corresponding number of Ψ			
0	2	3	6
1	4	7	
5	8		
9			

where

$$\mathbf{y} = \left[y(\boldsymbol{\xi}^{(1)}), \ldots, y(\boldsymbol{\xi}^{(Q)})\right]^\top, \tag{7}$$

$$\boldsymbol{\Psi} = \begin{bmatrix} \Psi_0(\boldsymbol{\xi}^{(1)}) & \ldots & \Psi_{P-1}(\boldsymbol{\xi}^{(1)}) \\ \vdots & & \vdots \\ \Psi_0(\boldsymbol{\xi}^{(Q)}) & \ldots & \Psi_{P-1}(\boldsymbol{\xi}^{(Q)}) \end{bmatrix} \tag{8}$$

with $\boldsymbol{\xi}^{(i)}, i \in \{1, ..., Q\}$ representing $Q > P$ samples of the M dimensional random vector $\boldsymbol{\xi}$. These samples are generated using a Q sized M dimensional standard normal LHS sampling.

The optimal Q number of samples needed to assess the coefficients with a good accuracy is still an open research area, but an empirical rule proposes $Q \geq (M-1) \times P$ [17]. Once the set of P coefficients $\{\gamma_0, ..., \gamma_P - 1\}$ has been determined, one may compute the statistical moments of y analytically avoiding Monte Carlo simulations. The first two moments are given by:

$$\mathbb{E}(y) = \gamma_0 \tag{9}$$

$$\sigma^2(y) = \sum_{j=1}^{P-1} \mathbb{E}\left(\Psi_j^2\right)\gamma_j^2 \tag{10}$$

For an accurate assessment of the statistical moments, a special attention has to be given to the computations of the P coefficients (9, 10). Thus, according to Eq. 6, the underlying model has to be as accurate as possible. Moreover, computing the whole set of coefficients may require a high number of calls $Q = (M-1) \times P$ to the underlying model as P (4) increases exponentially with the number of variables M and the degree N.

In the following section we introduce a test case and we quantify the precision requirements for the simulation model. We show that using typical FEM simulations may lead to inaccurate results for a reasonable computational cost when small perturbations are involved.

Inpact of through-thickness integration on the springback prediction

Test case

To illustrate the issue of model variability with regards to small perturbations, we choose to model a 2D deep drawn U-shaped metal sheet. The example used here corresponds to the B3 benchmark test proposed in the conference Numisheet '93 [18] (blank made of mild steel, blank holder force = 2.45 kN). We propose here to use the legacy software ABAQUS v6.10. The model we use is directly based on the implemented example [19].

The Fig. 1 gives the overall geometrical configuration of the deep drawing process.

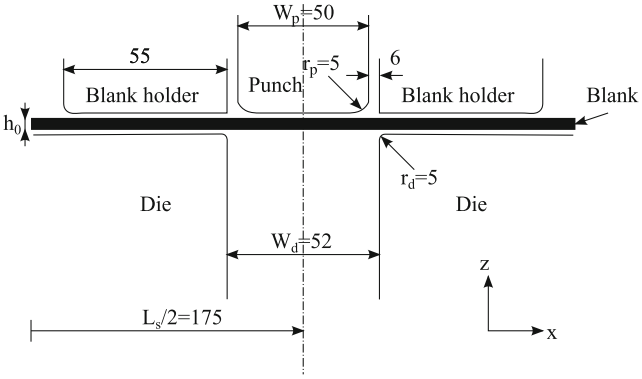

Fig. 1 Geometrical configuration of the modeled Numisheet'93 benchmark (values in *mm*)

The problem is symmetric (Fig. 1), thus only a half structure is modeled using appropriate symmetry boundary conditions. The blank is modeled using a single row of 175 first-order shell elements (S4R) with Simpson integration rules (7 integration points across the thickness). As the problem is essentially in plane strain state (the width of the blank is 35 mm and its thickness nominal value is 0.8 mm), corresponding boundary conditions are applied on each node. The blank is made of mild steel modeled as an elastic-plastic material. Isotropic elasticity and the Hill 48 [20] anisotropic yield criterion for the plasticity are considered. The following values are used:

- Young's modulus: 206 GPa,
- Poisson's ratio: 0.3,
- Yield strength: 167 MPa,
- Anisotropic yield criterion: $r_{00} = 1.79$, $r_{45} = 1.51$, $r_{90} = 2.27$.

The tools (punch, blank holder and die) are modeled as rigid body surfaces. The contact occurring during forming phase is modeled using contact pairs.

The punch velocity is taken here as 15 m/s and its displacement is $s = 70$ mm. The blank holder force is defined as $F_b = 2.45$ kN and a mass of 5 kg is attached.

The whole deep drawing process is simulated in two steps. The forming phase is modeled using the common dynamic explicit approach to solve the problem in a reasonable computational time. During this period, the blank holder force is applied with a smooth ramp to minimize the inertia effect and the punch velocity using a triangle step definition starting and ending with 0 velocity and reaching the 15 m/s with the half run.

To investigate the sensitivity limit of this model, we choose to uniformly vary the thickness of the blank from 0.7 mm to 0.9 mm with an 0.002 mm increment size. For each thickness value the springback shape parameters, the curvature ρ, the angles β_1 and β_2 are measured as shown in Fig. 2.

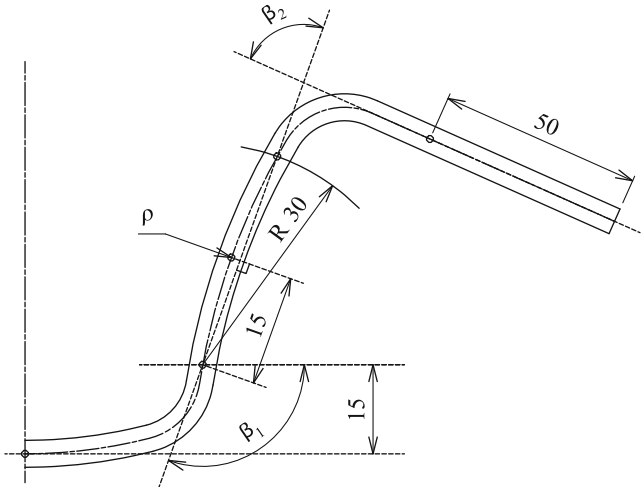

Fig. 2 Definition of springback parameters, ρ, β_1 and β_2

The results of the simulations are depicted in Fig. 3 for 7 integration points across the thickness.

The observed responses (Fig. 3(*left*)) highlight numerical instabilities for small variations (0.04 *mm*) of the thickness parameter. A deeper insight into the sensibilities (Fig. 3(*right*)) shows that the model may be used for thickness variations up to an order of $\Delta x \approx 10^{-5} m$ which is insufficient to perform a variability study. Moreover, to perform a variability study, an unaffordable number of calls to the fine FEM model may be necessary.

Investigation on the numerical instability on FEM modeling

We model a section of the metal sheet submitted to a typical 2D deep drawing process undergoing bending-unbending loading path and focus on the in-plane stress σ_{tt} distribution across the thickness.

When increasing the number of integration points across the thickness, the in-plane stress σ_{tt} profile through the section reaches numerical convergence shown in figure Fig. 4(*left*) when the number of integration points through the section is increased from 2 to around 200 (Fig. 4(*right*)). The convergence is assessed using the following mean square error

$$Err = \frac{\sum_{i=1}^{I} \left(\sigma_i - \sigma_i^{\text{ref}}\right)^2}{\sum_{i=1}^{I} \left(\sigma_i^{\text{ref}}\right)^2}, \tag{11}$$

where I is the number of integration points and σ_i^{ref} corresponds to the stress profile obtained with 200 integration points through the section.

This conclusion is in conformity with [7] where adaptive integration was investigated reducing the number of integration points (from 50 to 11). Moreover, among other numerical instability sources one may identify the coarsity

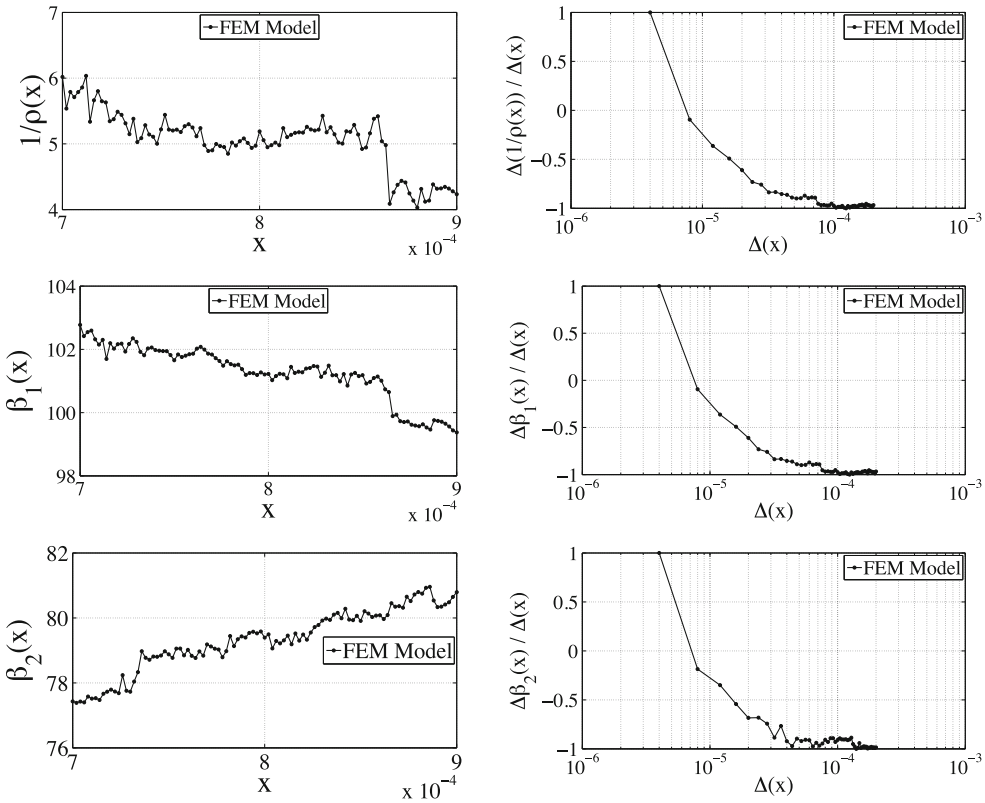

Fig. 3 Numerical instability for FEM simulations of the deep drawing process of 2-D U-shaped metal sheet under small variations of the thickness (m). On the *left side*, the obtained responses are depicted, as on the *right side* the numerical sensitivities of the model with regards to different order of magnitude of thickness variation is plotted

of the mesh. To reach a higher accuracy, the mesh of the FEM model has to be refined in every direction (preserving the same aspect ratio). Another limitation to FEM simulations of deep drawing process is contact modeling, also known to induce a non negligible numerical noise and low convergence rates. This leads to the conclusion that using a full scale refined FEM model to perform the variability study becomes rapidly unaffordable.

In the following two sections we successively describe the two ingredients of the proposed two-pronged approach: the semi-analytical B-U-T model (introduced in [21]) to alleviate the main FEM limitations for small variations of input parameters, and the sparse PCE to propagate the uncertainties at low computational cost.

A semi-analytical bending-under-tension model for deep drawing applications

In this section, we describe the first ingredient of the two-pronged approach, namely, the physics based reduced order model. We choose a semi-analytical approach introduced in [21] based on a B-U-T model, and highlight how it decreases numerical instabilities while preserving a reasonable precision and low computational costs.

Semi-analytical bending-under-tension model (B-U-T)

The semi-analytical B-U-T model considers the deep drawing process of a 2D U-shaped metal sheet as a 2D plain

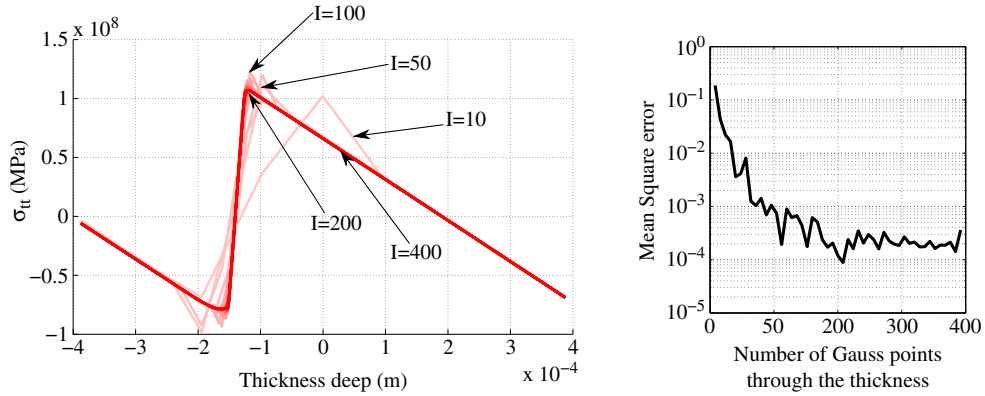

Fig. 4 Evolution of the stress across the section for different number of integration points (thickness 0.8 mm)

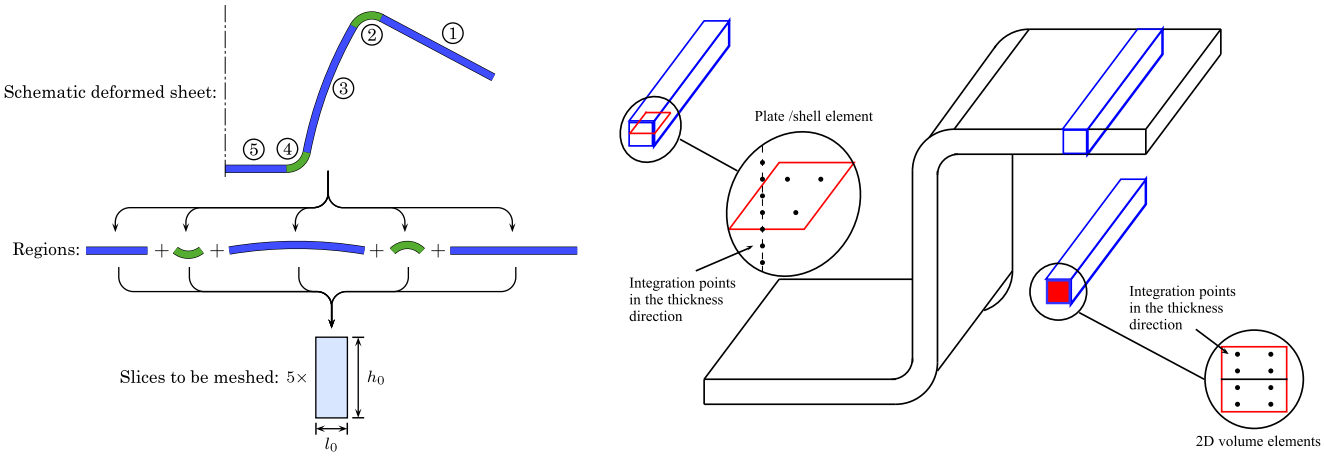

Fig. 5 Finite element description of one slice of the metal sheet

strain Bending-Under-Tension (B-U-T) forming process with negligible shear stress (the width of the sheet being sufficiently large). It is based on a semi-analytical numerical approach which combined an analytical approach with finite element modeling taking benefit from material laws independence and avoiding time consuming and low convergence issues such as contact modeling and high number of degrees of freedom. This model may be constructed in three steps [21]:

1. The first step consists in identifying a finite (usually small) number of regions of the metal sheet with an homogeneous loading state in the length direction. For the U-shaped sheet (as shown in the Fig. 5(*left*)) 5 regions are identified. Knowing the behavior of a single typical section of one of these regions is sufficient to deduce the behavior of the whole region as the loading state is supposed homogeneous in each region. This section (or slice) may be modeled by a handful of 2D/3D solid element or even a single shell element as shown in Fig. 5.
2. The second step consists in defining the loading path that the region is subjected to and to divide it into a sequence of loading states. For each sequence, particular boundary conditions are automatically applied (the reader is invited to refer to [21] for more details on the boundary conditions for each loading state.).
3. Finally, in the last step the whole model is integrated and the springback shape is reconstructed.

Assessment of the numerical noise in the springback shape parameters

Considering the semi-analytical B-U-T model, only very few finite elements are needed to model the deep drawing and springback phases. Moreover, the contact modeling of metal sheet with the punch and/or with the die does not induce numerical noise: the contact is modeled using an analytical uniform pressure applied on the lower or upper side of each slice. In this semi-analytical model no friction is directly applied, but its main effect, the induced tensile force, is taken into account [21]. To highlight the influence of the through-thickness integration, we use the B-U-T model with the configuration described in Table 2 and compare the springback shape parameters obtained for small variations of the thickness.

The same range of thickness values as in Fig. 3 is considered. Four nodes plate elements model each slice of the B-U-T model. P_{10}, P_{50}, P_{400} plates use respectively 10, 50, 400 integration points across the sections. As shown in Fig. 6, the through-thickness integration noise is non-negligible for the B-U-T model. For a large range of variation, numerical instabilities may be observed using 10 integration points, and a smooth response may be observed

Table 2 Geometrical, material, loading and contact parameter of the U-shaped B-U-T model

Geometry		Material		Loading		Contact	
L_s	300 mm	E	70.5 GPa	F_b	300 kN	μ	0.15
h_0	0.8 mm	ν	0.342	s	60 mm		
W_s	1 mm	ρ	2700 kg/m^3				
r_p	10 mm	H	1.5 GPa				
W_d	62 mm						
r_d	10 mm						

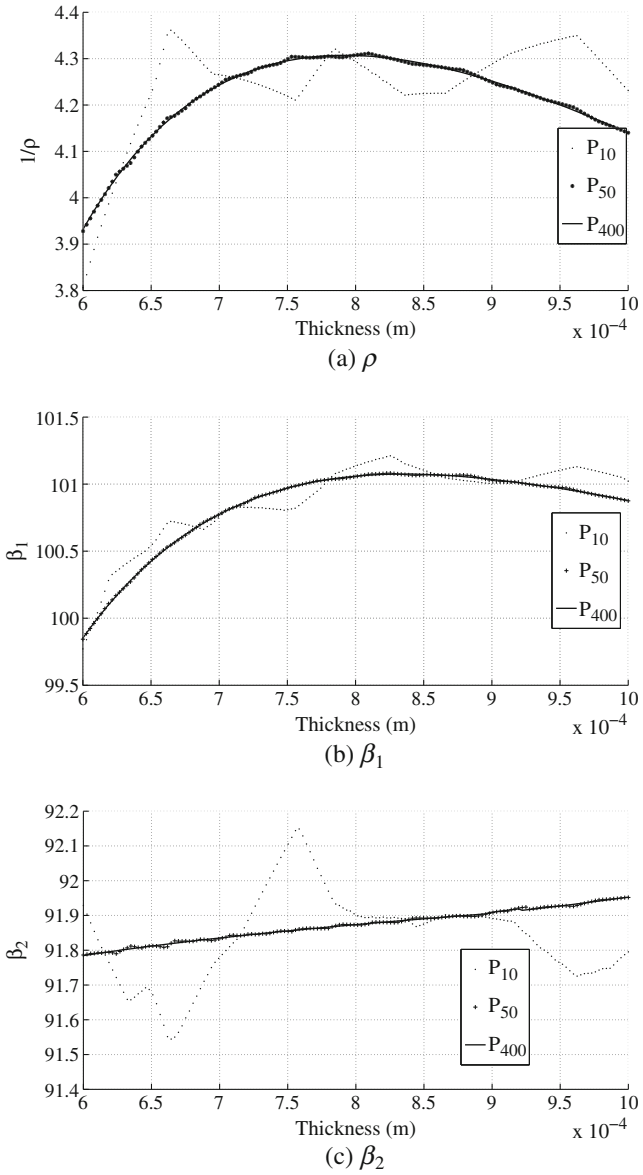

Fig. 6 Evolution of ρ, β_1 and β_2 with regards to small thickness variation for different numbers of through-thickness integration points

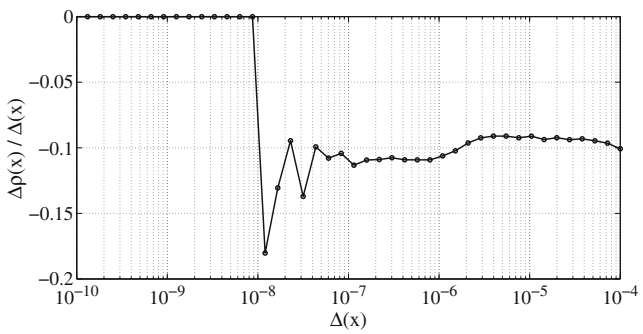

Fig. 7 Evolution of $\Delta\rho/\Delta(x)$ with regards to different order of magnitude of thickness variation Δx, around the nominal value of 0.8 mm

using 50 and 400 integration points. When focusing to a smaller range of variation a smooth response is only observed with 400 integration points.

As only one slice is considered at a time, considering as many integrations points through the sections becomes computationally affordable on the contrary to a full FEM. Moreover a variability study is possible for a variation range $[10^{-4}; 10^{-7}]$ m uncovered by the refined FEM model (Fig. 7). We thus retain the B-U-T model to construct the custom PCE surrogate introduced in the next section.

Sparse polynomial chaos expansion approach using least angle regression stagewise algorithm

In this section, the second ingredient of the two-pronged approach, namely, the sparse PCE is described. When using the regression scheme (6) in a high dimensional space, the computational cost to compute the full PCE rapidly becomes unaffordable. Strategies to truncate the PCE are needed in order to reduce the number of terms by retaining the most significant ones (*Sparsity of effect principle*).

Some methods inspired from model selection schemes have been proposed to create a sparse approximation of the PCE [11]. Among them l_1 penalization methods are the most popular. A review of these methods may be found in [22] and also in [23]. These studies highlight that among the great number of methods, Least Angle Regression Stagewise (LARS) is the most efficient method [24].

We build here a custom algorithm based on the Least Angle Regression Stagewise.

Let us first define the J^{th}-sparse approximation of the output function y by:

$$\tilde{y}^J_{\mathcal{A}}(\boldsymbol{\xi}) = \sum_{j\in\mathcal{A}} \gamma_j \Psi_j(\boldsymbol{\xi}) \tag{12}$$

where $\mathcal{A}$ is a sparse index set with $\text{card}(\mathcal{A}) = J$ and $J \leq P$. Then $\mathcal{A}$ only contains the set of J indices taken among $\{\Psi_j, j \in \{0, \ldots, P-1\}\}$.

The J^{th} residual vector is then defined as:

$$\mathbf{r}_J = \mathbf{y} - \tilde{\mathbf{y}}^J_{\mathcal{A}} \tag{13}$$

and the corresponding J^{th} correlation vector as

$$\tilde{\mathbf{c}}_J(\tilde{\mathbf{y}}) = \boldsymbol{\Psi}^\top \left(\mathbf{y} - \tilde{\mathbf{y}}^J_{\mathcal{A}}\right) \tag{14}$$

The proposed algorithm proceeds as follows:

Offline phase:

1 Build a stochastic design of experiments. Q samples on the hypercube $[0, 1]^M$ are performed using a "space filling" Latin Hypercube Sampling. The corresponding

normal standard realizations are then retrieved using an iso-probabilist transformation (using the invert multivariate Gaussian PDF):

$$\boldsymbol{\xi} = \{\boldsymbol{\xi}^{(1)}, \ldots, \boldsymbol{\xi}^{(M)}\} = \begin{pmatrix} \xi_1^{(1)} & \xi_2^{(1)} & \ldots & \xi_M^{(1)} \\ \xi_1^{(2)} & \xi_2^{(2)} & \ldots & \xi_M^{(2)} \\ \vdots & \vdots & \ddots & \vdots \\ \xi_1^{(Q)} & \xi_2^{(Q)} & \ldots & \xi_M^{(Q)} \end{pmatrix}$$

At this stage, $\boldsymbol{\xi}$ is a M-dimensional standard gaussian random variable: $\boldsymbol{\xi} \in \mathcal{N}_M(0, 1)$ represented by Q samples. Finally, the small random variations of the parameters are modeled by scaling each random variable to the desired means $\boldsymbol{\mu} = [\mu_1, \ldots, \mu_M]$ and standard deviations $\boldsymbol{\sigma} = [\sigma_1, \ldots, \sigma_M]$ according to the probabilistic model (see Table 3 as an example). We denote $\boldsymbol{\xi}_{\boldsymbol{\mu},\boldsymbol{\sigma}}$, the set of random variables matching the probabilistic models requirements.

2 For each $Q - sized$ sample $\{\boldsymbol{\xi}^{(1)}_{\boldsymbol{\mu},\boldsymbol{\sigma}}, \ldots, \boldsymbol{\xi}^{(M)}_{\boldsymbol{\mu},\boldsymbol{\sigma}}\}$ the corresponding evaluations of the "high fidelity" model are stored in $\mathbf{y}$ (7).

3 Choose an arbitrary N (high) degree PCE composed of P orthogonal multivariate monomials $\{\Psi_0, \Psi_{P-1}\}$. In the case where independent random Gaussian variables are considered as, multivariate Hermitian polynomials satisfy the orthogonality property (2) with regards to the measures $f_{\xi_i}(\xi_i) = \frac{1}{\sqrt{2\pi}} e^{-\frac{1}{2}\xi_i^2}, i = 1, \ldots, M$. Build the $\boldsymbol{\Psi}$ matrix (8) by evaluating each orthogonal multivariate monomial $\{\Psi_0, \Psi_{P-1}\}$ on the $Q - sized$ sampling $\{\boldsymbol{\xi}^{(1)}, \ldots, \boldsymbol{\xi}^{(M)}\}$.

Online phase:

1 Initialize the coefficients $\gamma_0, ..., \gamma_{P-1} = 0$ which sets the current residual $\mathbf{r}$ equals to $\mathbf{y}$ obtained in the *offline phase*.

2 Compute the correlation vector $\widetilde{\mathbf{c}}_0$ between each element of $\boldsymbol{\Psi}$ and $\mathbf{y}$. Retain the predictor ψ_{j^*} where $j^* = \arg max|\widetilde{\mathbf{c}}_0|$. The model then becomes $\mathbf{y} = \gamma_j \psi_j = \boldsymbol{\gamma}_{(1)}^{\top} \boldsymbol{\psi}$.

3 Update γ_j to $\gamma_j^* = \gamma_j + \epsilon_{(1)}^*$, where $\epsilon_{(1)}^*$ is the LARS step: at this step, another predictor ψ_{l^*} has as much correlation with the current residual as does ψ_{j^*} (see [24] for numerical computations of ϵ^*). Add ψ_l^* to the current basis: $\mathbf{y} = \gamma_j^* \psi^* + \gamma_l^* \psi_l^* = \boldsymbol{\gamma}_{(2)}^{\top} \boldsymbol{\psi}$.

4 Update jointly $\boldsymbol{\gamma}_{(2)} = \{\gamma_{j^*}, \gamma_{l^*}\}$ following the direction $\mathbf{u}_{(2)}$ ($\|\mathbf{u}_{(2)}\| = 1$) defined by the joint least-square coefficient on the current residual: $\boldsymbol{\gamma}_{(2)}^* = \boldsymbol{\gamma}_{(2)} + \boldsymbol{\epsilon}_{(2)}^* \times \mathbf{u}_{(2)}$. At this step another predictor ψ_k is found to have much correlation with the current residual and is added to the model.

5 Repeat step 4 until $m = min(P; Q)$ predictors have been entered or until the empirical error (15) has reached the desired threshold.

Each step of the algorithm allows us to add one term to the basis chosen according to its correlation with the current residual. The best obtained model $y_{\mathcal{A}^*}$ is chosen to give a low enough empirical error

$$\text{Err}_{\text{emp}} = \frac{\mathbb{E}\left[(\tilde{f}_{\mathcal{A}} - f)^2\right]}{\sigma(f)^2}. \tag{15}$$

Once the best model is obtained, the sparse coefficients values are computed according to Eq. 6. If the number Q of available simulations is too low to reach the condition $Q \geq (M - 1) \times P$ then the design of experiment may be enriched and the previous algorithm run again. As all computations are analytical, running the algorithm as many times as necessary is considered to have a negligible cost.

The combination of LARS and PCE allows us to propagate the uncertainties through the model at low computational costs. Nevertheless the accuracy of the results highly depends on the accuracy of the "high fidelity" model which has to be accurate for small random variations on the input parameters.

Table 3 Stochastic input normal random variables for the springback shape parameter study

Parameters	Mean	Std dev
Blank thickness	0.8 mm	3 %
Young's modulus	70.5 GPa	3 %
Yield Strength	0.180 GPa	3 %
Poisson's ratio	0.342	3 %
Friction coefficient	1.50e-1	3 %
Radius of the punch	10 mm	3 %
Radius of the matrix	10 mm	3 %
Clamp force	600 kN	3 %

Illustration of the two-pronged B-U-T/sparse PCE approach

In this section, we combine the ingredients of the two-pronged approach on the springback variability assessment of a 2D deep drawn U-shaped metal sheet introduced in section "Test case". We demonstrate the validity of the proposed approach firstly when a single random variable (blank initial thickness) is considered (*mono-variate case*) and then the whole probabilistic model is considered (*multi-variate case*) in which the standard variation has been arbitrarily fixed at 3 % of the mean value for each variable so that the

variation of each variable implies a variation in the input parameters with a comparable order of magnitude.

Mono-variate case using full PCE

As an introductory example, we consider the thickness as the unique random normal variable (according to the first line of Table 3) and use Hermitian PCE to assess the stochastic behavior of the springback shape parameters ρ, β_1 and β_2. As shown in Fig. 8, for each of these responses, the convergence is reached for the mean and standard deviation respectively for a PCE of order 5, 5 and 7. A 7^{th} order polynomial chaos expansion may be chosen for all the responses. This expansion contains 8 terms and thus $Q = 56$ calls to the model are needed to compute the whole set of coefficients (6). Additionally, the Fig. 8 also compares the values for the mean and the standard deviation obtained using a post-treatment of the coefficients (circles) (using the equations 9 and 10) and 10^4 Monte Carlo simulations (line) on the PCE surrogate. A good agreement is observed.

The Fig. 9(*left*) compares the 7^{th} order PCE surrogate to simulations using the "high-fidelity" B-U-T model around the nominal value of the thickness $x = 8.10^{-4}m$. It shows that the responses most affected by the thickness variation are ρ and β_1. For these responses, a good fit is observed. Considering the response β_2, a slight error may be observed specially when comparing the responses values corresponding to low probable values of the thickness. These localized errors on non probable values have a limited influence on the evaluation of the mean and standard deviation as noticed in Fig. 8.

The *right* side of the Fig. 9 illustrates good agreement of the probability density function obtained with 10^5 Monte Carlo simulations on the PCE metamodel with the one obtained by sampling the B-U-T model directly.

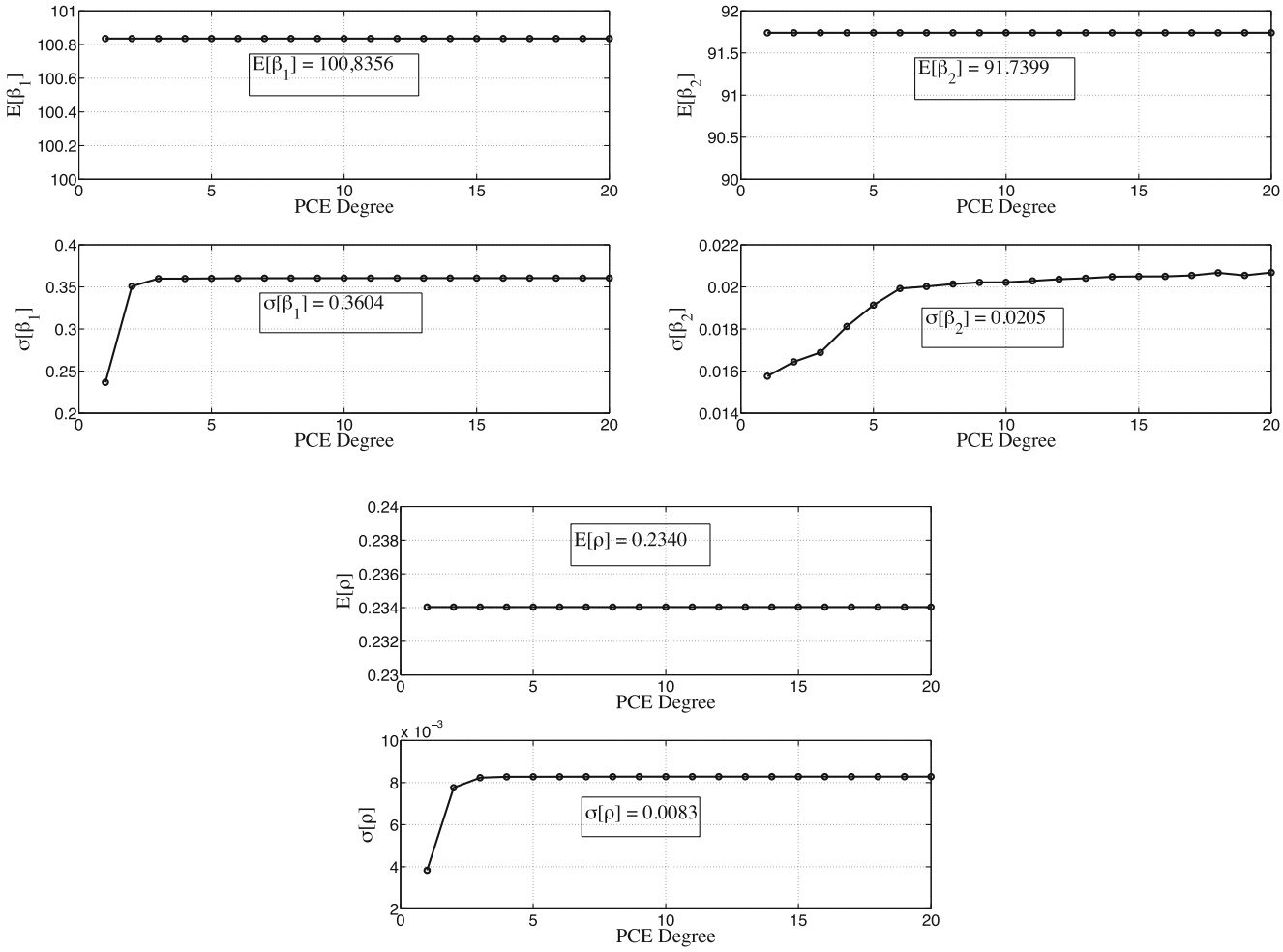

Fig. 8 Convergence in Mean and Standard deviation with regards to the polynomial degree for ρ, β_1, β_2

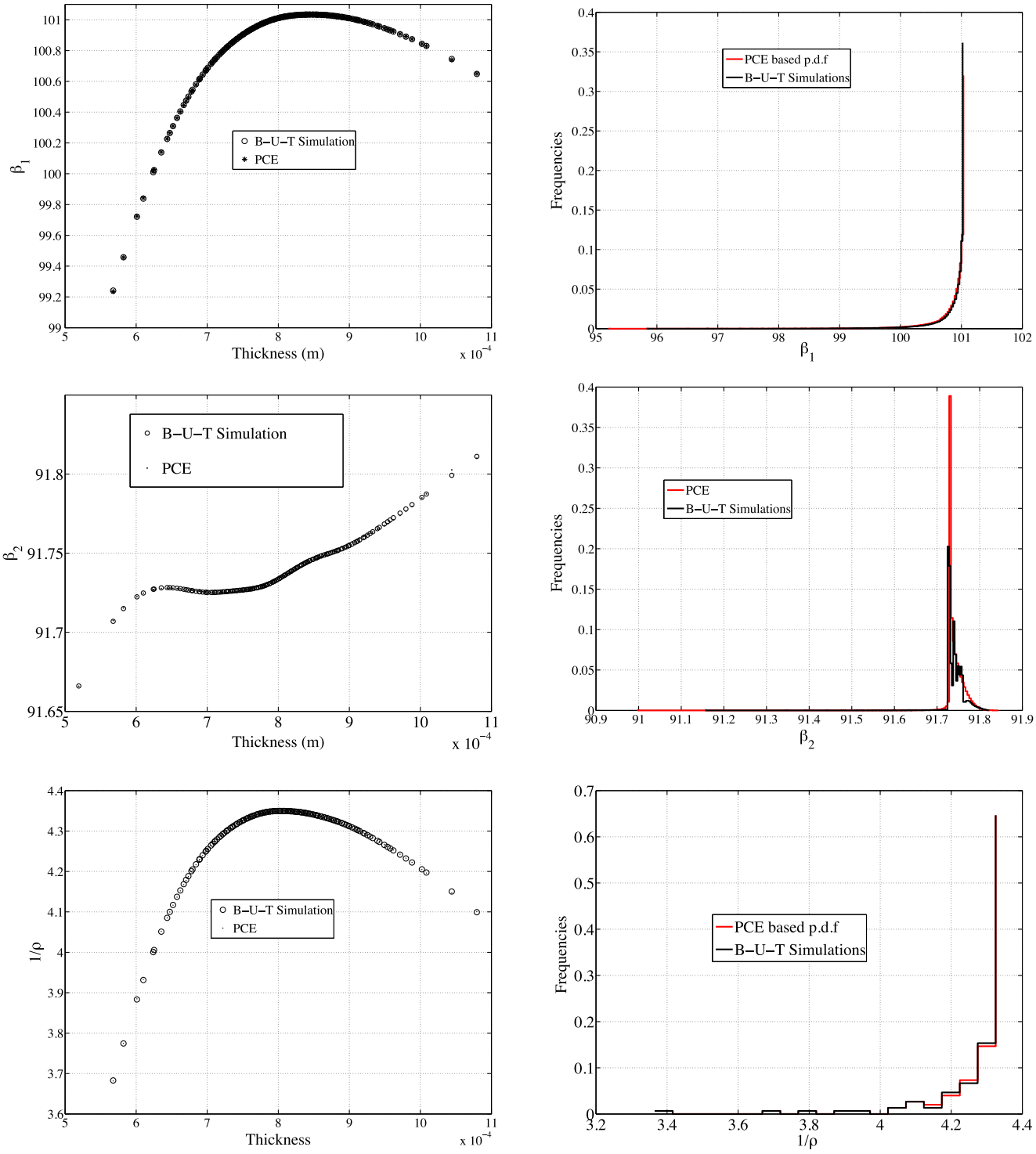

Fig. 9 PCE approximation of ρ, β_1, β_2 and its corresponding p.d.f in comparison the B-U-T simulations

Multi-variate case using LARS based sparse PCE

In order to illustrate the performance of the approach for an increasing number of variables, we consider now the full set of normal random variables described in Table 3.

In this study, we choose an a priori $N = 5^{\text{th}}$ order PCE with 8 variables yielding to $P = 1287$ polynomial terms. $Q = (M-1) \times P \approx 9000$ simulations would be necessary to compute the whole set of coefficients using the collocation scheme (6). We apply the LARS strategy proposed

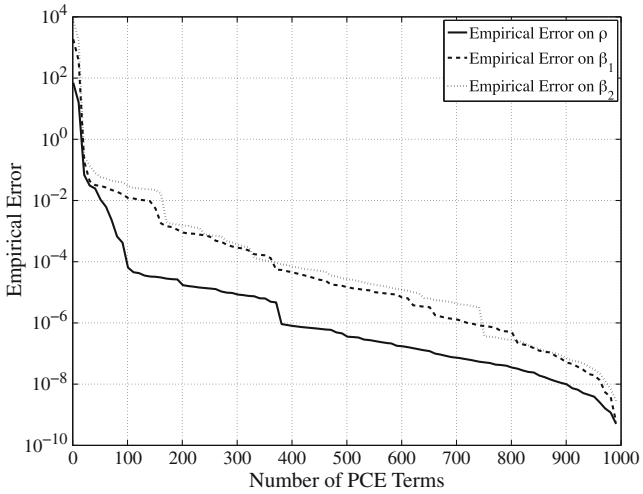

Fig. 10 Evolution of the empirical error when increasing the number of PCE terms using LARS algorithm

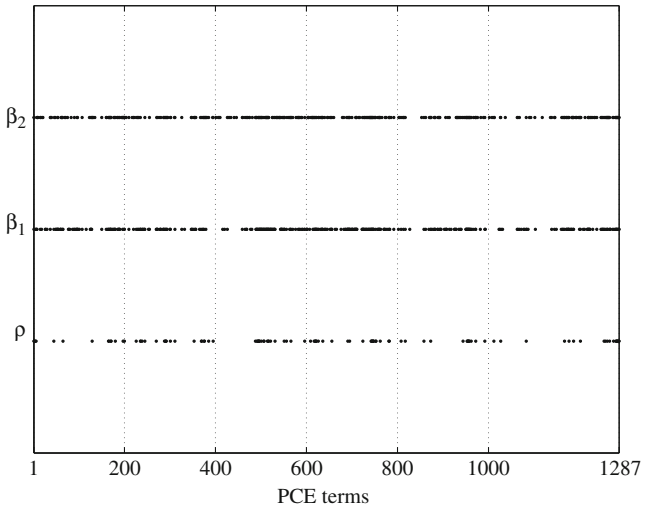

Fig. 11 Representation of the sparsity of the polynomial basis after the LARS algorithm (see section "Sparse polynomial chaos expansion approach using least angle regression stagewise algorithm") has been applied for each response ρ, β_1, β_2. A point corresponds to the presence in the basis of one polynomial according to the numbering scheme illustrated in Table 1

in the previous section, with a stopping criterion on the empirical error. We stop the algorithm when the criterion error reaches 10^{-4}.

The Fig. 10 exhibits the convergence rate of the empirical error as the terms are added step by step during the LARS procedure. The error threshold 10^{-4} is reached for the number of PCE terms given in the second column of the Table 4 for ρ, β_1, β_2.

Considering this empirical error, the Fig. 11 illustrates for each response the retained polynomials (numbered according to the procedure described in the first section.)

A more general insight is given in Table 5 which exhibits the number of polynomial terms with regards to their degree in the LARS PCE expansion. We show *a posteriori* that considering this level on the empirical error, a 4^{th} order polynomial approximation is enough to assess the springback variability of responses β_1 and β_2 while for ρ, only a sparse 3^{rd} PCE approximation is needed.

Considering the obtained histograms (using $1,000$ Monte Carlo simulations on the B-U-T model and the PCE model) in Fig. 12 a good agreement for each response is observed. Comparing with the obtained histograms in Fig. 9(*left*) (when only the thickness was considered as a random variable), we note that according to our stochastic model, the same variables ρ and β_1 are the most affected by randomness on the input parameters. Moreover, the mean value has moved for the responses $1/\rho$, β_1, β_2 respectively from $4.36\,\text{mm}^{-1}$, 100.83, 91.74 to $9.6\,\text{mm}^{-1}$, 112.28, 91.11. Except for β_2, whose variation range is small compared to ρ and β_1, considering the full stochastic model highly affects the variability responses: the mean computed in the mono-variate case corresponds to low probable values in the multi-variate case, and the type of the p.d.f for these responses is highly modified. An exponential type distribution is observed in the mono-variate case as with the full stochastic probabilistic model, a nearly symmetric distribution characterizes the responses variability.

Table 4 Empirical error and number of retained coefficients using LARS procedure

Springback parameters	Err_{emp}	Nb of terms	
		LARS	Full PCE
ρ	1,042e-4	112	1287
β_1	1,009e-4	381	1287
β_2	1,05e-4	383	1287

Table 5 Proportion of terms sorted according to their degree in LARS based PCE for each response ρ, β_1, β_2

Polynomial degree	Number of terms in PCE		
	ρ	β_1	β_2
0	1	1	1
1	8	6	8
2	33	28	31
3	69	92	97
4	0	254	245
5	0	0	0

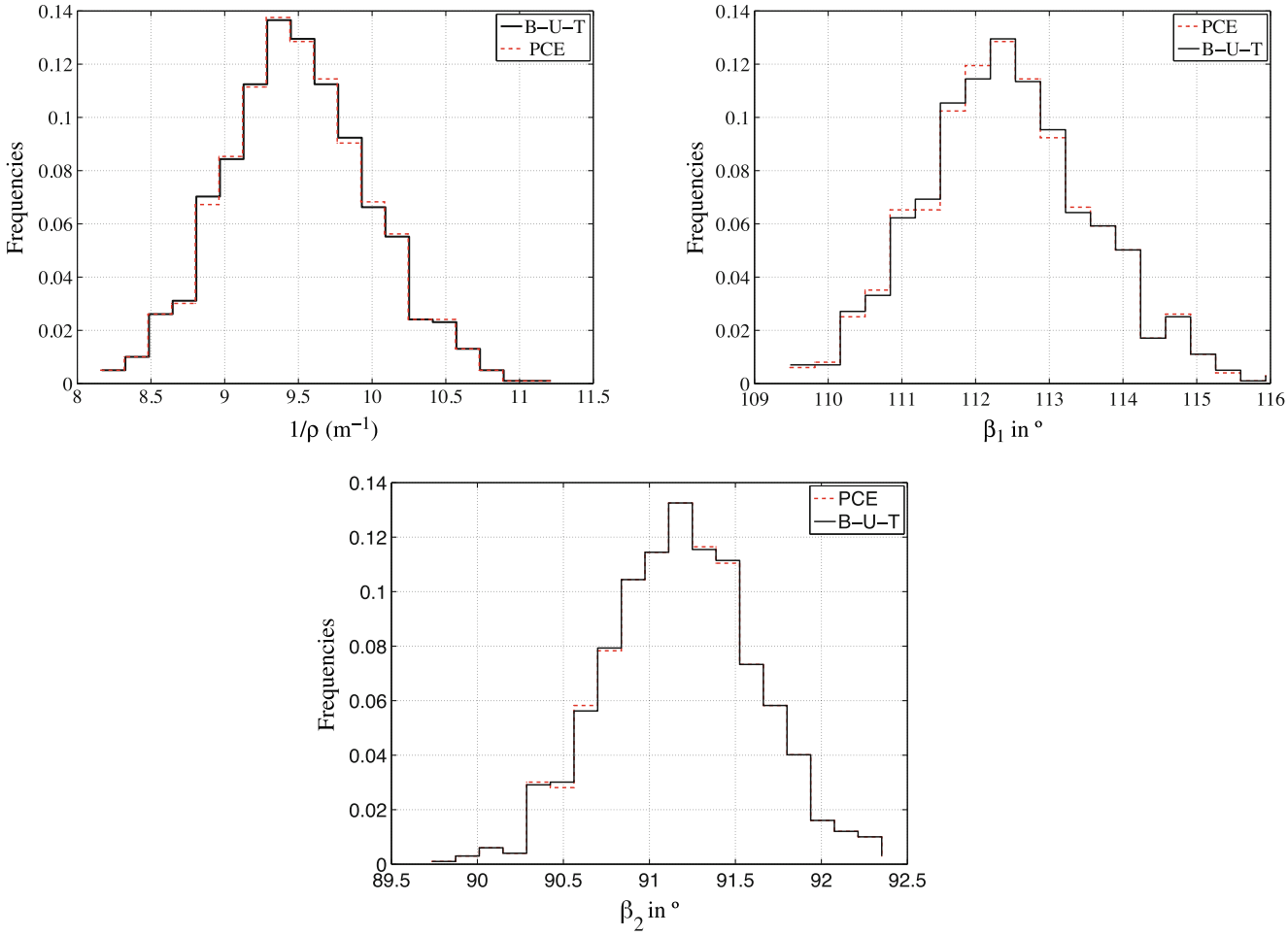

Fig. 12 Histograms of the springback shape responses obtained using the sparse PCE model

Conclusion and prospects

In this paper we combine a semi-analytical Bending-Under-Tension model and a custom Polynomial Chaos Expansion to accurately assess the springback parameters for small variations on the input parameters. The B-U-T model allows us to circumvent typical cost issues and numerical instability from full FEM simulations (contact modeling, through thickness integration). The use of such a model allows us to reach a sufficient numerical stability for small variations of the random parameters. Using these high resolution outputs, we are able to accurately train a custom stochastic surrogate to efficiently propagate the uncertainties through the model. Then, this approach allows us to accurately assess the springback variability when multiple random variables are taken into account with a limited budget.

In a more general way, our approach demonstrates that the use of simplified physics based model for large strain forming process allows to reduce the numerical instability and makes possible an accurate and low cost variability study. The approach is of course not limited to 2D plain strain and sparse PCE could be combined with other types of physics-based metamodels such as one-step or POD/PGD approaches could possibly presenting similar smoothing properties in 3D. In the current state of development we have demonstrated the validity of our the approach from numerical point of view using standard benchmarks. The comparison with experiment requires an implementation of the method within a specialized metal forming framework, which is beyond the scope of the current study dedicated to stochastic modeling. Moreover, further work is needed for sensitivity analysis performed using the polynomial chaos expansion to a priori identify the most influent input variables. Adaptive features may also be included in the sparse construction algorithm to keep on reducing the number of terms used, and increasing its prediction accuracy.

Acknowledgments This research was conducted as part of the OASIS project, supported by OSEO within the contract FUI no. F1012003Z. The first author is grateful to Innoviris for its support to BB2B project entitled multicriteria optimization with uncertainty quantification applied to the building industry. The authors also acknowledge the support of Labex MS2T.

References

1. Papeleux L, Ponthot J (2002) Finite element simulation of spring-back in sheet metal forming. J Mater Process Technol 125–126:785–791
2. Kleiber M, Rojek J, Stochi R (2002) Reliability assessment for sheet metal forming operations. Comput Methods Appl Mech Eng 191:4511–4532
3. de Souza T, Rolfe B (2008) Multivariate modelling of variability in sheet metal forming. J Mater Process Technol 203:1–12
4. Naceur H, Delaméziere A, Batoz J, Guo C, Knopf–Lenoir C (2004) Some improvement on the optimum process design in deep drawing using the inverse approach. J Mater Process Technol 146:250–262
5. Breitkopf P, Naceur H, Villon P (2005) Moving least squares response surface approximation: formulation and metal forming applications. Comput Struct 83:1411–1428
6. Kleiber M, Breitkopf P (1993) Finite elements in structural mechanics: an introduction with Pascal programs for micro-computers. Ellis Horwood
7. Meinders T, Burchitz I, Bonte M, Lingbeek R (2008) Numerical product design: Springback prediction, compensation and optimization. Int J Mach Tools Manuf 48(5):499–514
8. Radi B, El Hami A (2007) Reliability analysis of the metal forming process. Math Comput Model 45:431–439
9. Jansson T, Nilsson L, Moshfegh R (2008) Reliability analysis of a sheet metal forming process using monte carlo analysis and metamodels. J Mater Process Technol 202:255–268
10. Donglai W, Zhenshan C, Jun C (2007) Optimization and tolerance prediction of sheet metal forming process using response surface model. Comput Mater Sci 42:228–233
11. Blatman G, Sudret B (2011) Adaptive sparse polynomial chaso expansion based on least angle regression. J Comput Phys 230:2345–2367
12. Ghanem R, Spanos PD (1991) Spectral stochastic finite-element formulation for reliability analysis. J Eng Mech 117(10):2351–2372
13. Sudret B, Der Kiureghian A (2000) Stochastic finite elements methods and reliability- a state of the art. tech. rep. Department of civil and environmental engineering
14. Ghanem R, Spanos PD (1991) Stochastic finite elements: a spectral approach. Springer-Verlag, New York
15. Cameron R, Martin W (1944) Transformations of wiener integrals under translations. Ann Math 45(2):386–396
16. Xiu D (2009) Fast numerical methods for stochastic computations: a review. Commun Comput Phys 5:242–272
17. Berveiller M, Sudret B, Lemaire M (2006) Stochastic finite element: a non intrusive approach by regression. Rev Eur Méc Numér 15:81–92
18. Makinouchi A, Nakamachi E, Onate E, Wagoner R (eds) (1993) Numisheet'93 2nd international conference, numerical simulation of 3-D sheet metal forming process-verification of simulation with experiment, Riken Tokyo
19. Hibbit D, Karlsson B, Sorensen P. ABAQUS Example problems, vol 1, version 6.7. Dassault Système
20. Hill R (1948) A theory of the yielding and plastic flow of anisotropic metals. In: Proc R London, vol 193, pp 281–297
21. Le Quilliec G, Breitkopf P, Roelandt J, Juillard P (2013) Semi-analytical approach for plane strain sheet metal forming using a bending-under-tension numerical model. Int J Mater Form. doi:10.1007/s12289-012-1122-7
22. Hastie RT, Tibshirani J, Friedman G (2009) The elements of statistical learning, data mining, inference and prediction, Springer
23. Hesterberg T, Choi N, Meier L, Fraley C (2008) Least angle and l_1 penalized regression: a review. Stat Surv 2:61–93
24. Efron B, Hastie T, Johnstone I, Tibsirani T (2004) Least angle regression. Ann Stat 32(2):407–451

Chapter 4

Adapting the sampling to the model resolution: Fat Latin Hypercube sampling.

In this section we propose an alternative methodology to solve the same problematic: the stochastic analysis of the U-shaped deep drawing process of a metal sheet using a regression based Polynomial Chaos approach.

In many cases, the model resolution is not of the same order of magnitude of the range of variation of the random variable. In this case, the use of an intermediate non-physics based metamodel is not mandatory. One may solve the problem by focusing on the design of experiment. We defined a custom Latin Hypercube Sampling (LHS) taking the model resolution into account. A restricted area whose shape is parameterized by the resolution of the model is defined around each sampling point. The resulting LHS consists in sampling points, each characterized by a restricted area free of any other sampling points. This limits the total number of available points. We then propose to build a consistent regression-based PCE with the remaining number of samples points. This way this methodology aligns the stochastic model complexity with the limited number of trustworthy data at hand.

This approach has been described into a paper submitted in july 2013 to the journal CMAME and is currently under review.

The paper is given in its submitted version.

Fat Latin Hypercube Sampling and efficient Sparse Polynomial Chaos Expansion for uncertainty propagation on finite precision models – Application to 2D deep drawing process –

Jérémy LEBON[a,b], Guénhaël LE QUILLIEC[a], Piotr BREITKOPF[a], Rajan FILOMENO COELHO[b], Pierre VILLON[a]

[a] *Laboratoire Roberval, UMR 7337, Université de Technologie de Compiègne, BP 20529, 60205 Compiègne cedex, FRANCE*
Tel.: +33 (0)3 44 23 46 63
[b] *Université Libre de Bruxelles (ULB), BATir Department CP 194/2, 50, avenue Franklin Roosevelt, B-1050 Brussels (BELGIUM)*

Abstract

In the context of uncertainty propagation the random variable range of variation may be many orders of magnitude lower than its nominal value. When evaluating the non-linear Finite Element (FE) model involving contact/friction and material non linearity on such small perturbations of the input data, a numerical noise alters the output data and consequently distorts the statistical quantities. In this paper, a particular attention is given to the definition of adapted Design of Experiment (DoE) taking the model sensitivity into account and giving by consequence the maximum number of possible numerical experiments. In order to build acceptable Polynomial Chaos Expansion (PCE) with such sparse data, we implement a hybrid LARS+Q-norm approach. We illustrate our methodology using a deep drawing process of a 2D metal sheet, considering up to 8 random variables.

Keywords: Uncertainty Quantification, Model Sensitivity, Springback Variability Assessment, sensitivity-constrained Design of Experiment, Sparse Polynomial Chaos Expansion

1. Introduction

A profuse literature review reveals rigorous approaches to reduce the computational expense, combining in a hierarchical way a 'high-fidelity" (costly) model with a "lower-fidelity" model (less accurate but also less expensive) to perform parametric studies dedicated either to the search for optimal design [1, 2, 3] or to the characterization of system variability or finally to sensitivity studies [4, 5, 6]. In an optimization context, rigorous convergence proofs may be established as long as the "lower-fidelity" model is consistent (generally to the first [7] or second order [8]) with the "higher-fidelity" model. With regards to the nature of the metamodel involved one may classify these approaches as "multi-fidelity" or "variable-fidelity" when physical based surrogate model is involved [9, 10, 11, 12, 13] or in surrogate-based approaches when non-physics interpolating or

regression-based metamodels built from a Design of Experiment (DoE) are considered. [14, 15, 16].

These latter approaches are widely spread in stochastic analysis. For example, [17] uses a combination of Kriging model and subset simulations in order to efficiently assess structural failure probability at low computational costs. [18] uses Monte Carlo simulation and linear response surface to detect the most significant variable and to give an approximation of the probabilistic response. [19] uses the moving least square instead of the classical quadratic order response surface to better fit the limit state function and perform reliability analysis of the sheet metal forming process. [20, 21, 22, 6] demonstrates the advantages of adaptive scheme for Polynomial Chaos Expansion (PCE) to perform robust, reliability, and sensitivity analysis. A second order PCE is used in [23] to assess the variability of the tolerance prediction of the formed metal sheet submitted to random parameters. In the field of metal forming applications, a classical approach consists of using Monte Carlo simulation on a quadratic polynomial response surface method to quantify probabilistic characteristics (mean and standard deviation), e.g. [24] uses this classical approach to estimate the variability of the shape and dimensional errors in net-shape metal forming. In this approach, the exactness of the statistical quantity mainly depends on the capability of the metamodel of picking up the relationship between the dependent explanatory random variables. The training data may thus play a leading role.

In this work we focus our attention on the quality of the "high-fidelity" training data. We claim that there may exist a threshold on the magnitude of variation of the input variables below which the "high-fidelity" simulations may not be trustworthy. Thus, the number of achievable simulations using "high-fidelity" model is not only limited by the cost of a single simulation but more importantly by its intrinsic sensitivity to small perturbations. In this case, we face two competing issues. On one hand, a too small number of "high-fidelity" simulations harms the accuracy of the response surface. On the other hand, a too high number of simulations introduces numerical noise which also directly leads to a noisy response surface.

In the present paper, we address both issues simultaneously in order to propose a coherent PCE scheme taking into account the upper bound on sampling density given by sensitivity consideration, and the lower bound given by the regression approach to compute PCE coefficients.

The rest of the paper is organized as follows. In section 2, we investigate a sampling strategy taking into account the model precision leading to a non-noisy reduced set of sampling. Then, in section 3 we compare three sparse methodologies applied to PCE to efficiently and accurately propagate the uncertainty with the few number of remaining simulations. Finally, in section 4 we demonstrate the efficiency of the proposed methodology considering the deep drawing process of a 2D- U-shaped metal sheet as a test case.

2. Sampling schemes taking into account of model sensitivities

In the scope of this work, the FE model is referred to as the "high-fidelity" model and is used to train the analytical "lower-fidelity" model, namely the PCE. Firstly, we show that "very" small random perturbations on the input parameters $\boldsymbol{\xi} = [\xi^{(1)}, \xi^{(2)}, \ldots, \xi^{(M)}]$ around a nominal value $\boldsymbol{\xi}_{\text{nom}} = [\xi^{(1)}_{\text{nom}}, \xi(2)_{\text{nom}}, \ldots, \xi^{(M)}_{\text{nom}}]$ yield noisy training data set. We characterize the model output stability by the non-dimensional sensitivity for each considered variable $\xi^{(i)}$, $i \in \{1, \ldots, M\}$ using

the finite difference scheme

$$\mu_i = \frac{\Delta y(\xi^{(i)})}{\Delta \xi^{(i)}} \times \frac{\xi^{(i)}_{\text{nom}}}{y(\xi^{(i)}_{\text{nom}})} \tag{1}$$

where

$$\Delta y(\xi^{(i)}) = y\left(\xi^{(i)}_{\text{nom}} + \frac{\Delta\xi(i)}{2}\right) - y\left(\xi^{(i)}_{\text{nom}} - \frac{\Delta\xi^{(i)}}{2}\right). \tag{2}$$

When decreasing the order of magnitude of the perturbation ($-\log(\Delta\xi)$ increasing), the non-dimensional sensitivity μ_i computed for the "high-fidelity" model exhibits different behaviors:

1. Firstly, for "large" variation of $\Delta\xi_i$, the variation μ_i reveals the non-linear behavior of the model. No brutal variation of μ_i is observed and the model is considered as trustworthy.

2. Secondly, μ_i stabilizes around a constant value $\bar{\mu}_i$ where the model may be considered as linear.

3. Thirdly, on reaching the threshold , μ_i becomes unstable. Within the corresponding range of variation noisy data estranged from physical reality is generated. These data points have to be discarded to train a metamodel.

4. Finally, the threshold shows the model sensitivity limit: for this range of variation, the model is not sensitive anymore.

The model output is considered to be unstable when the following criterion is satisfied:

$$|\mu_i - \bar{\mu}_i| > \frac{\mu_i^*}{2}. \tag{3}$$

The Fig.1 illustrates the tendencies obtained for μ_i against the order of magnitude of the variation range in $\Delta\xi_i$. The results are issued from actual computations shown for a real case (section 4).

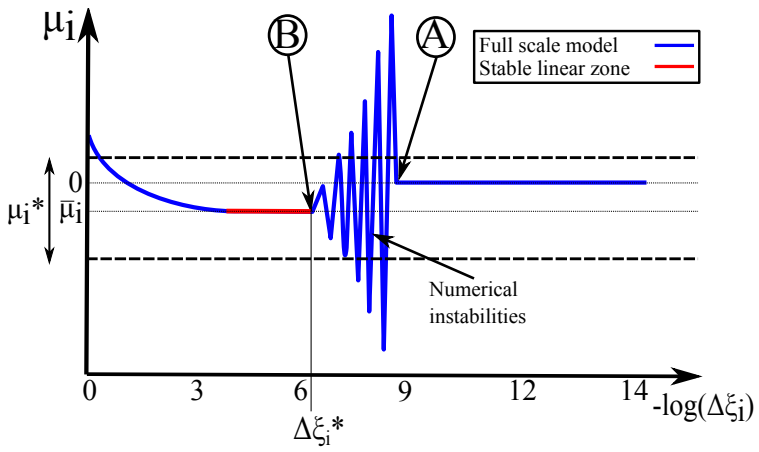

Figure 1: Typical sensitivity results issued from actual computation

We thus focus our attention on avoiding noisy training data which may lead to an inaccurate response surface for small variation of the input parameters. We propose to modify the traditional Latin Hypercube Sampling scheme in order to take into account model sensitivities.

2.1. A Fat-Latin Hypercube Sampling taking into account model sensitivities

Standard LHS. LHS ([25]) is an efficient technique to generate joint probability distributions by distributing samples in equiprobable bins. Let

$$\boldsymbol{\Xi} = \left\{\boldsymbol{\xi}^{(1)}, \boldsymbol{\xi}^{(2)}, \ldots, \boldsymbol{\xi}^{(M)}\right\} = \begin{Bmatrix} \boldsymbol{\xi}_1 \\ \boldsymbol{\xi}_2 \\ \vdots \\ \boldsymbol{\xi}_S \end{Bmatrix} = \begin{pmatrix} \xi_1^{(1)} & \xi_1^{(2)} & \cdots & \xi_1^{(M)} \\ \xi_2^{(1)} & \xi_2^{(2)} & \cdots & \xi_2^{(M)} \\ \vdots & \vdots & \ddots & \vdots \\ \xi_S^{(1)} & \xi_S^{(2)} & \cdots & \xi_s^{(M)} \end{pmatrix} \tag{4}$$

an S-sized and M-dimensional DoE and F_j, $j = 1, \ldots, M$ the joint cumulative distribution (assumed to be known) of each of the random variables. Let $\boldsymbol{\Xi}^{\mathcal{U}}$, the special case where F is an uniform joint distribution for all variables.

A possible 2D sampling for 2 independent uniform distributions laws is given in Fig.2(a) and for 2 independent normal distributions in Fig.2(b). By construction there is exactly one observation per row in each of the M directions.

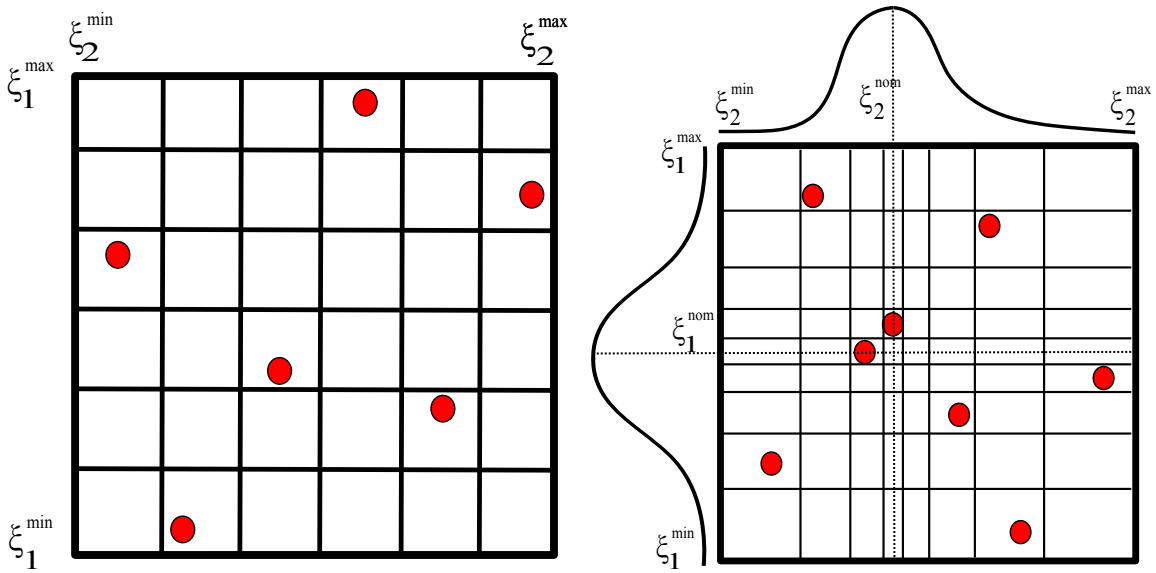

(a) Uniform distribution (b) Normal distribution

Figure 2: LHS sampling illustration for uniform distribution

The LHS advantages [26] are:

- as long as the number of samples S is large compared to the number of variables M, LHS eventually provides estimators with lower variances for any function with finite variance,

- in any case S-sized LHS does not perform worse than $(S-1)$-sized crude Monte Carlo.

However, LHS shows also some limitations:

- The error estimates may not be improved by iteratively increasing the number of samples: the resulting sampling is not a LHS anymore (see [27, 28, 29] for Nested LHS).
- When used for training response surfaces, a space-filling optimal design is interesting in order to sample the design space with a minimum number of response evaluations. When using LHS there is a risk that some of the random samples form a cluster to the detriment of some unexplored part of the design space. To circumvent these issues, some strategies may be found [30, 31, 32].

In the following we propose to alleviate another fundamental limitation: when performing stochastic studies small variations of the random input parameters result in noisy responses.

Fat-LHS. In the present paper, we propose to build a restricted area (free of other sampling points) around each sampling point is defined. The shape of this restricted area is parameterized by δ_i^* (Eq.3) and may be defined as follows:

$$\delta_i^* = \underset{\Delta\xi^{(i)}}{\operatorname{argmin}}\, \mu_i(\Delta\xi^{(i)}) > \mu_i^*, i \in \{1,\dots,M\}. \tag{5}$$

Depending on the chosen norm, different shapes are obtained for the restricted area (Fig.3). Fig.3(a) describes $\mathcal{L}_\infty$ related restricted area, the lengths of the border of the hypercube being $\delta_i^*, i \in \{1,\dots,M\}$. Fig.3(b) defines an elliptic sensitivity region restricted area, where the $\delta_i^*, i \in \{1,\dots,M\}$ define the lengths of the axes.

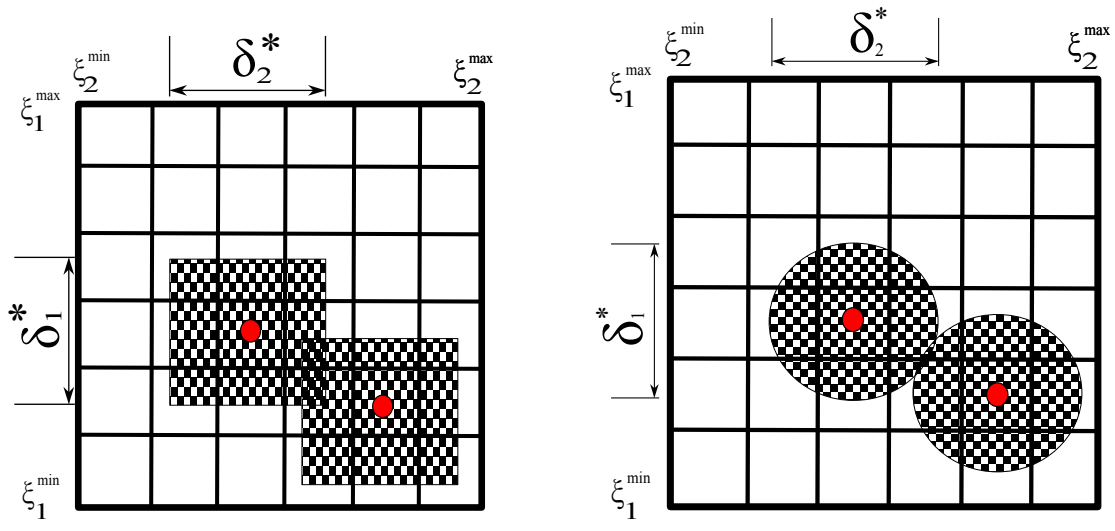

(a) Fat-LHS$^{\mathcal{L}_\infty}$ (b) Fat-LHS$^{\mathcal{L}_2}$

Figure 3: Sensitivity restricted area shape around two sampling points for $\mathcal{L}_\infty$ and $\mathcal{L}_2$ in 2D

This approach coupled with LHS requirements permits us to filter the spacial sensitivity but limits the maximum number of samples available for PCE determination. In the remainder of the paper we denote this upper bound on the number of samples at hand by S_{ub}.

2.2. Implementation of the Fat-LHS

We propose here an algorithm to identify the maximum number of points to be sampled for a given μ_i, $i \in \{1, \ldots, M\}$. We assume that for small variations of the input random parameters the shape and size of the restricted area stays identical for each sampling point. The general idea of the procedure is to start with a given LHS with a prescribed density probability on each random variable and then to:

1. identify the restricted area for each sampled point (Fig.4(a)),
2. iteratively remove the illegal neighbors (Fig.4(b))
3. re-adapt the bin's size to recover the equiprobability property (this makes the sampling loosing in empty bins and over-occupied bins (Fig.4(c))),
4. reconstruct an LHS sampling by randomly allocating the samples from over-occupied bins to the empty bins (Fig.4(d)).

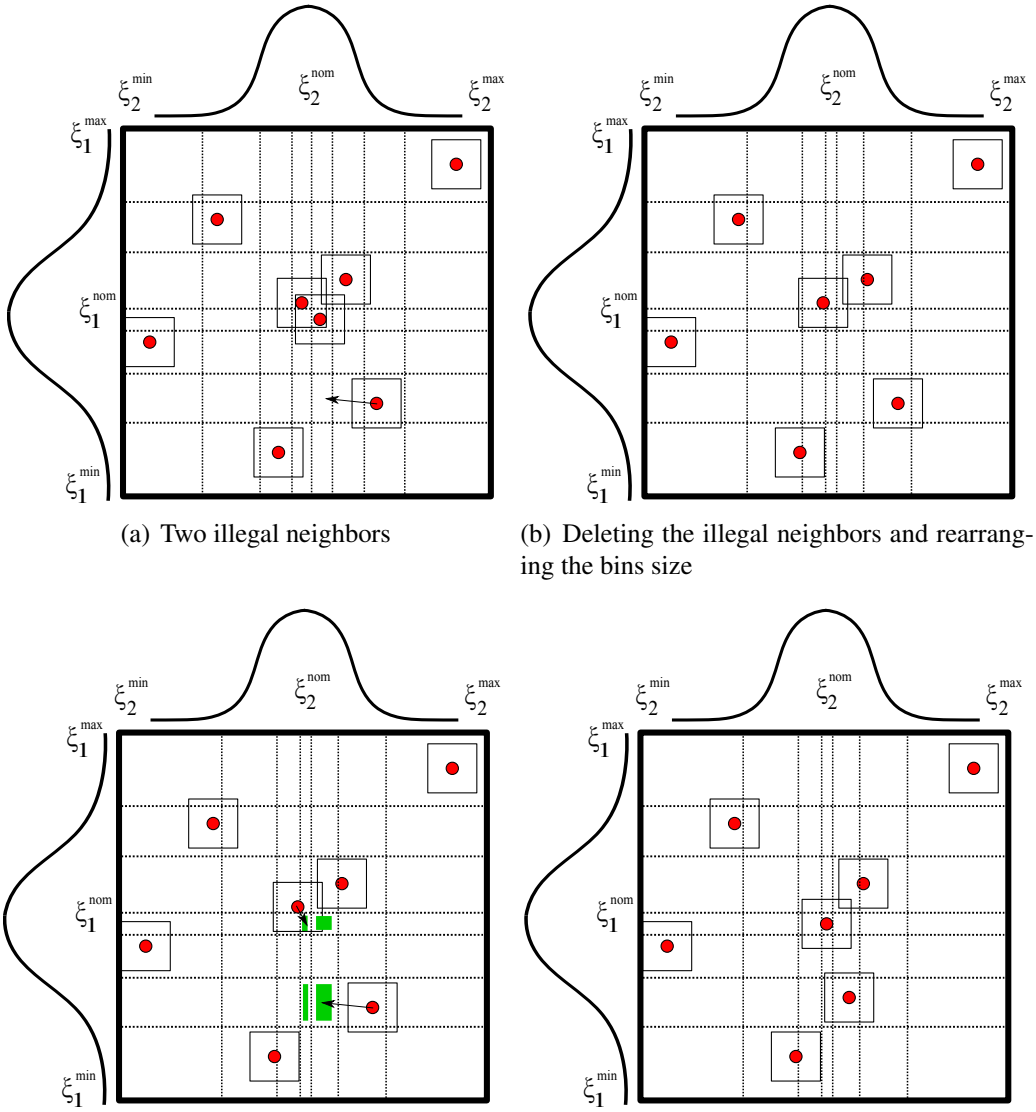

(a) Two illegal neighbors

(b) Deleting the illegal neighbors and rearranging the bins size

(c) Moving the samples in over-occupied bins to empty bins

(d) Legal neighbors only

Figure 4: Illustration of the Fat Latin Hypercube Sampling procedure

The procedure is described in **Algorithm** 1.

Algorithm 1 Fat-LHS algorithm

- Let M be the number of stochastic variables
- Let $\boldsymbol{s}_{\text{set}}(1) = \{1, \ldots, S\}$ be the initial set numbering the sampling points and $\boldsymbol{s}_{\text{set}}(2) = \varnothing$
- Let $\boldsymbol{\mu} = [\mu_1, \mu_2, \ldots, \mu_M]$ be the given sensitivity for each parameter

Generate a first LHS sampling with the desired properties

- Generate an $\boldsymbol{s}_{\text{set}}(iter1)-$sized and $M-$dimensional LHS denoted $\boldsymbol{\Xi}$ with minimum correlation or maximin distance between points.

Find and suppress the illegal neighbors

- Let $i = 1$
while $\text{card}(\boldsymbol{s}_{\text{set}}(i)) > \text{card}(\boldsymbol{s}_{\text{set}}(i+1))$ **do**
  for $s = 1 : card(s_{\text{set}}(i))$ **do**
    - Compute: $\boldsymbol{D}_s = \text{sign}\begin{pmatrix} \|\xi_s^{(1)} - \xi_1^{(1)}\| - \mu^{(1)} & \ldots & \|\xi_s^{(M)} - \xi_1^{(M)}\| - \mu^{(M)} \\ \|\xi_s^{(1)} - \xi_1^{(2)}\| - \mu^{(1)} & \ldots & \|\xi_s^{(M)} - \xi_2^{(M)}\| - \mu^{(M)} \\ \vdots & \ddots & \vdots \\ \|\xi_s^{(1)} - \xi_S^{(1)}\| - \mu^{(1)} & \ldots & \|\xi_s^{(M)} - \xi_S^{(M)}\| - \mu^{(M)} \end{pmatrix}$
    if $\exists j | \boldsymbol{D}^{(s)}(j,:) = \underbrace{[1, 1, \ldots, 1]}_{\text{m times}}$ **then**
      - $\boldsymbol{s}_{\text{set}}(i+1) = \boldsymbol{s}_{\text{set}}(i) - \{j\}$
      - $\boldsymbol{\Xi}_{\{-i\}} = \begin{pmatrix} \xi_1^{(1)} & \xi_1^{(2)} & \ldots & \xi_1^{(M)} \\ \xi_2^{(1)} & \xi_2^{(2)} & \ldots & \xi_2^{(M)} \\ \vdots & \vdots & \ddots & \vdots \\ \xi_{i-1}^{(1)} & \xi_{i-1}^{(2)} & \ldots & \xi_{i-1}^{(M)} \\ \xi_{i+1}^{(1)} & \xi_{i+1}^{(2)} & \ldots & \xi_{i+1}^{(M)} \\ \vdots & \vdots & \ddots & \vdots \\ \xi_S^{(1)} & \xi_S^{(2)} & \ldots & \xi_S^{(M)} \end{pmatrix}.$
    end if
  end for
  i=i+1
end while

Re-build an LHS sampling

- Considering the number of remaining points, adapt the "bin" size to recover the equiprobability property.
- Identify the bins with more than one sampling and the empty bins
- Randomly distribute the points from the over occupied bins to the empty bins

3. Hybrid $Q-$norm+LARS Polynomial Chaos Expansion (PCE) scheme

In this section we introduce the theoretical aspects for the construction of a sparse PCE decreasing its computational cost and thus allowing us to consider only a limited number of sampling points at hand.

3.1. Multivariate PCE

The PCE [33] is a stochastic metamodel, that is intended to give an approximation of the stochastic behavior of a functional y (*scalar random process*) that is defined as a function of an input random vector $\boldsymbol{\xi} = \{\xi_1, \xi_2, \ldots, \xi_M\}$ with M coordinates. We assume that y is a second order random variable ($\mathbb{E}(y^2) < \infty$) and that the probability density function $f_{\boldsymbol{\xi}}(\boldsymbol{\xi})$ may be decomposed on a product of the marginal probability density functions $f_{\xi^{(i)}}$ (Eq.6):

$$f(\boldsymbol{\xi}) = \prod_{i=1}^{M} f_{\xi_i}(\xi_i) \tag{6}$$

Given the natural inner product for arbitrary function ϕ with respect to each of the marginal probability function $f_{\xi}(\xi)$ defined on $\mathcal{D}$

$$< \phi_1, \phi_2 >= \int_{\mathcal{D}} \phi_1(\xi)\phi_2(\xi) f_{\xi}(\xi) d\xi \tag{7}$$

one may define an infinite set of mono-variate orthogonal polynomials $\boldsymbol{\varphi} = \{\varphi_k, k \in \mathbb{N}\}$ verifying $< \varphi_j, \varphi_k >= \delta_{jk}$. Hermitian polynomials respect this condition for Gaussian random variables.

For other types of random variables, different orthogonal polynomials may be retained (Table 1) leading to the generalized PCE or Wiener-Askey scheme [34].

Probabilistic measure	Orthogonal Polynomial
Uniform: $\mathbf{1}_{]-1,1[}(\xi)/2$	Legendre: $P_k(\xi)$
Gaussian: $\frac{1}{\sqrt{(2\pi)}} e^{-\xi^2/2}$	Hermite: $H_{e_k}(\xi)$
Gamma: $\xi^a e^{-\xi} \mathbf{1}_{\mathbb{R}^+}(\xi)$	Laguerre: $L_a^k(\xi)$
Beta: $\mathbf{1}_{]-1;1[}(\xi) \frac{(1-\xi)^a (1+\xi)^b}{B(a)B(b)}$	Jacobi: $J_k(\xi)$

Table 1: Some orthogonal polynomial types with respect to different continuous probability density function types

Using the tensor product on these mono-variate polynomials one may obtain an infinite set of multi-variate polynomials (with a preserved orthogonality property) $\boldsymbol{\psi} = \{\psi_{\boldsymbol{\alpha}}, \boldsymbol{\alpha} \in \mathbb{N}^M\}$ where $\boldsymbol{\alpha} \in \mathbb{N}^M$ is a multi-index set.

According to the theorem of Cameron Martin [35], the exact polynomial expansion of the functional y is

$$y(\boldsymbol{\xi}) = \sum_{\boldsymbol{\alpha} \in \mathbb{N}^M} \gamma_{\boldsymbol{\alpha}} \psi_{\boldsymbol{\alpha}}(\boldsymbol{\xi}). \tag{8}$$

where $\{\gamma_{\boldsymbol{\alpha}}\}$, $\boldsymbol{\alpha} \in \mathbb{N}^M$ are the coefficients of the PCE to be identified

3.2. *Truncating multi-variate polynomials expansion*

For practical use, one may truncate the full set of tensor product polynomials in order to only retain a *finite set* of polynomial terms. For Fat-LHS sampling scheme, we need an economical PCE scheme requiring less than $S_{lb} \leq S_{ub}$ samples. In the following we revisit three classical truncation schemes needed for the construction of our hybrid approach.

Classical truncation scheme. Among all $\{\psi_{\boldsymbol{\alpha}}, \boldsymbol{\alpha} \in \mathbb{N}^M\}$ the classical truncation scheme [33, 21, 36] retains only the multi-variate polynomial terms whose degree does not exceed an arbitrarily fixed N leading to the following multi-index set:

$$\mathcal{A}_q^M = \{\boldsymbol{\alpha} \in \mathbb{N}^M, \|\boldsymbol{\alpha}\|_q \leq p\}, \tag{9}$$

where $\|\boldsymbol{\alpha}\|_q = \left(\sum_{i=1}^{M} \alpha_i^q\right)^{1/q}$ and $q = 1$. Then, the truncated model may be written as:

$$y^{\mathcal{A}_q^M}(\boldsymbol{\xi}) \approx \sum_{\boldsymbol{\alpha} \in \mathcal{A}_q^M} \gamma_{\boldsymbol{\alpha}} \psi_{\boldsymbol{\alpha}}(\boldsymbol{\xi}). \tag{10}$$

Fig.5 gives an illustration of this scheme for a 2-variate 7$^{\text{th}}$ order PCE.

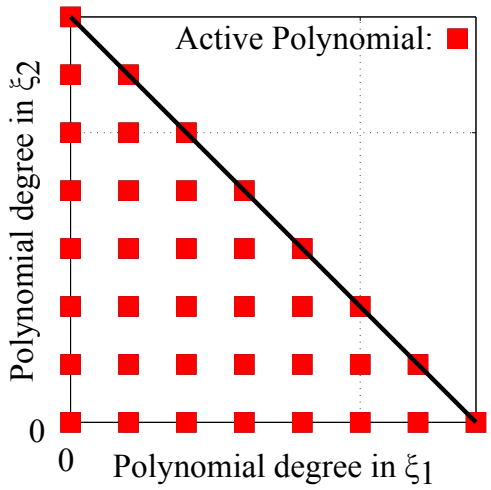

Figure 5: Illustration of the classical truncation scheme for a 7$^{\text{th}}$ order PCE

The number P of coefficients in the PCE is given by

$$P = \sum_{k=0}^{N} C_{M+k+1}^{k} = \frac{(N+M)!}{N!M!} \tag{11}$$

and increases exponentially both with N and M. So does the number of "high-fidelity" function evaluations needed to compute the number of PCE coefficients: whatever the method used, at least $S = P + 1$ samples are necessary.

Q−norm based truncation. This approach relies on the "sparsity of effects principle": a system is usually dominated by main effects and low-order interactions. Q-norm generalizes the classical truncation scheme by varying $0 \leq q \leq 1$ [37]. Fig.6 illustrates a typical truncated index set different for $q = 0.6$ and a 7^{th} order 2-variate PCE.

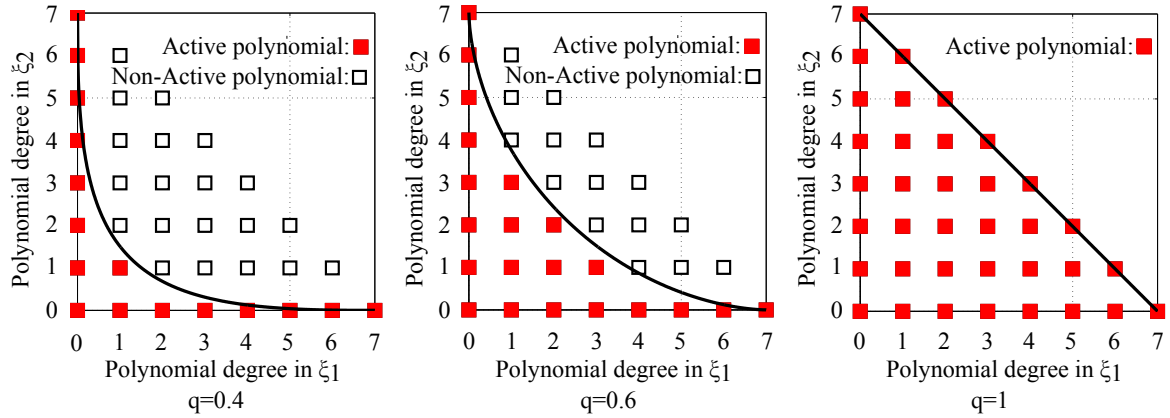

Figure 6: Illustration of $Q-$norm truncation with different values of the truncation parameter q for a 7^{th} order PCE

The set of active polynomials in the PCE decomposition is decreased when q decreases. Fig.7(a) illustrates the evolution of the number of 2-variate polynomial terms in linear scale against q values, and Fig.7(b) shows it for an 8-variate polynomial in log scale.

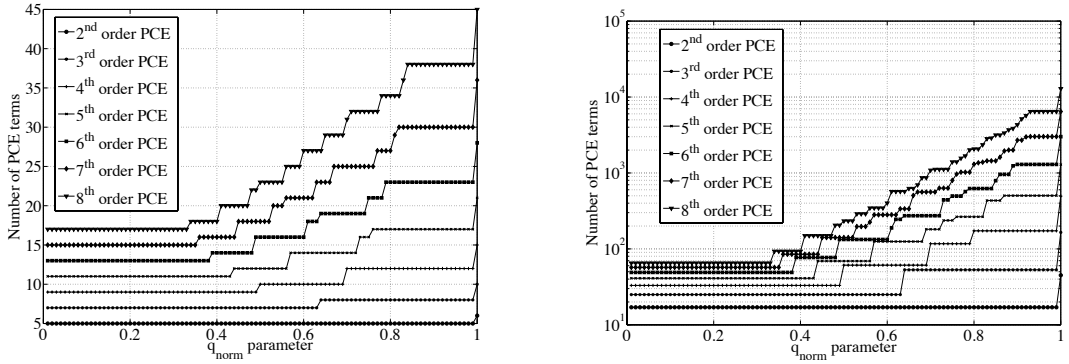

(a) 2-variate (b) 8-variate

Figure 7: Number of polynomials terms in *q-truncated* PCE with regards to the q truncation parameter for 2 and 8 variables

LARS truncation scheme. The Least Angle Regression Stagewise algorithm [39, 37] is issued from the variable selection community [38]. Roughly speaking, it iteratively adds to the current model the polynomial terms which are the most correlated with the residual response (**Algorithm** 2).

Fig.8 illustrates truncated index obtained after $k = 24$ iterations of the LARS algorithm applied to a 2-variate 7^{th} order polynomial chaos expansion.

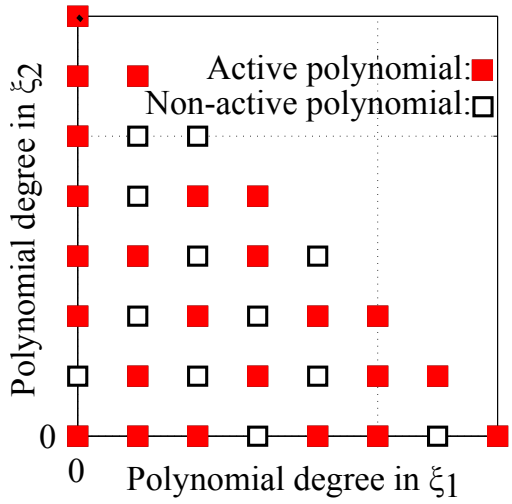

(a) $k = 24$

Figure 8: Illustration of $Q-$norm truncation with different values of the truncation parameter q for a 7^{th} order PCE

At step k, k predictors have been added to the approximated model

$$y^{\mathcal{A}^M_{\text{LARS}}(k)} = \sum_{\boldsymbol{\alpha}\in\mathcal{A}^M_{\text{LARS}}(k)} \gamma_{\boldsymbol{\alpha}}\psi_{\boldsymbol{\alpha}}^{\mathcal{A}^M_{\text{LARS}}(k)} \tag{12}$$

where $\mathcal{A}^M_{\text{LARS}}(k)$ is the corresponding multi-index set whose cardinal is k. The current residual response $\mathbf{r}^{(k)}$ and correlation vector $\tilde{\mathbf{c}}_0^{(k)}$ are respectively defined by

$$\mathbf{r}^{(k)} = \mathbf{y} - \mathbf{y}^{\mathcal{A}^M_{\text{LARS}}(k)} \tag{13}$$

and

$$\tilde{\mathbf{c}}_0^{(k)} = \frac{(\mathbf{y} - \mathrm{E}[\mathbf{y}])(\mathbf{r}^{(k)} - \mathrm{E}[\mathbf{r}^{(k)}])}{\sqrt{(\mathbf{y} - \mathrm{E}[\mathbf{y}])^2 \times (\mathbf{r}^{(k)} - \mathrm{E}[\mathbf{r}^{(k)}])^2}}. \tag{14}$$

Algorithm 2 Least Angle Regression Algorithm

Offline phase

• Build a stochastic S-sized and M-dimensional design of experiments according to the stochastic model denoted $\boldsymbol{\Xi}$.
For each $S - sized$ sample $\{\boldsymbol{\xi}_1, \ldots, \boldsymbol{\xi}_M\}$ store the corresponding evaluations of the "high-fidelity" model in $\mathbf{y}$.
• Build a (truncated) polynomial chaos basis $\boldsymbol{\Psi}_{\mathcal{A}_q^M}$ and evaluate it at each sample.

Online phase

• Initialize the coefficients $\boldsymbol{\gamma}_{\boldsymbol{\alpha}}$ which sets the current residual $\mathbf{r}$ equals to $\mathbf{y}$ obtained in the *offline phase*.
• Compute the correlation vector $\tilde{\mathbf{c}}_0^{(k)}$. Retain the predictor $\psi_{\boldsymbol{\alpha}^*}$ where $\boldsymbol{\alpha}^* = \text{argmax}|\tilde{\mathbf{c}}_0^{(k)}|$. The model becomes $y^{\mathcal{A}^M_{\text{LARS}}(k)}$.
• Update $\gamma_{\boldsymbol{\alpha}}$ to $\gamma^*_{\boldsymbol{\alpha}} = \gamma_{\boldsymbol{\alpha}} + \epsilon^*_{(1)}$, where $\epsilon^*_{(1)}$ is the LARS step where another predictor $\psi_{\boldsymbol{\beta}^*}$ has as much correlation with the current residual as does $\psi_{\boldsymbol{\alpha}^*}$ (see Tibshirani and al. 2009 for numerical computations of ϵ^*). Add $\boldsymbol{\beta}^*$ to the current index set of retained polynomial and update $y^{\mathcal{A}^M_{\text{LARS}}(k)}$.
• Update jointly $\{\boldsymbol{\gamma}_{\boldsymbol{\alpha}}\}_{\boldsymbol{\alpha}\in\mathcal{A}^M_{\text{LARS}}(k)}$ following the direction $\mathbf{u}^{(k)}$ ($\|\mathbf{u}^{(k)}\| = 1$) defined by the joint least-square coefficient on the current residual. At this step another predictor $\psi_{\boldsymbol{\theta}^*}$ is found to have much correlation with the current residual and is added to the model.
• Repeat the previous step until $m = min(P; Q)$ predictors have been entered or until a previously chosen error estimate has reached a minimal value.

3.3. Combining Q−norm and LARS

Considering the limited Fat-LHS sampling, we need to find the optimal sparse index set $\mathcal{A}^*$ such that the error produced on the resulting approximation model $y_{\mathcal{A}^*}$ is as low as possible. To perform this optimization task, we combine in an iterative manner the $Q-$ norm and LARS truncations. We index by $\mathcal{A}^M_{\text{q}}$ the set of polynomials $\boldsymbol{\Psi}_{\text{q-truncated}}$ obtained by a $Q-$norm. From this set, one may apply the LARS which selects the most correlated polynomial. We thus index by $\mathcal{A}^M_{\text{q+LARS}}$ the sparser set of polynomials $\boldsymbol{\Psi}_{\text{q+k}}$ obtained after a $Q-$norm and k steps using LARS.

Fig.9 illustrates this method by showing a sparse set of active polynomials obtained for $q = 0.6$ and $k = 8$.We note that $\text{card}(\mathcal{A}^M_{\text{q+k}}) \leq \text{card}(\mathcal{A}^M_{\text{q}})$.

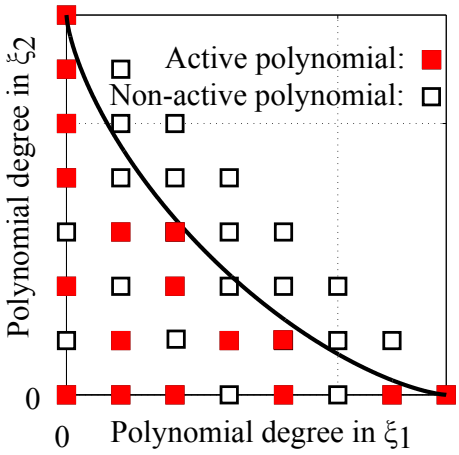

(a) LARS+Q−norm ($q = 0.6, k = 8$)

Figure 9: Illustration of combined Q−norm + LARS truncation for a 7^{th} PCE order

We thus face a combinatorial optimization problem:

$$\begin{cases} \underset{N,q,k}{\text{argmin}}\ Error(\mathcal{A}^{M}_{\text{q+k}}) \\ \quad s.t.\ S_{\text{lb}} \leq S \leq S_{\text{ub}} \end{cases} \tag{15}$$

where *Error* is an estimator of the PCE quality that we describe in the section 3.4, and S is the available number of samples.

Eq. 15 may be solved using any appropriate algorithm (genetic approach, simulated annealing, etc.). The strategy we adopt here is inspired by [22] and is shown in **Algorithm** 3.

Algorithm 3 Optimization of $Q-$norm + LARS parameters

- Arbitrarily choose a set $\mathbf{N} = \{N_1, \ldots, N_n\}$ of PCE orders, (N_n possibly high).
- Store the response obtained using an Fat-LHS sampling in a vector $\boldsymbol{y} = [y_1, \ldots, y_N]$

for $idx_n = 1 : n$ **do**

- Choose a set of significant q values

$q \in \{q_{(i)} | i \in 1, \ldots, Q\}$

for $idx_q = 1 : Q$ **do**

- Compute the $N^{\text{th}}_{idx_n}$ order full polynomial basis $\boldsymbol{\Psi}_{\text{full}}$.
- Truncate the full polynomial basis using the $q_{(idx_q)}$ norm giving $\boldsymbol{\Psi}_{\text{q-truncated}}$
- Let $P_{\text{remain}} = card(\mathcal{A}^M_{\text{q}})$ be the number of remaining polynomials after truncation
- Perform a V-fold cross validation as follows, with K=2.

for $idx_P = 1 : \min(P_{\text{remain}}, N)$ **do**

- Divide the sampling in 2 populations of equal size $\boldsymbol{\xi}_{\text{test}}$ and $\boldsymbol{\xi}_{\text{verif}}$

for $v = 1 : V$ **do**

- Compute the LARS Algorithm on the P_1 population
- Verify the results on the P_2 population by computing the chosen error estimate.

end for

- Retain the best LARS step k^* according to the selected error criterion

end for

end for

end for

- Retain the best model with the best N^*, q^*, k^* according to the selected error criterion

3.4. Error evaluation of the polynomial expansion

According to Cameron Martin's theorem [35], when truncating the multi-index set, one may not reach the convergence to the exact solution in the $\mathcal{L}_2$ sense. We assess the results for an another classical error estimate called the corrected Leave-One-Out (LOO) error estimate taking into account the overfitting phenomenon [37].

Global error estimate. An estimation of the exact $\mathcal{L}_2$ error is given by the empirical error:

$$\text{Err}_{\text{emp}} = \frac{1}{N} \sum_{i=1}^{N} (\mathbf{y}(\boldsymbol{\xi}_i) - \mathbf{y}^{\mathcal{A}^M_{\text{q+k}}}(\boldsymbol{\xi}_i))^2 \tag{16}$$

However, this estimator is known to under-predict the exact $\mathcal{L}_2$ error: when increasing the complexity of the PCE, the empirical error is systematically reduced, as the exact $\mathcal{L}_2$ error may increase (overfitting phenomenon). By construction, the Leave-One-Out error (LOO error) [22] may be less sensitive to the overfitting. It relies on the computation of the predicted residual

$$\Delta^{(i)} = \mathbf{y}(\boldsymbol{\xi}_i) - \mathbf{y}^{\mathcal{A}^M_{\text{q+k}}}_{-i}(\boldsymbol{\xi}_i), \tag{17}$$

for each evaluation $\boldsymbol{\xi}_i$, $i \in \{1, \ldots, N\}$, where $\mathbf{y}^{\mathcal{A}^M_{\text{q+k}}}_{-i}(\boldsymbol{\xi}_i)$ denotes the approximated model evaluated

in $\boldsymbol{\xi}_i$ trained in $\boldsymbol{\Xi}/\{\boldsymbol{\xi}_i\}$. The LOO error is then computed as

$$\mathrm{Err}_{\mathrm{LOO}} = \frac{1}{N}\sum_{i=1}^{N}\Delta^{(i)2}. \tag{18}$$

In the general case, the computation of the predicted residuals is a greedy process. In our case, these may be analytically computed

$$\Delta^{(i)} = \frac{\mathbf{y}(\boldsymbol{\xi}_i) - \mathbf{y}^{\mathcal{A}^M_{\mathrm{q+k}}}(\boldsymbol{\xi}_i)}{1-h_i} \tag{19}$$

where h_i is the i^{th} diagonal term of the $\boldsymbol{\Psi}^{\mathcal{A}^M_{\mathrm{q+k}}}\left(\boldsymbol{\Psi}^{\mathcal{A}^M_{\mathrm{q+k}}\top}\boldsymbol{\Psi}^{\mathcal{A}^M_{\mathrm{q+k}}}\right)^{-1}\boldsymbol{\Psi}^{\mathcal{A}^M_{\mathrm{q+k}}\top}$ matrix.

Finally, we compute the absolute LOO as

$$\mathrm{Err}_{\mathrm{LOO}} = \frac{1}{N}\sum_{i=1}^{N}\left(\frac{\mathbf{y}^{\mathcal{A}^M_{\mathrm{q+k}}}(\boldsymbol{\xi}_i) - \mathbf{y}^{\mathcal{A}^M_{\mathrm{q+k}}}(\boldsymbol{\xi}_i)}{1-h_i}\right)^2. \tag{20}$$

and its relative counterpart

$$\epsilon_{\mathrm{LOO}} = \frac{\mathrm{Err}_{\mathrm{LOO}}}{\sigma(\mathbf{y})^2}. \tag{21}$$

3.4.1. Computing the coefficients of the truncated multi-variate PCE

To compute the coefficients of the PCE, intrusive Galerkin type approach has been proposed by [33]. Among non intrusive, projection based methods take advantage of the orthogonal properties of the multivariate polynomials of the expansion. Stochastic collocation is based on a Lagrangian interpolation in the stochastic space. It may be proved that this method is equivalent to the former [40].

The regression based approach (on which we focus in this paper) consists in solving the overdetermined system of equations, where each $\boldsymbol{\Xi}^{(i)}, i \in \{1,...,S\}$ represent $S > P$ samples of the random vector $\boldsymbol{\Xi} = \{\boldsymbol{\xi}_1,...,\boldsymbol{\xi}_M\}$. The optimal number of realizations needed to assess the coefficients with a good accuracy is still an open research area, but [21] proposes an empirical rule (Eq.22). In the following, we consider this empirical requirement as a lower bound in the simulation requirements ($S \geq S_{lb}$) to build a PCE.

$$S_{lb} = (M-1)\times P. \tag{22}$$

The set of coefficients may be computed as

$$\boldsymbol{\gamma} = argmin(\|\mathbf{y}(\boldsymbol{\xi}) - \boldsymbol{\Psi}(\boldsymbol{\xi})\boldsymbol{\gamma}^\top\|^2) \tag{23}$$

yielding

$$\boldsymbol{\gamma} = (\boldsymbol{\Psi}(\boldsymbol{\xi})\boldsymbol{\Psi}(\boldsymbol{\xi})^\top)^{-1}\boldsymbol{\Psi}(\boldsymbol{\xi})\mathbf{y}(\boldsymbol{\xi}) \tag{24}$$

with $\boldsymbol{\xi}^{(i)}, i \in \{1,...,S\}$ representing $S > P$ samples of the M dimensional random vector $\boldsymbol{\xi}$. These samples are generated using a S-sized M-dimensional Fat-LHS.

The overdetermined system of equations (Eq.24) may be solved using a singular value decomposition of the $\mathbf{\Psi}\mathbf{\Psi}^\top$ matrix.

Once the set of P coefficients $\{\gamma_\alpha\}_{\alpha\in\mathcal{A}}$ has been determined, one may compute the statistical moments of y analytically avoiding Monte Carlo simulations. The first two moments are given by:

$$\mathbb{E}(y) = \gamma_0 \tag{25}$$

$$\sigma^2(y) = \sum_{\alpha\in\mathcal{A}-\{0\}} \mathbb{E}(\Psi_\alpha^2)\gamma_\alpha^2 \tag{26}$$

4. Results and discussions

4.1. Experiment description

We model the variability of the springback parameter of a 2D deep drawn U-shaped metal sheet from the B3 Numisheet '93 [41] benchmark.

The overall geometrical configuration of the deep drawing process is illustrated in Fig.10.

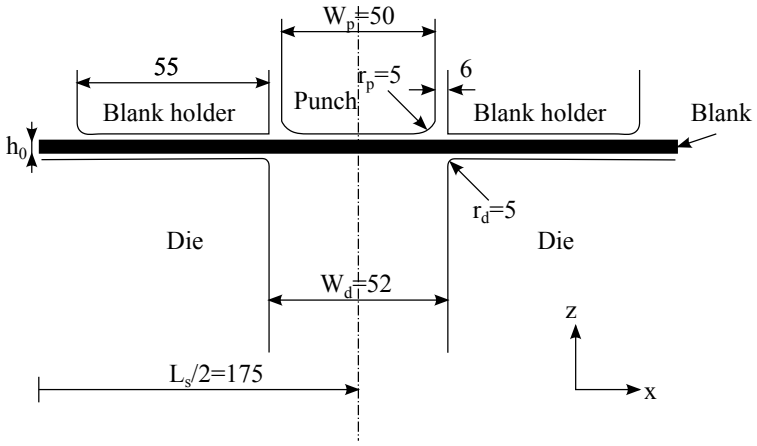

Figure 10: Geometrical configuration of the modeled Numisheet'93 benchmark (values in *mm*).

The process is modeled using a legacy software [42] (Fig.10) using appropriate symmetry boundary conditions. A single row of 175 first-order shell elements is used to model the blank with Simpson integration rule with 10 integration points across the thickness. As the problem is essentially in plane strain state (the width of the blank is 35 mm and its thickness nominal value is 0.8 mm), corresponding boundary conditions are applied on each node. The blank is made of mild steel modeled as an elastic-plastic material. Isotropic elasticity and the Swift isotropic hardening law are considered

$$\sigma = K_0(\epsilon_0 + \epsilon_p)^{n_0}. \tag{27}$$

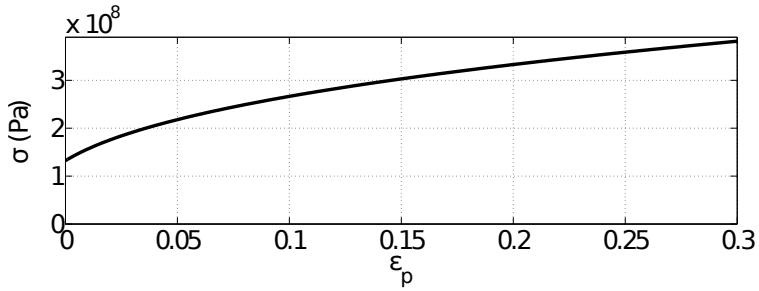

Figure 11: Representation of the Swift hardening law for the parameters described in Table 2

The value of the geometrical, material, loading and contact parameters are summarized in Table 2.

Geometry	Material	Loading	Contact
L_s : 300 mm	E : 71 GPa	F_b : 300 N	μ : 0.15
h_0 : 0.81 mm	ν : 0.342	s : 60 mm	
W_s : 1 mm	ρ : 2700 kg/m^3		
r_p : 10 mm	K_0 : 576.79 MPa		
W_d : 62 mm	ϵ_0 : 0.3593		
r_d : 10 mm	n_0 : 0.01658		

Table 2: Geometrical, material, loading and contact parameter of the U-shaped B-U-T model .

The tools (punch, blank holder and die) are modeled as rigid body surfaces. The punch velocity is taken here as 15 m/s and its displacement is $s = 70$ mm. The blank holder force is defined as $F_b = 2.45$ kN. The whole deep drawing process is simulated in two steps.

1. The forming phase is modeled using the explicit dynamic approach to solve the problem in a reasonable computational time. During this period, the blank holder force is applied with a smooth ramp to minimize the inertia effect and the punch velocity using a triangle step definition starting and ending with 0 velocity and reaching the 15 m/s with the half run. The contact occurring during forming phase is modeled using contact pairs.

2. The springback phase is modeled using an implicit approach. At the end at this phase, the springback shape parameters (output functions of interest), the curvature ρ, the angles β_1 and β_2 are measured as shown in Fig.12.

4.2. Sensitivity analysis

Results of the sensitivity according to the method presented in section 2 are given in Table 3.

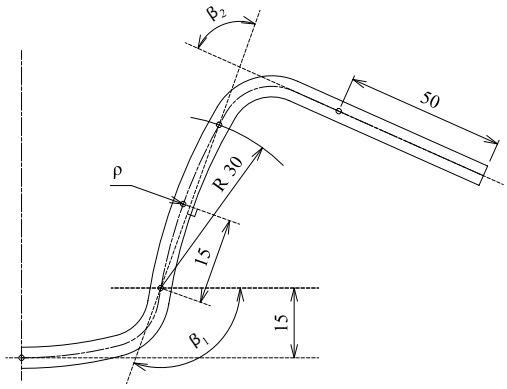

Figure 12: Definition of springback parameters, ρ, β_1 and β_2.

Variables	Responses		
	ρ	β_1	β_2
Thickness	1e-5	1e-5	1e-5
Young's Modulus	1e6	1e6	1e6
K_0	1e6	1e6	1e6
ϵ_0	1e-2	1e-2	1e-2
ν_0	1e-2	1e-2	1e-2
Poisson's coefficient	1e-2	1e-2	1e-2
Friction coefficient	1e-2	1e-2	1e-2
Clamp force	1e1	1e1	1e1

Table 3: Sensitivity threshold obtained for $\mu_i^* = 2$

4.3. Stochastic model

In Table 4, we identify the set of independent random variables considered in the model. If the variation range of the parameters may be considered as realistic, the Gaussian hypothesis is only illustrative.

The mean values correspond to the nominal values, and the standard deviations are adjusted so that $\xi_{\min} = \xi_{\text{mean}} - 3\sigma$ and $\xi_{\max} = \xi_{\text{mean}} + 3\sigma$.

4.4. 2D validation test case

In this paragraph, we consider only 2 random variables: the thickness of the blank and the Young modulus. If we consider the identified sensitivity in section 4.2, the sampling methodology developed in section 2.1 allows us to consider $S_{ub} = 343$ samples respecting the sensitivity criterion Eq.3.

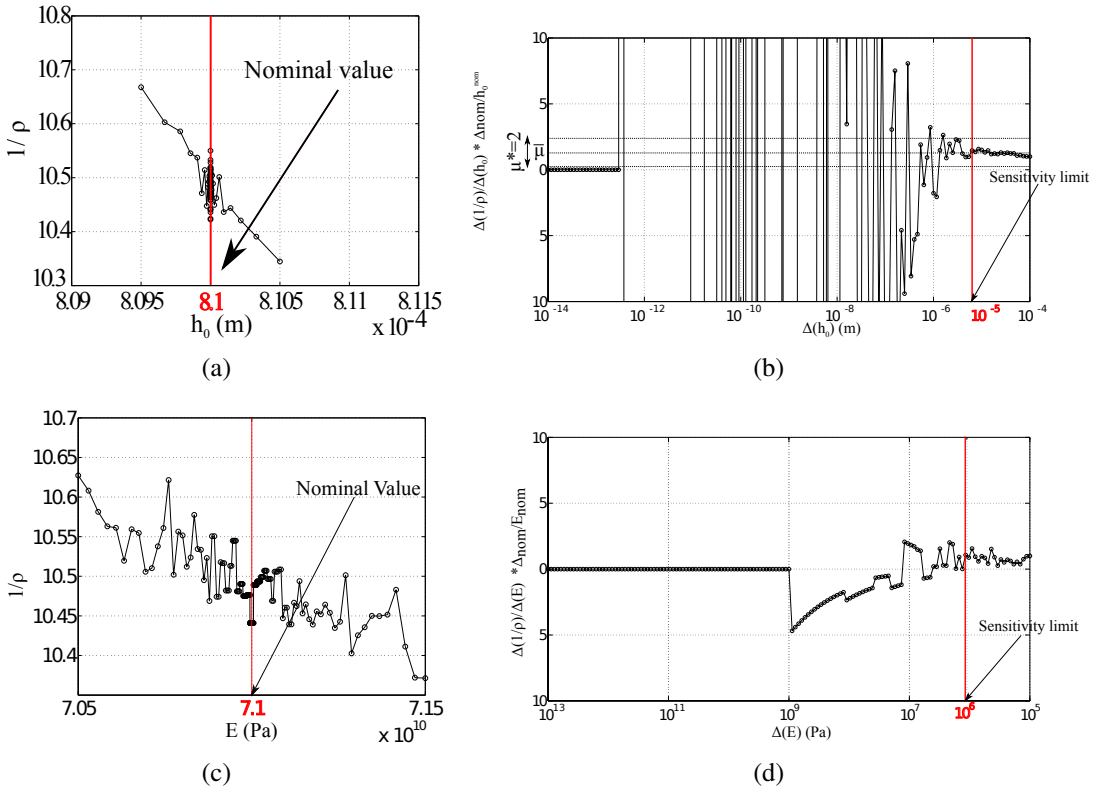

Figure 13: Numerical instability for FEM simulations of the deep drawing process of 2-D U-shaped metal sheet under small variations of the Thickness and Young modulus (MPa) for the ρ response. On the *left side*, the obtained responses are depicted, as on the *right side* the numerical sensitivities of the model with regards to different order of magnitude of thickness variation is plotted.

ξ	min	max	E[ξ]
Thickness (h_0)	0.805	0.815	0.8 mm
Young's Modulus (E_b)	70.5	71.5	71 GPa
K_0	575.79	577.79	576.79 MPa
ϵ_0	0.3493	0.3693	0.3593 -
ν_0	0.015	0.017	0.01658
Poisson's Coefficients (ν)	0.325	0.335	0.33
Friction coefficients (μ)	0.155	0.170	0.162
Clamp force (F)	34.5e3	35.5e3	35e3 kN

Table 4: Full stochastic model under study for the deep drawing process application

4.4.1. Validation of Fat-LHS

In order to illustrate the efficiency of the Fat-LHS, we propose to compare the value of the two first statistical moments of each response and illustrates for two different sampling methodologies:

a classical LHS sampling and the proposed sensitivity constrained LHS sampling. We illustrate the results only on the $1/\rho$ response, the interpretation remaining unchanged for the other outputs.

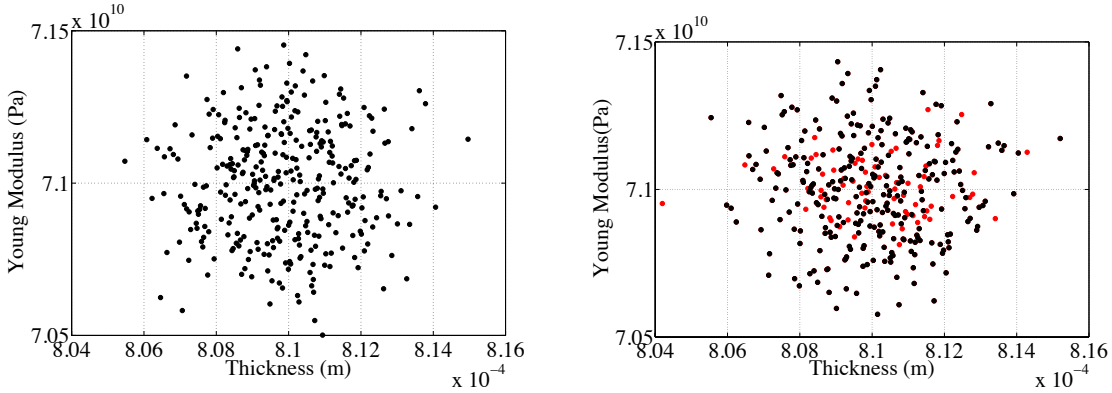

(a) Fat-LHS with 343 samplings

(b) LHS with 343 samplings

Figure 14: Illustration of LHS samplings obtained with taking (a) and not taking (b) into account the sensitivity constraint for 343 samplings. In red appears the illegal neighbors.

The Fig.15 is obtained using the classical LHS and Fat-LHS. For the same number of samples a non-negligible bias in the mean value is observed when the number of sampling becomes high, the classical LHS mean and standard deviation converges to the values produced by the Fat-LHS for a smaller number of sampled points.

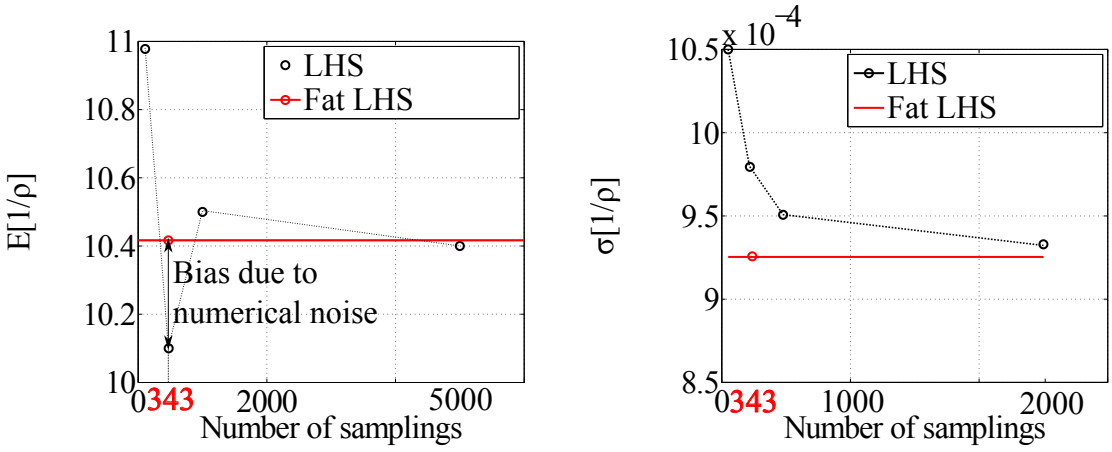

(a)

(b)

Figure 15: Comparison of the mean and the standard deviation evolution for different sampling size of classical LHS with the Fat-LHS

4.5. 8D example

4.5.1. Comparison of sparse PCE strategies

We here compare the convergence results of the different truncation strategies for different 2-variate PCE of increasing order. We consider a limited number of 457 simulations issued from the Fat-LHS previously described.

We choose a polynomial order $N \in \{1, \ldots, n\}$ for the PCE approximation. For each PCE order N we apply 3 truncation strategies:

1. We select the Q-norm parameters such that $S_{lb} \leq S \leq S_{ub}$. For all the possible q parameters we compute the approximate model $y_{\mathcal{A}_q^{\mathcal{M}}}$, and retain the one with the lowest LOO error.

2. We use the LARS based algorithm on the classical truncation scheme and retain the best model.

3. We combine the $Q-$norm and LARS approach and retain the best approximate model.

Fig.16 shows the evolution of the LOO corrected error with regards to the number of terms contained in the best PCE approximation. Each point refers to the best model obtained during the truncation for different PCE order. LARS alone provides the worst results, most of the time less accurate and more costly than the two other methods. Comparing the $Q-$norm and the combined LARS+$Q-$norm we observe similar results in terms of accuracy. However, a slight advantage may be given to the Combined LARS+Q-norm as it gives similar accuracy for a sparse PCE expansion. In addition, we note that due to smooth training data, we finally obtain the best results for truncated low order PCE.

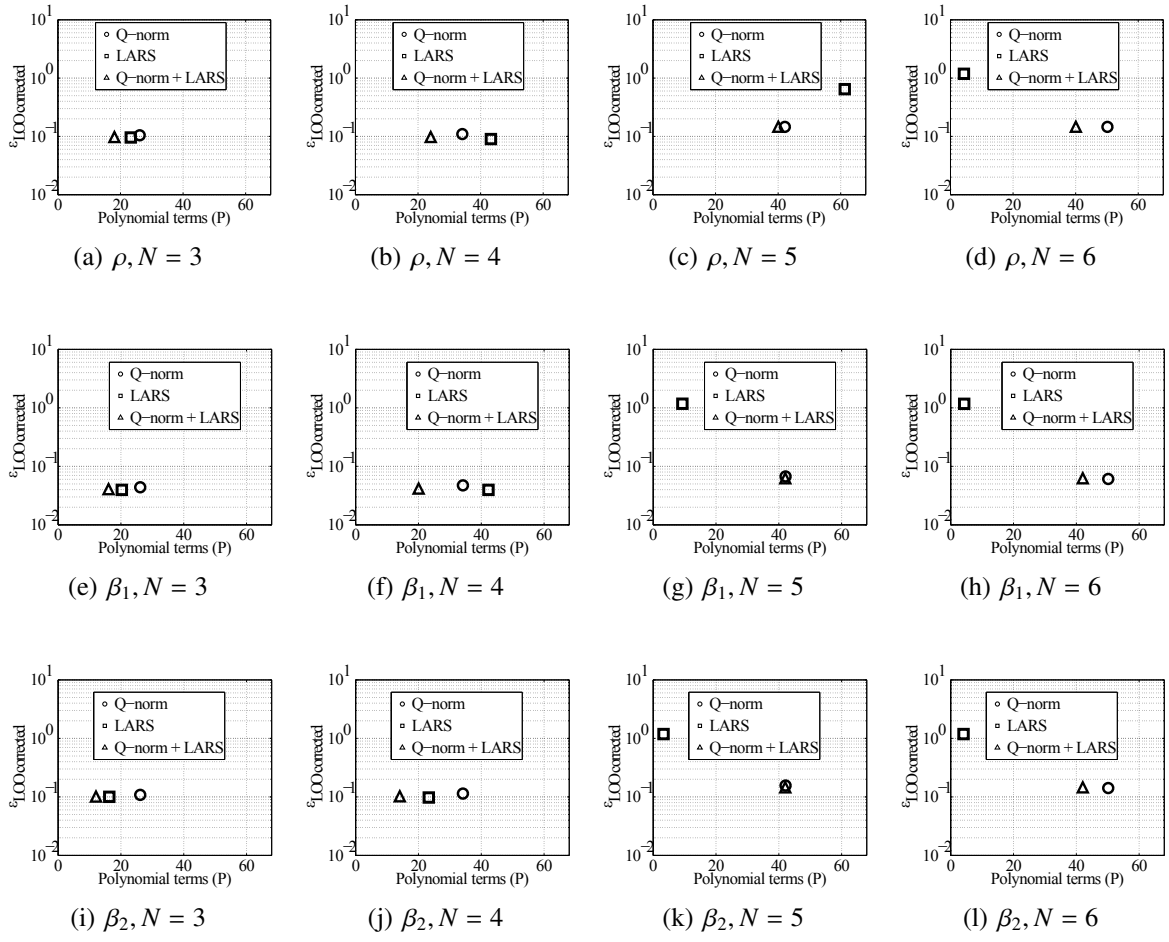

(a) $\rho, N = 3$ (b) $\rho, N = 4$ (c) $\rho, N = 5$ (d) $\rho, N = 6$

(e) $\beta_1, N = 3$ (f) $\beta_1, N = 4$ (g) $\beta_1, N = 5$ (h) $\beta_1, N = 6$

(i) $\beta_2, N = 3$ (j) $\beta_2, N = 4$ (k) $\beta_2, N = 5$ (l) $\beta_2, N = 6$

Figure 16: Comparison of the evolution of the LOO error corrected for different polynomial degree with regards to springback parameter ρ (a), β_1 (b), β_2 (c). The parameters considered as random variable are depicted in table 4

The histograms (Fig.17) illustrate the variability obtained for the best retained model for each response obtained using the **Algorithm** 3. A good agreement is observed with the exact "high-fidelity" simulations as the relative error in mean is close to 0 and in standard deviation lower than 1% as depicted in table 5.

H

	$\frac{\Delta E}{E_{\text{high-fidelity}}}$	$\frac{\Delta \sigma}{\sigma_{\text{high-fidelity}}}$
ρ	$\approx 10^{-9}$	$3.7e-3$
β_1	$\approx 10^{-7}$	$4.5e-3$
β_2	$\approx 10^{-12}$	$8.5e-3$

Table 5: Relative error in mean and standard deviation obtained for each response

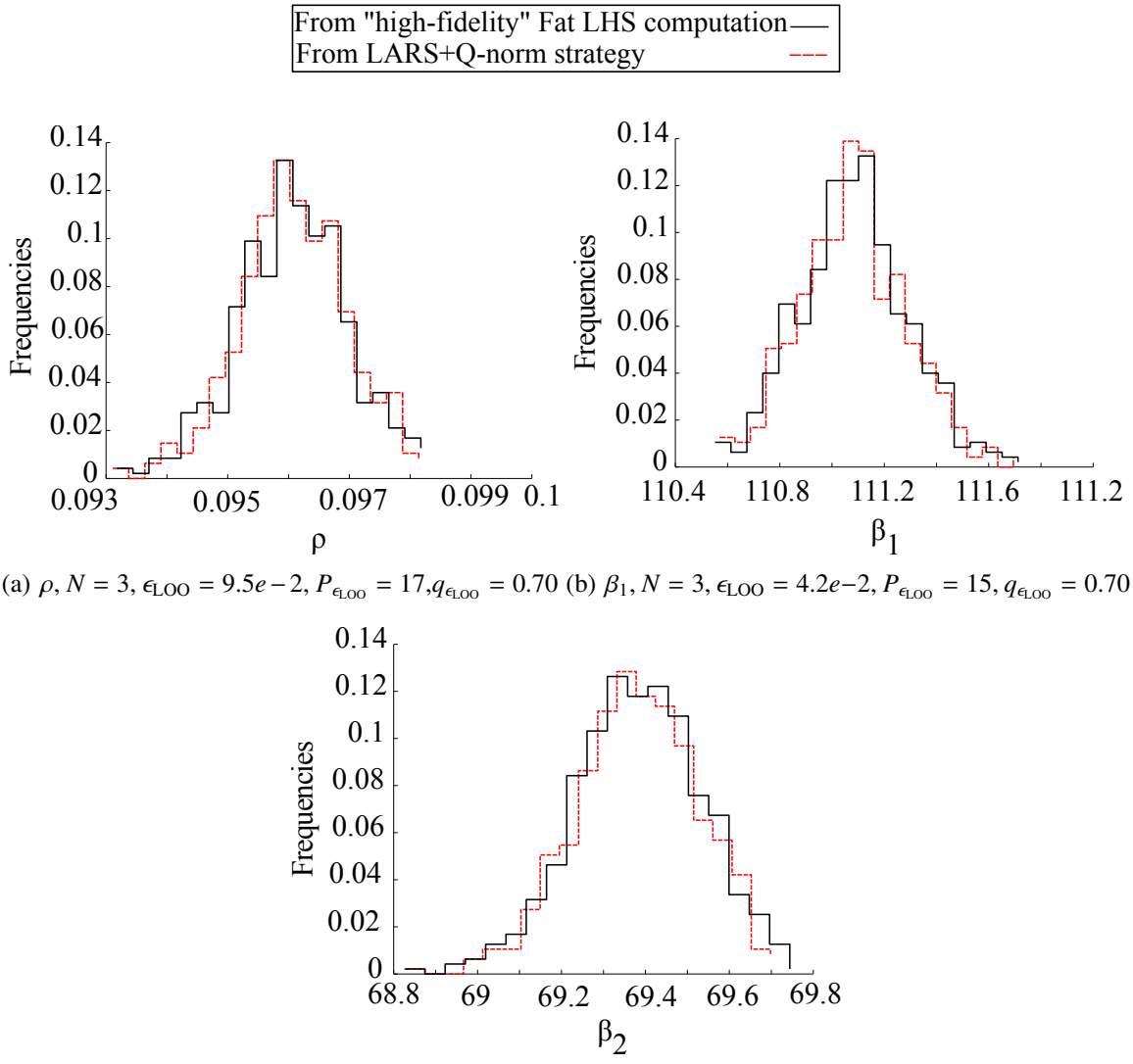

(a) ρ, $N = 3$, $\epsilon_{\text{LOO}} = 9.5e-2$, $P_{\epsilon_{\text{LOO}}} = 17$,$q_{\epsilon_{\text{LOO}}} = 0.70$ (b) β_1, $N = 3$, $\epsilon_{\text{LOO}} = 4.2e-2$, $P_{\epsilon_{\text{LOO}}} = 15$, $q_{\epsilon_{\text{LOO}}} = 0.70$

(c) β_2, N=3, $\epsilon_{\text{LOO}} = 8.5e-2$, $P_{\epsilon_{\text{LOO}}} = 10$, $q_{\epsilon_{\text{LOO}}} = 0.5$

Figure 17: Histograms obtained for the modified cross validation strategy for the 8-variate case using the $\epsilon_{\text{LOO corrected}}$

5. Conclusions and prospects

In this paper, we highlighted a fundamental limitation of the surrogate-based approach for uncertainty propagation. We showed that when using non linear FE scheme as "high-fidelity" simulation, small variations of the random input parameters may lead to noisy input training which alters the accuracy of the training data set and may distort the statistical quantities of interest. We illustrate this claim using the non-linear FEM simulation (involving contact/friction and material non linearities) of the springback of a 2D deep drawing process of U shaped metal sheet. We propose a sampling methodology called *Fat-LHS* allowing us to filter noisy data preserving their LHS property. This heuristic strategy provides the maximum number of simulations available considering the finite model sensitivity. We then use this limited number of non-noisy samples to build a PCE in order to propagate the uncertainty. But, the low number of samples leads us to consider sparse strategies to make affordable possible identification of the PCE terms. We compare three different methodologies to build a sparse PCE (LARS, $Q-$norm and LARS+$Q-$norm) and retain the best possible PCE for each of them. The comparison of the results shows that generally the $Q-$norm+LARS hybrid is more efficient. We obtain the best results for truncated low order sparse PCE leading to unbiased estimation. Further work is required to

- economically compute the model sensitivity threshold,
- generate more space–filling LHS design (in this paper, only the min-max strategy has been tested)

Finally, to assess the PCE accuracy, we use a LOO corrected PCE error in order to

- assess the goodness of fit of the PCE
- and to limit the overfilling phenomenon simultaneously.

Thus it is difficult to separate which part of the inaccuracy comes from the model misspecification and which part comes from the overfitting phenomenon. A formulation of an overfitting measure for PCE approximation inspired from [43] may open a new way to efficiently select the most significant polynomials terms in a sparse PCE expansion.

Acknowledgements

This research was conducted as part of the OASIS project, supported by OSEO within the contract FUI no. F1012003Z. The first author is grateful to Innoviris for its support to BB2B project entitled multicriteria optimization with uncertainty quantification applied to the building industry. The authors also acknowledge the support of Labex MS2T.

References

[1] G. G. Wang, S. Shan, Review of metamodeling techniques in support of engineering design optimization, Journal of Mechanical Design 129 (2007) 370.

[2] T. W. Simpson, V. Toropov, V. Balabanov, F. A. Viana, Design and analysis of computer experiments in multidisciplinary design optimization: a review of how far we have come or not, in: 12th AIAA/ISSMO Multidisciplinary Analysis and Optimization Conference, 2008, pp. 10–12.
[3] N. M. Alexandrov, R. M. Lewis, C. R. Gumbert, L. L. Green, P. A. Newman, Approximation and model management in aerodynamic optimization with variable-fidelity models, Journal of Aircraft 38 (6) (2001) 1093–1101.
[4] B. Sudret, Global sensitivity analysis using polynomial chaos expansions, Reliability Engineering & System Safety 93 (7) (2008) 964–979.
[5] T. Crestaux, O. Le Maıtre, J.-M. Martinez, Polynomial chaos expansion for sensitivity analysis, Reliability Engineering & System Safety 94 (7) (2009) 1161–1172.
[6] M. Eldred, Design under uncertainty employing stochastic expansion methods, International Journal for Uncertainty Quantification 1 (2) (2011) 119–146.
[7] N. M. Alexandrov, R. M. Lewis, An overview of first-order model management for engineering optimization, Optimization and Engineering 2 (4) (2001) 413–430.
[8] M. Eldred, A. Giunta, S. Collis, N. Alexandrov, R. Lewis, Second-order corrections for surrogate-based optimization with model hierarchies, in: Proceedings of the 10th AIAA/ISSMO Multidisciplinary Analysis and Optimization Conference, Albany, NY,, Aug, 2004.
[9] M. H. Bakr, J. W. Bandler, K. Madsen, J. E. Rayas-Sanchez, J. Sondergaard, Space-mapping optimization of microwave circuits exploiting surrogate models, Microwave Theory and Techniques, IEEE Transactions on 48 (12) (2000) 2297–2306.
[10] T. de Souza, B. Rolfe, Multivariate modelling of variability in sheet metal forming, Journal of Material Processing Technology 203 (2008) 1–12.
[11] N. M. Alexandrov, R. M. Lewis, C. R. Gumbert, L. L. Green, P. A. Newman, Optimization with variable-fidelity models applied to wing design, Tech. rep., DTIC Document (1999).
[12] R. Vitali, R. T. Haftka, B. V. Sankar, Multi-fidelity design of stiffened composite panel with a crack, Structural and Multidisciplinary Optimization 23 (5) (2002) 347–356.
[13] G. Sun, G. Li, S. Zhou, W. Xu, X. Yang, Q. Li, Multi-fidelity optimization for sheet metal forming process, Structural and Multidisciplinary Optimization 44 (1) (2011) 111–124.
[14] L. Wang, R. V. Grandhi, Improved two-point function approximations for design optimization, AIAA Journal 33 (9) (1995) 1720–1727.
[15] P. Breitkopf, H. Naceur, P. Villon, Moving least squares response surface approximation: Formulation and metal forming applications, Computers and Structures and Structures 83 (2005) 1411–1428.
[16] M. Eldred, D. Dunlavy, Formulations for surrogate-based optimization with data fit, multifidelity, and reduced-order models, in: Proceedings of the 11th AIAA/ISSMO Multidisciplinary Analysis and Optimization Conference, number AIAA-2006-7117, Portsmouth, VA, Vol. 199, 2006.
[17] V. Dubourg, B. Sudret, J. . Bourinet, Reliability-based design optimization using kriging surrogates and subset simulation, Structural and Multidisciplinary Optimization 44 (5) (2011) 673–690.
[18] T. Jansson, L. Nilsson, R. Moshfegh, Reliability analysis of a sheet metal forming process using monte carlo analysis and metamodels, Journal of Material Processing Technology 202 (2008) 255–268.
[19] S.-C. Kang, H.-M. Koh, J. F. Choo, An efficient response surface method using moving least squares approximation for structural reliability analysis, Probabilistic Engineering Mechanics 25 (4) (2010) 365 – 371.
[20] R. Ghanem, Adaptative polynomial chaos expansions applied to statistics of extremes in non linear random vibration, Probabilistic engineering mechanics 12 (2) (1998) 125–136.
[21] M. Berveiller, B. Sudret, M. Lemaire, Stochastic finite element : a non intrusive approach by regression, Revue Européenne de Mécanique Numérique 15 (2006) 81–92.
[22] G. Blatman, B. Sudret, Sparse polynomial chaos expansions and adaptive stochastic finite elements using a regression approach, Comptes Rendus Mécanique 336 (2008) 518–523.
[23] W. Donglai, C. Zhenshan, C. Jun, Optimization and tolerance prediction of sheet metal forming process using response surface model, Computational Materials Science 42 (2007) 228–233.
[24] H. Ou, P. Wang, B. Lu, H. Long, Finite element modelling and optimization of net-shape metal forming processes with uncertainties, Computers and Structures 90-91 (2012) 13–27.
[25] M. McKay, W. Conover, R. Beckman, A comparison of three methods for selecting values of input variables in

the analysis of output from a computer code, Technometrics 21 (1979) 239–245.
[26] M. Stein, Large sample properties of simulations using latin hypercube sampling, Technometrics 29 (2) (1987) 143–151.
[27] P. Z. Qian, M. Ai, C. Wu, Construction of nested space-filling designs, The Annals of Statistics 37 (6A) (2009) 3616–3643.
[28] P. Z. Qian, Nested latin hypercube designs, Biometrika 96 (4) (2009) 957–970.
[29] P. Z. Qian, B. Tang, C. Jeff Wu, Nested space-filling designs for computer experiments with two levels of accuracy, Statistica Sinica 19 (1) (2009) 287.
[30] G. D. Wyss, K. H. Jorgensen, A user's guide to lhs: Sandia's latin hypercube sampling software, SAND98-0210, Sandia National Laboratories, Albuquerque, NM.
[31] K. R. Dalbey, G. N. Karystinos, Fast generation of spacefilling latin hypercube sample designs, in: Proc. of the 13th AIAA/ISSMO Multidisciplinary Analysis and Optimization Conference, 2010.
[32] K. R. Dalbey, G. N. Karystinos, Generating a maximally spaced set of bins to fill for high-dimensional space-filling latin hypercube sampling, International Journal for Uncertainty Quantification 1 (3) (2011) 241–255.
[33] R. Ghanem, Stochastic finite Elements: A spectral approach, Springer, 1991.
[34] D. Xiu, G. E. Karniadakis, The wiener–askey polynomial chaos for stochastic differential equations, SIAM Journal on Scientific Computing 24 (2) (2002) 619–644.
[35] R. Cameron, W. Martin, Transformations of wiener integrals under translations, The annals of Mathematics 45 (2) (1944) 386–396.
[36] B. Sudret, A. Der Kiureghian, Stochastic finite elements methods and reliability- a state of the art, Tech. rep., Department of civil and environmental engineering (2000).
[37] G. Blatman, B. Sudret, Sparse polynomial chaos expansions and adaptive stochastic finite elements using a regression approach, Comptes-Rendus Mécanique 336 (2008) 518–523.
[38] T. Hesterberg, N. Choi, L. Meier, C. Fraley, Least angle and l_1 penalized regression: A review, Statistics Surveys 2 (2008) 61–93.
[39] R. T. Hastie, J. Tibshirani, G. Friedman, The Elements of Statistical Learning, Data Mining, Inference and Prediction, Springer, 2009.
[40] B. Sudret, Uncertainty propagation and sensitivity analysis in mechanical models – Contributions to structural reliability and stochastic spectral methods, habilitation à diriger des recherches, Université Blaise Pascal, Clermont-Ferrand, France (2007).
[41] A. Makinouchi, E. Nakamachi, E. Onate, R. Wagoner (Eds.), Numisheet'93 2nd International Conference, Numerical Simulatoin of 3-D Sheet Metal Forming Process - Verification of Simulation with Experiment., Riken Tokyo, 1993.
[42] LSTC, LS-Dyna Keyword User's Manual, Livermore Software Technology Corporation (LSTC), 2009th Edition.
[43] M. Bilger, W. G. Manning, Measuring overfitting and mispecification in nonlinear models, Tech. rep., HEDG, c/o Department of Economics, University of York (2011).

Chapter 5

Towards multi-objective optimization under uncertainty

As a natural step forward, incorporating the treatment of uncertainties into an optimization process may provide the engineer with additional valuable information concerning for example, the robustness and the reliability performances of the system to design. Most of the time such studies are made in a single objective context. However, in many real-life cases, the performance of a system is defined by multiple criteria, some of them competing.

In this section we thus propose an efficient metamodel-based strategy in order to tackle the issue of multi-objective optimization under uncertainty. Most of the time, evolutionary algorithms offer a reasonable way to solve this multiobjective optimization problem. However, these populations based algorithms are known to require a large number of evaluation of the numerical models. Inserting the treatment of uncertainties as an inner loop of the multiobjective optimization process may make the process become unaffordable. Moreover, the concepts defined in single objective optimization are not directly appliable in multiobjective optimization as they usually do not take into account the intrinsic multiobjective nature of the problem.

Both issues are addressed in this section. An original hierarchical metamodel approach is provided in order to perform a multiobjective optimization task at affordable computational costs. It is then applied in an original formulation to take uncertainties into account in a multiobjective context as well as an efficient approach to solve it based on a hierarchical approach.

The following paper has been published in the journal Structural Multidisciplinary Optimization.

As a second author in this paper, I particularly focus my attention on the definition of the hierarchical metamodel strategy for uncertainty propagation.

Struct Multidisc Optim (2011) 43:707–729
DOI 10.1007/s00158-010-0608-5

RESEARCH PAPER

Hierarchical stochastic metamodels based on moving least squares and polynomial chaos expansion

Application to the multiobjective reliability-based optimization of space truss structures

Rajan Filomeno Coelho · Jérémy Lebon · Philippe Bouillard

Received: 9 July 2010 / Revised: 26 October 2010 / Accepted: 6 December 2010 / Published online: 24 December 2010

Abstract While surrogate-based optimization has encountered a growing success in engineering design, the development of stochastic metamodels, i.e. capable of representing the complete random responses with respect to random inputs, is still an open issue, although they could be fruitfully used in optimization under uncertainty, both with single and multiple objectives. Therefore, the contribution of the paper is twofold. First, hierarchical stochastic metamodels based on moving least squares and spectral decomposition (by polynomial chaos expansion) are proposed in order to obtain a complete description of the random responses with respect to the deterministic and random input parameters. Then, these metamodels are incorporated into a novel multiobjective reliability-based formulation leaning on the concept of probabilistic nondominance. The whole procedure is applied to an analytical test case as well as to the design optimization of space truss structures, demonstrating the ability of the proposed method to provide accurate solutions at an affordable computational time.

Keywords Surrogate-based optimization · Optimization under uncertainty · Reliability-based design optimization · Polynomial chaos expansion · Moving least squares · Multiobjective evolutionary optimization · Space trusses

R. Filomeno Coelho (✉) · J. Lebon · P. Bouillard
BATir Department, Université Libre de Bruxelles,
50, avenue F.D. Roosevelt (CP 194/2), 1050, Brussels, Belgium
e-mail: rfilomen@batir.ulb.ac.be

J. Lebon
e-mail: jlebon@batir.ulb.ac.be

P. Bouillard
e-mail: pbouilla@batir.ulb.ac.be

1 Introduction

Despite the invaluable increase of computer hardware performances, the growing demands in computational time and memory resources required by structural and multidisciplinary optimization (involving numerical simulations such as the finite element analysis) explain the popularity of surrogate-based optimization (Breitkopf and Filomeno Coelho 2010). The current challenges met in surrogate-based optimization include the development of metamodels (e.g. kriging, moving least squares, artificial neural networks, radial basis function networks, support vector regression (Forrester and Keane 2009)) or ensemble of metamodels (Acar and Rais-Rohani 2008), the design space sampling (before and during the optimization), the selection, construction, tuning and validation of the surrogate models (Viana et al. 2009), and of course their efficient combination with optimization algorithms.

In this paper, three key features are specifically investigated. First, the use of complex in-house or commercial software often dictates the choice for *non-intrusive* strategies, i.e. requiring no modification of the simulation code. On this matter, a comprehensive survey covering the various modeling and optimization strategies available in the literature to tackle high-dimensional and computationally-expensive black-box simulations has recently been published in this journal (Shan and Wang 2010).

However, the role of *uncertainties*—which may have a significant impact on the optimal solutions, as investigated in robust design optimization (RDO) and reliability-based design optimization (RBDO) (Schuëller and Jensen 2008)—is generally not considered in the development of metamodels, although complete probabilistic descriptions might be useful, especially in reliability-based formulations where safety index assessment is required.

Finally, these issues should be extended to *multiobjective* optimization—generally handled by evolutionary algorithms (Coello Coello et al. 2002)—both in terms of formulation and practical implementations. This also rises new challenges, for instance regarding the updating of the metamodels when the region of interest is not a small neighborhood around the optimum (as in single-objective optimization), but a wider area surrounding the nondominated set.

From these considerations, the contribution of the paper is twofold:

(1) developing non-intrusive hierarchical stochastic metamodels based on moving least squares and polynomial chaos expansion;
(2) applying the proposed stochastic metamodels to the multiobjective reliability-based design optimization of space truss structures.

The paper is organized as follows: after the complete description of the stochastic metamodeling methodology (Section 2), their integration within a multiobjective reliability-based formulation is presented (Section 3), followed by the numerical results obtained for the optimization of space truss structures (Section 4). Finally, the conclusions and future prospects are discussed (Section 5).

2 Stochastic metamodels

2.1 Handling uncertainties through spectral decomposition

This study is concerned with random uncertainty modeled by probability distributions (Der Kiureghian and Ditlevsen 2009). Without loss of generality, it will be assumed in the remainder of the paper that the structural model inputs are decomposed into deterministic design variables x_i, and random design variables ξ_i which can represent perturbations around the design variables (e.g. random uncertainty around the nominal values of cross-sections to be optimized), or system parameter uncertainty (e.g. on material properties, loading or boundary conditions). We will make the additional assumption that the ξ_i are uncorrelated normal random variables.

Before building stochastic metamodels to approximate random scalar functions at limited cost, a preliminary step should be devoted to the representation of random responses. A profuse research on decomposition methods for random responses has been undertaken over the past fifteen years, roughly separable in two major trends: *perturbation* methods and *spectral* methods (Stefanou 2009).

In the perturbation approach, the sensitivities are used to compute probability measures by means of classical reliability methods (*First-Order Reliability Methods* or FORM, and *Second-Order Reliability Methods* or SORM), as stated in Haldar and Mahadevan (2000). In *spectral* decomposition, the aim is rather to obtain complete probability distributions for the random outputs. The main decomposition strategy available in the literature is the *polynomial chaos expansion* (PCE) (Ghanem and Kruger 1996). In structural mechanics, where models are solved by finite elements, the *stochastic Krylov subspaces* or *stochastic reduced basis methods* also encounter a growing interest; specifically adapted to stochastic finite elements, the random response is expressed using basis vectors spanning the stochastic Krylov subspace (Sachdeva et al. 2007). Other decomposition schemes have been proposed for highly nonlinear or discontinuous random processes, like piecewise approximations for example (Acharjee and Zabaras 2007).

In this paper, the use of polynomial chaos expansion is investigated in combination with metamodeling techniques in a hierarchical framework.

Let us focus first on random variables. A response s depending on a single normal variable ξ can be decomposed exactly as follows:

$$s(\xi) = \bar{s} + \sum_{j=1}^{\infty} \gamma_j^s H_j(\xi) = \sum_{j=0}^{\infty} \gamma_j^s H_j(\xi) \tag{1}$$

where $\bar{s}(= \gamma_0^s)$ is the mean of s, $\{\gamma_1^s, \dots\}$ are coefficients independent from ξ and $H_j(\xi)$ is the jth Hermite polynomial. The first five Hermite polynomials are explicitly given below:

$$\begin{aligned} H_0(\xi) &= 1; \\ H_1(\xi) &= \xi; \\ H_2(\xi) &= \xi^2 - 1; \\ H_3(\xi) &= \xi^3 - 3\xi; \\ H_4(\xi) &= \xi^4 - 6\xi^2 + 3. \end{aligned} \tag{2}$$

Of course, for real-life applications, an approximation of s is produced by keeping only a finite number of PCE terms:

$$s(\xi) = \sum_{j=0}^{N} \gamma_j^s H_j(\xi), \tag{3}$$

where N is the maximum degree of ξ appearing in the PCE.

Extended to M random variables, the complete N-order PCE is defined as the set of all multidimensional Hermite polynomials whose degree does not exceed N (Eldred et al. 2008):

$$s(\xi_1, \dots, \xi_M) = \sum_{j=0}^{P-1} \gamma_j^s \psi_j(\boldsymbol{\xi}), \tag{4}$$

where P is the number of terms whose degree $\leq N$:

$$P = \sum_{k=0}^{N} C_{M+k-1}^{k} = \frac{(M+N)!}{M!N!}, \tag{5}$$

and where:

$$\psi_{\boldsymbol{\kappa}}(\xi_1, \ldots, \xi_M) = \prod_{k=1}^{M} H_{\kappa_k}(\xi_k), \tag{6}$$

for which all combinations of $\{\kappa_1, \ldots, \kappa_M\}$ are covered with $\kappa_k \geq 0\ \forall k$ and:

$$\partial_{\boldsymbol{\kappa}} = \sum_{k=1}^{M} \kappa_k \leq N. \tag{7}$$

Other families of polynomials (e.g. Legendre, Jacobi, Laguerre) could be adopted depending on the nature of the random distribution (e.g. uniform, beta, exponential). The construction of PCE in the general case is referred to as the Wiener–Askey scheme (Eldred et al. 2008).

The key point in PCE lies in the determination of the coefficients γ_j^s, which can be achieved by the *Galerkin* method, by *non-intrusive spectral projection* (e.g. Monte Carlo sampling, importance sampling, Gauss quadrature, Smolyak's coarse tensorization), or by *collocation* (Crestaux et al. 2009).

The *collocation* method has been selected in this study due to its flexibility and limited computational cost. For a sample (= collocation point) $\boldsymbol{\xi}^{(i)}$, the corresponding N-order PCE approximation is defined as follows:

$$s(\boldsymbol{\xi}^{(i)}) = \sum_{j=0}^{P-1} \gamma_j^s \psi_j(\boldsymbol{\xi}^{(i)}), \tag{8}$$

where P is given by (5). In matrix form, for Q collocation points, this leads to:

$$\left\{ \begin{array}{c} s(\boldsymbol{\xi}^{(1)}) \\ \vdots \\ s(\boldsymbol{\xi}^{(Q)}) \end{array} \right\} = \left[\begin{array}{ccc} \psi_0(\boldsymbol{\xi}^{(1)}) & \ldots & \psi_{P-1}(\boldsymbol{\xi}^{(1)}) \\ \vdots & & \vdots \\ \psi_0(\boldsymbol{\xi}^{(Q)}) & \ldots & \psi_{P-1}(\boldsymbol{\xi}^{(Q)}) \end{array} \right] \times \left\{ \begin{array}{c} \gamma_0^s \\ \vdots \\ \gamma_{P-1}^s \end{array} \right\} \tag{9}$$

or, in compact form:

$$\mathbf{s}(\boldsymbol{\Xi}) = \boldsymbol{\Psi}(\boldsymbol{\Xi})\, \boldsymbol{\gamma}^s, \tag{10}$$

where $\boldsymbol{\Xi}$ is the set of collocation samples $\{\boldsymbol{\xi}^{(1)}, \ldots, \boldsymbol{\xi}^{(Q)}\}$.

The Q collocations points are computed by the "high-fidelity" simulation to obtain $\mathbf{s}(\boldsymbol{\Xi}) = [s(\boldsymbol{\xi}^{(1)}) \ldots s(\boldsymbol{\xi}^{(Q)})]^{\mathsf{T}}$. If $Q = P$, $\boldsymbol{\Psi}$ is a square matrix, and the corresponding linear system can be solved by Gauss algorithm for example. For $Q > P$ (i.e. there are more samples than the number of coefficients to determine), a linear least squares problem is set up:

$$\boldsymbol{\gamma}^s = \arg\min_{\boldsymbol{\gamma}^s} e_{\mathrm{LS}} = \frac{1}{2} \left\| \boldsymbol{\Psi}\boldsymbol{\gamma}^s - \mathbf{s} \right\|^2. \tag{11}$$

The solution $\boldsymbol{\gamma}^s$ of system (11) is typically found by *singular value decomposition* or SVD, with $\boldsymbol{\Psi}$ decomposed as follows:

$$\boldsymbol{\Psi} = \mathbf{U} \left[\begin{array}{c} \mathbf{D} \\ \mathbf{0} \end{array} \right] \mathbf{V}^{\mathsf{T}} = [\mathbf{U}_1\, \mathbf{U}_2] \left[\begin{array}{c} \mathbf{D} \\ \mathbf{0} \end{array} \right] \mathbf{V}^{\mathsf{T}} = \mathbf{U}_1 \mathbf{D} \mathbf{V}^{\mathsf{T}}, \tag{12}$$

where $\mathbf{U}$ and $\mathbf{V}$ are respectively $Q \times Q$ and $P \times P$ orthogonal matrices, $\mathbf{U}_1$ contains the first P columns of $\mathbf{U}$, $\mathbf{U}_2$ its last $Q - P$ columns, and $\mathbf{D}$ is a $P \times P$ diagonal matrix, with ranked diagonal elements $d_1 \geq \ldots \geq d_P > 0$.

The solution $\boldsymbol{\gamma}^s$ can be written explicitly as:

$$\boldsymbol{\gamma}^s = \mathbf{V}\mathbf{D}^{-1}\mathbf{U_1}^{\mathsf{T}}\mathbf{s}(\boldsymbol{\Xi}) \equiv \mathbf{C}(\boldsymbol{\Xi})\, \mathbf{s}(\boldsymbol{\Xi}). \tag{13}$$

In the optimization context, when multiple responses $f_1, \ldots, f_m$ (objectives), $g_1, \ldots, g_p$ (constraints) are considered, the $\mathbf{C}$ matrix (depending only on the $\boldsymbol{\xi}$ sites) can be computed once for all if common sites $\{\boldsymbol{\xi}^{(1)}, \ldots, \boldsymbol{\xi}^{Q}\}$ are chosen for all responses. The coefficients for the objectives and constraints are then retrieved directly by (13):

$$\left\{ \begin{array}{lcl} \boldsymbol{\gamma}^{f_1} & = & \mathbf{C}(\boldsymbol{\Xi})\, \mathbf{f}_1(\boldsymbol{\Xi}) \\ \ldots & & \\ \boldsymbol{\gamma}^{f_m} & = & \mathbf{C}(\boldsymbol{\Xi})\, \mathbf{f}_m(\boldsymbol{\Xi}) \\ & & \\ \boldsymbol{\gamma}^{g_1} & = & \mathbf{C}(\boldsymbol{\Xi})\, \mathbf{g}_1(\boldsymbol{\Xi}) \\ \ldots & & \\ \boldsymbol{\gamma}^{g_p} & = & \mathbf{C}(\boldsymbol{\Xi})\, \mathbf{g}_p(\boldsymbol{\Xi}) \end{array} \right. \tag{14}$$

or simply:

$$\boldsymbol{\Gamma} = \mathbf{C}(\boldsymbol{\Xi})\, \mathbf{S}(\boldsymbol{\Xi}), \tag{15}$$

where $\boldsymbol{\Gamma} = [\boldsymbol{\gamma}^{f_1} \ \ldots \ \boldsymbol{\gamma}^{g_p}]$ is a $P \times (m+p)$-matrix, $\mathbf{C}$ is a $P \times Q$-matrix and $\mathbf{S} = \left[\mathbf{f}_1 \ \ldots \ \mathbf{g}_p\right]$ is a $[Q \times (m+p)]$-matrix.

2.2 Hierarchical stochastic metamodels

The use of PCE, through a methodology similar to what is described above, has already been applied to robust

multiobjective optimization by Poles and Lovison (2009), but by considering PCE of all uncertain design variables and calculating the PCE coefficients at each function evaluation through a collocation method. The computational cost can be decreased through this decomposition, but a further gain can still be achieved through an hierarchical reduction strategy, as advocated in this paper.

In the general case, the responses depend on random variables $\boldsymbol{\xi}$, but also on deterministic variables $\mathbf{x}$. The multivariate PCE should thus be re-written as follows:

$$s(\mathbf{x}, \boldsymbol{\xi}) = \gamma_0^s(\mathbf{x}) + \sum_{j=1}^{P-1} \gamma_j^s(\mathbf{x}) \psi_j(\boldsymbol{\xi}). \tag{16}$$

For any set $\mathbf{x}$ of design variables, the whole procedure described in the previous section can be repeated, and assuming a common set $\boldsymbol{\Xi}$ of random samples $\{\boldsymbol{\xi}^{(1)}, \ldots, \boldsymbol{\xi}^{(Q)}\}$ for all PCE developments, the coefficients are directly computable as follows:

$$\boldsymbol{\Gamma}(\mathbf{x}) = \mathbf{C}(\boldsymbol{\Xi})\, \mathbf{S}(\mathbf{x}, \boldsymbol{\Xi}). \tag{17}$$

Therefore, a mapping can be traced out between the deterministic parameters $\mathbf{x}$ (to be optimized), and the PCE coefficients γ_j^s representing the different components of the random responses projected in the PCE basis; in other words, the PCE coefficients contain all the information about the stochastic behavior of the objectives and constraints.

Therefore, the idea proposed in this paper is to build hierarchical metamodels of the PCE coefficients with respect to the design variables $\mathbf{x}$:

$$\mathbf{x} \xrightarrow{\text{stochastic metamodels}} \boldsymbol{\Gamma}(\mathbf{x}) \xrightarrow{\text{PCE reconstruction}} \mathbf{s}(\mathbf{x}, \boldsymbol{\xi}). \tag{18}$$

This has similarities to what has been accomplished for multidisciplinary design optimization (Filomeno Coelho et al. 2008, 2009), where surrogate models were built by kriging or moving least squares interpolation of *Proper Orthogonal Decomposition* (POD) coefficients, through a bi-level reduction approach. Related work concerned with geometric filtration using POD for aerodynamic design optimization (Toal et al. 2010) also discusses the comparison between direct approximation and decomposition-based screening of geometric variables.

Surrogate model development for optimization purposes has been extensively discussed in recent contributions by Schuëller and Jensen (2008) as well as Forrester and Keane (2009), showing that the notion of stochasticity in metamodeling is still an open issue. In this topic, a feature worth pointing out is the ability of kriging metamodels to provide statistical information on the output predictions, since the response functions can be seen as the realization of a random process (Jones 2001).

However, in this study, the role of the general metamodeling technique is played by the *moving least squares* (MLS) method (Lancaster and Salkauskas 1981), also called *diffuse approximation* (Nayroles et al. 1992). It consists in a generalization of the least squares technique.

In univariate problems, the moving least squares approximation of a PCE coefficient $\gamma(x)$ can be written as follows (Breitkopf et al. 2002):

$$\gamma(x) \approx \gamma_{\text{MLS}}(x) = \mathbf{p}^{\mathsf{T}}(x)\mathbf{a}(x), \tag{19}$$

where:

$$\mathbf{p}^{\mathsf{T}}(x) = [1 \quad x \quad x^2 \ldots]. \tag{20}$$

$\mathbf{a}(x)$ are the minimizers of functional $J_x(\mathbf{a})$ defined by:

$$J_x(\mathbf{a}) = \frac{1}{2} \sum_i w_i(x^{(i)}, x) \left(\mathbf{p}^{\mathsf{T}}(x^{(i)})\mathbf{a} - \gamma^{(i)}\right)^2, \tag{21}$$

where:

- $\mathbf{p}(x)$ is the polynomial (here, a second-order basis has been selected);
- $x^{(i)}$ are the sample points;
- w_i are the weights depending the Euclidean norm between $x^{(i)}$ and x:

$$w_i = w_{\text{ref}}\left(\frac{\left\|x^{(i)} - x)\right\|}{r}\right), \tag{22}$$

where w_{ref} is chosen here as a piecewise cubic spline expressed by (23):

$$w_{\text{ref}}(s) = \begin{cases} 1 - 3s^2 + 2s^3 & \text{if } 0 \le s \le 1, \\ 0 & \text{if } s \ge 1, \end{cases} \tag{23}$$

and r is a radius defining the (local) influence zone. In this study, r is defined at each evaluation point x such that the influence zone covers the k closest sample points $x^{(i)}$, with $k = n_p + d$ (n_p is number of terms in the polynomial basis whereas d is the dimension of the inputs).

The surrogate surface established by this technique will usually not pass through all sample points. Therefore, to

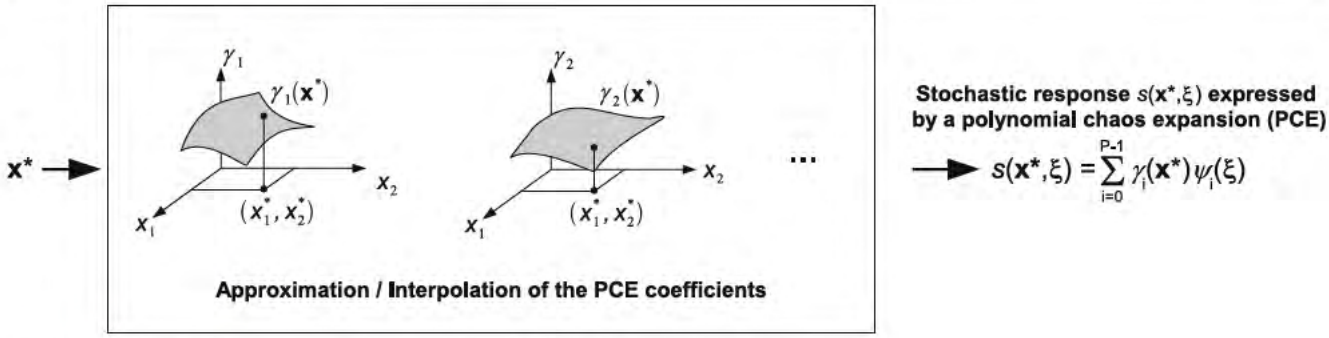

Fig. 1 Synthesis of the hierarchical stochastic metamodels

make the approximation *interpolating*, singular weights can be specifically scaled from the initial weights to fit the data points (Breitkopf et al. 2002):

$$w_{\text{interpolating}} = \frac{w_{\text{init}}}{1 + \varepsilon - w_{\text{init}}}, \tag{24}$$

where ε is set to 10^{-10} in this study. Should the singular weights approach lead to numerical difficulties, other techniques (e.g. Shepard weights) could be used to ensure interpolation.

To build the approximate model for the PCE coefficient matrix (Fig. 1), a two-step procedure is thus necessary:

(I) first, a *design of experiments* (DOE) or *sampling* in the variable domain is carried out: $\{\mathbf{x}^{(1)} \dots \mathbf{x}^{(n_{\text{DOE}})}\}$. These samples are selected in order to cover as widely as possible the design space, for instance through *Latin Hypercube Sampling* (LHS) (Swiler and Wyss 2004). For each $\mathbf{x}^{(i)}$, Q collocation points are calculated for a predefined set of normal random variables $\{\boldsymbol{\xi}^{(1)}, \dots, \boldsymbol{\xi}^{(Q)}\}$ (according to a LHS), and the corresponding PCE coefficients for all responses $\boldsymbol{\Gamma}^{(i)}$ are calculated following (17). This results in a database relating n_{DOE} design points to their corresponding PCE coefficient matrices:

$$\left\{\mathbf{x}^{(1)}, \dots, \mathbf{x}^{(n_{\text{DOE}})}\right\} \Rightarrow \left\{\boldsymbol{\Gamma}^{(1)}, \dots, \boldsymbol{\Gamma}^{(n_{\text{DOE}})}\right\}; \tag{25}$$

(II) by using the information gathered in step (I), MLS response surfaces can be devised to predict the PCE coefficient matrix for any vector $\mathbf{x}$ in order to reconstruct complete descriptions $s_i(\mathbf{x}, \boldsymbol{\xi})$ of the random responses.

The next section discusses the integration of these stochastic metamodels within a multiobjective formulation accounting for uncertainties.

3 Multiobjective reliability-based design optimization

3.1 A state of the art

The general formulation of a multiobjective optimization problem with deterministic and random variables can be written as follows (Beyer and Sendhoff 2007):

$$\begin{cases} \min_{\mathbf{x}} & \mathbf{f}(\mathbf{x}, \boldsymbol{\xi}) \\ \text{subject to:} & \mathbf{g}(\mathbf{x}, \boldsymbol{\xi}) \leq 0, \end{cases} \tag{26}$$

where:

- $\mathbf{x}$ is the deterministic design variable vector (to be optimized);
- $\boldsymbol{\xi}$ is the vector of random variables encompassing all uncertainties;
- $\mathbf{f} = [f_1, \dots, f_m]^{\mathrm{T}}$ is a vector of m objective functions;
- $\mathbf{g} = [g_1, \dots, g_p]^{\mathrm{T}}$ is a vector of p inequality constraints (it is assumed that all equality constraints are converted into inequalities).

To solve system (26), the first approach consists in the elimination of the random variables. The optimization can be undertaken deterministically at an upper level, leaving the uncertainty quantification at a basic stage. For instance, Achenie and Ostrovsky (2005) achieved a global optimization on objectives f_i' depending only on the deterministic variables $\mathbf{x}$, where each f_i' has been obtained by a local-level maximization of f_i (*worst case analysis*) with respect to the random variables $\boldsymbol{\xi}$.

Another approach to deal with uncertainties consists in incorporating robust measures or reliability indexes as additional objectives or constraints. For instance, Barakat et al. (2004) performed the reliability-based design of pre-stressed concrete beams by an *a priori* multicriteria technique (ε-constraint method), where the objectives included the system, flexural strength and tensile strength reliability indexes. Other examples are provided in Sinha

(2007), where the reliability-based multiobjective optimization of automotive crash-worthiness and occupant safety was undertaken by imposing an additional constraint on the probability of failure, or Kumar et al. (2008) concerning robust design using Bayesian Monte Carlo simulations to analyze the trade-off between mean performance and variability for compressor blades.

A similar approach mentioned in Achenie and Ostrovsky (2005) in the case of robust optimization consists in considering the objective function means (μ) and standard deviations (σ) as objectives to be minimized:

$$\min_{\mathbf{x}} \left[\mu\left[f_1\right], \sigma\left[f_1\right], \ldots, \mu\left[f_m\right], \sigma\left[f_m\right]\right]^{\mathsf{T}}. \tag{27}$$

For instance, Parashar and Bloebaum (2006) devised a *Robust Multi-Objective Genetic Algorithm Concurrent Subspace Optimization* (R-MOGACSSO) by integrating means and standard deviations in the multiobjective formulation, within a multidisciplinary architecture.

A theoretical insight into robust multiobjective optimization has been accomplished by Deb and Gupta (2005, 2006), who suggest a variant of this idea in the context of multiobjective evolutionary optimization, and advocated two definitions of multiobjective robustness:

– $\mathbf{x}^*$ is a *multiobjective robust solution of type I* if it is a global feasible Pareto-optimal solution to the following multiobjective problem defined with respect to a δ-neighborhood $\mathscr{B}(\mathbf{x}, \delta)$ (of hypervolume $|\mathscr{B}(\mathbf{x}, \delta)|$):

$$\begin{cases} \min_{\mathbf{x}} f_i^{\text{eff}}(\mathbf{x}) \equiv \dfrac{1}{|\mathscr{B}(\mathbf{x}, \delta)|} \displaystyle\int_{\mathbf{x}' \in \mathscr{B}(\mathbf{x}, \delta)} f_i(\mathbf{x}') d\mathbf{x}', \\ i = 1, \ldots, m \\ \text{subject to: } \mathbf{x} \in \mathscr{F} \ (\equiv \text{feasible domain}); \end{cases} \tag{28}$$

– $\mathbf{x}^*$ is a *multiobjective robust solution of type II* if it is a global feasible Pareto-optimal solution to the following multiobjective problem defined with respect to a δ-neighborhood $\mathscr{B}(\mathbf{x}, \delta)$:

$$\begin{cases} \min_{\mathbf{x}} \quad \mathbf{f}(\mathbf{x}) = \left[f_1(\mathbf{x}), \ldots, f_m(\mathbf{x})\right]^{\mathsf{T}} \\ \text{subject to:} \quad \dfrac{\left\|\mathbf{f}(\mathbf{x}) - \mathbf{f}^{\text{eff}}(\mathbf{x})\right\|}{\|\mathbf{f}(\mathbf{x})\|}, \mathbf{x} \in \mathscr{F}. \end{cases} \tag{29}$$

The integration of these formulations within NSGA-II (*Nondominated Sorting Genetic Algorithm-II*, Deb et al. 2002), and their application to several analytical test cases showed that it is an easy-to-implement and efficient way to obtain robust Pareto fronts (Deb and Gupta 2006). However, the number of function evaluations necessary to estimate the effective functions f_i makes this method expensive if finite element models are used to retrieve the values of the functions. Therefore, the use of an archive of points calculated in the former generations of the evolutionary algorithm is advised to decrease the global CPU time, as proposed by Gunawan and Azarm (2005).

Another method set up to decrease the computational effort consists in building surrogates based on a limited number of "exact" fitness evaluations, as performed by Paenke et al. (2006) with local linear and quadratic regression models.

In comparison with the aforementioned strategies, a different scenario is considered in Basseur and Zitzler (2006), where the objective vector is inherently associated with an unknown probability distribution, and where the optimization goal is specified by a quality indicator (namely: the ε-indicator). Practically, the fitness of an individual $\mathbf{x}$ is defined as the estimated expected loss in quality if $\mathbf{x}$ would be removed from the population.

Finally, a possible axis of research for multiobjective optimization under uncertainty would be to re-define the Pareto dominance criterion, as in the *fuzzy-Pareto-dominance* developed in the context of high numbers of objectives (Köppen et al. 2005), or in the epistemic uncertainty management (Limbourg 2005).

3.2 Formulation and implementation

As sketched above in the literature review, the current investigations are generally concerned with the robustness of the objective functions, and preferably for uncertainties defined by intervals. However, as the uncertainties are often described by probability distributions, robustness measures are not always prone to furnish sufficient insight on probability levels (what is the probability of attaining a specific value f'? or: for a given probability level p', what is the worst-case value of f?). In those situations, a reliability-based approach might be a more convenient option.

A reliability-based procedure is proposed in Deb et al. (2007, 2009), using objective means and probability-based constraints:

$$\begin{cases} \min_{\mu_{\mathbf{x}}, \mathbf{d}} & \left(\mu_{f_1}(\mu_{\mathbf{x}}), \ldots, \mu_{f_m}(\mu_{\mathbf{x}})\right), \\ \text{subject to:} & P\left[g_j(\mathbf{x}, \mathbf{d}, \mathbf{p}) \geq 0\right] \geq R_j, j = 1, \ldots, J, \\ & h_k(\mathbf{d}) \geq 0, k = 1, \ldots, K, \\ & \mathbf{x}^{(L)} \leq \mu_{\mathbf{x}} \leq \mathbf{x}^{(U)}, \\ & \mathbf{d}^{(L)} \leq \mathbf{d} \leq \mathbf{d}^{(U)}, \end{cases} \tag{30}$$

where $\mathbf{d}$, $\mathbf{p}$ are respectively the deterministic design variables and parameters, and $\mathbf{x}$ are the random design variables.

Minimum-risk optimal solutions are also defined in Levi et al. (2005) and Caballero et al. (2001) by maximizing the probability of keeping the objectives below a given threshold (in a minimization context).

However, in probability-based formulations, the computation of quantiles is an expensive task, usually involving an iterative process. This issue can be easily circumvented by introducing slack variables ζ_i to account for probability levels. More fundamentally, the presence of multiple objectives could lead to a different handling of the objective probabilities, accounting for the inherent multicriteria nature of the problem to address. Instead of comparing each objective function separately, the key point would rather be to check the *probabilistic nondominance* (Teich 2001):

$$\begin{cases} \min_{\mathbf{x},\boldsymbol{\zeta}} & \boldsymbol{\zeta} = [\zeta_1, \ldots, \zeta_m]^{\mathsf{T}} \\ \text{subject to:} & P_{\text{nondominance}} \equiv P\left[\mathbf{f}(\mathbf{x},\boldsymbol{\xi}) \succ \boldsymbol{\zeta}\right] \geq \alpha^{\mathbf{f}}, \\ & P_{\text{safety}} \equiv P\left[\mathbf{g}(\mathbf{x},\boldsymbol{\xi}) \leq 0\right] \geq \alpha^{\mathbf{g}}, \end{cases} \tag{31}$$

where the nondominance condition means that the objective vector $\mathbf{f}(\mathbf{x},\boldsymbol{\xi})$ should dominate ($\succ$) $\boldsymbol{\zeta}$ with a minimum probability level equal to $\alpha^{\mathbf{f}}$. The constraints can also be embraced into a single probabilistic constraint P_{safety} defined by a minimum threshold $\alpha^{\mathbf{g}}$. Both parameters $\alpha^{\mathbf{f}}$ and $\alpha^{\mathbf{g}}$ are reliability levels determined by the user.

The probability of Pareto nondominance with respect to a given vector $\boldsymbol{\zeta}$ is thus equal to:

$$P_{\text{nondominance}} = \int_{\mathbf{f}(\mathbf{x},\boldsymbol{\xi}) \succ \boldsymbol{\zeta}} p(\boldsymbol{\xi}) d\boldsymbol{\xi}, \tag{32}$$

where $p(\boldsymbol{\xi})$ is the joint probability density function of $\boldsymbol{\xi}$, while the probability of safety is given by:

$$P_{\text{safety}} = \int_{\mathbf{g}(\mathbf{x},\boldsymbol{\xi}) \leq 0} p(\boldsymbol{\xi}) d\boldsymbol{\xi}. \tag{33}$$

Formulation (31) could be applied directly within a multiobjective evolutionary algorithm (Coello Coello et al. 2002); in that case, each individual tested during the optimization process is represented by a *chromosome* containing the values of all design variables for this specific individual, through a coding defined in the evolutionary algorithm (e.g. binary coding, real coding, etc.). Consequently, each chromosome contains at once the parameters x_i, and the guess values ζ_i for the corresponding quantiles of f_i. Nevertheless, since design variables within chromosomes might be interchanged and modified throughout the generations by the crossover and mutation operators, the guess values ζ_i may not correspond at all to the values of the objectives $f_i(\mathbf{x},\boldsymbol{\xi})$, leading to a majority of unnecessary points with extreme probability values (0 or 1).

To alleviate this difficulty, a more efficient albeit equivalent formulation can be set up by considering *relative* additional variables η_i:

$$\begin{cases} \min_{\mathbf{x},\boldsymbol{\eta}} & \boldsymbol{\zeta} = [\zeta_1, \ldots, \zeta_m]^{\mathsf{T}} \\ \text{subject to:} & P_{\text{nondominance}} \equiv P\left[\mathbf{f}(\mathbf{x},\boldsymbol{\xi}) \succ \boldsymbol{\zeta}\right] \geq \alpha^{\mathbf{f}}, \\ & P_{\text{safety}} \equiv P\left[\mathbf{g}(\mathbf{x},\boldsymbol{\xi}) \leq 0\right] \geq \alpha^{\mathbf{g}}, \\ \text{and with:} & \zeta_i = \mu\left[f_i(\mathbf{x},\boldsymbol{\xi})\right] + \eta_i . \sigma\left[f_i(\mathbf{x},\boldsymbol{\xi})\right], \end{cases} \tag{34}$$

where $\mu\left[f_i(\mathbf{x},\boldsymbol{\xi})\right]$ and $\sigma\left[f_i(\mathbf{x},\boldsymbol{\xi})\right]$ are respectively the mean and standard deviation at $\mathbf{x}$ (with respect to the random variables $\boldsymbol{\xi}$). The use of relative coefficients η_i leads to a more active search for the quantiles, since they remain in the vicinity of the objectives f_i corresponding to the current design parameters x_i.

To solve (34), a multiobjective evolutionary algorithm can be implemented without modification; NSGA-II (*Non-dominated Sorting Genetic Algorithm-II*) will be used for this purpose (Deb et al. 2002) .

The probability measure $P_{\text{nondominance}}$ can be further expressed by considering the notion of Pareto dominance: a vector $\mathbf{f}^A$ is said to dominate $\mathbf{f}^B$ ($\mathbf{f}^A \succ \mathbf{f}^B$) if and only if $\forall i \in I = \{1, \ldots, m\} : f_i^A \leq f_i^B$, and for at least one $j \in I$: $f_j^A < f_j^B$. Therefore, $P_{\text{nondominance}}$ is equivalent to:

$$\begin{aligned} & P_{\text{nondominance}} \\ & \quad \equiv P\left[\mathbf{f}(\mathbf{x},\boldsymbol{\xi}) \succ \boldsymbol{\zeta}\right] \\ & \quad = P\left[\{f_1(\mathbf{x},\boldsymbol{\xi}) \leq \zeta_1\} \wedge \cdots \wedge \{f_m(\mathbf{x},\boldsymbol{\xi}) \leq \zeta_m\}\right] \\ & \quad = P\left[\{f_1(\mathbf{x},\boldsymbol{\xi}) - \zeta_1 \leq 0\} \wedge \ldots\right] \\ & \quad = P\left[\max_{i=1,\ldots,m} \{f_i(\mathbf{x},\boldsymbol{\xi}) - \zeta_i\} \leq 0\right]. \end{aligned} \tag{35}$$

Similarly, for the probability of safety:

$$\begin{aligned} P_{\text{safety}} &\equiv P\left[\mathbf{g}(\mathbf{x},\boldsymbol{\xi}) \leq 0\right] \\ &= P\left[\{g_1(\mathbf{x},\boldsymbol{\xi}) \leq 0\} \wedge \cdots \wedge \{g_p(\mathbf{x},\boldsymbol{\xi}) \leq 0\}\right] \\ &= P\left[\max_{j=1,\ldots,p} \{g_j(\mathbf{x},\boldsymbol{\xi})\} \leq 0\right]. \end{aligned} \tag{36}$$

Since the $\max\{\ldots\}$ expressions in (35) and (36) may lack of regularity (in the general case, it is only C^0-continuous with respect to $\boldsymbol{\xi}$), a smoother formulation can

be obtained by using Kreisselmeier–Steinhauser aggregation (Haftka and Gürdal 1992), classically encountered in constrained optimization to aggregate a set of constraints into a single one:

$$g_j \leq 0,\ j = 1, \ldots, p \rightarrow g_{\text{KS}} = \frac{1}{\rho} \ln \left[\sum_{j=1}^{q} \exp\left(\rho g_j\right) \right] \leq 0, \tag{37}$$

where ρ (≥ 1) is a parameter of the method.

An example of Kreisselmeier–Steinhauser aggregation function g_{KS} of constraints is illustrated in Fig. 2. g_{KS} is guaranteed by construction to be greater (or equal) than the maximum of the g_i. A control of the relation between g_{KS} and $\max\{g_i\}$ can be made through the parameter ρ: by increasing the value of ρ, g_{KS} gets closer to the maximum of the functions g_i. In any case, the KS-function is bounded by:

$$g_{\max} \leq g_{\text{KS}} \leq g_{\max} + \frac{\ln(p)}{\rho}. \tag{38}$$

The maximum functions appearing in (35) and (36) are thus replaced by:

$$\begin{cases} f_{\text{KS}}(\mathbf{x}, \boldsymbol{\xi}) = \dfrac{1}{\rho} \ln \left[\displaystyle\sum_{i=1}^{m} \exp\left[\rho\left(f_i(\mathbf{x}, \boldsymbol{\xi}) - \zeta_i\right)\right] \right] \\ g_{\text{KS}}(\mathbf{x}, \boldsymbol{\xi}) = \dfrac{1}{\rho} \ln \left[\displaystyle\sum_{j=1}^{q} \exp\left[\rho g_j(\mathbf{x}, \boldsymbol{\xi})\right] \right]. \end{cases} \tag{39}$$

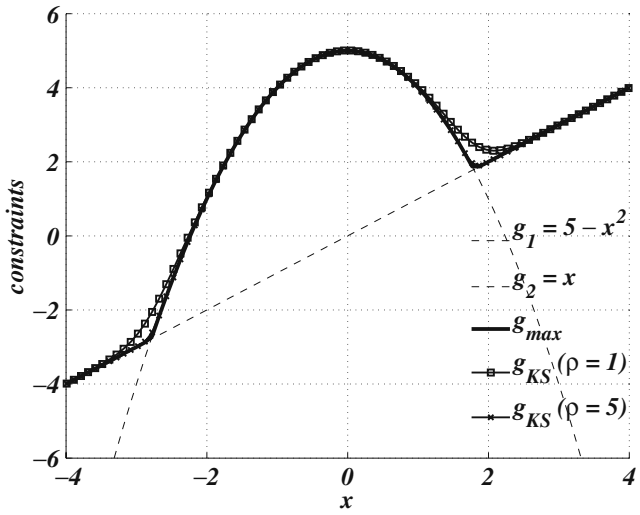

Fig. 2 Example of Kreisselmeier–Steinhauser aggregation for two constraints $g_1 = 5 - x^2$ and $g_2 = x$

Moreover, since any function $s(\mathbf{x}, \boldsymbol{\xi})$ depending on random variables $\boldsymbol{\xi}$ can be approximated through a PCE:

$$s(\mathbf{x}, \boldsymbol{\xi}) = \sum_{j=0}^{P-1} \gamma_j^s(\mathbf{x}) \psi_j(\boldsymbol{\xi}), \tag{40}$$

where its mean and variance are expressed by:

$$\begin{cases} E\left[s(\mathbf{x}, \boldsymbol{\xi})\right] = \gamma_0^s \\ \sigma^2\left[s(\mathbf{x}, \boldsymbol{\xi})\right] = \displaystyle\sum_{j=1}^{P-1} E\left[\psi_j^2\right] \left(\gamma_j^s\right)^2, \end{cases} \tag{41}$$

formulation (34) can be made explicit by substituting the stochastic responses by their corresponding PCE developments within the Kreisselmeier–Steinhauser aggregation functions:

$$\begin{cases} \min_{\mathbf{x},\boldsymbol{\eta}} \quad \zeta_i^{\text{PCE}} \equiv \gamma_0^{f_i}(\mathbf{x}) + \eta_i \sqrt{\displaystyle\sum_{j=1}^{P-1} E\left[\psi_j^2\right] \gamma_j^{f_i}(\mathbf{x})^2}, \\ \qquad\qquad i = 1, \ldots, m \\ \text{s.t.:} \quad P\left[\frac{1}{\rho} \ln \left(\displaystyle\sum_{i=1}^{m} \exp\left(\rho \sum_{j=0}^{P-1} \psi_j(\boldsymbol{\xi}) \gamma_j^{f_i}(\mathbf{x}) - \rho \zeta_i^{\text{PCE}} \right) \right) \leq 0 \right] \geq \alpha^{\mathbf{f}} \\ \qquad P\left[\frac{1}{\rho} \ln \left(\displaystyle\sum_{i=1}^{q} \exp\left(\rho \sum_{j=0}^{P-1} \psi_j(\boldsymbol{\xi}) \gamma_j^{g_i}(\mathbf{x}) \right) \right) \leq 0 \right] \geq \alpha^{\mathbf{g}}, \end{cases} \tag{42}$$

equivalent to:

$$\begin{cases} \min_{\mathbf{x},\boldsymbol{\eta}} \quad \gamma_0^{f_i}(\mathbf{x}) + \eta_i \sqrt{\displaystyle\sum_{j=1}^{P-1} E\left[\psi_j^2\right] \gamma_j^{f_i}(\mathbf{x})^2}, \quad i = 1, \ldots, m \\ \text{s.t.:} \quad P\left[\frac{1}{\rho} \ln \left(\displaystyle\sum_{i=1}^{m} \exp\left(\rho \sum_{j=1}^{P-1} \psi_j(\boldsymbol{\xi}) \gamma_j^{f_i}(\mathbf{x}) - \rho \eta_i \sqrt{\displaystyle\sum_{j=1}^{P-1} E\left[\psi_j^2\right] \gamma_j^{f_i}(\mathbf{x})^2} \right) \right) \leq 0 \right] \geq \alpha^{\mathbf{f}} \\ \qquad P\left[\frac{1}{\rho} \ln \left(\displaystyle\sum_{i=1}^{q} \exp\left(\rho \sum_{j=0}^{P-1} \psi_j(\boldsymbol{\xi}) \gamma_j^{g_i}(\mathbf{x}) \right) \right) \leq 0 \right] \geq \alpha^{\mathbf{g}} \end{cases} \tag{43}$$

or more concisely:

$$\Leftrightarrow \begin{cases} \min_{\mathbf{x},\boldsymbol{\eta}} & \gamma_0^{f_i}(\mathbf{x}) + \eta_i \sqrt{\sum_{j=1}^{P-1} E\left[\psi_j^2\right] \gamma_j^{f_i}(\mathbf{x})^2}, \\ & i = 1, \ldots, m \\ \text{s.t.:} & P\left[\sum_{i=1}^{m} \exp\left(\rho \mu_i^{\text{PCE}}(\mathbf{x}, \boldsymbol{\xi})\right) \leq 1\right] \geq \alpha^{\mathbf{f}} \\ & P\left[\sum_{i=1}^{q} \exp\left(\rho \nu_i^{\text{PCE}}(\mathbf{x}, \boldsymbol{\xi})\right) \leq 1\right] \geq \alpha^{\mathbf{g}} \end{cases} \tag{44}$$

where:

$$\begin{cases} \mu_i^{\text{PCE}}(\mathbf{x}, \boldsymbol{\xi}) &= \sum_{j=1}^{P-1} \psi_j(\boldsymbol{\xi}) \gamma_j^{f_i}(\mathbf{x}) \\ & \quad - \eta_i \sqrt{\sum_{j=1}^{P-1} E\left[\psi_j^2\right] \gamma_j^{f_i}(\mathbf{x})^2} \\ \nu_i^{\text{PCE}}(\mathbf{x}, \boldsymbol{\xi}) &= \sum_{j=0}^{P-1} \psi_j(\boldsymbol{\xi}) \gamma_j^{g_i}(\mathbf{x}). \end{cases} \tag{45}$$

The probabilities in formula (44) could be calculated by importance sampling (Tsompanakis and Papadrakakis 2004), FORM/SORM (First-Order/Second-Order Reliability Methods) or sparse grid (Xiong et al. 2010); however, in this work, simple Monte Carlo simulations (with 10,000 samples) are performed on the PCE.

However, it is worth mentioning that since the probabilities of nondominance and safety are defined by *limit surfaces* $b(\mathbf{x}, \boldsymbol{\xi}) = 0$:

$$\begin{cases} b_{\text{nondominance}}(\mathbf{x}, \boldsymbol{\xi}) \\ \quad = \sum_{i=1}^{m} \exp\left[\rho\left(\sum_{j=1}^{P-1} \psi_j(\boldsymbol{\xi}) \gamma_j^{f_i}(\mathbf{x}) \right.\right. \\ \qquad \left.\left. - \eta_i \sqrt{\sum_{j=1}^{P-1} E\left[\psi_j^2\right] \gamma_j^{f_i}(\mathbf{x})^2}\right)\right] - 1, \\ b_{\text{safety}}(\mathbf{x}, \boldsymbol{\xi}) = \sum_{i=1}^{q} \exp\left[\rho\left(\sum_{j=0}^{P-1} \psi_j(\boldsymbol{\xi}) \gamma_j^{g_i}(\mathbf{x})\right)\right] - 1, \end{cases} \tag{46}$$

the sensitivities of these functions b with respect to ξ_i can be derived explicitly (for example for further use with gradient-based methods to calculate the reliability index). The derivatives $\frac{\partial b}{\partial \xi_i}$ are detailed in the Appendix.

3.3 Adaptive sampling of the metamodels

The two-step procedure consisting in: (a) *creating a database of computer experiments* and (b) *training the metamodels and use them for optimization* might not be accurate enough for large number of variables and/or highly nonlinear responses. In those situations, an updating of the database with additional data from the high-fidelity simulation is mandatory to guarantee reliable predictions.

Infill criteria (i.e. conditions to add new points in the training set) include:

- minimizing the prediction error of the metamodels (e.g. by leave-one-out cross validation);
- exploring new regions of the design space, not yet covered in the sampling set;
- building a compromise between exploration and exploitation, accounting for the fact that it is generally not necessary to have an accurate description of suboptimal areas of the search space;
- maximizing the probability of improvement of the objective function (Jones 2001); this idea has also been proposed for multiobjective improvement by Forrester and Keane (2009). Metamodel assisted fitness evaluation procedures and adaptive design of experiments have also been successfully combined with a multiobjective genetic algorithm (Li et al. 2009).

In this work, a simple updating scheme is proposed, consisting in performing PCE collocation (with the high-fidelity simulation) for a fixed percentage of the genetic algorithm population at each generation. The individuals undergoing this process are the ones endowed with the highest fitness value, i.e. the feasible individuals of the population characterized by the best nondominance ranking.

The next section illustrates the proposed methodology on four test cases.

4 Numerical results

4.1 Description of the validation process

The flow-chart of the general optimization methodology is depicted in Figs. 3, 4 and 5 following the approach used to calculate the stochastic responses:

(A) for each design point $\{\mathbf{x}, \boldsymbol{\eta}\}$, the stochastic responses are computed by Monte Carlo simulations of the high-fidelity responses (objectives and constraints);
(B) for each design point $\{\mathbf{x}, \boldsymbol{\eta}\}$, a set $\{\boldsymbol{\xi}^{(1)}, \ldots, \boldsymbol{\xi}^{(Q)}\}$ of collocation points are defined and sent to the high-fidelity simulation. From the results obtained, the PCE

Table 1 Genetic parameters used for the multiobjective evolutionary optimizer endowed with the simulated binary crossover and mutation (Deb et al. 2002)

Genetic parameter	Value
Number of generations	30
Population size	200
Probability of SBX crossover	0.9
Probability of SBX mutation	0.5
Distribution index η_c for SBX crossover	10
Distribution index η_m for SBX mutation	20

coefficients are derived and used to build explicit PCE of the responses. Finally, the response means and standard deviations can be directly calculated from the PCE coefficients, while probability measures are computed by Monte Carlo simulations on the PCE;

(C) before the optimization, a LHS design of experiments (DOE) is performed on the deterministic variables $\mathbf{x}$; for each of the DOE point, Q collocation points are evaluated by the high-fidelity simulation, the corresponding PCE are derived, and MLS response surfaces are carried out for each of the PCE coefficients. Then, during the optimization, these metamodels are used to get an approximation of the PCE coefficients for further assessments of the probabilistic measures required by the multiobjective reliability-based formulation.

In this study, the number of collocation points Q is equal to the minimum number of samples necessary to build the polynomial chaos, while the degree of the (moving) least squares polynomial basis is equal to two (Table 1).

First, an analytical example available in Coello Coello et al. (2002) is presented to illustrate the principle of the proposed method (Section 4.2). Then, three space truss structures are investigated in detail in two steps: a *validation of the hierarchical stochastic metamodels* (including a comparison with a direct approach of the structural responses with respect to the deterministic and random variables altogether, see Section 4.3.1), followed by their application in *multiobjective optimization under uncertainty* (Section 4.4).

4.2 Case 1: analytical example

The goal of this first test case is to illustrate the hierarchical stochastic metamodeling methodology on a two-variable example where the analytical expression of the outputs will allow for calculating the theoretical expressions of the PCE coefficients (with respect to the design variables x_1 and x_2). These expressions will then be confronted to the corresponding response surfaces obtained by least squares approximation of the PCE coefficients.

The analytical test case is defined as follows (Coello Coello 2002):

$$\begin{cases} \min_{\mathbf{x}} \begin{cases} f_1(\mathbf{x},\boldsymbol{\xi}) = -u_1 - u_2^2 \\ f_2(\mathbf{x},\boldsymbol{\xi}) = -u_1^2 - u_2 \end{cases} \\ \text{s.t.: } u_1 + u_2 - 12 \le 0, \\ \quad -u_1^2 - 10u_1 + u_2^2 - 16u_2 + 80 \le 0, \\ \quad u_i = x_i + \xi_i, x_1 \in [2,7], x_2 \in [5,10], \\ \quad \xi_i = \mathcal{N}\left(\mu = 0, \sigma_i = 0.05\left(x_i^{\max} - x_i^{\min}\right)\right). \end{cases} \tag{47}$$

In this simple example, no adaptive scheme is used for the PCE-based metamodels, which are based on least squares approximation with a second-degree polynomial

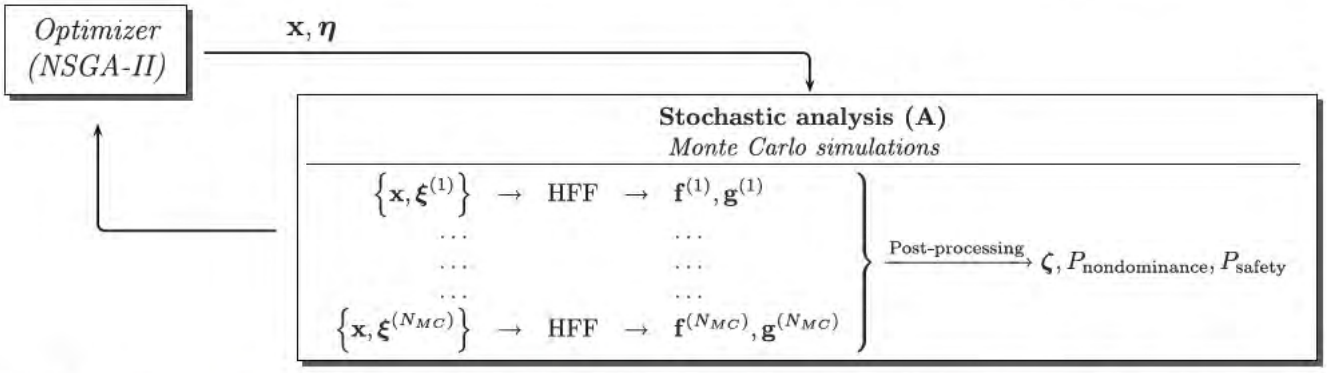

Fig. 3 Flow-chart of the general methodology developed for multiobjective reliability-based optimization—approach (A): the responses are obtained by Monte Carlo simulations on the "high-fidelity" functions HFF

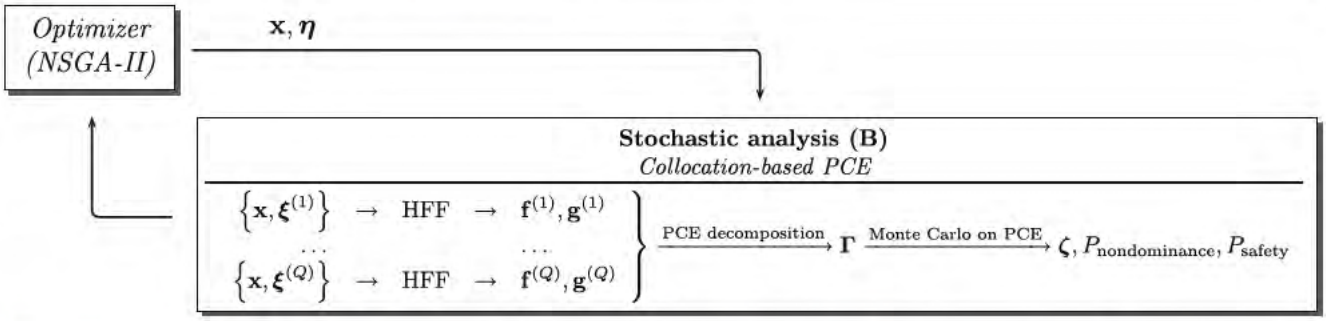

Fig. 4 Flow-chart of the general methodology developed for multiobjective reliability-based optimization—approach (B): the responses are obtained by Monte Carlo simulations on the collocation-based PCE (built on the "high-fidelity" functions HFF)

basis. Furthermore, a second-degree polynomial chaos basis is selected.

The Pareto fronts found through deterministic and nondeterministic optimizations are exhibited in Fig. 6. The interpretation of the results is the following: for each point $\boldsymbol{\zeta}$ $(= [\zeta_1, \zeta_2]^{\mathrm{T}})$ of the nondeterministic Pareto front, there is a probability equal to $\alpha^{\mathbf{f}}$ that the actual value of the objective vector dominates $\boldsymbol{\zeta}$ (with a probability $\alpha^{\mathbf{g}}$ of satisfying the constraints). Therefore, the values of $\boldsymbol{\zeta}$ drawn in the figure represent accurate estimates of the objective quantiles (assessed with respect to the nondominance concept). Of course, for higher levels of α (99% compared to 90%), the nondeterministic Pareto front moves farther from its deterministic counterpart. Besides, the Pareto fronts obtained for the three approaches (A), (B), and (C) are very similar, showing the accuracy of the PCE approaches in this example.

In this example, as stated above, the explicit form of the model responses (here: first- and second-order polynomials) allows for calculating analytically all non-zero PCE coefficients since the Hermite polynomials constitute a complete polynomial basis. Indeed, a further investigation (on f_1 for instance) can be performed by comparing a closed-form of the PCE coefficients to the numerical results. The second-degree polynomial chaos is expanded as follows:

$$\begin{cases} \psi_0(\xi) = 1, & \psi_1(\xi) = \xi_1, & \psi_2(\xi) = \xi_1^2 - 1, \\ \psi_3(\xi) = \xi_2, & \psi_4(\xi) = \xi_1\xi_2, & \psi_5(\xi) = \xi_2^2 - 1. \end{cases} \tag{48}$$

Consequently, objective f_1 is explicitly given by:

$$\begin{aligned} f_1(\mathbf{x}, \boldsymbol{\xi}) &= -(x_1 + \xi_1) - (x_2 + \xi_2)^2 \\ &= -x_1 - x_2^2 - \xi_1 - 2x_2\xi_2 - \xi_2^2 \\ &= (-x_1 - x_2^2 - 1)\psi_0(\xi) - \psi_1(\xi) \\ &\quad - 2x_2\psi_3(\xi) - \psi_5(\xi) \\ &\equiv \sum_{j=0}^{5} \gamma_j^{f_1}(\mathbf{x})\psi_j(\xi) \\ &= \underbrace{\gamma_0^{f_1}(\mathbf{x})}_{\text{quadratic in } \mathbf{x}} \psi_0(\xi) + \underbrace{\gamma_1^{f_1}}_{\text{constant}} \psi_1(\xi) \\ &\quad + \underbrace{\gamma_3^{f_1}(\mathbf{x})}_{\text{linear in } \mathbf{x}} \psi_3(\xi) + \underbrace{\gamma_5^{f_1}}_{\text{constant}} \psi_5(\xi). \end{aligned} \tag{49}$$

The response surfaces are depicted in Fig. 7 for the first six PCE coefficients $\gamma_0^{f_1}$ to $\gamma_5^{f_1}$ of objective f_1: the nature

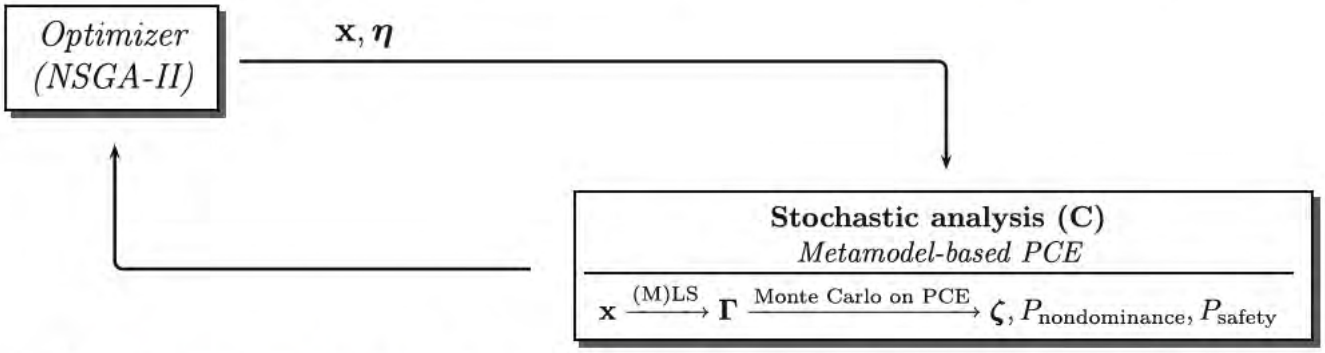

Fig. 5 Flow-chart of the general methodology developed for multiobjective reliability-based optimization—approach (C): the responses are obtained by Monte Carlo simulations on the metamodel-based PCE

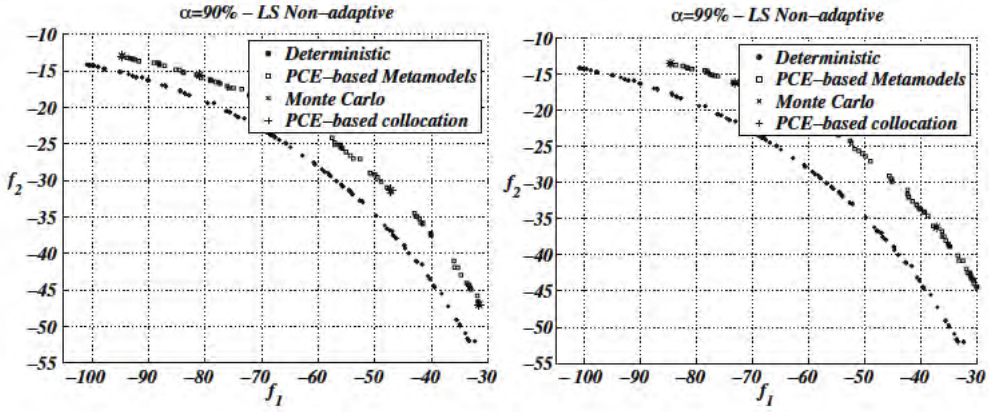

Fig. 6 Analytical test case: non-adaptive least squares approximation for probability thresholds $\alpha = 90\%$ (*left*) and $\alpha = 99\%$ (*right*)

of the surrogates for $\gamma_0^{f_1}$, $\gamma_1^{f_1}$, $\gamma_3^{f_1}$, and $\gamma_5^{f_1}$ correspond to the theoretical prediction, while absolute values close to zero ($< 10^{-13}$ due to numerical and round-off errors) are logically observed for $\gamma_2^{f_1}$ and $\gamma_4^{f_1}$.

4.3 Case 2: sizing optimization of space truss structures

The space truss sizing optimization problems treated in this section are characterized by the following features:

- the trusses are made of a linear elastic material (steel), but a geometrically nonlinear behavior is considered, by means of nonlinear shallow truss element endowed with Green's definition of the strain tensor (Crisfield 2000);
- the dead load of the bars is taken into account by adding for each bar half of the weight as a vertical force distributed on the nodes;
- the examples are two truss benchmarks—t25b and t72b (Haftka and Gürdal 1992)—and a dome (Greco et al. 2006);
- the boundary conditions are (x, y, z)-fixations on given nodes (depicted as dots in Figs. 8, 9, 10, 11, 12 and 13);
- the design variables are groups of common cross-section areas, identified by different line styles in Figs. 8–13;
- there are two objectives (the mass and the maximum vertical displacement), and two constraints (the Eulerian buckling critical load is checked, as well as the maximum axial stress).

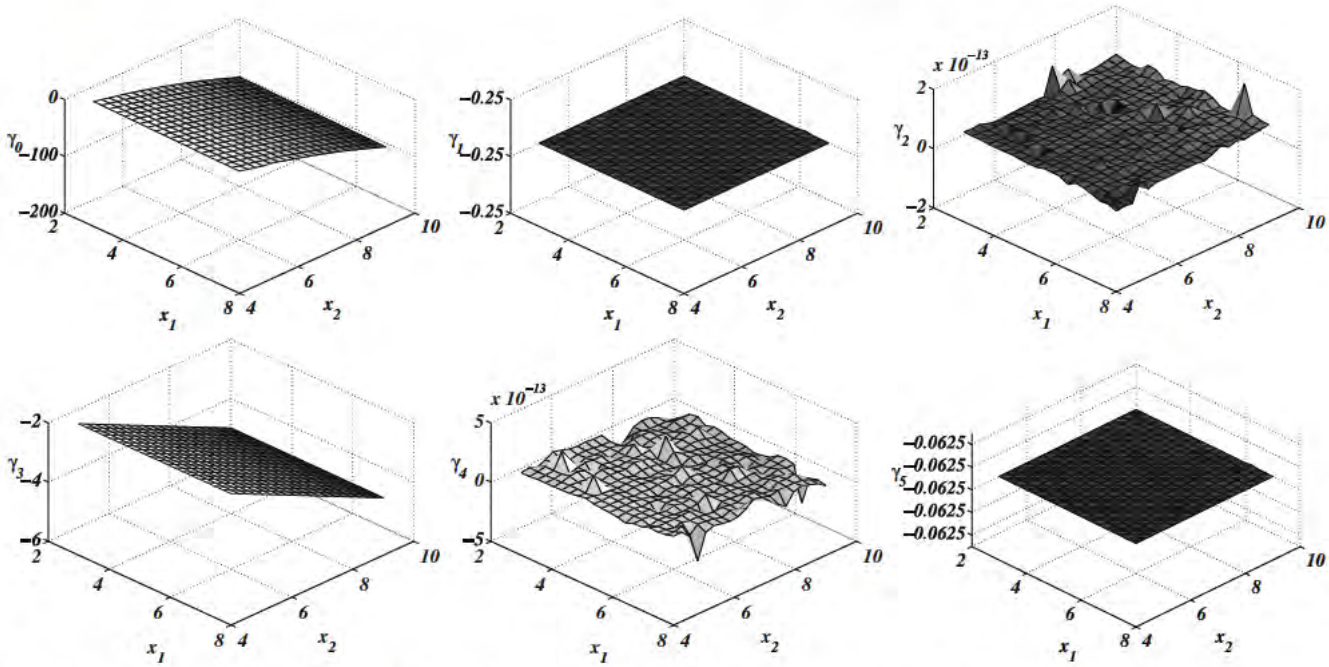

Fig. 7 Response surfaces of the first six PCE coefficients of objective f_1 with respect to the design variables x_1 and x_2 (for the analytical test case)

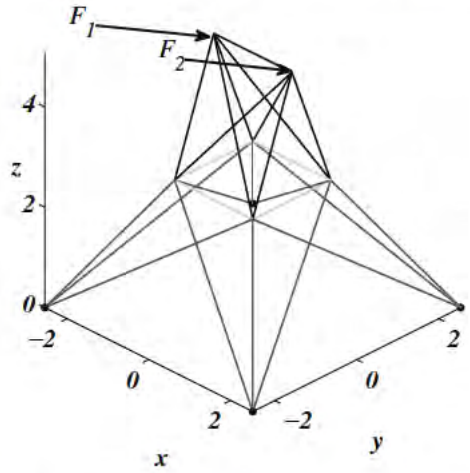

Fig. 8 Truss configuration for test case t25b

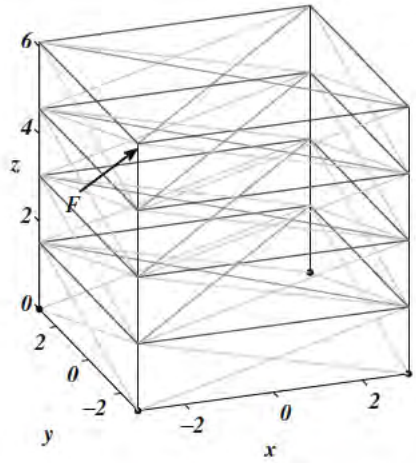

Fig. 10 Truss configuration for test case t72b

4.3.1 *Validation of the hierarchical stochastic metamodels*

Before incorporating the stochastic metamodeling strategy within a multiobjective process for truss design optimization, the pertinency of the proposed method has to be validated. Generally speaking, three main options are available when the estimation of statistical measures is performed with approximation techniques:

(I) *direct approximation of the responses*: metamodels for the structural responses are built with respect to the deterministic and random variables (altogether).

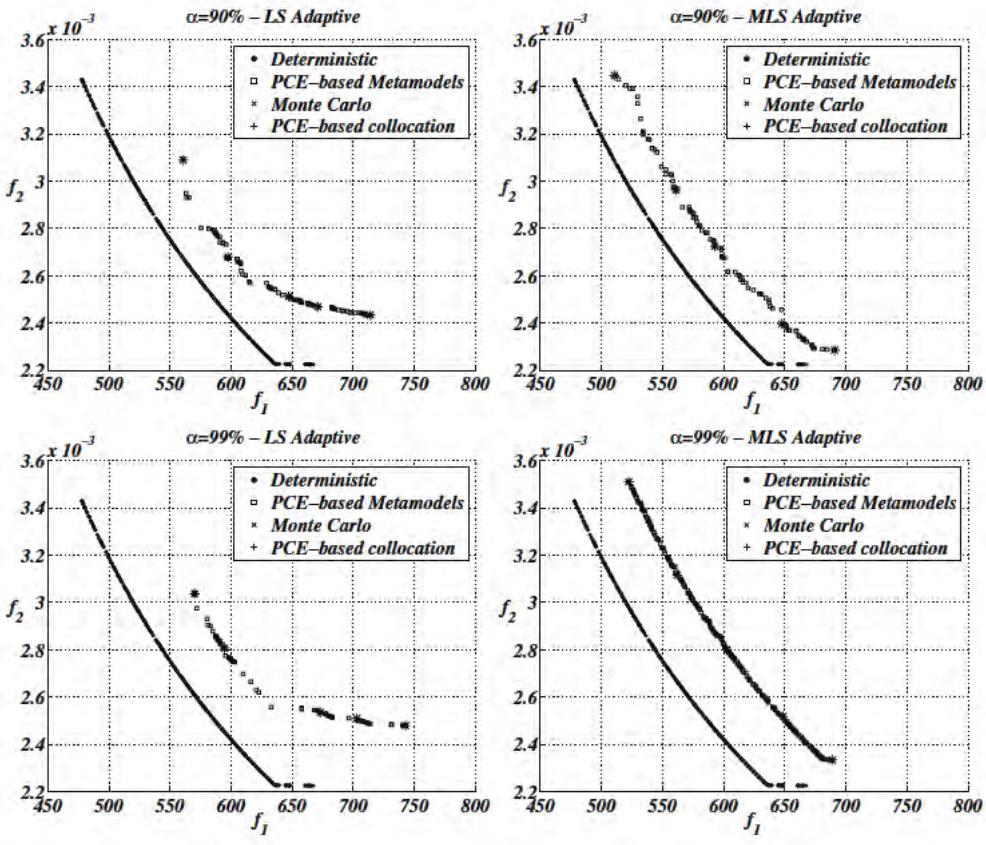

Fig. 9 Test case t25b: adaptive LS (*left*) vs. adaptive MLS (*right*) for probability thresholds $\alpha = 90\%$ (*top*) and $\alpha = 99\%$ (*down*)

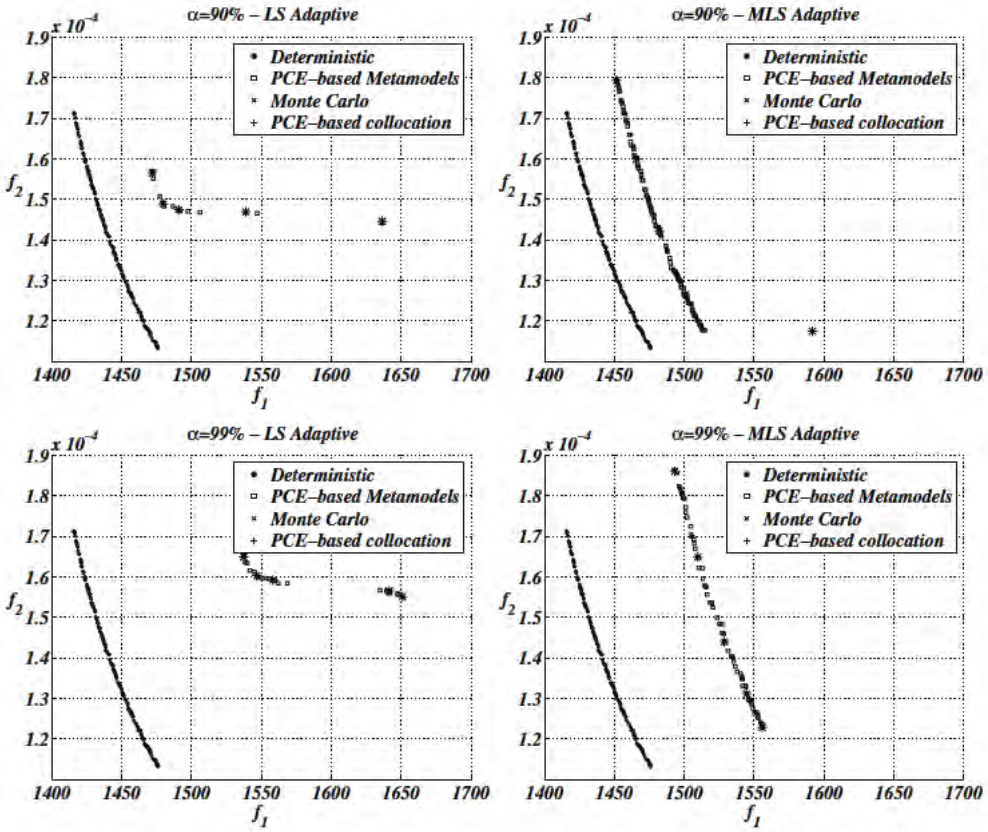

Fig. 11 Test case t72b: adaptive LS (*left*) vs. adaptive MLS (*right*) for probability thresholds $\alpha = 90\%$ (*top*) and $\alpha = 99\%$ (*down*)

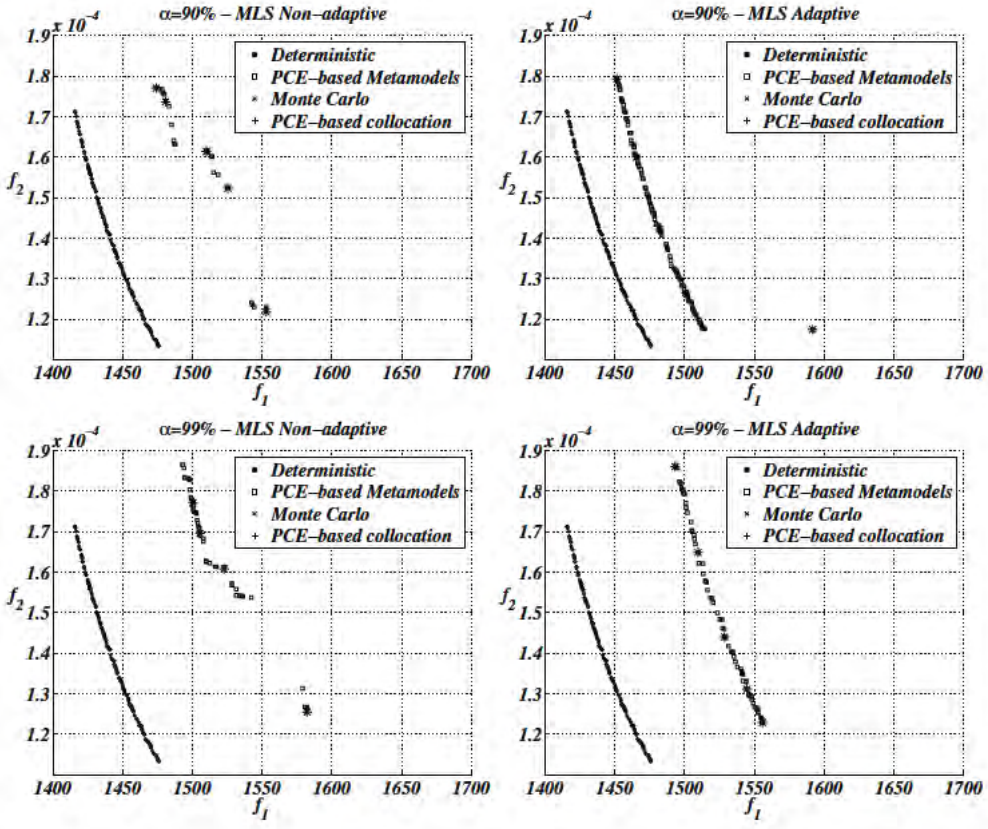

Fig. 12 Test case t72b: non-adaptive MLS (*left*) vs. adaptive MLS (*right*) for probability thresholds $\alpha = 90\%$ (*top*) and $\alpha = 99\%$ (*down*)

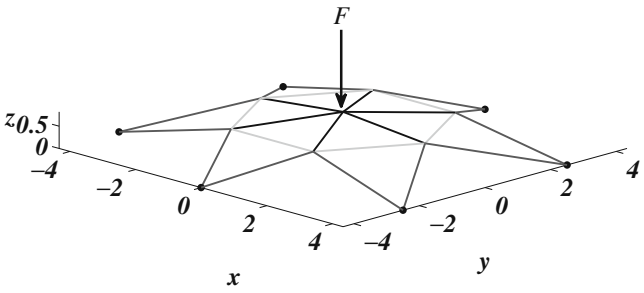

Fig. 13 Truss configuration for test case dome

The corresponding metamodels $\tilde{y}(\mathbf{x}, \boldsymbol{\xi})$ are then used to evaluate the statistical outputs (e.g. means and standard deviations) by Monte Carlo simulations on $\tilde{y}(\mathbf{x}, \boldsymbol{\xi})$;

(II) *direct approximation of the statistical outputs*: the statistical measures of the responses (e.g. mean E, standard deviation σ) can be approximated with respect to the deterministic and random variables: $\tilde{E}_y(\mathbf{x}, \boldsymbol{\xi})$, $\tilde{\sigma}_y(\mathbf{x}, \boldsymbol{\xi})$. This is not suitable here since probabilities of nondominance need eventually to be calculated within the multiobjective reliability-based formulation in this study, which requires an (explicit) expression of the responses with respect to all variables;

(III) *hierarchical stochastic metamodels*: a two-level decomposition is performed, assuming that the PCE coefficients can be accurately approximated by general metamodeling strategies: $\tilde{y}(\mathbf{x}, \boldsymbol{\xi}) = \sum_i \tilde{\gamma}_i^y(\mathbf{x}) \Psi_i(\boldsymbol{\xi})$.

Based on these considerations, the validation process consists in:

(a) comparing the errors obtained with the direct approximation of the responses (I) and the hierarchical stochastic metamodels (III);

(b) investigating the influence of the main parameters of the approximation, i.e. least squares (LS) / moving least squares (MLS), approximating MLS vs. interpolating MLS, degree of the (M)LS polynomial basis, degree of the PCE, etc.

The numerical results of the comparison between the direct approximation of the responses and the use of hierarchical stochastic metamodels are collected in Tables 2, 3, 4, 5, 6 and 7, by focusing on the means, standard deviations and 90%-quantiles of two structural responses (the maximum displacement in direction z and the maximum stress constraint), for the three truss design test cases, and with $1i0^3$ samples for the Monte Carlo simulations. It is clearly observed that a combination of second-order MLS interpolation of the PCE coefficients provide the most accurate results in almost all situations investigated.

To further analyze the parameters of the proposed method, the following aspects are discussed (and tested when applicable on the dome example):

- the *influence of the PCE polynomial basis order*: the results obtained with second-degree and third-degree PCE bases (both with a MLS interpolation) are compared in Tables 8 and 9, showing that although better accuracy would be expected with higher order terms, their approximation through metamodeling techniques also reveal to be more difficult, and suggests to use larger design of experiments to correctly estimate their values;
- the *approximation* used in the stochastic metamodels: moving least squares methods interpolation is compared with kriging (see Tables 10 and 11), as initially proposed by the authors in a previous study (Filomeno Coelho et al. 2010). The kriging method used in this work is a universal kriging with second-order polynomial basis and Gaussian kernel functions, as available in DACE toolbox. (Lophaven et al. 2002). The results show that due to its specific parameter determination

Table 2 Validation error for test case t25b: means, standard deviations and 90%-quantile of the maximum z-displacement (direct approximation of the responses vs. hierarchical stochastic metamodels based on a second-degree PCE) (the best values are written in bold)

Error (in %)	Means		Standard deviations		90%-quantiles	
	Direct	Hierarchical	Direct	Hierarchical	Direct	Hierarchical
1st-order least squares (LS)	4.49	4.25	26.6	4.18	5.12	4.26
2nd-order least squares (LS)	0.617	0.658	2.72	0.645	0.685	0.658
1st-order MLS approximation	0.469	0.39	3.16	0.385	0.466	0.39
2nd-order MLS approximation	0.053	0.0308	**0.000776**	0.0303	0.0488	0.0308
1st-order MLS interpolation	0.415	0.0411	3.26	0.0409	0.398	0.0412
2nd-order MLS interpolation	0.0461	**0.00298**	0.2	0.00295	0.0448	**0.00298**

Table 3 Validation error for test case t25b: means, standard deviations and 90%-quantile of the stress constraint (direct approximation of the responses vs. hierarchical stochastic metamodels based on a second-degree PCE) (the best values are written in bold)

Error (in %)	Means		Standard deviations		90%-quantiles	
	Direct	Hierarchical	Direct	Hierarchical	Direct	Hierarchical
1st-order least squares (LS)	2.15	2.14	46.3	1.58	1.15	2.06
2nd-order least squares (LS)	5.85	5.71	0.709	5.03	5.73	5.49
1st-order MLS approximation	4.82	3.81	5.46	3.25	4.51	3.66
2nd-order MLS approximation	2.49	1.61	16.9	1.39	1.88	1.55
1st-order MLS interpolation	3.53	0.615	8.88	0.534	2.81	0.591
2nd-order MLS interpolation	1.79	**0.529**	26.3	**0.461**	0.942	**0.508**

Table 4 Validation error for test case t72b: means, standard deviations and 90%-quantile of the maximum z-displacement (direct approximation of the responses vs. hierarchical stochastic metamodels based on a second-degree PCE) (the best values are written in bold)

Error (in %)	Means		Standard deviations		90%-quantiles	
	Direct	Hierarchical	Direct	Hierarchical	Direct	Hierarchical
1st-order least squares (LS)	2.05	1.89	5.78	1.8	1.97	1.88
2nd-order least squares (LS)	0.127	0.0628	1.78	0.0221	0.096	0.0609
1st-order MLS approximation	1.8	1.2	4.77	1.25	1.64	1.2
2nd-order MLS approximation	**0.00885**	0.042	0.691	0.0423	0.0244	0.04
1st-order MLS interpolation	1.42	0.133	5.47	0.121	0.996	0.133
2nd-order MLS interpolation	0.0165	0.0103	0.399	**0.0146**	0.0102	**0.00974**

Table 5 Validation error for test case t72b: means, standard deviations and 90%-quantile of the stress constraint (direct approximation of the responses vs. hierarchical stochastic metamodels based on a second-degree PCE) (the best values are written in bold)

Error (in %)	Means		Standard deviations		90%-quantiles	
	Direct	Hierarchical	Direct	Hierarchical	Direct	Hierarchical
1st-order least squares (LS)	0.148	0.127	2.47	3.01	0.141	0.129
2nd-order least squares (LS)	0.0041	0.00221	3.6	0.207	**0.000416**	0.00247
1st-order MLS approximation	0.141	0.0925	4.57	1.22	0.123	0.0926
2nd-order MLS approximation	0.00489	0.00386	0.612	0.0309	0.00375	0.00383
1st-order MLS interpolation	0.11	0.00896	5.27	0.122	0.0751	0.00897
2nd-order MLS interpolation	0.00479	**0.00113**	0.206	**0.0105**	0.00114	0.00113

Table 6 Validation error for test case dome: means, standard deviations and 90%-quantile of the maximum z-displacement (direct approximation of the responses vs. hierarchical stochastic metamodels based on a second-degree PCE) (the best values are written in bold)

Error (in %)	Means		Standard deviations		90%-quantiles	
	Direct	Hierarchical	Direct	Hierarchical	Direct	Hierarchical
1st-order least squares (LS)	2.25	2.2	16.7	3.36	1.94	2.18
2nd-order least squares (LS)	0.498	0.504	4.93	0.947	0.62	0.494
1st-order MLS approximation	1.82	1.24	3.81	1.8	1.6	1.22
2nd-order MLS approximation	0.209	0.0479	2.92	0.106	0.231	0.0469
1st-order MLS interpolation	1.31	0.128	4.7	0.202	1.03	0.126
2nd-order MLS interpolation	0.152	**0.0305**	2.98	**0.0602**	0.197	**0.0295**

Table 7 Validation error for test case dome: means, standard deviations and 90%-quantile of the stress constraint (direct approximation of the responses vs. hierarchical stochastic metamodels based on a second-degree PCE) (the best values are written in bold)

Error (in %)	Means		Standard deviations		90%-quantiles	
	Direct	Hierarchical	Direct	Hierarchical	Direct	Hierarchical
1st-order least squares (LS)	1.09	0.831	15.4	2.93	0.971	0.801
2nd-order least squares (LS)	0.574	0.499	1.18	2.34	0.572	0.476
1st-order MLS approximation	0.751	0.519	2.62	1.84	0.639	0.5
2nd-order MLS approximation	0.232	**0.00837**	1.03	0.0807	0.168	0.00919
1st-order MLS interpolation	0.527	0.0502	4.33	0.193	0.391	0.0482
2nd-order MLS interpolation	0.146	0.00987	1.11	**0.0681**	0.115	**0.00914**

Table 8 Influence of the PCE order for test case dome: means, standard deviations and 90%-quantile of the maximum z-displacement (the best values are written in bold)

Error (in %)	Means		Standard deviations		90%-quantiles	
	Direct	Hierarchical	Direct	Hierarchical	Direct	Hierarchical
Second-order PCE (with 2nd-order MLS interpolation)	0.152	**0.0305**	2.98	0.0602	0.197	**0.0295**
Third-order PCE (with 2nd-order MLS interpolation)	0.152	0.0308	2.98	**0.0213**	0.197	0.0312

Table 9 Influence of the PCE order for test case dome: means, standard deviations and 90%-quantile of the stress constraint (the best values are written in bold)

Error (in %)	Means		Standard deviations		90%-quantiles	
	Direct	Hierarchical	Direct	Hierarchical	Direct	Hierarchical
Second-order PCE (with 2nd-order MLS interpolation)	0.146	0.00987	1.11	**0.0681**	0.115	**0.00914**
Third-order PCE (with 2nd-order MLS interpolation)	0.146	**0.00716**	1.11	3.25	0.115	0.0463

Table 10 Influence of the metamodel (MLS vs. kriging) for test case dome: means, standard deviations and 90%-quantile of the maximum z-displacement (the best values are written in bold)

Error (in %)	Means		Standard deviations		90%-quantiles	
	Direct	Hierarchical	Direct	Hierarchical	Direct	Hierarchical
Kriging	0.0831	**0.000313**	1.72	**0.00579**	0.0248	**0.000782**
2nd-order MLS interpolation	0.152	0.0305	2.98	0.0602	0.197	0.0295

Table 11 Influence of the metamodel (MLS vs. kriging) for test case dome: means, standard deviations and 90%-quantile of the stress constraint (the best values are written in bold)

Error (in %)	Means		Standard deviations		90%-quantiles	
	Direct	Hierarchical	Direct	Hierarchical	Direct	Hierarchical
Kriging	0.0439	0.0177	19.9	**0.00929**	0.163	0.0175
2nd-order MLS interpolation	0.146	**0.00987**	1.11	0.0681	0.115	**0.00914**

features (Jones 2001), kriging interpolation is an excellent competitor to MLS interpolation. Therefore, the main motivation for using MLS in this work lies in its flexibility in the definition of the polynomial basis. Indeed, with a higher number of deterministic design variables, the number of polynomial terms can dramatically increase (the same phenomenon occuring for the number of PCE terms when the number of random variables increases). Fortunately, to address this major issue, LARS (Least-Angle Regression) or other so-called model selection methods can be used to reduce the number of terms in the basis by keeping only the most significant terms; in that case, similar methodologies (already proposed PCE basis reduction, see Blatman and Sudret (2008)) can be applied both for the MLS and the PCE in order to end up with a limited number of basis functions in both levels of the hierarchical stochastic metamodels. A dramatic reduction of the computational cost is expected by following this methodology;

– the *computation of the PCE coefficients* during the design of experiments phase: as indicated above, other methods than collocation can be used to determine the values of the PCE coefficients, like sparse grid quadratures (Klimke 2008), etc., and are expected to furnish more accurate results. In this study, as the number of collocation points is equal to the number of the PCE terms, the number of high-fidelity simulations is set to its minimum, hence limiting the computational effort required to calculate the PCE coefficients needed to train the hierarchical stochastic metamodels;
– the *number of samples* in the Monte Carlo simulations: in this study, because of the relatively low probability levels used eventually in the multiobjective optimization test cases (Section 4.4), a sample size of $N_{MC} = 10^3$ has been selected. Additional results obtained for $N_{MC} = 10^4$ did not reveal significant differences for the truss examples studied here, but this could be an issue for test cases with higher numbers of random variables, and should require specific care (Keane 2009). In that case, the Monte Carlo simulations used to assess the statistical responses could be accelerated, e.g. through *importance sampling* techniques (Tokdar and Kass 2010).

4.4 Application to multiobjective optimization under uncertainty

Due to the relatively high CPU cost of the function evaluation (i.e. making unaffordable the systematic use of Monte Carlo simulations within a multiobjective optimization procedure), the strategy followed to validate the reliability-based multicriteria optimization combined with PCE-based metamodeling consists in:

– launching the nondeterministic multiobjective optimization on the PCE-based metamodels;
– once the corresponding reliability-based Pareto set has been found, five selected points (whose images in the objective space are distributed along the nondeterministic Pareto front) are recomputed for comparison through Monte Carlo simulations and PCE-based collocation.

A second-degree polynomial chaos basis is selected for all examples, and the rate of individuals used at each generation for the updating of the database (in the adaptive scheme) is equal to 20%.

4.4.1 25-bar truss

The 25-bar truss (see Fig. 8) is characterized by three design variables (cross-sections), and two normal random variables ξ_1 and ξ_2:

– ξ_1 is related to the external forces F_1 and F_2 applied to the structure:

$$F_1 = \bar{F}_1(1+\xi_1),\ F_2 = \bar{F}_2(1+\xi_1), \tag{50}$$

– ξ_2 is related to the material density ρ (assumed to share the same value for all bars):

$$\rho = \bar{\rho}(1+\xi_2). \tag{51}$$

The results are exhibited in Fig. 9. A simple least squares approximation of the PCE coefficients is clearly not sufficient to furnish the dense and well spread fronts observed with moving least squares. Concerning the multiobjective reliability-based formulation, as shown in the

Table 12 Comparison of the results obtained with adaptive/non-adaptive (moving) least squares: average error on five optimal points located on the nondeterministic Pareto front ($\alpha = 90\%$)

Test case	# Design var.	# Objectives	# Constraints	Non-adaptive LS	Adaptive LS	Non-adaptive MLS	Adaptive MLS
t25b	3	2	2	5.9296e–06	6.3871e–06	6.1225e–06	6.2308e–06
t72b	3	2	2	4.5038e–06	5.1425e–06	4.7918e–06	4.9987e–06
dome	4	2	2	6.3327e–06	5.8209e–06	6.0269e–06	7.0233e–06

Table 13 Comparison of the results obtained with adaptive/non-adaptive (moving) least squares: average error on five optimal points located on the nondeterministic Pareto front ($\alpha = 99\%$)

Test case	# Design var.	# Objectives	# Constraints	Non-adaptive LS	Adaptive LS	Non-adaptive MLS	Adaptive MLS
t25b	3	2	2	8.4394e–06	1.0349e–05	1.0073e–05	9.6280e–06
t72b	3	2	2	7.5687e–06	7.7400e–06	7.6762e–06	7.6251e–06
dome	4	2	2	9.7939e–06	9.7474e–06	1.0105e–05	9.4782e–06

analytical example, an increase of the probability threshold α ($= \alpha^{\mathbf{f}} = \alpha^{\mathbf{g}}$) from 90 to 99% leads to a trade-off surface located farther from the deterministic Pareto front.

The results obtained for standard and moving least squares (without and with adaptivity) are compared in Tables 12 and 13 for probability thresholds of 90 and 99%. The numerical values display the error e between the objective function values obtained by the hierarchical stochastic metamodels (HSM) and the reference Monte Carlo simulations (MCS), averaged over $N_{\text{eval}} = 5$ points distributed along the nondeterministic Pareto front:

$$e = \frac{1}{N_{\text{eval}}} \sum_{i=1}^{N_{\text{eval}}} \sqrt{\left(\tilde{f}_1^{\text{HSM}} - \tilde{f}_1^{\text{MCS}}\right)^2 + \left(\tilde{f}_2^{\text{HSM}} - \tilde{f}_2^{\text{MCS}}\right)^2}, \tag{52}$$

where:

$$\tilde{f}_i^{\cdots} = \frac{f_i^{\cdots} - f_i^{\min}}{f_i^{\max} - f_i^{\min}} \tag{53}$$

and $f_i^{\min}$ and $f_i^{\max}$ are respectively the minimum and maximum value found in the nondeterministic Pareto front for objective f_i. All values collected in Tables 12 and 13 demonstrate the good agreement between the hierarchical stochastic metamodels and the reference simulations.

4.4.2 72-bar truss

The 72-bar truss (see Fig. 10) is characterized by three design variables (cross-sections), and two normal random variables: ξ_1 is related to the external force F applied at the

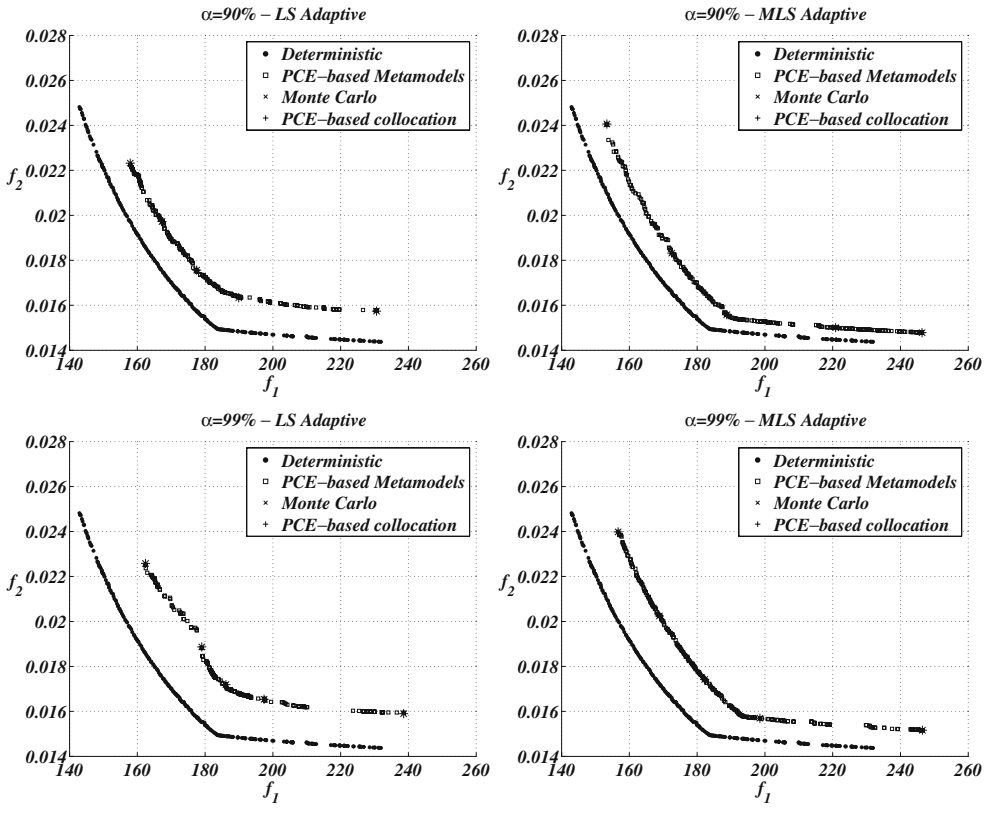

Fig. 14 Test case dome: adaptive LS (*left*) vs. adaptive MLS (*right*) for probability thresholds $\alpha = 90\%$ (*top*) and $\alpha = 99\%$ (*down*)

top of the structure through $F = \bar{F}(1+\xi_1)$ while ξ_2 is related to the material density ρ (assumed to share the same value for all bars) by $\rho = \bar{\rho}(1+\xi_2)$.

Again, the results show the benefit of moving least squares to approximate the PCE coefficients and thus provide dense and well distributed solutions. Additionally, in order to look at the effects of adaptivity of the metamodels in terms of size, accuracy and spread of the nondeterministic Pareto solutions, Fig. 12 depicts the results obtained without/with an updating strategy, demonstrating the need to update the database with new points during the optimization process to capture the whole Pareto front.

4.4.3 Dome

The last example is the dome shown in Fig. 13, parameterized by four design variables (cross-sections), and two normal random variables: ξ_1 is related to the external forces F (by $F = \bar{F}(1+\xi_1)$) whereas ξ_2 is related to Young's modulus E (assumed to share the same value for all bars) by $E = \bar{E}(1+\xi_2)$.

The same trend as in the previous examples is observed in Fig. 14 in the objective space, demonstrating for this problem that moving least squares outperforms its standard counterpart, due to the fact that the outputs cannot be modeled by quadratic responses throughout the whole domain. An insight on the Pareto set is also depicted in Fig. 15. The deterministic Pareto-optimal solutions are different from the reliability-based solutions (especially with respect to variable x_1), which motivates the use of this multiobjective formulation under uncertainty to provide more reliable Pareto-optimal solutions.

4.5 Discussion

The numerical experiments have illustrated the prominent features of the proposed methodology. First, a formulation based on reliability levels applicable both to the objectives (according to probabilistic nondominance) and to the constraints is advocated. The user can define probability thresholds, which makes the method well adapted to structural engineering problems constrained by probabilistic safety requirements.

Regarding the computational time, the hierarchical metamodeling technique (C) helps diminishing drastically the amount of simulations N_{sim} with respect to Monte Carlo simulations on the high-fidelity models (A) or collocation for each individual (B), as expressed below:

$$\begin{aligned}
&\text{(A)} \quad N^A_{\text{sim}} = N_{\text{gen}} N_{\text{pop}} N_{\text{MC}},\\
&\text{(B)} \quad N^B_{\text{sim}} = N_{\text{gen}} N_{\text{pop}} k_Q \tfrac{(N+M)!}{N!M!},\\
&\text{(C)} \quad N^C_{\text{sim}} = N_{\text{pop}}(1 + N_{\text{gen}}.R_{\text{updating}}) k_Q \tfrac{(N+M)!}{N!M!},
\end{aligned}$$

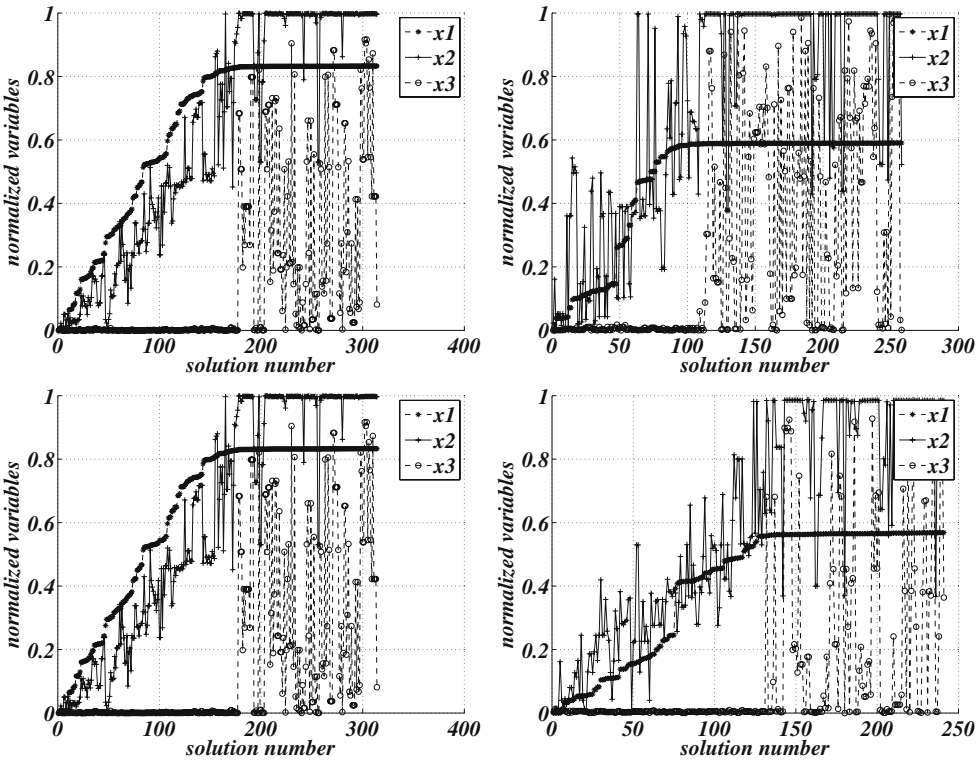

Fig. 15 Test case dome: deterministic (*left*) vs. nondeterministic (by adaptive MLS; *right*) Pareto sets obtained for probability thresholds $\alpha = 90\%$ (*top*) and $\alpha = 99\%$ (*down*)

where:

- M is the number of random variables;
- N is the degree of the polynomial chaos expansion;
- N_{gen} is the number of generations of the genetic algorithm;
- N_{pop} is the size of the population of the genetic algorithm (also set as the size of the initial training database for the surrogate models);
- N_{MC} is the number of Monte Carlo simulations;
- R_{updating} is the rate of individuals undergoing the updating scheme at each generation;
- $k_Q > 1$ is the ratio between the number of collocation points Q and the minimum number of points P necessary to build the polynomial chaos, i.e. $Q = k_Q P$ (in this study: $k_Q = 1$).

According to these expressions, the number of simulations required by the dome example is the following:

(A) $N_{\text{sim}}^{A} = 200 \times 30 \times 10{,}000 = 6.10^7$ (not affordable);
(B) $N_{\text{sim}}^{B} = 200 \times 30 \times 1 \times 15 = 90{,}000$;
(C) $N_{\text{sim}}^{C} = 735$ (observed for $\alpha = 90\%$).

Although the theoretical number of simulations required by method (C) with a rate of updating equal to 20% and 30 generations is 1,400, a much lower value is observed during the numerical experiments (735 for $\alpha = 90\%$) due to the presence in the offspring of individuals already present in the previous generations; these duplicates, already members of the database, are thus detected and not recomputed through the high-fidelity simulation.

It is also interesting to observe that the nondeterministic Pareto sets (i.e. the optimal solutions in the design space) are different from the deterministic ones, justifying the need for an alternative reliability-based formulation (see Fig. 15).

5 Conclusions and future prospects

In this paper, a non-intrusive procedure has been proposed to construct hierarchical stochastic metamodels based on a moving least squares interpolation of polynomial chaos expansion coefficients. This procedure is achieved for all simulation responses required by the optimization (objectives and constraints). Furthermore, those metamodels have been thoroughly validated and incorporated into an original multiobjective reliability-based formulation, and successfully applied to the structural design optimization of space trusses.

Our current investigations are mainly concerned with the following topics:

- the examples treated in this work are characterized by small numbers of variables and rather smooth responses. For more complex problems, higher degrees of PCE and MLS bases might be required, which would considerably increase the size of the training database, hence the overall CPU cost. In that case, considering sparse PCE to discard from the PCE coefficient matrix the terms that bring no significant contribution to the random response might be an option, in addition to a finer updating process during the optimization;
- for wider design spaces, improving the adaptive strategy of the stochastic metamodels should also be considered, for example by including a prediction error procedure to validate the surrogate model accuracy during the optimization. Another approach could imply screening or space reduction techniques (Shan and Wang 2010);
- tackling correlated non-normal random variables;
- applying the proposed methodology to large-scale civil engineering applications, also characterized by higher safety constraints.

Acknowledgments The authors are grateful to the Institute for the encouragement of Scientific Research and Innovation of Brussels (ISRIB) for their support under a BB2B project entitled "Multicriteria optimization with uncertainty quantification applied to the building industry". The authors also wish to thank the Reviewers for their fruitful comments.

Appendix

To give the closed-form expression of the sensitivities of the limit surfaces b with respect to ξ_i (Section 3.2), the chain rule is applied:

$$\frac{\partial b}{\partial \xi_i} = \sum_j \frac{\partial b}{\partial \psi_j} \frac{\partial \psi_j}{\partial \xi_i}, \tag{54}$$

Since ψ_j is expressed as a product of Hermite polynomials of each variable ξ_i:

$$\psi_j(\boldsymbol{\xi}) = \prod_{l=1}^{M} H_{\kappa_l(j)}(\xi_l), \tag{55}$$

the derivative of ψ_j with respect to a variable ξ_i is given by:

$$\begin{aligned} \frac{\partial \psi_j}{\partial \xi_i} &= \frac{\partial}{\partial \xi_i} \left(\prod_{l=1}^{M} H_{\kappa_l(j)}(\xi_l) \right) \\ &= \left(\prod_{l=1, l\neq i}^{M} H_{\kappa_l(j)}(\xi_l) \right) \frac{\partial H_{\kappa_i(j)}}{\partial \xi_i}. \end{aligned} \tag{56}$$

If $\kappa_i(j) = 0$, $\frac{\partial H_0}{\partial \xi_i} = 0$; otherwise, the definition of Hermite polynomials leads to:

$$\frac{\partial \psi_j}{\partial \xi_i} = \left(\prod_{l=1, l\neq i}^{M} H_{\kappa_l(j)}(\xi_l) \right) \left(\kappa_i(j) H_{\kappa_i(j)-1}(\xi_i) \right). \tag{57}$$

Therefore, we obtain explicitly:

$$\begin{aligned}
&\frac{\partial b_{\text{nondominance}}}{\partial \xi_k} \\
&= \frac{\partial}{\partial \xi_k} \left\{ \sum_{i=1}^{m} \exp\left(\rho \sum_{j=1}^{P-1} \psi_j(\boldsymbol{\xi}) \gamma_j^{f_i}(\mathbf{x}) \right. \right. \\
&\qquad \left. \left. - \rho \eta_i \sqrt{\sum_{j=1}^{P-1} E\left[\psi_j^2\right] \gamma_j^{f_i}(\mathbf{x})^2} \right) - 1 \right\} \\
&= \sum_{i=1}^{m} \left\{ \exp(\ldots) \rho \sum_{j=1}^{P-1} \gamma_j^{f_i}(\mathbf{x}) \frac{\partial \psi_j}{\partial \xi_k} \right\} \\
&= \sum_{i=1}^{m} \left\{ \exp(\ldots) \rho \sum_{j=1}^{P-1} \gamma_j^{f_i}(\mathbf{x}) \right. \\
&\qquad \left. \times \left[\prod_{l=1, l\neq k}^{M} H_{\kappa_l(j)}(\xi_l) \right] \kappa_k(j) H_{\kappa_k(j)-1}(\xi_k) \right\}
\end{aligned} \tag{58}$$

and:

$$\begin{aligned}
\frac{\partial b_{\text{safety}}}{\partial \xi_k} = \sum_{i=1}^{m} \left\{ \exp(\ldots) \rho \sum_{j=1}^{P-1} \gamma_j^{g_i}(\mathbf{x}) \right. \\
\left. \times \left[\prod_{l=1, l\neq k}^{M} H_{\kappa_l(j)}(\xi_l) \right] \kappa_k(j) H_{\kappa_k(j)-1}(\xi_k) \right\},
\end{aligned} \tag{59}$$

where the expression $(\kappa_k(j) H_{\kappa_k(j)-1})$ is equal to 0 when $\kappa_k(j) = 0$.

References

Acar E, Rais-Rohani M (2008) Ensemble of metamodels with optimized weight factors. Struct Multidis Optim 37:279–294

Acharjee S, Zabaras N (2007) A non-intrusive stochastic Galerkin approach for modeling uncertainty propagation in deformation processes. Comput Struct 85:244–254

Achenie LEK, Ostrovsky GM (2005) Multicriteria optimization under parametric uncertainty. In: Attoh-Okine NO, Ayyub BM (eds) Applied research in uncertainty modeling and analysis. Springer, New York

Barakat S, Bani-Hanib K, Taha MQ (2004) Multi-objective reliability-based optimization of prestressed concrete beams. Struct Saf 26:311–342

Basseur M, Zitzler E (2006) Handling uncertainty in indicator-based multiobjective optimization. Int J Comput Intell Res 2(3):255–272

Beyer HG, Sendhoff B (2007) Robust optimization—a comprehensive survey. Comput Methods Appl Mech Eng 196:3190–3218

Blatman G, Sudret B (2008) Sparse polynomial chaos expansions and adaptive stochastic finite elements using a regression approach. C R Méc 336:518–523

Breitkopf P, Filomeno Coelho R (eds) (2010) Multidisciplinary design optimization in computational mechanics, 1 vol. ISTE/Wiley, Chippenham, 549 pp

Breitkopf P, Rassineux A, Villon P (2002) An introduction to moving least squares meshfree methods. Rev Eur Élém Fin 11(7–8):825–867

Caballero R, Cerdá E, Muñoz MM, Rey L, Stancu-Minasian IM (2001) Efficient solution concepts and their relations in stochastic multiobjective programming. J Optim Theory Appl 110(1):53–74

Coello Coello CA, Van Veldhuizen DA, Lamont GB (2002) Evolutionary algorithms for solving multi-objective problems. Kluwer/Plenum, New York

Crestaux T, Le Maître O, Martinez JM (2009) Polynomial chaos expansion for sensitivity analysis. Reliab Eng Syst Saf 94:1161–1172

Crisfield MA (2000) Non-linear finite element analysis of solids and structures, vol 1. Essentials. Wiley, Chichester

Deb K, Gupta H (2005) Searching for robust pareto-optimal solutions in multi-objective optimization. In: Coello Coello CA, Aguirre AH, Zitzler E (eds) Evolutionary multi-criterion optimization, third international conference, EMO 2005, Guanajuato, Mexico, March 9–11, pp 150–164

Deb K, Gupta H (2006) Introducing robustness in multi-objective optimization. Evol Comput 14(4):463–494

Deb K, Pratap A, Agarwal S, Meyarivan T (2002) A fast and elitist multiobjective genetic algorithm: NSGA-II. IEEE Trans Evol Comput 6(2):182–197

Deb K, Padmanabhan D, Gupta S, Mall AK (2007) Reliability-based multi-objective optimization using evolutionary algorithms. In: Evolutionary multi-criterion optimization. Springer, Berlin

Deb K, Gupta S, Jaum D, Branke J, Mall AK, Padmanabhan D (2009) Reliability-based optimization using evolutionary algorithms. IEEE Trans Evol Comput 13(5):1054–1074

Der Kiureghian A, Ditlevsen O (2009) Aleatory or epistemic? Does it matter? Struct Saf 31:105–112

Eldred MS, Webster CG, Constantine PG (2008) Evaluation of non-intrusive approaches for Wiener–Askey generalized polynomial chaos. In: Proceedings of the 49th AIAA/ASME/ASCE/AHS/ASC structures, structural dynamics, and materials conference, Schaumburg, IL, April 7–10

Filomeno Coelho R, Breitkopf P, Knopf-Lenoir C (2008) Model reduction for multidisciplinary optimization—application to a 2D wing. Struct Multidisc Optim 37(1):29–48

Filomeno Coelho R, Breitkopf P, Knopf-Lenoir C, Villon P (2009) Bi-level model reduction for coupled problems—application to a 3D wing. Struct Multidisc Optim 39(4):401–418

Filomeno Coelho R, Lebon J, Bouillard Ph (2010) Multiobjective reliability-based optimization of truss structures with stochastic surrogate models. In: ECCM 2010 (IV European conference on computational mechanics), Palais des Congrès, Paris, France, May 16–21

Forrester AIJ, Keane AJ (2009) Recent advances in surrogate-based optimization. Prog Aerosp Sci 45(1–3):50–79

Ghanem RG, Kruger RM (1996) Numerical solution of spectral stochastic finite element systems. Comput Methods Appl MechEng 129:289–303

Greco M, Gesualdo FAR, Venturini WS, Coda HB (2006) Nonlinear positional formulation for space truss analysis. Finite Elem Anal Des 42:1079–1086

Gunawan S, Azarm S (2005) Multi-objective robust optimization using a sensitivity region concept. Struct Multidisc Optim 29:50–60

Haftka RT, Gürdal Z (1992) Elements of structural optimization. Kluwer, Dordrecht

Haldar A, Mahadevan S (2000) Reliability assessment using stochastic finite element analysis. Wiley, Chichester

Jones DR (2001) A taxonomy of global optimization methods based on response surfaces. J Glob Optim 21:345–383

Keane AJ (2009) Comparison of several optimisation strategies for robust turbine blade design. J Propul Power 25(5):1092–1099

Klimke A (2008) Sparse grid interpolation toolbox user's guide, v5.1

Köppen M, Vicente-Garcia R, Nickolay B (2005) Fuzzy-Pareto-dominance and its application in evolutionary multi-objective optimization. In: Coello Coello CA, Aguirre AH, Zitzler E (eds) Evolutionary multi-criterion optimization, Third international conference, EMO 2005, Guanajuato, Mexico, March 9–11, pp 399–412

Kumar A, Nair PB, Keane AJ, Shahpar S (2008) Robust design using Bayesian Monte Carlo. Int J Numer Methods Eng 73:1497–1517

Lancaster P, Salkauskas K (1981) Surfaces generated by moving least squares methods. Math Comput 37(155):141–158

Levi F, Gobbi M, Mastinu G (2005) An application of multi-objective stochastic optimisation to structural design. Struct Multidisc Optim 29:272–284

Li G, Li M, Azarm S, Al Hashimi S, Al Ameri T, Al Qasas N (2009) Improving multi-objective genetic algorithms with adaptive design of experiments and online metamodeling. Struct Multidisc Optim 37:447–461

Limbourg P (2005) Multi-objective optimization of problems with epistemic uncertainty. In: Evolutionary multi-criterion optimization, third international conference, EMO 2005, Guanajuato, Mexico, March 9–11, pp 413–427

Lophaven SN, Nielsen HB, Søndergaard J (2002) DACE—a Matlab kriging toolbox (version 2.0). Tech. rep., Informatics and Mathematical Modelling, Technical University of Denmark

Nayroles B, Touzot G, Villon P (1992) Generalizing the finite element method: Diffuse approximation and diffuse elements. Comput Mech 10:307–318

Paenke I, Branke J, Jin Y (2006) Efficient search for robust solutions by means of evolutionary algorithms and fitness approximation. IEEE Trans Evol Comput 10(4):405–420

Parashar S, Bloebaum CL (2006) Robust multi-objective genetic algorithm concurrent subspace optimization (R-MOGACSSO) for multidisciplinary design. In: 11th AIAA/ISSMO multidisciplinary analysis and optimization conference, Portsmouth, Virginia, September 6–8, AIAA paper 2006-6907

Poles S, Lovison A (2009) A polynomial chaos approach to robust multiobjective optimization. In: Deb K, Greco S, Miettinen K, Zitzler E (eds) Hybrid and robust approaches to multiobjective optimization, Schloss Dagstuhl—Leibniz-Zentrum fuer Informatik, Germany, Dagstuhl, Germany, Dagstuhl seminar proceedings

Sachdeva SK, Nair PB, Keane AJ (2007) On using deterministic FEA software to solve problems in stochastic structural mechanics. Comput Struct 85:277–290

Schuëller GI, Jensen HA (2008) Computational methods in optimization considering uncertainties—an overview. Comput Methods Appl Mech Eng 198(1):2–13

Shan S, Wang GG (2010) Survey of modeling and optimization strategies to solve high-dimensional design problems with computationally-expensive black-box functions. Struct Multidisc Optim 41:219–241

Sinha K (2007) Reliability-based multiobjective optimization for automotive crashworthiness and occupant safety. Struct Multidisc Optim 33:255–268

Stefanou G (2009) The stochastic finite element method: past, present and future. Comput Methods Appl Mech Eng 198:1031–1051

Swiler LP, Wyss GD (2004) A user's guide to Sandia's Latin hypercube sampling software: LHS UNIX library/standalone version. Tech. rep., Sandia National Laboratories, Albuquerque, New Mexico

Teich J (2001) Pareto-front exploration with uncertain objectives. In: Evolutionary multi-criterion optimization. LNCS, vol 1993. Springer, pp 314–328

Toal D, Bressloff N, Keane AJ, Holden C (2010) Geometric filtration using proper orthogonal decomposition for aerodynamic design optimization. AIAA J (American Institute of Aeronautics and Astronautics) 48(5):916–928

Tokdar ST, Kass RE (2010) Importance sampling: a review. Wiley Interdisc Rev Comput Stat 2:54–60

Tsompanakis Y, Papadrakakis M (2004) Large-scale reliability-based structural optimization. Struct Multidisc Optim 26:429–440

Viana FAC, Haftka RT, Steffen V Jr (2009) Multiple surrogates: how cross-validation errors can help us to obtain the best predictor. Struct Multidisc Optim 39:439–457

Xiong F, Greene S, Chen W, Xiong Y, Yang S (2010) A new sparse grid based method for uncertainty propagation. Struct Multidisc Optim 41:335–349

Chapter 6

General conclusions and prospectives

6.1 Conclusions

In this thesis we investigated the following question in the scope of variability studies when small variations are concerned: how far may we trust the "high-fidelity" models? We have shown on a classical metal forming test problem than when using the non-linear FE scheme as "high-fidelity" simulations, small variations of the random input parameters lead to noisy training data and may distort the statistical data of interest.

When using non linear FE scheme as "high-fidelity" simulation, small variations of the random input parameters may lead to noisy input training data which alters the accuracy of the training data set and may distort the statistical quantities of interest. We have illustrated this claim using the non-linear FEM simulation (involving contact/friction and material non linearities) of the springback of a 2D deep drawing process of U shaped metal sheet.

We have introduced two methodologies in order to bypass this limitation. The first methodology consists in combining a physical reduced order metamodel (semi-analytical Bending-Under-Tension model) and a custom Polynomial Chaos Expansion to accurately assess the springback parameters for small variations on the input parameters. The B-U-T model allowed us to circumvent typical cost issues and numerical instability from full FEM simulations (contact modeling, through thickness integration). The use of such a model has allowed us to reach a sufficient numerical stability for small variations of the random parameters. Using these high resolution outputs, we have been able to accurately train a custom stochastic surrogate to efficiently propagate the uncertainties through the model. Then, this approach allowed us to accurately assess the springback variability when multiple random variables are taken into account with a limited budget.

However, physics-based metamodels with higher resolution are not always available. To circumvent this issue, one opportunity is to take into account the model sensitivity in the sampling scheme. We proposed a modified Latin Hypercube Sampling methodology called *Fat-LHS* allowing to filter noisy data and to preserve their Latin Hypercube Sampling property. This heuristic strategy provides the maximum number of simulations available considering the finite model sensitivity. We then used this limited number of non-noisy samples to build a PCE in order to propagate the uncertainty. But, the low number of samples has lead us to consider sparse strategies to make affordable possible identification of the PCE terms. We have compared three different methodologies to build a sparse PCE (LARS, Q-norm and LARS+Q-norm) and have retained the best possible PCE for each of them. The comparison of the results has shown that generally the Q-norm+LARS hybrid is more efficient. We have obtained the best results for truncated low order sparse PCE.

Moreover, the combination of optimization and uncertainty quantification has been addressed. In most of the studies, these both fields have been combined when only one objective function is considered. However, most of real life problem involved the simultaneous optimization of possibly competing objectives. Then two issues have to be tackled: the definition of a formulation of MOOU, and its resolution. In this thesis, we particularly focused on the resolution phase. Most of the time this task is achieved using a nested combination of metamodels constructed separately either in the deterministic design variables space or in the stochastic variables space. Here, we have proposed a computationally efficient non-intrusive procedure to construct a metamodel in both deterministic and stochastic spaces. It is based on a moving least squares interpolation of polynomial chaos coefficients. Those metamodels have

been thoroughly validated and incorporated into an original multi-objective reliability-based formulation, and successfully applied to the cost-effective structural design optimization of space trusses.

6.2 Prospects

To deal with real-life multi-objective optimization problem under uncertainty, one has to take into account the eventually high dimensionality of the problem and to develop robust methodologies to this purpose. The examples treated in this work are characterized by small numbers of variables and rather smooth responses. For more complex problems, higher degrees of PCE and MLS bases might be required, which would considerably increase the size of the training database, hence the overall CPU cost. In that case, considering sparse PCE to discard from the PCE coefficient matrix the terms that bring no significant contribution to the random response might be an option, in addition, to a finer updating process during the optimization; Moreover, tackling wider design spaces, improving the adaptive strategy of the stochastic metamodels should also be considered, for example by including a prediction error procedure to validate the surrogate model accuracy during the optimization. Another approach could imply screening or space reduction techniques in a MOOU framework.

Finally, focusing on the UQ part of the problem, our approach demonstrates that the use of simplified physics based model for large strain forming process allows to reduce the numerical instability and makes possible an accurate and low cost variability study. The approach is of course not limited to 2D plain strain and sparse PCE opens the way to a combination with other types of physics-based metamodels such as one-step or POD/PGD approaches presenting similar smoothing properties in 3D. The consistency between the different fidelities levels in the approach have not been addressed as [NE12] recently investigates this issue. In the current state of development we have demonstrated the validity of our the approach from numerical point of view using standard benchmarks. The comparison with experiment requires an implementation of the method within a specialized metal forming framework, which is beyond the scope of the current study dedicated to stochastic modeling, but may be done in further studies.